Jianming Wei
Hong Wang
Fang Liu

Iterative Learning Control for Nonlinear Time-Delay System

国防工業出版社
National Defense Industry Press

Springer

Iterative Learning Control for Nonlinear Time-Delay System

Jianming Wei · Hong Wang · Fang Liu

Iterative Learning Control for Nonlinear Time-Delay System

国防工業出版社
National Defense Industry Press

Springer

Jianming Wei
College of Weapons Engineering
Naval University of Engineering
Wuhan, Hubei, China

Hong Wang
Naval Aviation University
Yantai, Shandong, China

Fang Liu
College of Weapons Engineering
Naval University of Engineering
Wuhan, Hubei, China

ISBN 978-981-19-6316-2 ISBN 978-981-19-6317-9 (eBook)
https://doi.org/10.1007/978-981-19-6317-9

Jointly published with National Defense Industry Press
The print edition is not for sale in China (Mainland). Customers from China (Mainland) please order the print book from: National Defense Industry Press.

Translation from the Chinese language edition: "FeiXianXing ShiZhi XiTong Diedai XueXi KongZhi" by Jianming Wei, © National Defense Industry Press 2020. Published by National Defense Industry Press.

This Springer imprint is published by the registered company Springer Nature Singapore Pte Ltd.
The registered company address is: 152 Beach Road, #21-01/04 Gateway East, Singapore 189721, Singapore

Preface

The essence of the world is nonlinear, and practical control systems are always impacted by nonlinearity. Non-smooth and nonlinear characteristics exist broadly in the practical plants, such as dead zone, saturation and hysteresis, which may deteriorate the system performances and even at worst may become a source of instability. Consequently, the control problem of nonlinear systems under nonlinearity attracts much attention in the control community. On the other hand, time delays are inevitable, which is usually arose by the detection, computation and transmission of signals and the reaction time of actuators. The existence of time delays will also impose a negative effect on the control performances. The interaction of non-smooth nonlinear characteristics and time delays make it very difficult to design the learning controllers for such systems. Hence, there are few results reported in literatures.

This book, in turn, investigates the adaptive iterative learning control problems for parametric nonlinear time-delay systems, nonparametric, nonlinear time-delay systems, nonlinear time-delay systems with unknown control direction and nonlinear time-delay systems with only output measurable in a logical order from easy to difficult and from shallow to deep, and proposes a series of adaptive iterative learning control schemes, eventually solving the adaptive iterative learning controller design problems under an unified framework.

As a treatise focusing on iterative learning control methods of nonlinear time-delay systems, this book has a good professionalism and pertinence, and also has great theoretical significance and academic value to the study and promotion of learning control theory, and so it may offer beneficial reference for scholars and engineers working on researches on related theories and technologies.

The publication of this book has been sponsored by Defense Technology Book Publishing Fund of National Defense Industry Press and Shandong Natural Science Foundation (ZR2017QF016). Moreover, the publication is also supported by the College of Weapons Engineering, Naval University of Engineering. The authors gratefully acknowledge these supports.

We would like to give thanks to authors of the referenced materials in this book.

Some mistakes are unavoidable owing to the authors' limited knowledge. Comments and suggestions are always welcome.

Wuhan, China Jianming Wei
Yantai, China Hong Wang
Wuhan, China Fang Liu
May 2021

About This Book

The iterative learning control problem of nonlinear time-delay systems is investigated in this book. On the basis of deep investigation of previous works, we innovatively propose a class of adaptive iterative learning control schemes and solve a series of adaptive iterative learning control design problems for nonlinear time-varying systems with unknown nonlinear input characteristics and time delays under a unified framework, step by step, from easy to difficult. The book includes six chapters. In Chap. 1, the research background and significance of the book are discussed; moreover, the developments of iterative learning control, especially adaptive iterative learning control, are deeply analyzed. In Chap. 2, a novel adaptive iterative learning control scheme is proposed for a class of nonlinear parameterized systems with dead-zone input and unknown time-varying delays. In Chap. 3, neural network approximation method is employed to design the adaptive iterative learning control scheme for a class of uncertain nonparameterized, nonlinear time-varying systems with unknown dead-zone input and time-varying state delays. In Chap. 4, the neural network method and Nussbaum gain method are comprehensively integrated to establish the adaptive iterative learning control scheme for a class of nonlinear systems with unknown time delays and control direction preceded by backlash-like hysteresis. In Chap. 5, the adaptive iterative learning control problem for nonlinear time-delay systems with unmeasurable states is studied; two different adaptive iterative learning schemes are put forward based on state observer and tracking error observer, respectively. In Chap. 6, the research for plants with unmeasurable states and unknown control gain is carried out by taking manipulator as investigation object, and a kind of state observer-based adaptive iterative learning control scheme is presented.

As a book discussing the iterative learning control problems of nonlinear time-delay systems, it may be referential to the scholars and engineering technicians who engage in relevant research works.

Contents

Chapter 1
Introduction

1.1 Background

The history of science and technology has witnessed a rapid development in the twentieth century. The great achievements of science and technology have completely changed the appearance of the world. In this process, control science plays an essential role, just as what Dr. Hsue-shen Tsien has pointed out in the Preface of Engineering Cybernetics (3rd Edition): we can declare unequivocally that relativity theory, quantum theory and Cybernetics are three great achievements in the first half of the twentieth century from the perspective of scientific theory which can be called as three revolutions in the natural sciences and are three big leaps about the knowledge of the objective world [1]. In twentieth century, the developments of many technologies that can be called as technical revolution, for example, nuclear technology, electronic computer technology, astronautical technology and life technology, all have a direct connection to Cybernetics. Therefore, in Dr. Hsue-shen Tsien's opinion, Cybernetics as the technical science has a profound meaning to the research on engineering technology, bioscience, economic science and social sciences, which is not less than the effects of relativity theory quantum theory on the human beings [1]. Nowadays, control technologies have a wide application in all kinds of fields, such as industrial manufacture, transportation, aerospace and so on, from airplanes, missiles, aircraft carriers, warships to mobiles, computers, air conditioners that are closely related to daily life, control technologies are everywhere and make great contributions to the progress of human civilization.

In the development of science and technology, they supplement each other and are inextricably intertwined. The developments of technology promote the births of new scientific principal, in turn new science theory can promote great progress of technology and will be tested by production practice and scientific experiments. Before a few years of the birth of Cybernetics, V-1 and V-2 missile had come out, and it is in the technical engineering practice of designing the guidance and control system of modern missiles, the idea of Cybernetics gradually grew up. But the electromechanical guidance systems of V-1 and V-2 were very simple and crude, which

J. Wei et al., *Iterative Learning Control for Nonlinear Time-Delay System*,
https://doi.org/10.1007/978-981-19-6317-9_1

results in a low accuracy. However, the guidance systems of intercontinental missile that are designed by using engineering Cybernetics can achieve a high accuracy less than the CEP of tens of meters after a flight of thousands of kilometers. During the latter half of the twentieth century, the control theory were greatly improved by the requirements of control technology. Since the Cybernetics was proposed by Wiener in 1948, control science has gone through three stages of development: classical control theory, modern control theory, postmodern control theory.

Classical control theory was developed during the 1940s and 1950s when Bertalanffy finished his book “General system theory” and Wiener wrote the famous “Cybernetics” in 1948, which marked the formation of the rounded system of classical control theory. Classical control theory takes single-input single-output (SISO) linear time-invariant system as the research subject and use the input-output characteristic that is mainly described by transfer function as mathematical model to analyze the system performance (transient performance and steady-state performance), or designs control devices according to performance and chooses controllers that are economical, highly reliable and easily realized in engineering, where the frequently-used analysis and design method include time response method, root locus method and frequency response method. Therefore, classical control theory essentially neglects the inner characteristics of the control system which leads to the fact that it is only applicable to SISO time-invariant systems and difficult to optimize the systems performance index. In this way, classical control theory can hardly meet the needs for modern industrial process and space technology which is impetus for promoting the development of modern control theory.

The control scholars initiated the research on modern control in 1960s, which investigated the problem for multi-variables linear systems and nonlinear systems. Modern control theory uses time domain method, especially state-space method, as the main research method, furthermore uses linear algebra and differential equation as the main analytical method. Modern control theory breaks through many limitations of classical control theory that leads to its wider range of research objects compared with classical control theory and satisfies the control needs for complex systems in modern industrial control, aerospace industry and so on, to a certain extent. However, modern control theory is established on the basis of the fact that the studied systems are known. But strictly speaking, for all kinds of plants in various industrial manufacture process and aerospace vehicles, it is difficult to build an accurate model to describe the dynamic characteristics. On the other hand, the characteristics of the plant itself will change with operating conditions and environment. Consequently, it is almost impossible to build an accurate mathematical model for a controlled system and there inevitably exist errors between the established model and the actual dynamic characteristics of the system. Meanwhile, the systems are usually influenced by external unknown disturbances when operating. Therefore, in engineering practice, for more and more complex systems, such as hypersonic vehicles that are difficult to be modeled precisely but require more accurate and faster control systems, the controllers that are designed by modern control theory is difficult to acquire the desired control performance and sometimes even can’t guarantee the system stability. Moreover, as the controlled objects become more and more complex, modern control theory already has no ability to deal with some strong-nonlinear dynamics. In this case, control scholars introduced the uncertainty into system models and started researching the analysis and synthesis (design) problem for dynamic systems with uncertainties and strong-nonlinearities. Subsequently, post-modern control theory developed gradually.

In classical and modern control theories, the researches on the control theory of linear systems have gradually matured. However, all the systems in the real world are nonlinear in nature and linear models are nothing but the linearized results of nonlinear systems in the neighborhood of some specified points. The main research objects of post-modern control theory are various nonlinear systems in the real world. The post-modern control theory is a joint name of many advanced control methods, such as robust control, adaptive control, variable structure control, backstepping, intelligent control and so on. In particular, on account of the development of computer technology, neural network (NN) theory and fuzzy theory in 1980s, the NN and fuzzy system were introduced into controller design, which enriched and promoted nonlinear control theory.

In the development of post-modern control, inspired by artificial intelligence, control scholars have been always exploring how to endow the controller certain intelligences which enable it to improve constantly by learning in the control process and eventually achieve perfect control performance. As early as 1960s, Sklansky put forward the ideology of control system learning. In the early 1970s, Chinese American scholar Fu proposed the concept of learning control [2]. Since then the researches on learning control have been active and a variety of learning control schemes have been presented successively. Especially in 1980s, as the rapid development of computer technology and artificial intelligence, the researches about the learning control theory ushered in a new breakthrough. Nowadays, learning control theories have developed into an important branch.

In the learning control theory, iterative learning control (ILC) is a branch of rigorous mathematical descriptions. The basic principle of traditional ILC is to generate current control action by exploiting information collected from previous executions based on a learning mechanism in order to improve control performance from iteration to iteration, and eventually realize highly accurate tracking of the system states or output to the desired reference trajectories within a finite time interval after a few times of learning. The basic idea of ILC was proposed by Japanese scholar Uchiyama [3]. In 1984 Arimoto theorized and systematized the idea of ILC and put forward two ILC algorithms with convergence analysis for the first time [4]. Arimoto's work attracted much attention from control peers and opened up a wide development prospection. Hereafter, ILC obtained rapid development in theoretical research and practical applications and developed into a hot topic in the field of intelligent control. Because of its simpleness, easy realization, intelligence and broad application prospects in industrial robots and manipulators, the researches on ILC theory and the learning controller design to solve the tracking problems for uncertain systems that repeated running on a finite interval are of important academic significance and application value.

In a lot of actual physical systems, the current states of the system may be affected by past states, in other words, the change rate of current states is not only related to current states but also dependent on the states of some time or an interval in the past, this kind of characteristic is called as time-delay. In control systems, time delay exists widely and it may be caused by many factors, such as signal detection time of detection equipment, transmission time of control signals, response time of actuators. The existence of time-delay may degrade the system dynamic performance and cause oscillation, in the worst case, it will even destroy the system stability. Therefore, the research on the control problem for time-delay systems has great theoretical significance and application value. Since 1960s, the research on the control problems of time-delay systems developed continuously and has formed an important subject and is still a hot topic at present in field of control theory.

In essence, all the systems in the real world are nonlinear, which is not only determined by the nonlinearity of the physical laws that the system, but also because of the influence of various nonlinear characteristics, for example, saturation, deadzone, friction, hysteresis and so on. These nonlinearities exist widely in practical physical systems. Just like time-delay, nonlinearities will also degrade the control system performance and destroy the system stability in the worst situation. So, it is necessary to consider the influence of nonlinear characteristic in the controller design for nonlinear systems which is of research significance and application value as well.

In conclusion, because of the wide existence of time-delay and nonlinear characteristics and the difficulty of theoretical analysis, it is necessary to investigate the ILC problem for nonlinear systems with unknown nonlinearities and time-delays. Meanwhile, we should recognize that the research on this type nonlinear systems is not a simple combination of the respective research results for nonlinearity, time-delay and ILC, but a deep investigation for the problems arising. In this book, we lucubrate the problem of ILC theory of time-delay systems and systematically propose an adaptive iterative learning control (AILC) scheme to solve a series of control problems for several kinds of time-delay systems with nonlinearities under an uniform framework, which try to provide some reference for the further research and relative engineering practice of similar problems (especially the AILC problem for time-delay systems).

1.2 Research Status of ILC

In 1978, Uchiyama published the paper about the idea of ILC in Japanese, so the works didn't attract much attention from other control scholars until Arimoto systematized Uchiyama's thought and published it in English in 1984. Throughout thirty years of development, ILC has formed three main frames of research work: contraction mapping theorem based classical ILC, composite energy function based AILC and 2-D theorem based ILC.

1.2.1 Contraction Mapping Theorem Based Classical ILC

The so-called classical ILC is the control algorithm proposed in the stages of ILC research. Unlike other methods that starts with linear systems, ILC takes nonlinear systems as research object at the beginning, i.e., robotic systems [4], furthermore, its control objective is very high, i.e., driving the system output to track the desired trajectory $y_d(t) \in C^1[0, T]$ on a finite interval $[0, T]$ completely. Consider the following nonlinear dynamical system that is globally Lipschitz continuous

$$\dot{x}_k = f(x_k, u_k, t),\ y_k(t) = g(x_k, u_k, t) \tag{1.1}$$

Classical ILC uses the previous control experience and control errors to obtain the control actions for current iteration. Specifically, after an iteration, the control signal $u_{k-1}(t)$ (the subscript "k-1" denotes the times of iteration) and tracking error $e_{k-1}(t)$ (the system output is indicated as $y_{k-1}(t)$ and $e_{k-1}(t)$ is defined as $e_{k-1}(t) = y_d(t) - y_{k-1}(t)$) are obtained. When executing the control task once again, the control signals should be constructed based on error feedback and the control signals of the previous running, i.e.,

$$u_k(t) = u_{k-1}(t) + qe_k(t) \tag{1.2}$$

where, $q > 0$ is the feedback gain and is also the learning gain. The block diagram of this type ILC algorithm is presented in Fig. 1.1.

According to the analysis in [5], the term $u_{k-1}(t)$ in learning algorithm (1.2) plays a role of feedforward in $u_k(t)$, the term $qe_k(t)$ works as feedback and at the same time plays a role of error correction. From the viewpoint of learning, the previous control experience $u_{k-1}(t)$ is used effectively to make up for the shortage of current control effect. This is similar to the learning process of human beings that practices and corrects a movement over and over again in order to get the right way. From the viewpoint of control, through learning the feedforward has taken the place of feedback as the leading role in the control process of ILC algorithm (1.2). From Fig. 1.1 it can be seen that algorithm (1.2) is closed loop due to the feedback

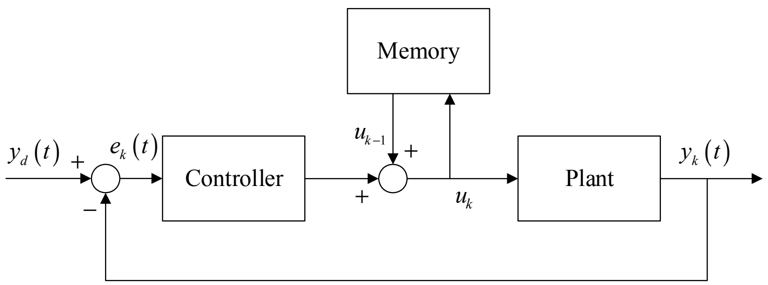

Fig. 1.1 The block diagram of ILC

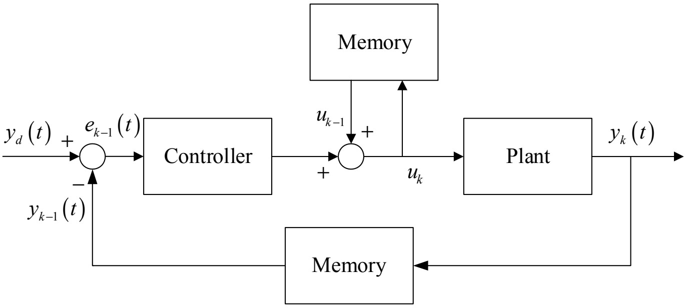

Fig. 1.2 The block diagram of open-loop ILC

function. So, the algorithm with form of (1.2) can be referred to as Closed-Loop ILC. Correspondingly, Open-Loop ILC has the following form:

$$u_k(t) = u_{k-1}(t) + qe_{k-1}(t) \tag{1.3}$$

The block diagram of Open-Loop ILC is shown in Fig. 1.2.

In Open-Loop ILC, the feedback term has been removed and the feedforward bears the responsibility alone. Here "q" is only the learning gain, which avoids the problem that it is difficult to reasonably balance the feedback stability and learning convergence when "q" plays both roles of feedback gain and learning gain in Closed-Loop ILC.

The theoretical core of learning convergence of classical ILC is to ensure the geometrical convergence of tracking error in the pointwise manner by using contraction mapping methodology, i.e., $\|e_k(t)\| \le \gamma\|e_{k-1}(t)\|$, $0 < \gamma < 1$, $\forall t \in [0, T]$. For the ILC algorithms (1.2) and (1.3) for system (1.1), in order to achieve learning convergence, the system should satisfy the convergence condition [5]: $\left|1 - q\partial g / \partial u_k\right| \le \gamma$. Then it is obvious that we just need to know the upper and lower bounds of $\partial g / \partial u_k$ and then we can choose approximate gain "q" to guarantee that the convergence condition holds.

The ILC algorithm (1.3) is the simplest expression of ILC. Since (1.3) only contains the proportional term of error, so it is called as P-type ILC algorithm. Accordingly, if there exist the integral or differential term of tracking error in the ILC algorithm, then it is called as integral-type or differential-type ILC algorithm. Moreover, in learning algorithm design, integral signals and differential signals will also be incorporated with proportional signals to form mixed-type ILC algorithm, such as PI-type, PD-type, and PID-type.

In practical applications, the performance of open-loop ILC and closed-loop ILC are both unsatisfactory, as closed-loop ILC may cause oscillation because of signal lag caused by the sampler, while open-loop ILC is not robust because of absence of feedback term. Besides, although closed-loop ILC has the problem that it is difficult to reasonably balance the feedback gain and learning gain, they are not contradictory. Moreover, the feedback signals enable the control system to obtain better dynamical performance and accelerate the convergence speed. Consequently, for the purpose of complementing each other, some scholars combined the characteristics of open-loop ILC and closed-loop ILC and further put forward Open-Closed-Loop ILC method. Through comparative study, Xu [6] found that Open-Closed-Loop ILC can achieve better control performance than pure Open-Loop ILC or pure Closed-Loop ILC and enhance the robustness.

Now that the usage of previous control information can obtain better control effect in the control process, then will it be improved further if we use the control information of more than one iteration? Based on this idea, South Korean scholar Bien proposed high-order ILC algorithm for the first time in 1989 and derived the advantage of accelerating convergence speed for high-order ILC [7]. The general form of high-order ILC can be expressed as

$$u_k = \sum_{i=1}^{n} a_i u_{k-i}(t) + \sum_{i=1}^{n} b_i e_{k-i}(t),\ 1 \leq n \leq k-1 \tag{1.4}$$

But through research Xu found that if the control information of the past multi-iterations were simply combined linearly, high-order ILC may not be able to speed up the convergence [8]. The reason lies in that in the information of past multi-iterations only the latest one can accurately describe the situation of iterative convergence and a simple linear combination of the earlier information that is not accurate for the current iteration may degrade control performance. Norrlöf carried out the comparative research of first-order ILC algorithm and second-order ILC algorithm through an industrial manipulator. He found out that second-order ILC algorithm can't achieve better performance than first-order ILC algorithm, but if there exist uncertainties in the plant the control effects of second-order ILC are better than first-order ILC. Moreover, he also discovered that second-order ILC can obtain more smooth control effects [9]. In Xu's book [10], he has proved theoretically by using min–max and Q-factor method that first-order ILC had faster convergence speed from the viewpoint of Q-factor. But Xu pointed out simultaneously that the investigation of the performance of first-order and high-order ILC using other performance index remains an open problem, so there has been no corresponding conclusion about it. In fact, when there exist zero-mean disturbances and measurement noises along iteration axis, since high-order ILC plays a role of average operator for disturbances and noises, it can obtain better control performance compared with first-order ILC. The control community has been continuously studying high-order ILC schemes since it was proposed. Many scholars have designed a great number of high-order ILC algorithms for various ILC problems, aiming at improving control performance, accelerating convergence speed and enhancing the robustness of control systems.

If the system is not affected by disturbances or noises, ILC algorithm is able to achieve perfect control performance. But in practice the control systems are inevitably influenced by disturbances or noises. Consequently, the control performance of Open-Closed-Loop ILC algorithm is unsatisfactory, the learning errors always decrease early and then increase. The main reason for this lies in that ILC is a typical integrator along iteration axis. If the noise is fixed and repeatable ILC can learn it together, but conversely, if the noise is not repeatable, the compensation signal will become higher and higher as the iteration continues which eventually leads to the problem of snowball effect and learning divergence [5]. To address this problem, ILC scholars came up with the method of filters, then the ILC expression is changed to

$$u_k(t) = A(t)u_{k-1}(t) + B(t)e_{k-1}(t) + C(t)e_k(t) \tag{1.5}$$

where, $A(t)$, $B(t)$ and $C(t)$ represents various kinds of filter. The simplest form of (1.5) is adding a forgetting factor, i.e.,

$$u_k(t) = pu_{k-1}(t) + q_1 e_{k-1}(t) + q_2 e_k(t) \tag{1.6}$$

where, $0 < p \leq 1$ is the forgetting factor. One drawback of this method is that it will forget all the signals, whether they are useful or useless. To avoid this problem, we can choose $A(t)$ as a low pass filter which can retain the useful low-frequency signal and filter out high frequency noise. If the controlled plant is linear system, we can employ Kalman filter method to determine the filter in (1.5).

Except the aforementioned classical ILC laws, many other ILC laws were proposed for different problems from different angles. For example, for linear systems model predictive control and optimal control have been extended to ILC methods in which the optimal ILC law were determined by defining objective function and finding its extrema. The research result of Amann shows that the prediction function in control law can speed up convergence and improve interference rejection [11]. Until now, a few kinds of predictive ILC algorithms has been proposed and applied to practical control systems [12, 13]. Moreover, D-type methods are not suitable for practical applications, which lies in the following reasons: firstly, the differential signal is not measurable and usually obtained by differentiating the position signals; secondly, differential signals are sensitive to high frequency noises. Since the upper bound of tracking error is proportionate to the magnitude of noise, the existence of noises will degrade the effect and accuracy of D-type algorithms. As for P-type algorithm (1.2), the error convergence can be guaranteed only in the case without uncertainties and disturbances. To overcome above contradiction, anticipatory ILC scheme [14] was proposed and gained a series of developments [15, 16]. Furthermore, in order to speed up learning speed and improve control effect, Xu put forward two kinds of nonlinear ILC laws: Newton-type ILC law [17] and secant ILC law [10].

Through above analysis, we can conclude that classical ILC don't need any information about the system, neither state variables nor state space, it deals with high uncertainty and strong nonlinearity using the simples learning law. But classical ILC is limited to the system that satisfies global Lipschitz continuous condition, otherwise, it may escape in finite time, then contraction mapping theorem is not applicable. Thus, it greatly restricts the application range of ILC. Besides, classical ILC hardly ever takes full advantage of system information and usually neglects the system dynamical characteristics. But in practical control system design, although we can't obtain accurate model of the system, we can build the nominal model, which means we can obtain partial information of the plant. Obviously, the controllers using known information are able to improve control performance and speed up convergence. Additionally, classical ILC takes contraction mapping theorem but not Lyapunov method as the key of design and analysis, which makes it difficult to incorporate with advanced nonlinear control methods, such as adaptive control, sliding mode control, NN control, fuzzy control and so on. Hence, it is necessary to consider the combination of above nonlinear control methods and the idea of ILC, and introduce the Lyapunov based stability analysis method into the learning convergence analysis. Inspired by above motivations, adaptive ILC (AILC) is developed.

1.2.2 Composite Energy Function Based Adaptive ILC

The first task of AILC is rightly to deal with locally Lipschitz continuous controlled object, and secondly, consider the systems uncertainties, including parameterized uncertainties and non-parameterized uncertainties. Take the following first-order system as example

$$\dot{x}(t) = f(x, t) + u(t) \tag{1.7}$$

If the expression of $f(x, t)$ is $f(x, t) = \theta(t)\xi(x)$, where $\theta(t)$ is unknown time-varying parameter that is independent of states, $\xi(x)$ is the nonlinear function of x, for example $\xi(x) = x^2$ or $\xi(x) = x\sin(x)$, then the (1.7) is called as parameterized uncertain system. On the contrary, if $f(x, t)$1.7 can't be decomposed as the product of a known function of states and an unknown parameter, Eq. (1.7) is referred as to non-parameterized system, for example, $f(x, t) = x^2 \sin(x \cos t)$. In nonlinear control theories, adaptive control and robust control are used to deal with above two kinds of uncertainties respectively. So AILC should not only handle above two kinds of uncertainties, but also succeed the advantage of ILC in achieving learning convergence in iteration domain. Meanwhile, the Lyapunov method of modern nonlinear control theories needs to be employed in the stability analysis of AILC.

French directly introduced adaptive control methodology when studying the learning problem for parameterized systems running in finite interval and used Lyapunov analysis method. The designed parameter adaptive learning law and Lyapunov function are as follows:

$$\dot{\hat{\theta}}_k(t) = q\xi(x)e_k(t), \ \ t \in [0, T] \tag{1.8}$$

$$V\left(\tilde{\theta}_k, t\right) = e_k^2(t) + \tilde{\theta}_k^2(t) \tag{1.9}$$

where, $\hat{\theta}_k(t)$ denotes the estimated value of $\theta(t)$ at the k-th iteration, $\tilde{\theta}_k(t) = \theta(t) - \hat{\theta}(t)$, $e_k(t) = x_k(t) - x_r(t)$, q is the parameter learning gain. It can be seen that differential-type parameter adaptive law (1.8) is exactly the same as that of adaptive control for each iteration in finite interval. But since the system runs in a finite interval, this method can't ensure the asymptotic convergence along time axis as adaptive control method. For this problem, French's solution was to link up the initial value and final value of the contiguous iterations, which is specified by

$$\hat{\theta}_k(0) = \hat{\theta}_{k-1}(T) \tag{1.10}$$

This method can be regarded as the transitional form of learning control and adaptive control. However, differential-type adaptive law can only estimate unknown constant parameter, so it is not suitable for the system (1.7) whose unknown parameter is time-varying. Moreover, this method works depending on the condition that the control system can guarantee the stability in time domain. For the plants that are difficult to design control systems in time domain, this method is not applicable.

Qu's team firstly studied the learning control problem of time-varying parametric systems and put forward the following parameter iterative learning law and Lyapunov functional in American Control Conference in 1995 [18]:

$$\hat{\theta}_k(t) = \hat{\theta}_{k-1}(t) + q\xi(x)e_k(t), \ t \in [0, T] \tag{1.11}$$

$$V\left(\tilde{\theta}_k, t\right) = \int_0^t \tilde{\theta}_k^2(\sigma)\mathrm{d}\sigma, \ t \in [0, T] \tag{1.12}$$

Based on this kind of idea, Xu and Qu designed a robust ILC algorithm by combining ILC and robust control [19] and demonstrated the stability condition using Lyapunov direct method, which guaranteed the global asymptotic stability by using variable structure control and the iterative convergence through estimating unknown parameter along iterative axis. Two control schemes complement each other. Whereafter, they solved the control problem for some classes of parameterized nonlinear systems by using this kind of integral-type Lyapunov performance index [20–22]. On the basis of summarizing previous result results, Xu proposed a kind of Composite Energy Function (CEF) design method which are given by [23]

$$E_k(t) = V(e_k(t)) + \int_0^t \tilde{\theta}_k^2(\sigma)\mathrm{d}\sigma \tag{1.13}$$

where, $V(e_k(t))$ is the standard Lyapunov function containing the quadratic term of tracking error. From (1.13), it can be seen that CEF contains not only the information of state tracking along time axis, but also the information of parameter learning performance along iteration axis. In other words, the CEF simultaneously considers the dynamical process in both time domain and iteration domain which enables us to obtain the stability for single run along time axis and the learning convergence of tracking error along iteration axis with the boundedness of all the closed-loop signals. The AILC design method based on CEF is a milestone in the development of ILC, it normalizes the main idea of controller design, stability and convergence analysis for AILC and provides an important reference to the ILC problem of various time-varying parameterized systems. Based on this design idea, Xu and other scholars carried out a series of theoretical research of AILC for various nonlinear systems and the AILC problems of many nonlinear systems.

Take the following parameterized dynamical system running in finite time interval $[0, T]$ repeatedly for example:

$$\dot{x}_k(t) = \theta(t)\xi(x_k) + u_k(t) \tag{1.14}$$

As mentioned above, $\theta(t)$ is unknown time-varying parameter, $\xi(x_k)$ is known continuous smooth function, tracking error id defined as $e_k(t) = x_k(t) - x_r(t)$, $t \in [0, T]$, then the control law for the k-th iteration can be designed as

$$u_k(t) = -Ke_k(t) + \dot{x}_r(t) - \hat{\theta}_k(t)\xi(x_k) \tag{1.15}$$

where, $K > 0$ is design parameter. According to the AILC design method, design adaptive iterative updating law for unknown time-varying parameter as

$$\begin{cases} \hat{\theta}_k(t) = \hat{\theta}_{k-1}(t) + q\xi(x_k)e_k(t) \\ \hat{\theta}_0(t) = 0, t \in [0, T] \end{cases} \tag{1.16}$$

According to Eq. (1.13), choose CEF as

$$E_k(t) = \frac{1}{2}e_k(t) + \frac{1}{2q}\int_0^t \tilde{\theta}_k(\sigma)\mathrm{d}\sigma \tag{1.17}$$

Employing CEF analysis method, it can be derived that

$$\Delta E_k(t) = E_k(t) - E_{k-1}(t) \le -\int_0^t (e_k(\sigma))^2\mathrm{d}\sigma < 0 \tag{1.18}$$

Furthermore, we can derive that

$$\lim_{k\to\infty}\int_0^T (e_k(\sigma))^2\mathrm{d}\sigma = 0 \tag{1.19}$$

Hence, as $k \to \infty$, the system state $x_k(t)$ converges to the reference signal $x_r(t)$ on $[0, T]$.

Xu's works on many problems of ILC improved greatly the relative researches and even initiated some works, which attracted much attention of peers. In [24], Xu investigated the ILC problem of uncertain time-varying systems, which considered two cases that unknown parameter was time-varying and time-invariant and designed difference-type and differential-type parameters for them respectively. Additionally, Xu discussed the problem that the desired reference trajectories vary with iterations as well. In [25], Xu mainly addressed the problem of initial condition for ILC, under the framework of Lyapunov analysis method, where they discussed the relation of five typical kinds of initial conditions and corresponding learning convergence conditions that carried out based on the AILC problem for a class of simple nonlinear time-varying parameterized system. Input nonlinearities are common in control problems. In [26] and [27], Xu designed AILC schemes for nonlinear systems with input saturation based on Lyapunov-like CEF method. In addition, for the nonlinear system with input uncertainty Xu put forward a kind of 'dual-loop' ILC scheme [28, 29], where 'loop 1' is intended to stabilize the nominal model of the system and 'loop 2' deals with input uncertainty through learning algorithm. On the basis of above results, Xu's team further studied the problem that unknown time-varying parameters also varied with iterations [30, 31]. To address this problem, they built the inner model of unknown time-varying parameter along iteration axis and described the change along iteration as an autoregressive process, then they designed corresponding high-order learning law for unknown parameter and control algorithm based on inner model and analyzed the learning convergence property of the control system by utilizing CEF method. In paper [32], Xu created a new CEF, named Barrier CEF (BCEF), by employing Barrier Lyapunov in CEF, and designed a new ILC scheme for a class of n-order SISO system with limited output by using backstepping technique. Here, they considered both parameterized and non-parameterized uncertainties, therein, non-parameterized uncertainty was handled through local Lipschitz condition and unknown time-varying parameter was estimated by difference-type learning algorithm, finally, the convergence of tracking errors was proven by using the BCEF under the alignment initial condition (i.e., $x_k(0) = x_{k-1}(T)$).

Prof. Zhongsheng Hou's research team of Beijing Jiaotong University obtained a series of research results for ILC [33–38]. They mainly investigated the ILC problem for discrete nonlinear systems [33, 34] and expanded the CEF based AILC design method to discrete nonlinear systems. In the design of adaptive learning laws for unknown parameters, they designed recursive least-squares method to adjust the learning gain along iterative axis. In their works, they also considered the problem of initial condition and iteration-varying desired reference trajectories. Moreover, they discussed the AILC problem for nonlinear parameterized systems with input saturation as well [35, 36], where they obtained the parameterized form by using parameter separation technique and further designed AILC (including feedback term and saturation adaptive learning term) and saturation difference updating laws for parameters. To prove the learning convergence of control schemes, in [35] and [36], they constructed time weighted Lyapunov-like CEF and Lyapunov–Krasovskii-like CEF respectively. In [37], they expanded the scheme in [36] to the control of brake process of high-speed trains which was described as a nonlinear parameterized system with speed lag and input saturation nonlinearity, whereafter, they designed AILC scheme for high-speed trains. In the latest results [38], they put forward a NN based adaptive terminal ILC method in which NN was used to approximate the initial states. In the adaptive learning law for neural weight, dead-zone model was employed to ensure that adaptation and learning are performed only if the terminal tracking error exceeds the predefined range.

Prof. Mingxuan Sun's team in Zhejiang Technical University deeply studied the nature of ILC and obtained a great deal of innovative results [39–46]. In the researches on AILC, they proposed a finite-time dead-zone ILC methods for several kinds of parameterized systems. To relax the requirement of identical initial condition, initial rectified attractor was introduced, which allowed the initial positions to be set arbitrarily without assuming the bound on the repositioning errors to be small enough. In controller design, they constructed a finite time-varying dead-zone that includes the proposed initial rectified attractor to drive the tracking error converge to the region defined by the dead-zone and achieve complete tracking in finite time interval. In [41], Sun and Liu put forward robust ILC based on time weighted Lyapunov-like method, where robust component was used to guarantee the boundedness of all closed-loop systems and ILC component was used to improve the tracking performance and achieve perfect tracking. In [42], Sun and Chen investigated the ILC problem for a class of SISO nonlinear non-minimum-phase systems, they firstly transformed the uncertain zero-dynamic of the non-minimum-phase system to asymptotically stable subsystem through redefining the output variable and then designed two controllers by using partially saturated and fully saturated ILC algorithms. To deal with unknown time-varying parameters, Sun's team came up with a new method [43, 44] which transformed the unknown time-varying parameter to unknown constant parameters by using Taylor expansion and designed differential-type adaptive learning law and alignment method to estimate unknown constant parameters. On this basis, they designed the AILC algorithm in which the hyperbolic tangent function was employed to deal with the influence of remainder term of Taylor expansion on tracking performance, meanwhile, restraining the chattering problem. Additionally, they introduced a convergent sequence to guarantee the learning convergence along iteration axis. In recent years, they studied ILC problems for error tracking systems [45, 46], where they considered different cases of unknown constant parameters, time-varying parameters and mixed (constant and time-varying) parameters, and designed AILC schemes based on Lyapunov-like method with non-saturated, partially saturated or completely saturated parameter learning laws. The proposed methods relaxed the requirements for initial positioning for ILC and allowed the initial values to be set arbitrarily.

The Prof. Chiang-Ju Chien's team in Taiwan Huafan University has devoted themselves to the study of ILC theory and published a great number of papers [47–59]. The creative works of Chiang-Ju Chien' team mainly include the following aspects. (1) In order to deal with identical initial condition of ILC, Chien presented a boundary layer function method. By employing a decreasing boundary layer function using exponent function, they introduced an auxiliary error variable by redefining the tracking error and imposed the zero initial error condition on the auxiliary error, thus relaxing the limitation of zero initial tracking error and allowing the initial states to be placed in an arbitrary position within the predefined range. Moreover, the property of boundary layer function makes it possible to replace the sign function with saturation function in the robust learning term design of some control schemes, which can smooth control signals in a certain degree and avoid the chattering problem when using sign function. (2) For uncertainties in the plants, they utilized fuzzy approximation technique and used fuzzy logic systems [48, 52], fuzzy NNs [50, 56, 57], Output-recurrent Fuzzy Neural Network (ORFNN) [53] to approximate the uncertainties, which transformed unknown functions to the parameterized form. Eventually, it facilitated the AILC design. (3) On the basis of Qu's works, they proposed difference-differential mixed type parameter adaptive learning law [50–53, 59] which is given by

$$(1-\gamma)\dot{\hat{\theta}}_k(t) = -\gamma\hat{\theta}_k(t) + \gamma\hat{\theta}_{k-1}(t) + q\xi(x)e_k(t) \tag{1.20}$$

where, $\gamma \in [0, 1]$ is adjustable parameter. It can be seen that for $\gamma = 0$, (1.20) changes to pure differential type adaptive learning law which coincides with (1.8); for $\gamma = 1$, (1.20) reduces to pure difference type adaptive learning law which is specified by (1.11); for $0 < \gamma < 1$, (1.20) is exactly the difference-differential mixed type. Obviously, (1.20) unifies adaptive learning laws (1.8) and (1.11), thus (1.8) and (1.11) become the special form of (1.20). This kind of parameter updating form is similar to the σ-modification method in adaptive control, and consequently it can enhance the robustness in a certain extent. Chien presented a specific discussion on this parameter adaptive learning law in [51]. Furthermore, in order to obtain learning convergence, Chien designed new index of estimation error in CEF for this parameter adaptive learning law. (4) They improved the proof process for a class of CEF-based stability analysis and added the discussion on dynamical performance except for the proof of boundedness of close-loop signals and learning convergence. Their works played an important role in the development of AILC. Except the above-mentioned works, they also investigated deeply the AILC problem for only output measurable nonlinear systems [54–57] and manipulator systems [58, 59].

The research team of Prof. Jun-min Li in Xidian University further improved the development of AILC in more kinds of nonlinear systems [60–73]. For a few classes of nonlinear parameterized systems, they used parameter separation technique and signal replacement method to reconstruct the system equation under the assumption of locally Lipschitz condition and designed differential-type and difference-type adaptive learning laws for unknown constant parameter and time-varying parameter respectively. The learning convergence of the control system in iteration domain is obtained through CEF analysis method [60, 61]. Further they expanded the above methods to time-delay systems [62–64] and designed AILC schemes after dealing with the time-delay functions by using Lyapunov–Krasovskii functional (L-K for short). In their works, for strict-feedback nonlinear systems, a salient feature of the controlled object is that time-varying nonlinear parameterized uncertainties are matched, this is decided by the characteristic of backstepping method. For the strict-feedback systems that don't satisfy the matched condition, i.e., time-varying uncertainties are un-matched, they referred to the Sun's method [43, 44] and used Fourier series expansion to transform the unknown time-varying parameters to constant parameters, which makes it possible to carry out the controller design by using backstepping technique [66, 67, 69, 70]. For the remainder term, they also employed the hyperbolic tangent function and a convergent sequence to guarantee the learning convergence along iteration axis [66–72]. In addition, they also conducted the research on the AILC problem for multi-agent systems [71, 72]. In [71] they used fuzzy logic method to approximate the unknown dynamics of the follower agent and designed differential-difference mixed type adaptive learning law. Whereas, differential type adaptive learning law was applied in [72].

Except for the above research teams, other scholars also studied the AILC problem for different kinds of nonlinear uncertain systems using similar idea and designed differential-type, difference-type and mixed type adaptive learning laws according to different situations [74–82]. Additionally, NN is another important approximation tool besides fuzzy approximation technique. Therefore, it is necessary and significative to introduce neural approximation technique into AILC design. In [83] and [84], the application of wavelet in ILC was discussed. Actually, similar to the parameter adaptive technique above, adaptive NN control method can be combined with ILC. In [85], Jiang proposed a kind of distributed NN structure which was composed of a series of local NNs and it approximated the unknown function on the finite time interval in the form that each local NN approximated the unknown function on a small fixed interval. Li further proved the realizability of this type NN by the way of mathematical analysis [85]. The distinguishing characteristic of this type NN is that the approximation accuracy depends on the number of local NNs. From the perspective of ILC, Sun proposed a kind of time-varying NN [86, 87] whose optimal weight was time varying and proved the convergence of approximation error using least square method. By using time-varying NN, they designed AILC schemes for several classes of systems [88–90] and used difference-type adaptive updating law to estimate the optimal weight. For nonlinear parameterized systems, Li relaxed the assumption of local Lipschitz condition and proposed a new iterative NN. The basic idea was that: firstly, estimating the unknown time-varying parameter via adaptive iterative learning law, and then taking the estimated value and state information as the input of NN to approximate the unknown function with time-varying parameter. By using this kind iterative NN, Li conducted research on several classes of strict-feedback systems and designed difference-type, differential-type, mixed type adaptive learning laws for unknown time-varying parameter, NN weight, unknown upper bound respectively. On this basis, they designed adaptive iterative learning controller containing NN learning term and robust term by making use of backstepping technique, where they introduced tracking-differentiator to obtain the differential signal of virtual control instead of differentiating it directly. But this method remained to be discussed further, because the usage of tracking-differentiator implied introducing a dynamical system into the original closed-loop system, but the influence of tracking-differentiator on the original system was not considered. It is worth pointing out that each research team in the field of ILC has their own special skills, but it doesn't mean they develop independently along their own research directions, on the contrary, they will learn from each other and improve the development of ILC theory.

In a word, the design methods for Lyapunov-like CEF based AILC have witnessed a great progress and produced a series of research results through the efforts of learning control scholars over the past decades. However, compared with other control theories that have been developed for several decades, the development of AILC has not matured. Particularly, the research on AILC for nonlinear systems with unknown input nonlinearity characteristics and time-delay needs further improvement.

1.2.3 2-D Theory Based ILC

When ILC system is running iteratively, it presents two kinds of dynamical process: time domain and iteration domain. In other words, it is in nature a two-dimensional dynamical process. This characteristic enlightened some researchers to apply 2-D methodology to ILC. The basic idea of 2-D theory based ILC is to describe the ILC system as 2-D system (generally 2-D Roesser model) and then use 2-D system theory to obtain the necessary and sufficient conditions of learning convergence. This method is very effective, simple and feasible. It not only inherits the advantages of classical ILC, but also reduces the limitations of convergence condition. Therefore, in the past decades, many scholars conducted the researches on 2-D theory based ILC and got a great deal of results [91–99]. However, 2-D theory based ILC is based on 2-D Roesser linear model. So one notable drawback is that it is only applicable to linear systems or the nonlinear systems that can be linearized. Therefore, the researches on modelling methods based on 2-D theory and 2-D theory based ILC for nonlinear systems needs to be further studied.

In the previous section, we summarize briefly the development of ILC theory. Through the development in the past decades, there have been a plenty of research results. But it is worth pointing out that there are still many topics for ILC problem, such as initial value problem, application research, frequency-domain analysis method and so on. Because these problems are out of the scope of this book, we will not discuss them in detail.

1.3 Main Contents of the Book

Based on summarizing and studying the previous results, this book presents a new kind of AILC design method and systematically solve a series of AILC design problems for nonlinear time-varying systems with input nonlinearities and time delays. The main contents of this book are as follows.

Chapter 1 presents the research background and significance of this book and a summary of the development of ILC. There into, the development and research status of AILC are discussed emphatically, which takes the works of several research teams as the main line and summarize the basic idea, characteristic and research actuality of ILC.

In Chap. 2, a novel adaptive iterative learning control scheme is proposed for a class of nonlinear time-varying parameterized with unknown dead-zone and time-varying delays. Firstly, a new dead-zone model with time-varying slopes is established, which has a simple form but extensive presentation. After compensating for the time delay term by L-K functional, the system is re-parameterized by using Young's inequality. On this basis, the adaptive iterative learning controller is designed. In the design, the boundary layer function is introduced to relax the limitation of identical initial condition for ILC, and the possible singularity problem is avoided by utilizing the hyperbolic tangent function.

In Chap. 3, the study on the AILC problem for a class of uncertain non-parameterized nonlinear time-varying systems with unknown dead-zone and time-varying state delays is carried out, where two time-varying NNs are used to approximate time-varying uncertainties and robust learning term is designed to deal with the NN approximation errors, which conquers the difficulty of time-varying uncertainties. The Lyapunov-like CEF analysis is presented to get the boundedness of system signals, the convergence of tracking errors and dynamical performance.

In Chap. 4, An AILC scheme is proposed for a class of nonlinear systems with unknown control direction, time-varying state delays and backlash-like hysteresis input by synthetically using Nussbaum type function method, time-varying NNs and robust adaptive control technique. The control gain is estimated by using Nussbaum type function method and a new CEF satisfying initial resetting is constructed to overcome the difficulty in stability analysis arouse by the usage of Nussbaum type function. For the first time, integral type Lyapunov function is utilized in the AILC design, which avoids the possible singularity problem by cooperation with hyperbolic tangent function.

In Chap. 5, a deep investigation is carried out for the AILC problem of nonlinear systems with states un-measurable and two kinds of observer-based AILC schemes are proposed, which overcomes the design difficulty from time delays, input saturation and the absence of measurement of states. In the state observer-based AILC scheme, state observer is designed on the basis of NN compensation. The observer gain is determined by using LMI method, which avoids the SPR condition. In the error observer-based AILC scheme, a new error variable is defined by introducing filter, which removes the identical initial condition and SPR condition. A new robust learning term is chosen by using hyperbolic tangent function and series convergent sequence to guarantee the learning convergence.

In Chap. 6, the research for plants with unmeasurable states and unknown control gain is carried out by taking manipulator as investigation object, which successfully overcomes the design difficulty from unknown control gain, absence of measurement of states and output delays. During the design the observer gain is determined by using LMI method and hyperbolic tangent function and convergent sequence are employed to design the robust term for purposed of guaranteeing the learning convergence.

The researches on the control problem for nonlinear systems with input nonlinear characteristics and time-delay have both theoretical and practical meaning. This book explores the researches on above-mentioned problems, in the future we can carry on a further study from the following two aspects:

(1) Further research on the development of the proposed AILC design methods in other kinds of systems, for example, multi-input multi-output nonlinear systems, distributed interconnected large-scale systems, non-affine nonlinear systems, discrete systems, fractional-order systems.
(2) Further research on the combination of AILC and other novel nonlinear control methods and the improvement in theory and applications.

References

1. Hsue-shen Tsien, Jian Song. Engineering Cybernetics (The Third Edition) [M]. Beijing: Science Press, 2011.
2. Fu K. Learning control systems and intelligent control systems: An intersection of artificial intelligence and automatic control[J]. IEEE Transactions on Automatic Control, 1971, 16(1): 70–72.
3. Uchiyama M. Formation of high-speed motion pattern of a mechanical arm by trial[J]. Transactions of the Society of Instrumentation and Control Engineers, 1978, 14(6):706–712.
4. Arimoto S, Kawamura S, Miyazaki F. Bettering operation of robots by learning[J]. Journal of Robotic Systems, 1984, 1(2): 123–140.
5. Xu Jian-Xin, Hou Zhong-Sheng. On Learning Control: The State of the Art and Perspective [J]. ACTA Automatica Sinica, 2005, 31(6): 943–955.
6. Xu J X, Lee T H, Zhang H W. Analysis and comparison of iterative learning control schemes[J]. Engineering Applications of Artificial Intelligence, 2004, 17(6): 675–686.
7. Bien Z, Huh K M. Higher-order iterative learning control algorithm [J]. IEE Proceedings D (Control Theory and Applications), IET Digital Library, 1989, 136(3): 105–112.
8. Xu J X, Tan Y. Robust optimal design and convergence properties analysis of iterative learning control approaches[J]. Automatica, 2002, 38(11): 1867–1880.
9. Norrlöf M. Comparative study on first and second order ILC-frequency domain analysis and experiments [C]. Proceedings of the 39th IEEE Conference on Decision Control, Sydney, Australia, 2000: 3415–3420.
10. Jian-Xin Xu, Ying Tan. Linear and nonlinear iterative learning control [M]. Berlin Heidelberg: Springer-Verlag, 2003.
11. Amann N, Owens D H, Rogers E. Predictive optimal iterative learning control[J]. International Journal of Control, 1998, 69(2): 203–226.
12. Wang Y, Dassau E, Doyle III F J. Closed-loop control of artificial pancreatic β-cell in type 1 diabetes mellitus using model predictive iterative learning control[J]. IEEE Transactions on Biomedical Engineering, 2010, 57(2): 211–219.
13. Shi J, Zhou H, Cao Z, et al. A design method for indirect iterative learning control based on two-dimensional generalized predictive control algorithm[J]. Journal of Process Control, 2014, 24(10): 1527–1537.
14. Wang D. On the D-type and P-type ILC designs and anticipatory approach[J]. International Journal of Control, 2000, 73(10): 890–901.
15. Sun M, Wang D. Anticipatory iterative learning control for nonlinear systems with arbitrary relative degree[J]. IEEE Transactions on Automatic Control, 2001, 46(5): 783–788.

16. Huang D, Xu J X, Li X, et al. D-type anticipatory iterative learning control for a class of inhomogeneous heat equations[J]. Automatica, 2013, 49: 2397–2408.
17. Xu J X, Tan Y. On the P-type and Newton-type ILC schemes for dynamic systems with non-affine-in-input factors[J]. Automatica, 2002, 38(7): 1237–1242.
18. Ham C, Qu Z H, Kaloust J H. Nonlinear learning control for a class of nonlinear systems based on Lyapunov's direct method [C]. Proc. 1995 IEEE American Control Conference, Seattle, 1995: 3024–3028.
19. Xu J X, Qu Z H. Robust iterative learning control for a class of nonlinear systems[J]. Automatica, 1998, 34(8): 983–988.
20. Xu J X, Badrinath V. Adaptive robust iterative learning control with dead zone scheme[J]. Automatica, 2000, 36(1): 91–99.
21. Qu Z H, Xu J X. Asymptotic learning control for a class of cascaded nonlinear uncertain systems[J]. IEEE Transactions on Automatic control, 2002, 47(8): 1369–1376.
22. Ham C, Qu Z, Kaloust J. Nonlinear learning control for a class of nonlinear systems[J]. Automatica, 2001, 37(3): 419–428.
23. Xu J X, Tan Y. A composite energy function-based learning control approach for nonlinear systems with time-varying parametric uncertainties[J]. IEEE Transactions on Automatic Control, 2002, 41(7): 1940–1945.
24. Xu J X, Xu J. On iterative learning from different tracing tasks in the presence of time-varying uncertainties[J]. IEEE Transactions on Systems, Man, and Cybernetics-Part B: Cybernetics, 2004, 34(1): 589–596.
25. Xu J X, Yan R. On initial conditions in iterative learning control[J]. IEEE Transactions on Automatic Control, 2005, 50(9): 1349–1355.
26. Xu J X, Tan Y, Tong-Heng Lee. Iterative learning control design based on composite energy function with input saturation [C]. Proceedings of the American Control Conference, Denver, Colorado, 2003: 5129–5134.
27. Xu J X, Tan Y, Lee T H. Iterative learning control design based on composite energy function with input saturation[J]. Automatica, 2004, 40(8): 1371–1377.
28. Huang D Q, Tan Y, Xu J X. A dual-loop iterative learning control for nonlinear systems with hysteresis input uncertainty [C]. IEEE International Conference on Control and Automation, Christchurch, New Zealand, 2009: 1116–1121.
29. Tan Y, Dai H, Huang D, et al. Unified iterative learning control schemes for nonlinear dynamic systems with nonlinear input uncertainties[J]. Automatica, 2012, 48(12): 3173–3182.
30. Yin C K, Xu J X, Hou Z S. An ILC scheme for a class of nonlinear continuous-time systems with time-iteration-varying parameters subject to second-order internal model[J]. Asian Journal of Control, 2011, 13(1): 126–135.
31. Yin C K, Xu J X, Hou Z S. A high-order internal model based iterative learning control scheme for nonlinear systems with time-iteration-varying parameters[J]. IEEE Transactions on Automatic Control, 2010, 55(11): 2665–2670.
32. Jin X, Xu J X. Iterative learning control for output-constrained systems with both parametric and nonparametric uncertainties[J]. Automatica, 2013, 49(8): 2508–2516.
33. Chi R, Hou Z, Xu J. Adaptive ILC for a class of discrete-time systems with iteration-varying trajectory and random initial condition[J]. Automatica, 2008, 44(8): 2207–2213.
34. CHI R H, SUI S L, HOU Z S. A new discrete-time adaptive ILC for nonlinear systems with time-varying parametric uncertainties[J]. Acta Automatica Sinca, 2008, 34(7): 805–808.
35. Zhang R, Hou Z, Ji H, et al. Adaptive iterative learning control for a class of non-linearly parameterised systems with input saturations[J]. International Journal of Systems Science, 2016, 47(5): 1084–1094.
36. Zhang R, Hou Z, Chi R H, et al. Adaptive iterative learning control for nonlinearly parameterised systems with unknown time-varying delays and input saturations[J]. International Journal of Control, 2015, 88(6): 1133–1141.
37. Ji H, Hou Z, Zhang R. Adaptive iterative learning control for high-speed trains with unknown speed delays and input saturations[J]. IEEE Transactions on Automation Science and Engineering, 2015, 13(1): 260–273.

38. Liu Y, Chi R H, Hou Z S. Neural network state learning based adaptive terminal ILC for tracking iteration-varying target points[J]. International Journal of Automation and Computing, 2015, 12(3): 266–272.
39. Ming-Xuan Sun, Xiong-Xiong He, Li Yu. Iterative learning controller designs: a finite time dead-zone approach [J]. Control Theory & Applications, 2007, 24(3): 349–355.
40. Hua-ying Xie, Ming-Xuan Xie. Design of iterative learning controllers with finite-time dead-zone modification[J]. Control Theory & Applications, 2009, 26(11): 1225–1231.
41. Li Liu, Minx-Xuan Sun. Robust learning control algorithms for uncertain time-varying systems [J]. Control Theory & Applications, 2010, 27(3): 323–328.
42. Bing-yu Chen, Ming-xuan Sun, Sheng Zhu. Output-redefinition-based iterative learning control for nonlinear non-minimum phase systems[J]. Control Theory & Applications, 2010, 27(7): 948–952.
43. Sheng Zhu, Ming-xuan Sun, Xiong-xiong He. Iterative Learning Control of Strict-feedback Nonlinear Time-varying Systems[J]. ACTA AUTOMATICA SINICA, 2010, 36(3): 454–458.
44. Sheng Zhu, Ming-xuan Sun, Xiong-xiong He. Iterative Learning Control for a Class of Nonlinear Systems with Input Backlash[J]. ACTA AUTOMATICA SINICA, 2011, 37(8): 1014–1017.
45. Ming-Xuan SUN, Qiu-Zhen YAN. Error tracking of iterative learning control systems[J]. Acta Automatica Sinca, 2013, 39(3): 251–262.
46. Mingxuan Sun, Qiu-Zhen YAN. Error-tracking iterative learning control with state constrained for nonparametric uncertain systems [J]. Control Theory & Applications, 2015, 32(7): 895–901.
47. Chien C J. An adaptive PID-type iterative learning controller for nonlinear systems with non-repeatable control tasks[J]. Journal of Chinese Institute of Engineers, 2006, 29(2): 279–287.
48. Chien C J, Hsu C T, Yao C Y. Fuzzy system-based adaptive iterative learning control for nonlinear plants with initial state errors[J]. IEEE Transactions on Fuzzy Systems, 2004, 12(5): 724–732.
49. Wang Y C, Chien C J, Teng C C. Direct adaptive iterative learning control of nonlinear systems using an output-recurrent fuzzy neural network[J]. IEEE Transactions on Systems, Man, and Cybernetics-Part B: Cybernetics, 2004, 34(4): 1348–1359.
50. Wang Y C, Chien C J, Lee D T. A hybrid adaptive scheme of fuzzy-neural iterative learning controller for nonlinear dynamic systems[J]. International Journal of Fuzzy Systems, 2005, 7(4): 147–157.
51. Tayebi A, Chien C J. A unified adaptive iterative learning control framework for uncertain nonlinear systems[J]. IEEE Transactions on Automatic Control, 2007, 52(10): 1097–1103.
52. Chien C J. A combined adaptive law for fuzzy iterative learning control of nonlinear systems with varying control tasks[J]. IEEE Transactions on Fuzzy Systems, 2008, 16(1): 40–51.
53. Wang Y C, Chien C J. Decentralized adaptive fuzzy neural iterative learning control for nonaffine nonlinear interconnected systems[J]. Asian Journal of Control, 2011, 13(1): 94–106.
54. Chien C J, Yao C Y. An output-based adaptive iterative learning controller for high relative degree uncertain linear systems[J]. Automatica, 2004, 40(1): 145–153.
55. Chien C J, Yao C Y. Iterative learning of model reference adaptive controller for uncertain nonlinear systems with only output measurement[J]. Automatica, 2004, 40(5): 855–864.
56. Wang Y C, Chien C J. An observer-based adaptive iterative learning control using filtered-FNN design for robotic systems[J]. Advances in Mechanical Engineering, 2014, 6: 471418.
57. Wang Y C, Chien C J, Er M J. An observer-based model reference adaptive iterative learning controller for MIMO nonlinear systems[C]. 11th IEEE International Conference on Control & Automation, Taiwan, 2014: 1168–1173.
58. Tayebi A. Adaptive iterative learning control for robot manipulators[J]. Automatica, 2004, 40(7): 1195–1203.
59. Chien C J, Tayebi A. Further results on adaptive iterative learning control of robot manipulators[J]. Automatica, 2008, 44(3): 830–837.
60. Jun-min Li, Yun-ping Sun, Yun Liu. Hybrid adaptive iterative learning control of non-uniform trajectory tracking[J]. Control Theory & Applications, 2008, 25(1): 100–104.

61. Yun-ping Sun, Jun-min Li, Jiang-an Wang. Adaptive learning control of nonlinear systems with iteration-varying trajectory[J]. Systems Engineering and Electronics, 2009, 31(7): 1715–1719.
62. Jun-min Li. Adaptive iterative learning control for nonlinearly parameterized systems with time-varying delays[J]. Acta Mathematica Scientia, 2011, 31A(3): 682–290.
63. Jun-min Li, Yuan-liang Wang, Xin-min Li. Adaptive iterative learning control for nonlinear parameterized-systems with unknown time-varying delays[J]. Control Theory & Applications, 2011, 28(6): 861–868.
64. Chen W, Zhang L. Adaptive iterative learning control for nonlinearly parameterized systems with unknown time-varying delays[J]. International Journal of Control, Automation and Systems, 2010, 8(2): 177–186.
65. Chen W, Li J, Li J. Practical adaptive iterative learning control framework based on robust adaptive approach[J]. Asian Journal of Control, 2011, 13(1): 85–93.
66. Zhang C L, Li J M. Adaptive iterative learning control for nonlinear time-delay systems with periodic disturbances using FSE-neural network[J]. International Journal of Automation and Computing, 2011, 8(4): 403–410.
67. Li D, Li J M. Adaptive iterative learning control for nonlinearly parameterized systems with unknown time-varying delay and unknown control direction[J]. International Journal of Automation and Computing, 2012, 9(6): 578–586.
68. Zhang C, Li J. Adaptive iterative learning control for nonlinear pure-feedback systems with initial state error based on fuzzy approximation[J]. Journal of the Franklin Institute, 2014, 351(3): 1483–1500.
69. Zhang C L, Li J M. Adaptive iterative learning control of non-uniform trajectory tracking for strict feedback nonlinear time-varying systems[J]. International Journal of Automation and Computing, 2014, 11(6): 621–626.
70. Zhang C L, Li J M. Adaptive iterative learning control of non-uniform trajectory tracking for strict feedback nonlinear time-varying systems with unknown control direction[J]. Applied Mathematical Modelling, 2015, 39(10): 2942–2950.
71. Li J M, Li J S. Adaptive fuzzy iterative learning control with initial-state learning for coordination control of leader-following multi-agent systems[J]. Fuzzy Sets and Systems, 2014, 248: 122–137.
72. Li J S, Li J M. Coordination control of multi-agent systems with second-order nonlinear dynamics using fully distributed adaptive iterative learning[J]. Journal of the Franklin Institute, 2015, 352: 2441–2463.
73. Li J, Li X, Xing K. Hybrid adaptive iterative learning control of non-uniform trajectory tracking for nonlinear time-delay systems[C]. Proceedings of the 26th Chinese Control Conference, Zhangjiajie, China, 2007: 515–519.
74. Jiang P, Chen H, Bamforth L C A. A universal iterative learning stabilizer for a class of MIMO systems[J]. Automatica, 2006, 42(6): 973–981.
75. Ding J, Yang H. Adaptive iterative learning control for a class of uncertain nonlinear systems with second-order sliding mode technique[J]. Circuits, Systems, and Signal Processing, 2014, 33(6): 1783–1797.
76. Fan L. Iterative learning and adaptive fault-tolerant control with application to high-speed trains under unknown speed delays and control input saturations[J]. IET Control Theory & Applications, 2014, 8(9): 675–687.
77. Marino R, Tomei P. An iterative learning control for a class of partially feedback linearizable systems[J]. IEEE Transactions on Automatic Control, 2009, 54(8): 1991–1996.
78. Li X D, Xiao T F, Zheng H X. Adaptive discrete-time iterative learning control for non-linear multiple input multiple output systems with iteration-varying initial error and reference trajectory[J]. IET Control Theory & Applications, 2011, 5(9): 1131–1139.
79. Li X D, Tommy W S, Cheng L L. Adaptive iterative learning control of non-linear MIMO continuous systems with iteration-varying initial error and reference trajectory[J]. International Journal of Systems Science, 2013, 44(4): 786–794.
80. Meng D, Jia Y, Du J, et al. Robust iterative learning control design for uncertain time-delay systems based on a performance index[J]. IET Control Theory & Applications, 2010, 4(5): 759–772.

81. Bouakrif F. Iterative learning control for strictly unknown nonlinear systems subject to external disturbances[J]. International Journal of Control, Automation and Systems, 2011, 9(4): 642–648.
82. Sun L, Wu T. Decentralized adaptive iterative learning control for interconnected systems with uncertainties[J]. Journal of Control Theory and Applications, 2012, 10(4): 490–496.
83. Xu J X, Yan R. Constructive learning control based on function approximation and wavelet [C]. 43rd IEEE Conference on Decision and Control, Atlantis, Paradise Island, Bahamas, 2004: 4952–4957.
84. Shan Liu, Tie-jun Wu. Robust iterative learning control using wavelet approximation for nonlinear plants [J]. Acta Automatica Sinica, 2004, 30(2): 270–276.
85. Jiang P, Li Z, Chen Y. Iterative learning neural network control for robot learning from demonstration[J]. Control Theory & Applications, 2004,21(3): 447–452.
86. Sun M X. Iterative learning neurocomputing [C]. 2009 International Conference on Wireless Networks and Information Systems, Shanghai, China, 2009: 158–161.
87. Sun M X. Time-varying neurocomputing: An iterative learning perspective [C]. Proceedings of Intelligent Computing Theories and Applications- 8th International Conference, Huangshan, China, 2012: 18–26.
88. Hua G, Sun M. Neural networks iterative learning control: a terminal sliding mode approach [C]. Proceedings of the 7th World Congress on Intelligent Control and Automation, Chongqing, China, 2008: 3119–3124.
89. Wei-li Yan, Ming-xuan Sun. Time-varying neural networks based indirect adaptive ILC for discrete-time varying nonlinear systems [C]. Proceedings of the 29th Chinese Control Conference, Beijing, China, 2010: 2060–2065.
90. Sheng Zhu, Ming-xuan Sun. Iterative learning control of a class of nonlinear systems with unknown input dead-zone[J]. Control and Decision, 2009, 24(1): 96–100.
91. Meng D, Jia Y, Du J, et al. Robust discrete-time iterative learning control for nonlinear systems with varying initial state shifts[J]. IEEE Transactions on Automatic Control, 2009, 54(11): 2626–2631.
92. Meng D, Jia Y, Du J, et al. Necessary and sufficient stability condition of LTV iterative learning control systems using a 2-D approach[J]. Asian Journal of Control, 2011, 13(1): 25–37.
93. Meng D, Jia Y, Du J. Robust ILC with iteration-varying initial state shifts: a 2D approach[J]. International Journal of Systems Science, 2015, 46(1): 1–17.
94. Fang Y, Chow T W S. 2-D analysis for iterative learning controller for discrete-time systems with variable initial conditions[J]. IEEE Transactions on Circuits and Systems: I: Fundamental Theory and Applications, 2003, 50(5): 722–727.
95. Kurek J E, Zaremba M B. Iterative learning control synthesis based on 2-D system theory[J]. IEEE Transactions on Automatic Control, 1993, 38(1): 121–125.
96. Wang L, Mo S, Zhou D, et al. Robust design of feedback integrated with iterative learning control for batch processes with uncertainties and interval time-varying delays[J]. Journal of Process Control, 2011, 21(7): 987–996.
97. Liu X, Kong X. Nonlinear fuzzy model predictive iterative learning control for drum-type boiler-turbine system[J]. Journal of Process Control, 2013, 23(8): 1023–1040.
98. Cichy B, Gałkowski K, Rogers E. 2D systems based robust iterative learning control using noncausal finite-time interval data[J]. Systems & Control Letters, 2014, 64: 36–42.
99. Liu Y, Jia Y. Robust formation control of discrete-time multi-agent systems by iterative learning approach[J]. International Journal of Systems Science, 2015, 46(2): 625–633.

Chapter 2
AILC of Parameterized Nonlinear Time-Delay Systems

2.1 Introduction

In control field, a broad category of plants can be modeled as parametric dynamic systems or transformed to parametrized form through some technical operations. The design problems of parameterized systems occupy an important position in control theories, the scholars studying all kinds of control theories proposed various control schemes for parametric systems. In general, if the unknown system parameters are time-invariant, adaptive control methods can be used to estimate them and Lyapunov method is applied to obtain asymptotic convergence. Conversely, if unknown parameters are time-varying variables, it is needed to take advantage of AILC method to design the control systems.

In practical control systems, time delay is a common physical phenomenon. The existence of time delays has a negative impact on the system performance, in the worst case, it will even destroy the system stability. Therefore, the research on the control problem for time-delay systems has great theoretical significance and application value. Because of the challenge in theoretical design and demand in practice, the issue of control system design for time-delay systems has drawn much attention in control community and a great deal of effective solutions have been put forward [1–7]. Most of these results are obtained by using control design methods in time domain and the results for ILC are relatively less in comparison. Chen, Meng and Sun et al. designed ILC algorithms for time-delay systems under the framework of contraction mapping theory and 2-D theory [8–11]. The research teams of Li [12–18] and Hou [19, 20] investigated the AILC design problems for time-delay systems by using CEF method. Wherein, the References [15, 18] and [15] presents AILC schemes for nonlinear systems with known delays. In the situation of unknown time delays, the L-K [21] is an effective design tool. For a large class of parameterized systems with unknown time-varying delays, Li et al. dealt with the impact of unknown time-varying delays by using L-K functional and designed AILC schemes on the basis of signal replacement method [12–16]. Based on the same idea, Hou et al. proposed AILC schemes for a class of nonlinear parameterized systems and high-speed train

J. Wei et al., *Iterative Learning Control for Nonlinear Time-Delay System*,
https://doi.org/10.1007/978-981-19-6317-9_2

dynamical systems in parameterized form [19, 20]. To carry out the analysis based on CEF, the above results all require identical initial condition, which is a common shortcoming of their work.

Non-smooth and nonlinear characteristics such as dead-zone, hysteresis, saturation and backlash, are common in practical control systems. There into, dead-zone is one of the most important non-smooth nonlinear characteristics in many industrial motion control systems. The existence of dead-zone can severely impact system performances. It gives rise to design difficulty of controller. Therefore, the effect of dead-zone has been taken into consideration and drawn much attention in the control community for a long time [22–32]. To handle the problem of unknown dead-zone in control system design, an immediate method is to construct an inverse model of dead-zone and compensate for its influence in the controller [22]. The continuous and discrete inverse models of dead-zone were established in [23] and [24] respectively. When there is no priori knowledge of dead-zone to build inverse model, we have to directly model the dead-zone characteristic and compensate for dead-zone model in the controller design. Wang et al. established linear model with same slopes for dead-zone in [25]. Zhang et al. built a general form model of dead-zone with wide generality which can be transformed once more by using mean value theorem in design [3, 26, 27]. Other scholars basically adopt the above approaches in their researches [28, 29]. In researches on ILC, the results considering dead-zone are relatively less. The references [30–32] present the studies of ILC problem for systems with dead-zone input and obtain the convergence of control system using contraction mapping theorem. For the CEF based AILC problem of the systems with dead-zone input, only Zhu et al. discussed it in [33], and they adopted the constant slope dead-zone model in [25].

In this chapter, we will conduct the research on the AILC problem for a class of nonlinear parameterized systems with dead-zone input and unknown time-varying delays. To the best of our knowledge, there is no result discussing it in the literature at present stage.

2.2 Problem Formulation and Preliminaries

2.2.1 Problem Formulation

Consider a class of nonlinear time varying systems with unknown time-varying time-delays and dead-zone running on a finite time interval $[0, T]$ repeatedly which is given by

$$\begin{cases} \dot{x}_{i,k}(t) = x_{i+1,k}(t), i = 1, \ldots, n-1 \\ \dot{x}_{n,k}(t) = f\big(X_k(t), X_{\tau,k}(t), \boldsymbol{\theta}(t)\big) + g(t)u_k(t) + d(t) \\ y_k(t) = x_{1,k}(t), u_k(t) = D(v_k(t)), t \in [0, T] \\ x_{i,k}(t) = \varpi_i(t), t \in [-\tau_{\max}, 0), i = 1, \ldots, n \end{cases} \tag{2.1}$$

where, t is the time, $k \in \mathbf{N}$ denotes the times of iteration ($\mathbf{N}$ is the integer set); $y_k(t) \in \mathbf{R}$ and $x_{i,k}(t) \in \mathbf{R}$ $(i = 1, \ldots, n)$ are the system output and states, respectively; $\boldsymbol{X}_k(t) \triangleq \left[x_{1,k}(t), \ldots, x_{n,k}(t)\right]^{\mathrm{T}}$ is the state vector; $\tau(t)$ is unknown time-varying delay of states, $x^{\tau}_{i,k} \triangleq x_{i,k}(t - \tau(t)), i = 2, \ldots, n, \boldsymbol{X}_{\tau,k}(t) = \left[x^{\tau}_{1,k}(t), \ldots, x^{\tau}_{n,k}(t)\right]^{\mathrm{T}}$; $f(\cdot, \cdot, \cdot)$ is unknown smooth continuous function; $g(t)$ is the unknown continuous time-varying gain of the system input; $\theta(t)$ is an unknown continuous time-varying parameter vector; $d(t)$ is unknown external disturbance. $\varpi_i(t)$ $(i = 1, \ldots, n)$ denotes initial functions for delayed states; $v_k(t) \in R$ is the control input and the actuator nonlinearity $D(v_k(t))$ presents the dead-zone characteristic.

Remark 2.1 One of the main tasks of control science is to design a suitable controller for the controlled object such that the closed-loop system can be stabilized or track the desired reference trajectory under the requirements of some performance indices, namely, regulation and tracking problem. In order to design a good control system, it is necessary to acquire the knowledge about the motion laws of controlled object, actuator and all the elements of the system as fully as possible. The so-called motion law refers to the corresponding motion that the system element inevitably generates under certain internal and external conditions. There exists fixed causal relationship between internal-external conditions and the motions of system elements, which mostly could be presented by mathematical expressions. This is the mathematical description of the motion laws of control systems. In control systems, the common physical phenomenons are nothing more than electricity, magnetism, optics, conduction of heat and the motion of rigid body, elastomer and fluid, the motion laws of these physical quantities could be determined by the fundamental laws of electromagnetism, optics, thermodynamics and mechanics, for example, Kirchhoff's law in electromagnetism, Maxwell's equations, Fourier's law in thermodynamics, the second law of thermodynamics, Fermat's principle in optics, Newton's laws and their variants in mechanics. These physical laws are generally described by differential equations, integral equations and algebraic equations. The differential equations similar to (2.1) describe the controlled object in this chapter, it has a broad representation and represents the mathematical model for a lot of dynamical process. This kind of form in (2.1) is known as Brunovsky canonical form.

Control Objective: for a given desired trajectory $y_d(t)$, design an AILC scheme, such that the output $y_k(t)$ of (2.1) track $y_d(t)$ accurately enough, and all the close-loop signals are bounded.

For system (2.1), define the desired trajectory vector as $\boldsymbol{X}_d(t) = \left[y_d(t), \dot{y}_d(t), \ldots, y_d^{(n-1)}(t)\right]^{\mathrm{T}}$ and tracking error vector as $\boldsymbol{e}_k(t) = \left[e_{1,k}, e_{2,k}, \ldots, e_{n,k}\right]^{\mathrm{T}} = \boldsymbol{X}_k(t) - \boldsymbol{X}_d(t)$. Then the control objective can be described as: designing an AILC algorithm, such that the elements of tracking error vector $\boldsymbol{e}_k(t)$ converge to a small neighborhood of the origin as $k \to \infty$, i.e., $\lim_{k\to\infty} \|e_k(t)\| \leq \varepsilon_{e\infty}$ with $\varepsilon_{e\infty}$ as a small positive error tolerance.

To facilitate control system design, make the following reasonable assumptions.

Assumption 2.1 The unknown state time-varying delays $\tau(t)$ satisfy: $0 \le \tau(t) \le \tau_{\max}$, $\dot{\tau}(t) \le \kappa < 1$, where $\tau_{\max}$ and κ are unknown positive constants.

Assumption 2.2 The unknown smooth functions $f(\cdot,\cdot,\cdot)$ satisfy the inequality

$$\begin{aligned} &\left| f\big(\boldsymbol{X}_k, \boldsymbol{X}_{\tau,k}, \boldsymbol{\theta}(t)\big) - f\big(\boldsymbol{X}_d, \boldsymbol{X}_{d,\tau}, \boldsymbol{\theta}(t)\big)\right| \le \\ &\|\boldsymbol{X}_k - \boldsymbol{X}_d\| h_1(\boldsymbol{X}_k, \boldsymbol{X}_d)\xi_1(\boldsymbol{\theta}) + \left\|\boldsymbol{X}_{\tau,k} - \boldsymbol{X}_{d,\tau}\right\| h_2\big(\boldsymbol{X}_{\tau,k}, \boldsymbol{X}_{d,\tau}\big)\xi_2(\boldsymbol{\theta}) \end{aligned} \tag{2.2}$$

where, $\boldsymbol{X}_{d,\tau} \triangleq \boldsymbol{X}_d(t-\tau(t))$, $h_1(\cdot,\cdot)$, and $h_2(\cdot,\cdot)$ are known continuous positive functions, $\xi_1(\boldsymbol{\theta})$ and $\xi_2(\boldsymbol{\theta})$ denote unknown smooth functions of $\boldsymbol{\theta}(t)$.

Assumption 2.3 The sign of control gain $g(t)$ is known, without lose of generality, we always assume $g(t) > 0$.

Assumption 2.4 The initial state errors $e_{i,k}(0)$ at each iteration are not necessarily zero small and fixed, but assumed to be bounded.

Assumption 2.5 The desired trajectory $y_d(t)$ up to its n-th derivative are continuous, bounded and available.

Assumption 2.6 The unknown external disturbance $d(t)$ is bounded, i.e., $|d(t)| \le d_{\max}$ with $d_{\max}$ being an unknown constant.

Assumption 2.7 For $t \in [-\tau_{\max}, 0)$, $e_{i,k}(t) = 0$, $i = 1, \ldots, n$.

Remark 2.2 Assumption 2.1 is necessary for the control problem of time-varying delay systems, which ensures that the time-delay parts can be eliminated by Lyapunov-Krasovskii functional. Moreover, Assumption 2.1 is milder than that in [12–16] which requires to know the true value of κ.

Remark 2.3 As $g(t)$ is continuous on $[0, T]$, there exist constants $0 < g_{\min} \le g_{\max}$ such that $g_{\min} \le g(t) \le g_{\max}$. However, the control gain bounds $g_{\min}$ and $g_{\max}$ are only used for analytical purposes, their true values are not necessarily known since they are not used for controller design.

Remark 2.4 In most ILC schemes, identical initial condition or fixed initial states are required, i.e., $\boldsymbol{X}_k(0) = \boldsymbol{X}_d(0)$ or $\boldsymbol{X}_k(0) = \boldsymbol{X}_0$ with $\boldsymbol{X}_0$ as a fixed constant vector. From the practical point of view, it is difficult to satisfy identical initial condition or fixed initial states due to the operation precision and existence of measurement noise. Therefore, Assumption 2.4 has much more practical significance.

Remark 2.5 Assumption 2.7 is only used for analysis and has no practical meaning.

2.2.2 Dead-Zone Characteristic

As mentioned above, dead-zone is a common nonlinear characteristic in practical control systems, which will severely impact system performances and even destroy the system stability. Different from existing results, a new simple dead-zone model in nonlinear form is proposed as follows.

$$u_k(t) = D(v_k(t)) = \begin{cases} m(t)(v_k(t) - b_r), & v_k(t) \geq b_r \\ 0, & b_l < v_k(t) < b_r \\ m(t)(v_k(t) - b_l), & v_k(t) \leq b_l \end{cases} \tag{2.3}$$

where, $b_r \geq 0$ and $b_l \leq 0$ are unknown constants, $m(t) > 0$ is unknown time-varying coefficient. $v_k(t)$ and $u_k(t)$ are the input and output of dead-zone characteristic respectively. A graphical representation of the proposed dead-zone is shown in Fig. 2.1.

We make the following assumption on the dead-zone parameters.

Assumption 2.8 The dead-zone parameters b_r, b_l and $m(t)$ are bounded, i.e., there exist unknown constants $b_{r\min}$, $b_{r\max}$, $b_{l\min}$, $b_{l\max}$, $m_{\min}$, $m_{\max}$ satisfying $b_{r\min} \leq b_r \leq b_{r\max}$, $b_{l\min} \leq b_l \leq b_{l\max}$ and $m_{\min} \leq m(t) \leq m_{\max}$.

To facilitate the subsequent design, rewrite the dead-zone as the following from

$$u_k(t) = D(v_k) = m(t)v_k(t) - d_1(v_k(t)) \tag{2.4}$$

$$d_1(v_k(t)) = \begin{cases} m(t)b_r, & v_k(t) \geq b_r \\ m(t)v_k(t), & b_l < v_k(t) < b_r \\ m(t)b_l, & v_k(t) \leq b_l \end{cases} \tag{2.5}$$

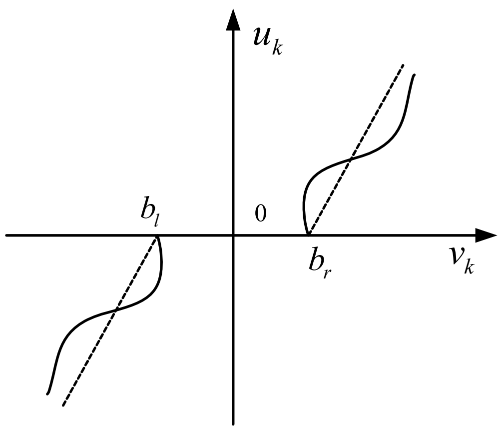

Fig. 2.1 Graphical representation of the dead-zone model

It is obvious that $d_1(v_k(t))$ is bounded.

Remark 2.6 In the research reports concerning dead-zone nonlinearity, the commonly used dead-zone model includes two forms: one is linear form, namely, $m(t)$ has equal or unequal values in negative and positive planes; the other one is nonlinear form, in this case, it is usually transformed into the parameterized form by using some mathematical method, such as mean-value theorem, in order to facilitate controller design. Obviously, the dead-zone model proposed here is a nonlinear form. As $m(t)$ could be any smooth continuous form which is more general than linear form. Meanwhile, the dead-zone model (2.3) is in parameterized form and can be directly estimated in design, in other words, it doesn't need mathematical approximation by using some mathematical techniques any more.

Throughout this book, σ denotes the integral variable and $||\cdot||$ denotes the Euclidean norm. $\mathbf{N}$ is the set of nonnegative integers. For a signal vector $\boldsymbol{r}_k(t)$, define the norm $\|\boldsymbol{r}_k(t)\|_{L_T^\infty} = \max_{(k,t)\in\mathbf{N}\times[0,T]} \|\boldsymbol{r}_k(t)\|$ and $\|\boldsymbol{r}_k(t)\|_{L_T^2} = \int_0^T \|\boldsymbol{r}_k(\sigma)\|^2 \mathrm{d}\sigma$. Then if $\|\boldsymbol{r}_k(t)\|_{L_T^\infty} < \infty$, we could say that $\boldsymbol{r}_k(t)$ is bounded in L_T^∞-norm, which is denoted by $\boldsymbol{r}_k(t) \in L_T^\infty$. Similarly, we denote the boundedness of $\boldsymbol{r}_k(t)$ in L_T^2-norm as $\boldsymbol{r}_k(t) \in L_T^2$. Obviously, the boundedness in L_T^∞-norm implies the boundedness in L_T^2-norm, because there exists the relationship between them: $\|\boldsymbol{r}_k(t)\|_{L_T^2} \le T\|\boldsymbol{r}_k(t)\|_{L_T^\infty}^2$.

2.3 AILC Scheme Design

Define a filtered tracking error variable as $e_{sk}(t) = [\boldsymbol{\Lambda}^{\mathrm{T}} 1]\boldsymbol{e}_k(t)$, where $\boldsymbol{\Lambda} = [\lambda_1, \lambda_2, \ldots, \lambda_{n-1}]^{\mathrm{T}}$ and $\lambda_1, \lambda_2, \ldots, \lambda_{n-1}$ are the coefficients of Hurwitz polynomial $H(s) = s^{n-1} + \lambda_{n-1}s^{n-2} + \cdots + \lambda_1$. According to Assumption 2.4, there exist known constants ε_i satisfying $|e_{i,k}(0)| \le \varepsilon_i$, $i = 1, 2, \cdots n$, $\forall k \in \mathbf{N}$.

In ILC, there are two common ways to deal with initial condition problem: one is design learning law for initial values, the other is employing the modification term. The first one is to use iterative learning process to realize the learning convergence of initial values along iteration axis. But this method requires the accurate positioning of the system initial values. So, similar to zero initial condition, this method is difficult to realize because of measurement noises or accuracy problem. In contrast, the second method is suitable for the needs of practical engineering. In existing results, there are mainly two ways to introduce modification term: one is to redefine the control errors such that the redefined error variables satisfy zero initial condition [23]; the other one is to directly introduce the modification quantity for initial errors in controller and eliminate the impacts of initial errors in finite time. The boundary layer function put forward by Chiang-Ju Chien's team is a method of control error redefinition. In this book, we will use their method for reference and improve it to deal with the initial condition problem.

Introduce the boundary layer and define a new tracking error variable as

$$s_k(t) = e_{sk}(t) - \eta(t)\mathrm{sat}\left(\frac{e_{sk}(t)}{\eta(t)}\right) \tag{2.6}$$

$$\eta(t) = \varepsilon e^{-Kt}, K > 0 \tag{2.7}$$

where, $\varepsilon = \left[\boldsymbol{\Lambda}^T 1\right][\varepsilon_1, \varepsilon_2, \ldots, \varepsilon_n]^{\mathrm{T}}$, K is design parameter, sat$(\cdot)$ denotes saturation function which is defined by

$$\mathrm{sat}(\cdot) = \mathrm{sgn}(\cdot) \cdot \min\{|\cdot|, 1\} \tag{2.8}$$

where, $\mathrm{sgn}(\cdot) = \begin{cases} 1\, if \cdot > 0 \\ 0\, if \cdot = 0 \\ -1\, if \cdot < 0 \end{cases}$ is the sign function.

Remark 2.7 According to the definition of boundary layer function, $\eta(t)$ is a decreasing function with respect to time, and $\eta(0) = \varepsilon$, $0 < \eta(T) \le \eta(t) \le \varepsilon$, $\forall t \in [0, T]$. If we can design a controller that derive $s_k(t)$ converge to zero, then the system states will asymptotically converge to the desired trajectory on $t \in [0, T]$, in other words, the tracking error $e_{sk}(t)$ will be always within the envelope that determined by boundary layer function $\eta(t)$. Then according to the Hurwitz property of coefficient vector $\boldsymbol{\Lambda}$, we can know that $e_{1,k}(t)$ will also locate in the envelope that determined by $\eta(t)$, i.e., the system output $y_k(t)$ will be able to track the desired reference trajectory $y_d(t)$. Moreover, by choosing suitable parameters ε and K, we can ensure the tracking error locate within the tolerance range.

According to previous definition, it can be easily shown that

$$\begin{aligned} |e_{sk}(0)| &= \left|\lambda_1 e_{1,k}(0) + \lambda_2 e_{2,k}(0) + \cdots + e_{n,k}(0)\right| \\ &\le \lambda_1 \left|e_{1,k}(0)\right| + \lambda_2 \left|e_{2,k}(0)\right| + \cdots + \left|e_{n,k}(0)\right| \\ &\le \lambda_1 \varepsilon_1 + \lambda_2 \varepsilon_2 + \cdots + \varepsilon_n = \varepsilon = \eta(0) \end{aligned} \tag{2.9}$$

which implies that $s_k(0) = e_{sk}(0) - \eta(0)\frac{e_{sk}(0)}{\eta(0)} = 0$ is satisfied for $\forall k \in \mathbf{N}$.

For the subsequent design, we firstly give the dynamical equation for $e_{n,k}(t)$

$$\begin{aligned} \dot{e}_{n,k}(t) &= f\big(\boldsymbol{X}_k(t), \boldsymbol{X}_{\tau,k}, \boldsymbol{\theta}(t)\big) + g(t)u_k + d(t) - y_d^{(n)}(t) \\ &= f\big(\boldsymbol{X}_k, \boldsymbol{X}_{\tau,k}, \boldsymbol{\theta}(t)\big) - f\big(\boldsymbol{X}_d, \boldsymbol{X}_{d,\tau}, \boldsymbol{\theta}(t)\big) + f\big(\boldsymbol{X}_d, \boldsymbol{X}_{d,\tau}, \boldsymbol{\theta}(t)\big) \\ &\quad + g(t)(m(t)v_k(t) - d_1(v_k(t))) + d(t) - y_d^{(n)}(t) \\ &= f\big(\boldsymbol{X}_k, \boldsymbol{X}_{\tau,k}, \boldsymbol{\theta}(t)\big) - f\big(\boldsymbol{X}_d, \boldsymbol{X}_{d,\tau}, \boldsymbol{\theta}(t)\big) + f\big(\boldsymbol{X}_d, \boldsymbol{X}_{d,\tau}, \boldsymbol{\theta}(t)\big) \\ &\quad + g(t)m(t)v_k(t) + d_2(t) - y_d^{(n)}(t) \end{aligned} \tag{2.10}$$

where, $d_2(t) = -b(t)d_1(v_k(t)) + d(t)$. According to Assumptions 2.3 and 2.6, it is obvious that $d_2(t)$ is bounded, namely, there exists an unknown smooth positive function $\overline{d}(t)$ such that $|d_2(t)| \le \overline{d}(t)$. For expression simplicity, define

$g_m(t) = g(t)m(t)$, $\Theta(t) = f\big(\boldsymbol{X}_d, \boldsymbol{X}_{d,\tau}, \boldsymbol{\theta}(t)\big)$, $\Delta_k(t) = f\big(\boldsymbol{X}_k, \boldsymbol{X}_{\tau,k}, \boldsymbol{\theta}(t)\big) - f\big(\boldsymbol{X}_d, \boldsymbol{X}_{d,\tau}, \boldsymbol{\theta}(t)\big)$. Obviously, $\Theta(t)$ is an unknown time-varying but iteration-invariant function. Additionally, there exists the relationship that $\underline{g}_m = m_{\min} g_{\min} \leq g_m(t) \leq m_{\max} g_{\max} = \overline{g}_m$ with $\underline{g}_m$ and $\overline{g}_m$ being unknown positive constants.

Define a smooth scalar function as

$$V_{s_k}(t) = \frac{1}{2} s_k^2(t) \tag{2.11}$$

Taking the time derivative of $V_{s_k}(t)$ yields

$$\begin{aligned}
\dot{V}_{s_k}(t) &= s_k(t)\dot{s}_k(t) \\
&= \begin{cases} s_k(t)(\dot{e}_{sk}(t) - \dot{\eta}(t)), & if\ e_{sk}(t) > \eta(t) \\ 0, \quad if \quad |e_{sk}(t)| \leq \eta(t) \\ s_k(t)(\dot{e}_{sk}(t) + \dot{\eta}(t)) \ , & if\ e_{sk}(t) < -\eta(t) \end{cases} \\
&= s_k(t)\big[\dot{e}_{sk}(t) - \dot{\eta}(t)\mathrm{sgn}(s_k(t))\big] \\
&= s_k(t)\left[\sum_{j=1}^{n-1} \lambda_j e_{j+1,k}(t) - \dot{\eta}(t)\mathrm{sgn}(s_k(t)) + \Theta(t) + \Delta_k(t) + g_m(t)v_k(t) \right. \\
&\quad \left. + d_2(t) - y_d^{(n)}(t)\right] \\
&= s_k(t)\left[\sum_{j=1}^{n-1} \lambda_j e_{j+1,k}(t) + K\eta(t)\mathrm{sgn}(s_k(t)) + Ke_{sk}(t) \right. \\
&\quad \left. - Ke_{sk}(t) + \Theta(t) + \Delta_k(t) + g_m(t)v_k(t) + d_2(t) - y_d^{(n)}(t)\right] \\
&= s_k(t)[\Theta(t) + \Delta_k(t) + g_m(t)v_k(t) + \mu_k(t) + d_2(t)] - Ks_k^2(t)
\end{aligned} \tag{2.12}$$

where, $\mu_k(t) = \sum_{j=1}^{n-1} \lambda_j e_{j+1,k}(t) + Ke_{sk}(t) - y_d^{(n)}(t)$ and using the following equality

$$\begin{aligned}
&s_k(t)(-Ke_{sk}(t) + K\eta(t)\mathrm{sgn}(s_k(t))) \\
&\quad = s_k(t)\left(-Ks_k(t) - K\eta(t)\mathrm{sat}\left(\frac{e_{sk}(t)}{\eta(t)}\right) + K\eta(t)\mathrm{sgn}(s_k(t))\right) \\
&\quad = -Ks_k^2(t) - K\eta(t)|s_k(t)| + K\eta(t)|s_k(t)| \\
&\quad = -Ks_k^2(t)
\end{aligned} \tag{2.13}$$

Using Young's inequality and noting Assumption 2.2, we have

$$\begin{aligned}
&s_k(t)\Delta_k(t) \\
&\leq |s_k(t)|\big(\|\boldsymbol{X}_k - \boldsymbol{X}_d\| h_1(\boldsymbol{X}_k, \boldsymbol{X}_d)\xi_1(\boldsymbol{\theta}) + \big\|\boldsymbol{X}_{\tau,k} - \boldsymbol{X}_{d,\tau}\big\| h_2\big(\boldsymbol{X}_{\tau,k}, \boldsymbol{X}_{d,\tau}\big)\xi_2(\boldsymbol{\theta})\big)
\end{aligned}$$

$$\leq \frac{1}{2}s_k^2(t)\xi_1^2(\boldsymbol{\theta}) + \frac{1}{2}\|\boldsymbol{e}_k\|^2 h_1^2(\boldsymbol{X}_k, \boldsymbol{X}_d) + \frac{1}{2}s_k^2(t)\xi_2^2(\boldsymbol{\theta}) + \frac{1}{2}\left\|\boldsymbol{e}_{\tau,k}\right\|^2 h_2^2\big(\boldsymbol{X}_{\tau,k}, \boldsymbol{X}_{d,\tau}\big) \tag{2.14}$$

Substituting (2.14) into (2.12) leads to

$$\dot{V}_{s_k}(t) \leq s_k(t)\bigg[\Theta(t) + g_m(t)v_k(t) + \mu_k(t) + d_2(t) + \frac{1}{2}s_k(t)\xi_1^2(\boldsymbol{\theta}) + \frac{1}{2}s_k(t)\xi_2^2(\boldsymbol{\theta})\bigg] - Ks_k^2(t) + \frac{1}{2}\|\boldsymbol{e}_k\|^2 h_1^2(\boldsymbol{X}_k, \boldsymbol{X}_d) + \frac{1}{2}\left\|\boldsymbol{e}_{\tau,k}\right\|^2 h_2^2\big(\boldsymbol{X}_{\tau,k}, \boldsymbol{X}_{d,\tau}\big) \tag{2.15}$$

To deal with the unknown time-varying delay term in (2.15), consider the following Lyapunov-Krasovskii functional

$$V_{U_k}(t) = \frac{1}{2(1-\kappa)}\int_{t-\tau(t)}^{t} \|\boldsymbol{e}_k(\sigma)\|^2 h_2^2(\boldsymbol{X}_k(\sigma), \boldsymbol{X}_d(\sigma))\mathrm{d}\sigma \tag{2.16}$$

According to Assumption 2.1, taking the time derivative of $V_{U_k}(t)$ results in

$$\begin{aligned}\dot{V}_{U_k}(t) &= \frac{1}{2(1-\kappa)}\|\boldsymbol{e}_k\|^2 h_2^2(\boldsymbol{X}_k, \boldsymbol{X}_d) - \frac{1-\dot{\tau}(t)}{2(1-\kappa)}\left\|\boldsymbol{e}_{\tau,k}\right\|^2 h_2^2\big(\boldsymbol{X}_{\tau,k}, \boldsymbol{X}_{d,\tau}\big)\\ &\leq \frac{1}{2(1-\kappa)}\|\boldsymbol{e}_k\|^2 h_2^2(\boldsymbol{X}_k, \boldsymbol{X}_d) - \frac{1}{2}\left\|\boldsymbol{e}_{\tau,k}\right\|^2 h_2^2\big(\boldsymbol{X}_{\tau,k}, \boldsymbol{X}_{d,\tau}\big)\end{aligned} \tag{2.17}$$

Choose the Lyapunov function as $V_k(t) = V_{s_k}(t) + V_{U_k}(t)$, recalling (2.15) and (2.17), we can obtain the time derivative of $V_k(t)$ as follows

$$\begin{aligned}\dot{V}_k(t) \leq\ & s_k(t)\bigg[\Theta(t) + g_m(t)v_k(t) + \mu_k(t) + d_2(t) + \frac{1}{2}s_k(t)\xi_1^2(\boldsymbol{\theta})\\ &+ \frac{1}{2}s_k(t)\xi_2^2(\boldsymbol{\theta})\bigg] - Ks_k^2(t) + \frac{1}{2}\|\boldsymbol{e}_k\|^2 h_1^2(\boldsymbol{X}_k, \boldsymbol{X}_d)\\ &+ \frac{1}{2(1-\kappa)}\|\boldsymbol{e}_k\|^2 h_2^2(\boldsymbol{X}_k, \boldsymbol{X}_d)\end{aligned} \tag{2.18}$$

For convenience of expression, denote $\zeta_k(t) = \frac{1}{2}\|\boldsymbol{e}_k\|^2 h_1^2(\boldsymbol{X}_k, \boldsymbol{X}_d) + \frac{1}{2(1-\kappa)}\|\boldsymbol{e}_k\|^2 h_2^2(\boldsymbol{X}_k, \boldsymbol{X}_d)$, then (2.18) can be simplified as

$$\begin{aligned}\dot{V}_k(t) \leq\ & s_k(t)\bigg[\Theta(t) + g_m(t)v_k(t) + \mu_k(t) + d_2(t) + \frac{1}{2}s_k(t)\xi_1^2(\boldsymbol{\theta})\\ &+\frac{1}{2}s_k(t)\xi_2^2(\boldsymbol{\theta}) + \frac{\zeta_k(t)}{s_k(t)}\bigg] - Ks_k^2(t)\end{aligned} \tag{2.19}$$

Examining Eq. (2.19), if we directly compensate for the term $\zeta_k(t)/s_k(t)$ in the feedback controller design, it will cause singularity problem as $s_k(t)$ approaches zero. In order to tackle this problem, we exploit the following characteristic of hyperbolic tangent function.

Lemma 2.1 [34] *For any constant* $\eta > 0$ *and any variable* $p \in R$, *the following equality holds*

$$\lim_{p\to 0}\frac{\tanh^2(p/\eta)}{p} = 0 \tag{2.20}$$

Introducing the hyperbolic tangent function, inequality (2.19) *can be rewritten as*

$$\begin{aligned}\dot{V}_k(t) \le s_k(t)\Big[&\Theta(t) + d_2(t) + g_m(t)v_k(t) + \mu_k(t) + \frac{1}{2}s_k(t)\xi_1^2(\theta) + \frac{1}{2}s_k(t)\xi_2^2(\boldsymbol{\theta})\\ &+ \frac{b}{2s_k(t)}\tanh^2\left(\frac{s_k(t)}{\eta(t)}\right)\|\boldsymbol{e}_k\|^2h_1^2(\boldsymbol{X}_k, \boldsymbol{X}_d)\\ &+\frac{b}{2(1-\kappa)s_k(t)}\tanh^2\left(\frac{s_k(t)}{\eta(t)}\right)\|\boldsymbol{e}_k\|^2h_2^2(\boldsymbol{X}_k, \boldsymbol{X}_d)\Big]\\ &- Ks_k^2(t) + \left(1 - b\tanh^2\left(\frac{s_k(t)}{\eta(t)}\right)\right)\zeta_k(t)\end{aligned} \tag{2.21}$$

where, $b > 1$ *is a design constant.*

From Lemma 2.1, it's clear that $\lim_{s_k(t)\to 0}\frac{b}{s_k(t)}\tanh^2\left(\frac{s_k(t)}{\eta(t)}\right)\zeta_k(t) = 0$. Hence, the singularity problem will not occur even at the point $s_k(t) = 0$. Upon multiplication of (2.21) by $1/g_m(t)$, it becomes

$$\begin{aligned}\frac{\dot{V}_k(t)}{g_m(t)} \le s_k(t)\Big[&\frac{1}{g_m(t)}(\Theta(t) + d_2(t)) + v_k(t) + \frac{1}{g_m(t)}\mu_k(t)\\ &+ \frac{1}{2g_m(t)}s_k(t)\big(\xi_1^2(\boldsymbol{\theta}) + \xi_2^2(\boldsymbol{\theta})\big)\\ &+ \frac{b}{2g_m(t)s_k(t)}\tanh^2\left(\frac{s_k(t)}{\eta(t)}\right)\|\boldsymbol{e}_k\|^2h_1^2(\boldsymbol{X}_k, \boldsymbol{X}_d)\\ &+\frac{b}{2g_m(t)(1-\kappa)s_k(t)}\tanh^2\left(\frac{s_k(t)}{\eta(t)}\right)\|\boldsymbol{e}_k\|^2h_2^2(\boldsymbol{X}_k, \boldsymbol{X}_d)\Big]\\ &- \frac{K}{g_m(t)}s_k^2(t) + \frac{1}{g_m(t)}\left(1 - b\tanh^2\left(\frac{s_k(t)}{\eta(t)}\right)\right)\zeta_k(t)\\ = s_k(t)&\big[\boldsymbol{\beta}^T(t)\boldsymbol{\Phi}(\boldsymbol{X}_k, \boldsymbol{X}_d) + v_k(t)\big] - \frac{K}{g_m(t)}s_k^2(t)\\ &+ \frac{1}{g_m(t)}\left(1 - b\tanh^2\left(\frac{s_k(t)}{\eta(t)}\right)\right)\zeta_k(t)\end{aligned} \tag{2.22}$$

where, $\boldsymbol{\beta}(t) = \left[\frac{1}{g_m(t)}(\Theta(t) + d_2(t)), \frac{1}{g_m(t)}, \frac{1}{g_m(t)}\left(\xi_1^2(\boldsymbol{\theta}) + \xi_2^2(\boldsymbol{\theta})\right), \frac{1}{(1-\kappa)g_m(t)}\right]^{\mathrm{T}}$ denotes an unknown time-varying parameter vector that is invariant along the iteration axis; $\boldsymbol{\Phi}(\boldsymbol{X}_k, \boldsymbol{X}_d) = \left[1, \mu_k(t) + \frac{b}{2s_k(t)} \tanh^2\left(\frac{s_k(t)}{\eta(t)}\right)\|\boldsymbol{e}_k\|^2 h_1^2(\boldsymbol{X}_k, \boldsymbol{X}_d), s_k(t), \frac{b}{2s_k(t)} \times \tanh^2\left(\frac{s_k(t)}{\eta(t)}\right)\|\boldsymbol{e}_k\|^2 h_2^2(\boldsymbol{X}_k, \boldsymbol{X}_d)\right]^{\mathrm{T}}$.

Based on (2.22), we can design the adaptive iterative learning controller as follows:

$$v_k(t) = -\hat{\boldsymbol{\beta}}_k^{\mathrm{T}}(t)\boldsymbol{\Phi}(\boldsymbol{X}_k, \boldsymbol{X}_d) - K_1 s_k(t) \tag{2.23}$$

where, $K_1 > 0$ is a design parameter, $\hat{\boldsymbol{\beta}}_k(t)$ represents the estimate of $\boldsymbol{\beta}(t)$ at the k-th iteration. Design the adaptive learning algorithm for $\boldsymbol{\beta}(t)$ as follows

$$\begin{cases} \hat{\boldsymbol{\beta}}_k(t) = \hat{\boldsymbol{\beta}}_{k-1}(t) + q s_k(t)\boldsymbol{\Phi}(\boldsymbol{X}_k, \boldsymbol{X}_d) \\ \hat{\boldsymbol{\beta}}_0(t) = 0, t \in [0, T] \end{cases} \tag{2.24}$$

where, $q > 0$ is parameter learning gain.

Define the parameter estimation error as $\tilde{\boldsymbol{\beta}}_k(t) = \hat{\boldsymbol{\beta}}_k(t) - \boldsymbol{\beta}(t)$. Then substituting the controller (2.23) into (2.22) yields

$$\begin{aligned} \frac{\dot{V}_k(t)}{g_m(t)} &\le -s_k(t)\tilde{\boldsymbol{\beta}}_k^{\mathrm{T}}(t)\boldsymbol{\Phi}(\boldsymbol{X}_k, \boldsymbol{X}_d) - \left(\frac{K}{g_m(t)} + K_1\right)s_k^2(t) \\ &\quad + \frac{1}{g_m(t)}\left(1 - b\tanh^2\left(\frac{s_k(t)}{\eta(t)}\right)\right)\zeta_k(t) \\ &\le -s_k(t)\tilde{\boldsymbol{\beta}}_k^{\mathrm{T}}(t)\boldsymbol{\Phi}(\boldsymbol{X}_k, \boldsymbol{X}_d) - \left(\frac{K}{\overline{g}_m} + K_1\right)s_k^2(t) \\ &\quad + \frac{1}{g_m(t)}\left(1 - b\tanh^2\left(\frac{s_k(t)}{\eta(t)}\right)\right)\zeta_k(t) \end{aligned} \tag{2.25}$$

For simplicity in expression, denote $K_2 = \left(K/\overline{g}_m + K_1\right)$. Then Eq. (2.25) can be rewritten as

$$s_k(t)\tilde{\boldsymbol{\beta}}_k^{\mathrm{T}}(t)\boldsymbol{\Phi}(\boldsymbol{X}_k, \boldsymbol{X}_d) \le -\frac{\dot{V}_k(t)}{g_m(t)} - K_2 s_k^2(t) + \frac{1}{g_m(t)}\left(1 - b\tanh^2\left(\frac{s_k(t)}{\eta(t)}\right)\right)\zeta_k(t) \tag{2.26}$$

In this section, we will analyze the stability of the closed-loop system and the convergence of tracking errors. The stability of the proposed AILC scheme is summarized as follows.

The block diagram of the proposed AILC is presented in Fig. 2.2.

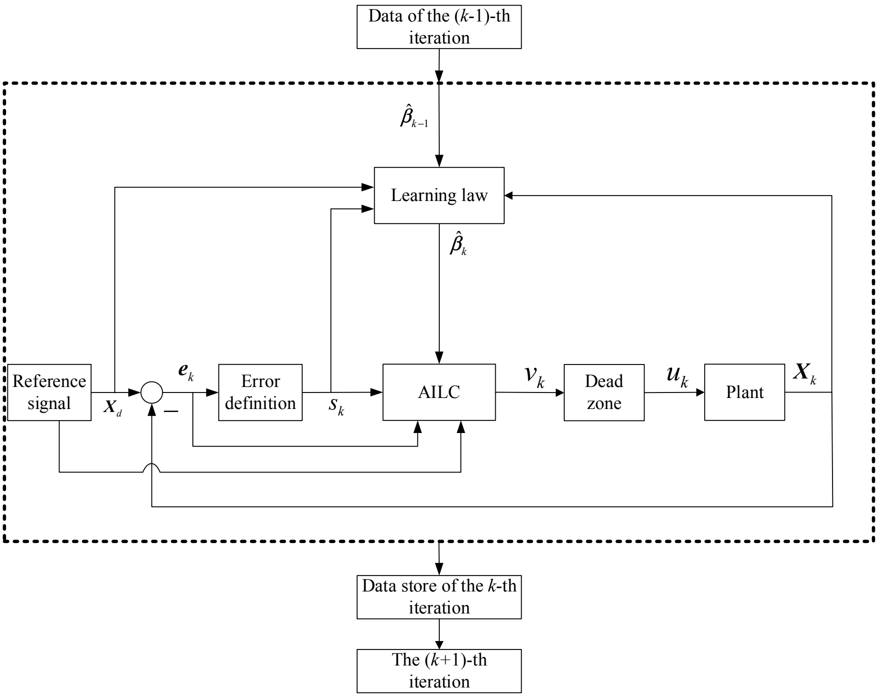

Fig. 2.2 The block diagram of the proposed AILC

2.4 Stability Analysis

In this section, we will analyze the system stability using Lyapunov-like CEF method. In the proof, we need to use the following characteristic of the tangent hyperbolic function.

Lemma 2.2 *Define a compact set*: $\mathbf{\Omega}_{s_k} := \{s_k(t) | |s_k(t)| \le m\eta(t)\}$, *the for* $\forall s_k(t) \notin \mathbf{\Omega}_{s_k}$, *the following inequality holds*:

$$1 - b \tanh^2\left(\frac{s_k(t)}{\eta(t)}\right) < 0 \tag{2.27}$$

where, $m = \ln\left(\sqrt{b/(b-1)} + \sqrt{1/(b-1)}\right)$.

Proof For expression convenience, denote $x = s_k(t)/\eta(t)$, then Eq. (2.27) can be expressed as

$$\frac{1}{b} < \tanh^2(x) = \left(\frac{e^x - e^{-x}}{e^x + e^{-x}}\right)^2 = 1 - \left(\frac{2}{e^x + e^{-x}}\right)^2 \tag{2.28}$$

Noting that e^x and e^{-x} are both positive, from Eq. (2.28) we can obtain

$$e^x + e^{-x} > 2\sqrt{\frac{b}{b-1}} \tag{2.29}$$

Multiplying both sides of the previous inequality by e^x and rearranging terms we get

$$e^{2x} - 2\sqrt{\frac{b}{b-1}}e^x + 1 > 0 \tag{2.30}$$

Solving the quadratic inequality (A.3), we can get the following solutions

$$0 < e^x < \sqrt{b/(b-1)} - \sqrt{1/(b-1)} \; or \; e^x > \sqrt{b/(b-1)} + \sqrt{1/(b-1)} \tag{2.31}$$

On the other hand, from $|s_k(t)| > m\eta(t)$ we have

$$x < -m \; or \; x > m \tag{2.32}$$

According to the expression of m, we obtain

$$\begin{aligned} 0 < e^x &< \frac{1}{\sqrt{b/(b-1)} + \sqrt{1/(b-1)}} = \sqrt{b/(b-1)} - \sqrt{1/(b-1)} \\ or \; e^x &> \sqrt{b/(b-1)} + \sqrt{1/(b-1)} \end{aligned} \tag{2.33}$$

Obviously, from the uniformity of inequality (2.31) and (2.33), we can easily know that Lemma 2.2 holds. □

For the proposed AILC scheme in this chapter, we have the following conclusion.

Theorem 2.1 *Considering the parameterized time-delay systems as* (2.1) *running repeatedly on finite time interval* $[0, T]$, *if* Assumption 2.1–Assumption 2.8 *are satisfied*, *design AILC scheme* (2.23) *with adaptive updating law* (2.24), *we can obtain the following conclusions*: ① *all the closed-loop signal are bounded*; ② *the tracking error* $e_{sk}(t)$ *converge to a small neighborhood of zero as* $k \to \infty$ *in* L_T^2*-norm, i.e.,* $\lim_{k\to\infty} \int_0^T (e_{sk}(\sigma))^2 d\sigma \le \varepsilon_{esk}$, $\varepsilon_{esk} = \frac{1}{2K}(1+m)^2\varepsilon^2$; ③ *the system transient performance*: *the output tracking error* $e_{1,k}(t)$ *satisfies* $\lim_{k\to\infty} |e_{1,k}(t)| = k_0 \sum_{i=1}^{n-1} \sqrt{\varepsilon_i^2} e^{-\lambda_0 t} + (1+m)\varepsilon k_0 \frac{1}{\lambda_0 - K}\left(e^{-Kt} - e^{-\lambda_0 t}\right)$.

Proof The sign of the last term in the right side of Eq. (2.26) depends on the sign of $\left(1 - b\tanh^2\left(s_k(t)/\eta(t)\right)\right)$, whereas the sign of $\left(1 - b\tanh^2\left(s_k(t)/\eta(t)\right)\right)$ depends on the value of S_k. Therefore, according to Lemma 2.2, we need to consider two cases.

Case 1. $s_k(t) \in \boldsymbol{\Omega}_{s_k}$.

For $s_k(t) \in \Omega_{s_k}$, $|s_k(t)| \leq m\eta(t)$ holds. Consider the following three situations. ① If $s_k(t) = 0$, we can know that $e_{sk}(t)$ lies in the envelope of $\eta(t)$ all the time, i.e., $|e_{sk}(t)| \leq \eta(t)$; ② If $s_k(t) > 0$, from the definition of $s_k(t)$, we know $s_k(t) = e_{sk}(t) - \eta(t)$. According to $|s_k(t)| \leq m\eta(t)$, it is clear that $s_k(t) = e_{sk}(t) - \eta(t) \leq m\eta(t)$, which implies that $0 < e_{sk} \leq (1+m)\eta(t)$; ③ Similarly, if $s_k(t) < 0$, we know $s_k(t) = e_{sk}(t) + \eta(t) \geq -m\eta(t)$, which is equivalent to $0 > e_{sk}(t) \geq -(1+m)\eta(t)$. In summary, we can obtain the conclusion that $|e_{sk}(t)| \leq (1+m)\eta(t)$. Obviously, since $\boldsymbol{X}_d(t)$ is bounded, then we can know that $x_{i,k}(t)$ is bounded. Furthermore, since $h_1(\cdot,\cdot)$ and $h_1(\cdot,\cdot)$ are continuous and bounded on $[0, T]$, then we can say that $\boldsymbol{\Phi}(\boldsymbol{X}_k, \boldsymbol{X}_d)$ is a bounded vector. According to Eq. (2.24), $\hat{\boldsymbol{\beta}}_0(t) = 0, t \in [0, T]$, then if $s_k(t) \in \boldsymbol{\Omega}_{s_k}$, $\hat{\boldsymbol{\beta}}_k(t)$ is bounded as well. Through above analysis, we can further obtain the boundedness of $v_k(t)$. Thus all the closed-loop signals are bounded.

Remark 2.8 In theory, m can be made arbitrarily small through the choose of b. For example, when $b = 100$, $m = 0.099$. Thus $s_k(t)$ can be driven arbitrarily small as well. However, overlarge b may lead to excessive control signal, which may degrade the transient performance. Therefore, in practical applications, designers should choose suitable parameters and obtain satisfactory transient performance and stable error.

Case 2. $s_k(t) \notin \boldsymbol{\Omega}_{s_k}$.

In this case, from Lemma 2.2 we know that the last term in the right side of (2.26) is less than zero, so it can be removed from inequality (2.26), i.e.,

$$s_k(t)\tilde{\boldsymbol{\beta}}_k^{\mathrm{T}}(t)\boldsymbol{\Phi}(\boldsymbol{X}_k, \boldsymbol{X}_d) \leq -\frac{\dot{V}_k(t)}{g_m(t)} - K_2 s_k^2(t) \tag{2.34}$$

Choosing the Lyapunov-like CEF as

$$E_k(t) = \frac{1}{2q}\int_0^t \tilde{\boldsymbol{\beta}}_k^{\mathrm{T}}(\sigma)\tilde{\boldsymbol{\beta}}_k(\sigma)\mathrm{d}\sigma \tag{2.35}$$

In the next text, we will prove the boundedness of signals and the convergence of tracking error in Theorem 2.1, which includes three parts. The main idea is presented in Fig. 2.3.

The specific proof is as follows.

(1) The difference of $E_k(t)$.

Compute the difference of $E_k(t)$ in the k-th iteration and the (k-1)-th iteration

$$\Delta E_k(t) = E_k(t) - E_{k-1}(t)$$

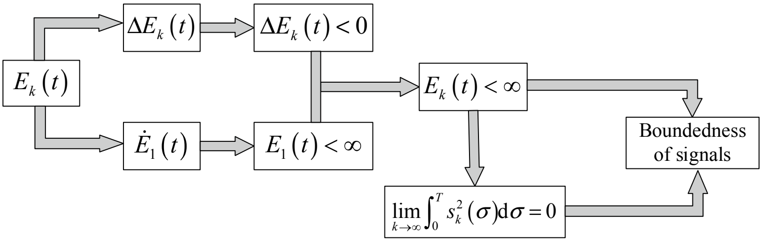

Fig. 2.3 The main idea of CEF-based proof for Theorem 2.1

$$= \frac{1}{2q}\int_0^t \left(\tilde{\boldsymbol{\beta}}_k^{\mathrm{T}}(\sigma)\tilde{\boldsymbol{\beta}}_k(\sigma) - \tilde{\boldsymbol{\beta}}_{k-1}^{\mathrm{T}}(\sigma)\tilde{\boldsymbol{\beta}}_{k-1}(\sigma)\right)\mathrm{d}\sigma \tag{2.36}$$

Utilizing the algebraic relation $(\boldsymbol{a}-\boldsymbol{b})^{\mathrm{T}}(\boldsymbol{a}-\boldsymbol{b}) - (\boldsymbol{a}-\boldsymbol{c})^{\mathrm{T}}(\boldsymbol{a}-\boldsymbol{c}) = (\boldsymbol{c}-\boldsymbol{b})^{\mathrm{T}}[2(\boldsymbol{a}-\boldsymbol{b}) + (\boldsymbol{b}-\boldsymbol{c})]$ and recalling adaptive iterative learning law (2.24), we can obtain the following inequality

$$\begin{aligned}\Delta E_k(t) &= \int_0^t s_k(\sigma)\tilde{\boldsymbol{\beta}}_k^{\mathrm{T}}(\sigma)\boldsymbol{\Phi}(\boldsymbol{X}_k, \boldsymbol{X}_d)\mathrm{d}\sigma - \frac{q}{2}\int_0^t s_k^2(\sigma)\|\boldsymbol{\Phi}(\boldsymbol{X}_k, \boldsymbol{X}_d)\|^2\mathrm{d}\sigma \\ &\le \int_0^t s_k(\sigma)\tilde{\boldsymbol{\beta}}_k^{\mathrm{T}}(\sigma)\boldsymbol{\Phi}(\boldsymbol{X}_k, \boldsymbol{X}_d)\mathrm{d}\sigma\end{aligned} \tag{2.37}$$

Substituting Eq. (2.34) into above inequality results in

$$\Delta E_k(t) \le -\int_0^t \frac{\dot{V}_k(\sigma)}{g_m(\sigma)}\mathrm{d}\sigma - \int_0^t K_2 s_k^2(\sigma)\mathrm{d}\sigma \le -\frac{1}{g_m}V_k(t) - K_2\int_0^t s_k^2(\sigma)\mathrm{d}\sigma < 0 \tag{2.38}$$

The above inequality indicates that $E_k(t)$ is decreasing along iteration axis. Accordingly, the boundedness of $E_k(t)$ can be ensured provided that $E_1(t)$ is bounded.

(2) The boundedness of $E_k(t)$.

According to the definition of CEF, we know

$$E_1(t) = \frac{1}{2q}\int_0^t \tilde{\boldsymbol{\beta}}_1^{\mathrm{T}}(\sigma)\tilde{\boldsymbol{\beta}}_1(\sigma)\mathrm{d}\sigma \tag{2.39}$$

Taking the time derivative of $E_1(t)$ yields

$$\dot{E}_1(t) = \frac{1}{2q}\tilde{\boldsymbol{\beta}}_1^{\mathrm{T}}(t)\tilde{\boldsymbol{\beta}}_1(t) \tag{2.40}$$

Recalling parameter adaptive law, we have $\hat{\boldsymbol{\beta}}_1(t) = qs_1(t)\boldsymbol{\Phi}(\boldsymbol{X}_1, \boldsymbol{X}_d)$, then we obtain

$$\begin{aligned}
\dot{E}_1(t) &= \frac{1}{2q}\tilde{\boldsymbol{\beta}}_1^{\mathrm{T}}(t)\tilde{\boldsymbol{\beta}}_1(t) \\
&= \frac{1}{2q}\Big(\tilde{\boldsymbol{\beta}}_1^{\mathrm{T}}(t)\tilde{\boldsymbol{\beta}}_1(t) - 2\tilde{\boldsymbol{\beta}}_1^{\mathrm{T}}(t)\hat{\boldsymbol{\beta}}_1(t)\Big) + \frac{1}{q}\tilde{\boldsymbol{\beta}}_1^{\mathrm{T}}(t)\hat{\boldsymbol{\beta}}_1(t) \\
&= \frac{1}{2q}\Big[\Big(\hat{\boldsymbol{\beta}}_1(t) - \boldsymbol{\beta}(t)\Big)^{\mathrm{T}}\Big(\hat{\boldsymbol{\beta}}_1(t) - \boldsymbol{\beta}(t)\Big) - 2\Big(\hat{\boldsymbol{\beta}}_1(t) - \boldsymbol{\beta}(t)\Big)^{\mathrm{T}}\hat{\boldsymbol{\beta}}_1(t)\Big] \\
&\quad + s_1(t)\tilde{\boldsymbol{\beta}}_1^{\mathrm{T}}(t)\boldsymbol{\Phi}(\boldsymbol{X}_1, \boldsymbol{X}_d) \\
&= \frac{1}{2q}\Big(-\hat{\boldsymbol{\beta}}_1^{T}(t)\hat{\boldsymbol{\beta}}_1 + \boldsymbol{\beta}^{\mathrm{T}}(t)\boldsymbol{\beta}(t)\Big) + s_1(t)\tilde{\boldsymbol{\beta}}_1^{\mathrm{T}}(t)\boldsymbol{\Phi}(\boldsymbol{X}_1, \boldsymbol{X}_d)
\end{aligned} \tag{2.41}$$

Recalling (2.26), we may have

$$\dot{E}_1(t) \le -\frac{\dot{V}_1(t)}{g_m(t)} - K_2 s_1^2(t) + \frac{1}{2q}\boldsymbol{\beta}^{\mathrm{T}}(t)\boldsymbol{\beta}(t) \tag{2.42}$$

Denote $\beta_{\max} = \max\limits_{t\in[0,T]}\left\{\frac{1}{2q}\boldsymbol{\beta}^{\mathrm{T}}(t)\boldsymbol{\beta}(t)\right\}$. Integrating the above inequality over $[0, t]$ yields

$$E_1(t) - E_1(0) \le -\frac{1}{\overline{g}_m}V_1(t) - K_2\int_0^t s_1^2(\sigma)\mathrm{d}\sigma + t\cdot\beta_{\max} \tag{2.43}$$

Obviously, $E_1(0) = 0$, then inequality (2.43) can be transformed to

$$E_1(t) \le t\cdot\beta_{\max} < \infty \tag{2.44}$$

which, therefore, implies the boundedness of $E_1(t)$, so $E_k(t)$ is finite for any $k \in \mathbf{N}$.

(3) The convergence of tracking error

Applying (2.38) repeatedly, we have

$$E_k(t) = E_1(t) + \sum_{l=2}^{k}\Delta E_l(t)$$

$$< E_1(t) - \frac{1}{\bar{b}_m}\sum_{l=2}^{k} V_l(t) - \sum_{l=2}^{k} K_2 \int_0^t s_l^2(\sigma)\mathrm{d}\sigma$$

$$\leq E_1(t) - \sum_{l=2}^{k} K_2 \int_0^t s_l^2(\sigma)\mathrm{d}\sigma \tag{2.45}$$

Rewrite the above inequality as

$$\sum_{l=2}^{k} K_2 \int_0^t s_l^2(\sigma)\mathrm{d}\sigma \leq (E_1(t) - E_k(t)) \leq E_1(t) \tag{2.46}$$

Letting $t = T$ in (2.46) and taking the limitation of (2.46), it follows that

$$\lim_{k\to\infty}\sum_{l=2}^{k} \int_0^T s_l^2(\sigma)\mathrm{d}\sigma \leq \frac{1}{K_2}E_1(T) \tag{2.47}$$

Since $E_1(T)$ is bounded, according to the convergence theorem of the sum of series, we have $\lim\limits_{k\to\infty}\int_0^T s_k^2(\sigma)\mathrm{d}\sigma = 0$, which implies that $\lim\limits_{k\to\infty} s_k(t) = s_\infty(t) = 0$, $\forall t \in [0, T]$. Moreover, from the definition (2.6), we can know that if $|e_{sk}(t)| \leq \eta(t)$, then $s_k(t) = 0$, therefore, $\lim\limits_{k\to\infty}\int_0^T s_k^2(\sigma)\mathrm{d}\sigma = 0$ is equivalent to $\lim\limits_{k\to\infty}|e_{sk}(t)| \leq \eta(t)$, furthermore, $\lim\limits_{k\to\infty}\int_0^T (e_{sk}(\sigma))^2\mathrm{d}\sigma \leq \int_0^T (\eta(\sigma))^2\mathrm{d}\sigma$.

According to the boundedness of $E_k(t)$, we can obtain the boundedness of $\hat{\boldsymbol{\beta}}_k(t)$. Moreover, from the boundedness of $\boldsymbol{X}_d(t)$ we further get the boundedness of $x_{i,k}(t)$. Similar to case 1, the boundedness of $v_k(t)$ can be derived.

Summarizing above conclusions in two cases, we can see that the AILC scheme proposed in this chapter is able to ensure the boundedness of closed-loop signals and $\lim\limits_{k\to\infty}|e_{sk}(t)| \leq (1+m)\eta(t)$.Consequently, we can further get $\lim\limits_{k\to\infty}\int_0^T (e_{sk}(\sigma))^2\mathrm{d}\sigma \leq \varepsilon_e$, $\varepsilon_e = \int_0^T ((1+m)\eta(\sigma))^2\mathrm{d}\sigma = \frac{1}{2K}(1+m)^2\varepsilon^2\left(1 - e^{-2KT}\right) \leq \frac{1}{2K}(1+m)^2\varepsilon^2 = \varepsilon_{esk}$. Moreover, $e_{s\infty}(t)$ satisfy $\lim\limits_{k\to\infty}|e_{sk}(t)| = e_{s\infty}(t) = (1+m)\varepsilon e^{-Kt}$, $\forall t \in [0, T]$.

Next, we continue to prove the conclusion about transient performance in Theorem 2.1.

(4) Transient performance

Define the vector $\boldsymbol{\psi}_k(t) = \left[e_{1,k}(t), e_{2,k}(t), \cdots, e_{n-1,k}(t)\right]^{\mathrm{T}}$, then from the definition $e_{sk}(t) = \left[\boldsymbol{\Lambda}^{\mathrm{T}} 1\right]\boldsymbol{e}_k(t)$ we have

$$\dot{\boldsymbol{\psi}}_k(t) = \boldsymbol{A}_s\boldsymbol{\psi}_k(t) + \boldsymbol{b}_s e_{sk}(t) \tag{2.48}$$

where,

$$\boldsymbol{A}_s = \begin{bmatrix} 0 & 1 & \cdots & 0 \\ \vdots & \vdots & \ddots & \vdots \\ 0 & 0 & \cdots & 1 \\ -\lambda_1 & -\lambda_2 & \cdots & -\lambda_{n-1} \end{bmatrix} \in \mathbf{R}^{(n-1)\times(n-1)}, \boldsymbol{b}_s = \begin{bmatrix} 0 \\ \vdots \\ 0 \\ 1 \end{bmatrix} \in \mathbf{R}^{n-1} \tag{2.49}$$

with A_s being a stable matrix. According to the proposition in [35], there exist two constants $k_0 > 0$ and $\lambda_0 > 0$ such that $\left\|\mathrm{e}^{\boldsymbol{A}_s t}\right\| \le k_0 e^{-\lambda_0 t}$ [35]. The solution of $\dot{\boldsymbol{\psi}}_k(t)$ is

$$\boldsymbol{\psi}_k(t) = \mathrm{e}^{\boldsymbol{A}_s t}\boldsymbol{\psi}_k(0) + \int_0^t \mathrm{e}^{\boldsymbol{A}_s(t-\sigma)}\boldsymbol{b}_s e_{sk}(\sigma)\mathrm{d}\sigma \tag{2.50}$$

Hence, $\boldsymbol{\psi}_k(t)$ is bounded by

$$\left\|\boldsymbol{\psi}_k(t)\right\| \le k_0\left\|\boldsymbol{\psi}_k(0)\right\|\mathrm{e}^{-\lambda_0 t} + k_0\int_0^t \mathrm{e}^{-\lambda_0(t-\sigma)}|e_{sk}(\sigma)|\mathrm{d}\sigma \tag{2.51}$$

Choosing suitable parameter such that $\lambda_0 > K$. The from $\lim\limits_{k\to\infty}|e_{sk}(t)| \le (1+m)\eta(t)$ it follows

$$\begin{aligned} \left\|\boldsymbol{\psi}_\infty(t)\right\| &\le k_0\left\|\boldsymbol{\psi}_\infty(0)\right\|e^{-\lambda_0 t} + k_0\int_0^t \mathrm{e}^{-\lambda_0(t-\sigma)}|e_{s\infty}(\sigma)|\mathrm{d}\sigma \\ &\le k_0\left\|\boldsymbol{\psi}_\infty(0)\right\|e^{-\lambda_0 t} + (1+m)\varepsilon k_0\int_0^t \mathrm{e}^{-\lambda_0(t-\sigma)}\mathrm{e}^{-K\sigma}\mathrm{d}\sigma \\ &= k_0\left\|\boldsymbol{\psi}_\infty(0)\right\|e^{-\lambda_0 t} + (1+m)\varepsilon k_0\frac{1}{\lambda_0 - K}\left(\mathrm{e}^{-Kt} - \mathrm{e}^{-\lambda_0 t}\right) \\ &\le k_0\left\|\boldsymbol{\psi}_\infty(0)\right\| + \frac{1}{\lambda_0 - K}(1+m)\varepsilon k_0 \end{aligned} \tag{2.52}$$

Noting $e_{sk}(t) = \left[\boldsymbol{\Lambda}^{\mathrm{T}} 1\right]\boldsymbol{e}_k(t)$ and $\boldsymbol{e}_k(t) = \left[\boldsymbol{\psi}_k^{\mathrm{T}}(t)\, e_{n,k}(t)\right]^{\mathrm{T}}$, we have

$$\begin{aligned} \|\boldsymbol{e}_k(t)\| &\le \left\|\boldsymbol{\psi}_k(t)\right\| + \left|e_{n,k}(t)\right| \\ &= \left\|\boldsymbol{\psi}_k(t)\right\| + \left|e_{sk}(t) - \boldsymbol{\Lambda}^{\mathrm{T}}\boldsymbol{\psi}_k(t)\right| \\ &\le (1 + \|\boldsymbol{\Lambda}\|)\left\|\boldsymbol{\psi}_k(t)\right\| + |e_{sk}(t)| \end{aligned} \tag{2.53}$$

Combining (2.52) and (2.53), it results in

$$
\begin{aligned}
\|\boldsymbol{e}_{\infty}(t)\| &\leq (1+\|\boldsymbol{\Lambda}\|)\left\|\boldsymbol{\psi}_{\infty}(t)\right\| + |e_{s\infty}(t)| \\
&\leq k_0\left\|\boldsymbol{\psi}_{\infty}(0)\right\|e^{-\lambda_0 t} + (1+m)\varepsilon k_0\frac{1}{\lambda_0 - K}\left(\mathrm{e}^{-Kt} - \mathrm{e}^{-\lambda_0 t}\right) + (1+m)\eta(t) \\
&\leq (1+\|\boldsymbol{\Lambda}\|)\left(k_0\sum_{i=1}^{n-1}\sqrt{\varepsilon_i^2} + \frac{1}{\lambda_0 - K}(1+m)\varepsilon k_0\right) + (1+m)\eta(t) \\
&\leq (1+\|\boldsymbol{\Lambda}\|)\left(k_0\sum_{i=1}^{n-1}\sqrt{\varepsilon_i^2} + \frac{1}{\lambda_0 - K}(1+m)\varepsilon k_0\right) + (1+m)\varepsilon = \varepsilon_{e\infty}
\end{aligned}
\tag{2.54}
$$

According to $\left|e_{1,k}(t)\right| \leq \left\|\boldsymbol{\psi}_k(t)\right\|$ we can get

$$
\begin{aligned}
\left|e_{1,\infty}(t)\right| &\leq k_0\left\|\boldsymbol{\psi}_{\infty}(0)\right\|\mathrm{e}^{-\lambda_0 t} + (1+m)\varepsilon k_0\frac{1}{\lambda_0 - K}\left(\mathrm{e}^{-Kt} - \mathrm{e}^{-\lambda_0 t}\right) \\
&\leq k_0\sum_{i=1}^{n-1}\sqrt{\varepsilon_i^2} + \frac{1}{\lambda_0 - K}(1+m)\varepsilon k_0
\end{aligned}
\tag{2.55}
$$

This concludes the proof. □

2.5 Simulation Analysis

In this section, a simulation study is presented to verify the effectiveness of the AILC scheme. Consider the following second-order nonlinear system with unknown time-varying delays and unknown dead-zone:

$$
\begin{cases}
\dot{x}_{1,k}(t) = x_{2,k}(t) \\
\dot{x}_{2,k}(t) = f\left(\boldsymbol{X}_k, \boldsymbol{X}_{\tau,k}, \theta(t)\right) + g(t)u_k(t) + d(t) \\
y_k(t) = x_{1,k}(t),\ u_k(t) = D(v_k(t))
\end{cases}
\tag{2.56}
$$

where, $f\left(\boldsymbol{X}_k, \boldsymbol{X}_{\tau,k}, \theta(t)\right) = -\left(x_{1,k}(t) + x_{2,k}(t)\right)\theta(t) + \exp(-\theta(t)((x_{1,k}^{\tau}(t))^2 + (x_{2,k}^{\tau}(t))^2))$, $g(t) = 2 + 0.5\sin t$, $d(t) = 0.1\sin t$. The unknown time-varying delay is $\tau(t) = 0.5(1+\sin t)$, then $\tau_{\max} = 1$, $\theta(t) = |\cos(t)|$. It can be easily verified that

$$
\left|\exp\left(-\theta(t)\|\boldsymbol{X}_k\|^2\right) - \exp\left(-\theta(t)\|\boldsymbol{X}_d\|^2\right)\right| \leq \|\boldsymbol{X}_k - \boldsymbol{X}_d\|\sqrt{2|\theta(t)|}e^{-0.5}
$$

Obviously, this system has the typical form of (2.1), and it satisfies Assumptions 2.1–2.3 and 2.5–2.7. Moreover, it is clear that $h_1 = 1$, $h_2 = 1$.

2.5.1 Verification of the AILC Scheme

To test above conclusion, conduct the following two experiments.

Experiment 1 The desired reference trajectory is given by $\boldsymbol{X}_d(t) = [\sin t, \cos t]^{\mathrm{T}}$. The design parameters are chosen as $\varepsilon_1 = \varepsilon_2 = 1$, $\lambda = 2$, $K = 3$, $K_1 = 2$, $q = 1$, $b = 5$, $\varepsilon = \lambda\varepsilon_1 + \varepsilon_2 = 3$. The parameters for dead-zone nonlinearity is specified by $m = 1 + 0.2 \sin t$, $b_r = 0.25$, $b_l = -0.25$. The initial condition for $x_{1,k}(0)$ and $x_{2,k}(0)$ are generated randomly on intervals $[-0.5, 0.5]$ and $[0.5, 1.5]$, respectively. The system runs on the interval [0, 10] for ten iterations. Part simulation results are presented in Figs. 2.4, 2.5, 2.6, 2.7 and 2.8.

Figures 2.4 and 2.5 show the tracking curves of the 1st iteration ($k = 1$) and the 10th iteration (k = 10), respectively, which shows that the tracking performance has been improved through nine times of learning. In Fig. 2.5, we can see that the it has achieved complete tracking except for the initial stage that is influenced by resetting error. This improvement performance is clearly shown by Fig. 2.8. Figures 2.6 and 2.7 show the control curves of the 1st iteration and 10th iteration respectively, which shows the boundedness of control signal and the influence of dead-zone nonlinearity.

Experiment 2 To show the control performance for more complicated desired reference trajectory, we choose the desired reference signal as $\boldsymbol{X}_d(t) = [\sin t + \sin(1.5t), \cos t + 1.5\cos(1.5t)]^{\mathrm{T}}$. The design parameters keep the same as Experiment 1. The initial conditions for states $x_{1,k}(0)$ and $x_{2,k}(0)$ are generated randomly on the intervals $[-0.5, 0.5]$ and $[2, 3]$ respectively. The system runs on

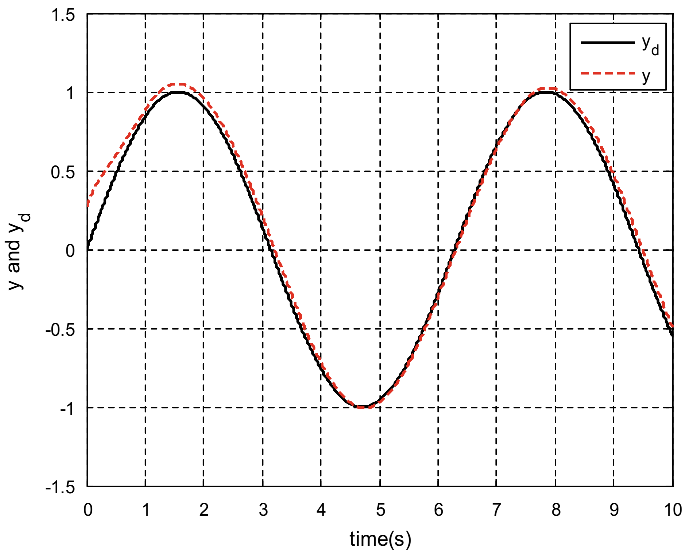

Fig. 2.4 System output y_k versus y_d ($k = 1$)

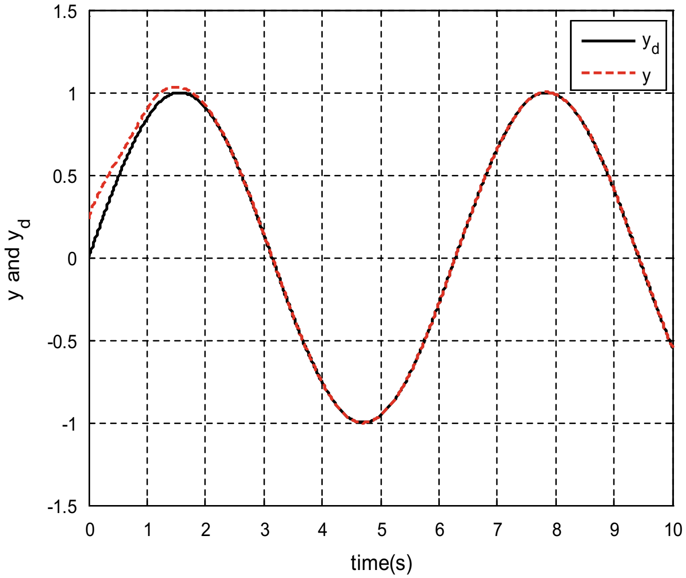

Fig. 2.5 System output y_k versus y_d ($k = 10$)

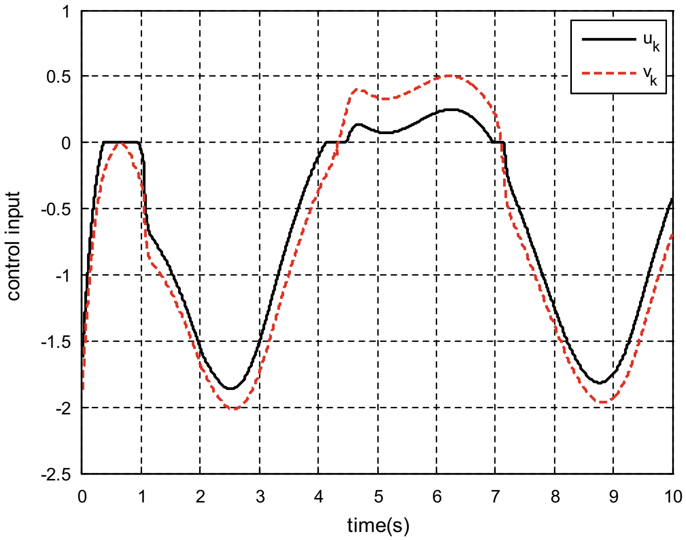

Fig. 2.6 The input v_k and output u_k of dead-zone characteristic ($k = 1$)

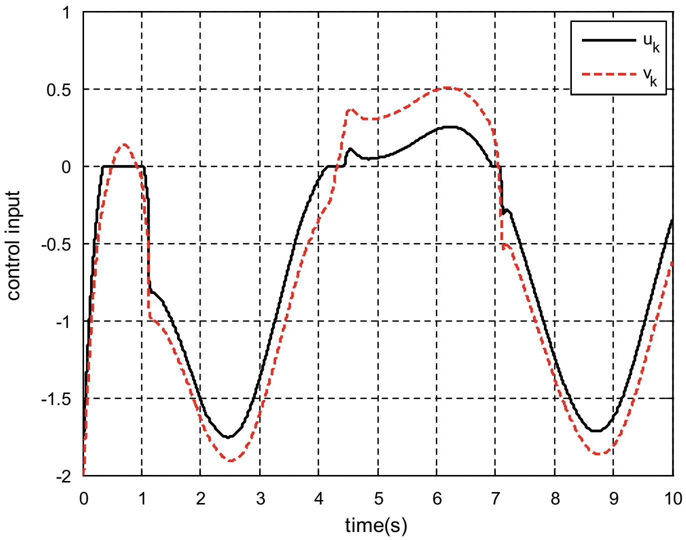

Fig. 2.7 The input v_k and output u_k dead-zone characteristic ($k = 10$)

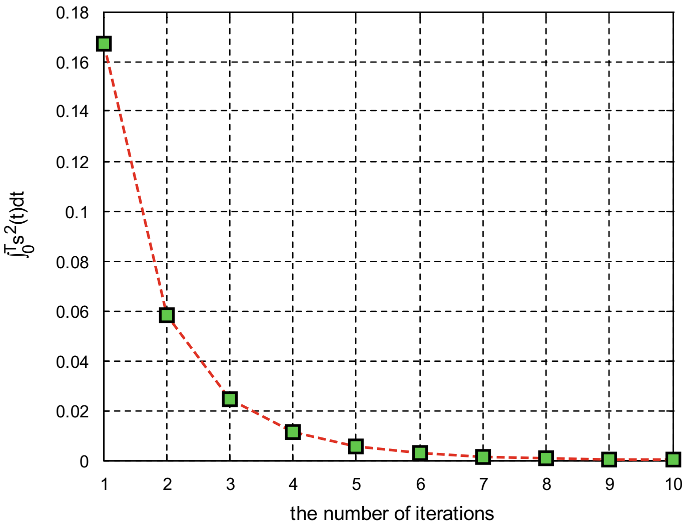

Fig. 2.8 $\int_0^T s_k^2(t)\mathrm{d}t$ versus the number of iterations (Experiment 1)

finite time interval [0, 10] for ten iterations. The simulation results are presented in Figs. 2.9, 2.10, 2.11, 2.12 and 2.13.

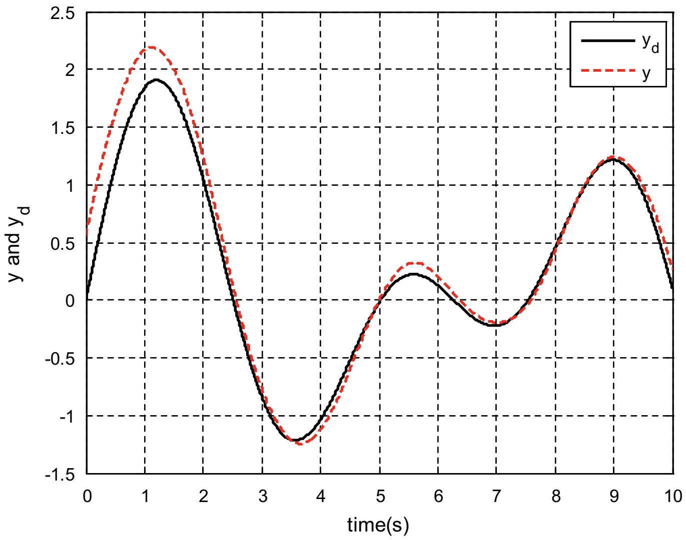

Fig. 2.9 System output y_k versus y_d ($k = 1$)

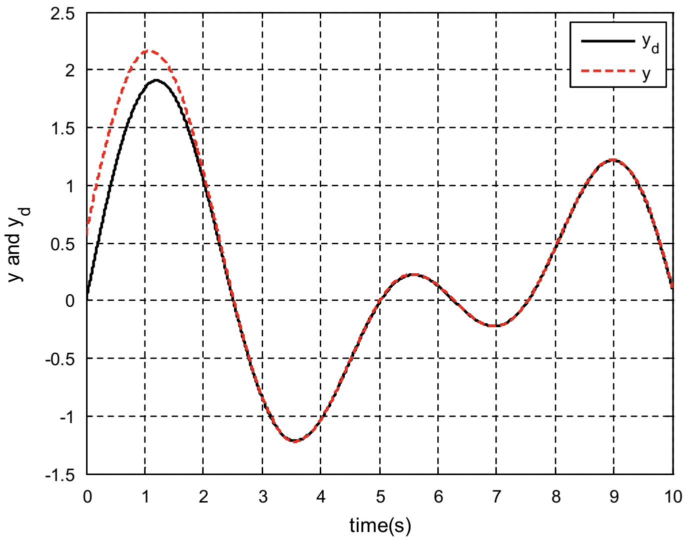

Fig. 2.10 System output y_k versus y_d ($k = 10$)

As shown in simulation Figure s, we can see that the proposed controller can also achieve perfect tracking performance for more complicated desired trajectory and accomplish the control objective.

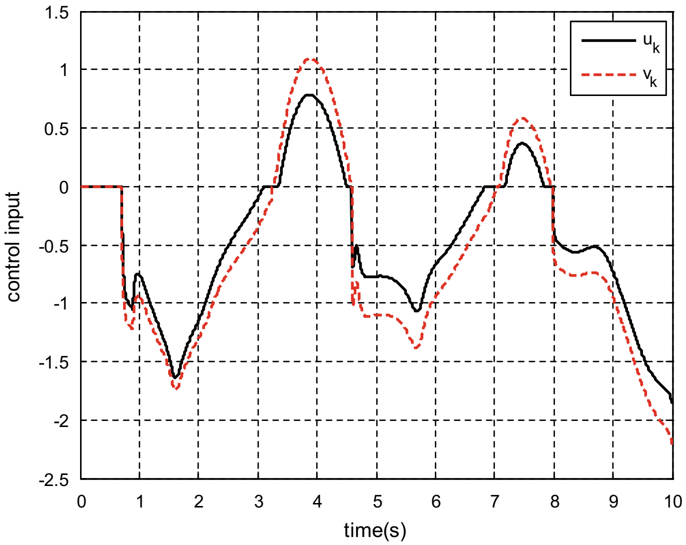

Fig. 2.11 The input v_k and output u_k of dead-zone characteristic ($k = 1$)

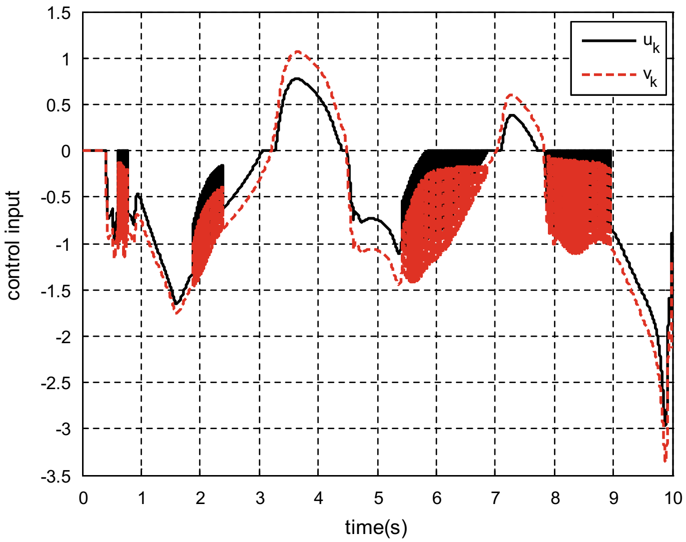

Fig. 2.12 The input y_k and output u_k of dead-zone characteristic ($k = 10$)

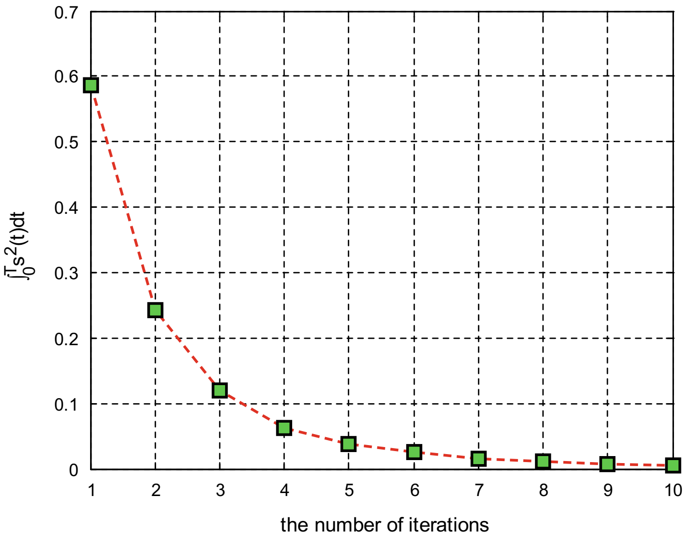

Fig. 2.13 $\int_0^T s_k^2(t)dt$ versus the number of iterations (Experiment 2)

2.5.2 Comparison Simulation: Adaptive Control

Experiment 3 Finally, the contribution of this chapter is shown by comparing the proposed controller with traditional adaptive controller. In adaptive control, the controller remains unchanged, but instead of (2.24) the adaptive law for unknown parameter changes to the σ-modification form which is given by

$$\dot{\hat{\beta}}(t) = -\mathbf{\Gamma}\Big[\mathbf{\Phi}_k(t)s_k + \sigma\hat{\boldsymbol{\beta}}(t)\Big], \hat{\boldsymbol{\beta}}(0) = 0$$

The design parameters are chosen as $\mathbf{\Gamma} = \mathrm{diag}\{0.01\}, \sigma = 0.5$. The desired reference signal is $\boldsymbol{X}_d(t) = [\sin t, \cos t]^{\mathrm{T}}$, other design parameters keeps the same as Experiment 1. As traditional adaptive controller runs in time domain, the notation “k” here doesn’t have any practical meaning. Figures 2.14, 2.15 and 2.16 provide the simulation results. From the simulation results shown below, it is obvious that the adaptive controller is unable to achieve good tracking performance, and the tracking error exists all the time and can’t be eliminated by adaptive law.

As observed in simulation results above, the proposed AILC can achieve a good tracking performance for parameterized nonlinear time-delay systems preceded by dead-zone characteristic and tracking errors decrease along the iteration axis, which demonstrates the validity of the proposed AILC approach in this chapter and achieve the control design objective.

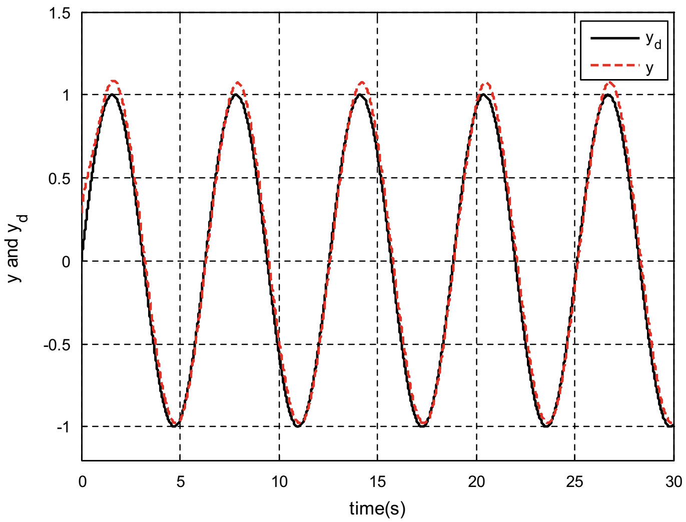

Fig. 2.14 The system output y_k versus desired trajectory y_d (Experiment 3)

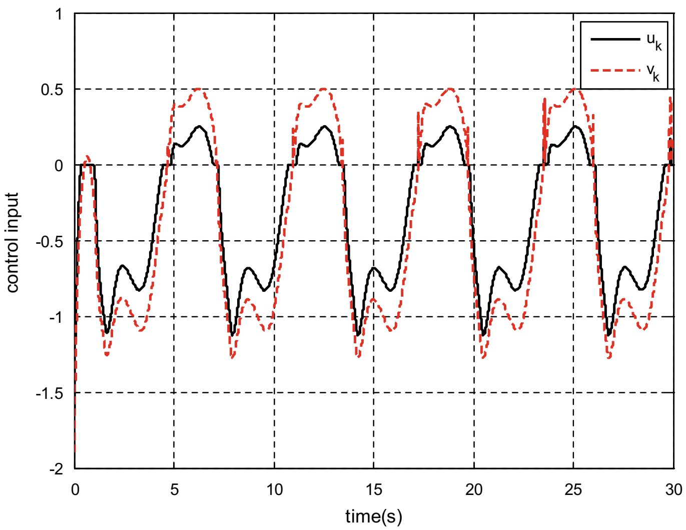

Fig. 2.15 The input v_k and output u_k of dead-zone characteristic (Experiment 3)

2.6 Summary and Comments

In this chapter, based on a deep investigation of research results concerning nonlinear systems with time-delay and dead-zone, a new AILC scheme is proposed for a class of nonlinear time-varying systems with unknown time-varying time-delays and

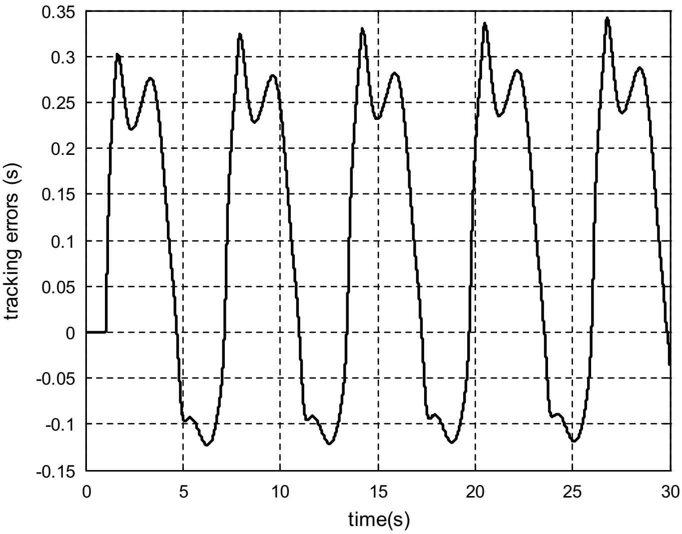

Fig. 2.16 The curve of tracking error $s\,(t)$

unknown input dead-zone nonlinearity running on a finite time interval repetitively. Firstly, a novel representation with time-varying slope for the dead-zone nonlinearity characteristic is built, this model for dead-zone is very simple in form and broadly representative. Using appropriate Lyapunov-Krasovskii functional in the Lyapunov function candidate, the uncertainties from unknown time-varying delays are removed such that control law is delay-independent. The identical initial condition for ILC has been relaxed by introducing the boundary layer function. The hyperbolic tangent function is employed to avoid the possible singularity problem, which guarantee the continuity of control signal. Theoretical analysis by constructing Lyapunov-like CEF has shown that the tracking errors converge to a small residual domain around the origin as iteration goes to infinity. At the same time, all the closed-loop signals remain bounded. Simulation results have been provided to show the effectiveness the proposed control scheme and the advantage in tackling this kind systems compared with traditional adaptive control method. The proposed AILC strategy widens the applicable scope of AILC and may provide useful reference ideas for relevant research.

References

1. Ge S S, Hong F, Lee T H. Adaptive neural control of nonlinear time-delay systems with unknown virtual control coefficients[J]. IEEE Transactions on Systems, Man, and Cybernetics, Part B: Cybernetics, 2004, 34(1): 499–516.
2. Ge S S, Hong F, Lee T H. Robust adaptive control of nonlinear systems with unknown time delays[J]. Automatica, 2005, 41(7): 1181–1190.

3. Zhang T P, Ge S S. Adaptive neural control of MIMO nonlinear state time-varying delay systems with unknown dead-zones and gain signs[J]. Automatica, 2007, 43(6): 1021–1033.
4. Bresch-Pietri D, Chauvin J, Petit N. Adaptive control scheme for uncertain time-delay systems[J]. Automatica, 2012, 48(8): 1536–1552.
5. Zhang X, Liu L, Feng G, et al. Output feedback control of large-scale nonlinear time-delay systems in lower triangular form[J]. Automatica, 2013, 49(11): 3476–3483.
6. Zhou B. Truncated predictor feedback for time-delay systems[M]. Heidelberg: Springer, 2014.
7. Zhang X, Lin Y. Adaptive output feedback control for a class of large-scale nonlinear time-delay systems[J]. Automatica, 2015, 52: 87–94.
8. Meng D, Jia Y, Du J, et al. Robust iterative learning control design for uncertain time-delay systems based on a performance index[J]. IET Control Theory & Applications, 2010, 4(5): 759–772.
9. Chen Y, Gong Z, Wen C. Analysis of a high-order iterative learning control algorithm for uncertain nonlinear systems with state delays[J]. Automatica, 1998, 34(3): 345–353.
10. Sun M, Wang D. Iterative learning control design for uncertain dynamic systems with delayed states[J]. Dynamics and Control, 2000, 10(4): 341–357.
11. Sun M, Wang D. Initial condition issues on iterative learning control for non-linear systems with time delay[J]. International Journal of Systems Science, 2001, 32(11): 1365–1375.
12. Jun-min Li. Adaptive iterative learning control for nonlinearly parameterized systems with time-varying delays[J]. Acta Mathematica Scientia, 2011, 31A(3): 682–290.
13. Jun-min Li, Yuan-liang Wang, Xin-min Li. Adaptive iterative learning control for nonlinear parameterized-systems with unknown time-varying delays[J]. Control Theory & Applications, 2011, 28(6): 861–868.
14. Chen W, Zhang L. Adaptive iterative learning control for nonlinearly parameterized systems with unknown time-varying delays[J]. International Journal of Control, Automation and Systems, 2010, 8(2): 177–186.
15. Zhang C L, Li J M. Adaptive iterative learning control for nonlinear time-delay systems with periodic disturbances using FSE-neural network[J]. International Journal of Automation and Computing, 2011, 8(4): 403–410.
16. Li D, Li J M. Adaptive iterative learning control for nonlinearly parameterized systems with unknown time-varying delay and unknown control direction[J]. International Journal of Automation and Computing, 2012, 9(6): 578–586.
17. Fan L. Iterative learning and adaptive fault-tolerant control with application to high-speed trains under unknown speed delays and control input saturations[J]. IET Control Theory & Applications, 2014, 8(9): 675–687.
18. Li J, Li X, Xing K. Hybrid adaptive iterative learning control of non-uniform trajectory tracking for nonlinear time-delay systems[C]. Proceedings of the 26th Chinese Control Conference, Zhangjiajie, China, 2007: 515–519.
19. Zhang R, Hou Z, Chi R H, et al. Adaptive iterative learning control for nonlinearly parameterised systems with unknown time-varying delays and input saturations[J]. International Journal of Control, 2015, 88(6): 1133–1141.
20. Ji H, Hou Z, Zhang R. Adaptive iterative learning control for high-speed trains with unknown speed delays and input saturations[J]. IEEE Transactions on Automation Science and Engineering, 2015, 13(1): 260–273.
21. Hale J K. Functional differential equations[M]. Berlin Heidelberg: Springer, 1971.
22. Tao G, Kokotovic P V. Adaptive control of plants with unknown dead-zones[J]. IEEE Transactions on Automatic Control, 1994, 39(1): 59–68.
23. Wang X S, Hong H, Su C Y. Model reference adaptive control of continuous-time systems with an unknown input dead-zone[J]. IEE Proceedings-Control Theory and Applications, 2003, 150(3): 261–266.
24. Tang X, Tao G, Joshi S M. Adaptive actuator failure compensation for parametric strict feedback systems and an aircraft application[J]. Automatica, 2003, 39(11): 1975–1982.
25. Wang X S, Su C Y, Hong H. Robust adaptive control of a class of nonlinear systems with unknown dead-zone[J]. Automatica, 2004, 40(3): 407–413.

26. Zhang T P, Ge S S. Adaptive dynamic surface control of nonlinear systems with unknown dead zone in pure feedback form[J]. Automatica, 2008, 44(7): 1895–1903.
27. Zhang T, Ge S S. Adaptive neural network tracking control of MIMO nonlinear systems with unknown dead zones and control directions[J]. IEEE Transactions on Neural Networks, 2009, 20(3): 483–497.
28. Ma H J, Yang G H. Adaptive output control of uncertain nonlinear systems with non-symmetric dead-zone input[J]. Automatica, 2010, 46(2): 413–420.
29. Gao Y, Tong S, Li Y. Fuzzy adaptive output feedback DSC design for SISO nonlinear stochastic systems with unknown control directions and dead-zones[J]. Neurocomputing, 2015, 167: 187–194.
30. Xu J X, Xu J, Lee T H. Iterative learning control for systems with input deadzone[J]. IEEE Transactions on Automatic Control, 2005, 50(9): 1455–1459.
31. Shen D, Mu Y, Xiong G. Iterative learning control for non-linear systems with deadzone input and time delay in presence of measurement noise[J]. IET control theory & applications, 2011, 5(12): 1418–1425.
32. Xu J X, Xu J, Lee T. Iterative learning control for a linear piezoelectric motor with a nonlinear unknown input deadzone[C]. Proc. of the 2004 IEEE Conference on Control Applications. 2004: 1001–1006.
33. Sheng Zhu, Ming-xuan Sun. Iterative learning control of a class of nonlinear systems with unknown input dead-zone[J]. Control and Decision, 2009, 24(1): 96–100.
34. Ge S S, Lee K P. Adaptive dynamic surface control of nonlinear systems with unknown dead zone in pure feedback form[J]. Automatica, 2007, 43(1): 31–43.
35. Ioannou P A, Sun J. Robust Adaptive Control[M]. Prentice-Hall, Englewood Cliffs, NJ, USA, 1995.

Chapter 3
NN AILC of Nonlinear Time-Delay Systems

3.1 Introduction

In Chap. 2, we solve the AILC problem of a class of nonlinear parameterized time-delay systems with dead-zone input that is described by (2.1). However, if the systems don't satisfy the parameterized condition, the proposed method in Chap. 2 is not yet applicable. In this chapter, we will investigate the AILC problem for a class of non-parameterized nonlinear systems with unknown dead-zone input and time-varying delays.

When there exist non-parameterized uncertainties in systems, neural networks or fuzzy logic systems are useful tool in dealing with them. Chien et al. employed fuzzy logic systems or fuzzy neural networks approximation technique and designed AILC scheme for SISO nonlinear systems, distributed interconnected large systems, non-affine nonlinear interconnected systems respectively, with difference-type adaptive law for estimating weights. In [1], Zhu utilized RBF NN to approximate the nonlinear uncertainty and designed differential-type adaptive law to estimate the NN weight. To deal with time-varying uncertainties, Prof. Sun put forward a kind of time-varying neural network [2, 3] whose optimal weights are time-varying. In this case, the NN weight can't be estimated by differential-type adaptive law, and Sun designed a kind of weight updating form along iteration axis and proved the convergence of approximation error by using least square method. By using time-varying NN, they designed AILC schemes for several classes of systems [1, 4, 5] and difference-type adaptive updating law for time-varying optimal weight.

In this chapter, we will study a class of nonlinear systems with unknown time-varying delay, dead-zone input and time-varying nonlinearity. The influences of these factors make it very difficult to design effective control scheme and existing methods in both time domain and iterative domain are not applicable. Here, we will employ time-varying NN technique to design a novel AILC scheme aiming at solving this control problem.

J. Wei et al., *Iterative Learning Control for Nonlinear Time-Delay System*,
https://doi.org/10.1007/978-981-19-6317-9_3

3.2 Problem Formulation and Preliminaries

3.2.1 Problem Formulation

In this paper, we consider a class of nonlinear time-varying systems with unknown time-varying delays and dead-zone running over a finite time interval $[0, T]$ repeatedly, that is described by

$$\begin{cases} \dot{x}_{i,k}(t) = x_{i+1,k}(t), i = 1, \ldots, n-1 \\ \dot{x}_{n,k}(t) = f(\boldsymbol{X}_k(t), t) + h\big(\boldsymbol{X}_{\tau,k}(t), t\big) + g(\boldsymbol{X}_k(t), t)u_k(t) + d(t) \\ y_k(t) = x_{1,k}(t), u_k(t) = D(v_k(t)), t \in [0, T] \\ x_{i,k}(t) = \varpi_i(t), t \in [-\tau_{\max}, 0), i = 1, \ldots, n \end{cases} \tag{3.1}$$

where, most notations are as same as that in previous chapter. What is different is that, $\tau_i(t)$ denote unknown time-varying delays of states, and $x_{\tau_i,k} \triangleq x_{i,k}(t - \tau_i(t))$, $i = 2, \ldots, n$, $\boldsymbol{X}_{\tau,k}(t) = \big[x_{\tau_1,k}(t), \ldots, x_{\tau_n,k}(t)\big]^{\mathrm{T}}$ denotes a vector of time-delay states; $f(\cdot, \cdot)$ and $g(\cdot, \cdot)$ are unknown smooth continuous functions; $h(\cdot, \cdot)$ is an unknown bounded continuous function of time-delay states. Here we will still consider the influence of dead-zone characteristic and use the model (2.3), where $v_k(t) \in R$ and $u_k(t)$ represent the input and output of dead-zone respectively. Moreover, the Assumption 2.8 on dead-zone model still holds her.

Remark 3.1 Comparing (2.1) with (3.1), we can see that, different from the controlled object in Chap. 2 in which the time delays of all states are same, the time delays of all states in (3.1) are independent of each other, which is consistent with practical situation.

The control objective of this chapter remains the same as Chap. 2. Before the control system design, we need to make some assumptions.

Assumption 3.1 The unknown state time-varying delays $\tau_i(t)$ satisfy $0 \leq \tau_i(t) \leq \tau_{\max}$, $\dot{\tau}_i(t) \leq \kappa < 1$, $i = 1, 2, \ldots, n$, where $\tau_{\max}$ and κ are unknown positive constants.

Assumption 3.2 The unknown smooth continuous function $h(\cdot, \cdot)$ satisfy the following inequality

$$\big|h\big(\boldsymbol{X}_{\tau,k}, t\big)\big| \leq \theta(t) \sum_{j=1}^{n} \rho_j\big(x_{\tau_j,k}(t)\big) \tag{3.2}$$

where $\theta(t)$ is unknown time-varying parameter, $\rho_j(\cdot)$ $j = 1, 2, \ldots, n)$ are known positive smooth functions.

Assumption 3.3 The sign of $h(\cdot,\cdot)$ is known, and there exist constants $0 < g_{\min} \leq g_{\max}$ such that $g_{min} \leq |g(\cdot,\cdot)| \leq g_{max}$). Without loss of generality, we always assume $g(\cdot,\cdot) > 0$.

The assumptions on initial resetting errors, desired state trajectories and unknown disturbance remain the same as Chap. 2.

Remark 3.2 Assumption 3.2 is mild on $h(\cdot,\cdot)$. Since $h(\cdot,\cdot)$ is continuous and smooth on $[0, T]$, then it is obvious that $h(\cdot,\cdot)$ is bounded on $[0, T]$. Compared with the assumption of local Lipschitz condition with known upper bound functions in [6–10], this assumption is largely relaxed and can be easily satisfied. Actually, $\rho_j(\cdot)$ are not necessarily known, because they are approximated by NNs as part of the uncertainties, which will be discussed in detail later.

Remark 3.3 The control gain bounds $g_{\min}$ and $g_{\max}$ are only required for analytical purposes, their true values are not necessarily known since they are not used for controller design.

3.2.2 RBF Neural Network

For control engineering, two types of artificial neural networks are usually used as approximator to approximate unknown functions, which specifically are linearly parameterized neural networks (LPNNs) and multilayer neural networks (MNNs). As a kind of LPNNs, the radial basis function (RBF) neural network (NN) [11] is usually used as a tool to model unknown nonlinear functions owing to its nice approximation capabilities. The RBF NN has attracted much attention because of its simple form and avoidance of unnecessary and lengthy computation and widely used in pattern recognition and control problems [12, 13]. Research shows that RBF NN is able to approximate any continuous functions with arbitrarily high accuracy on a compact set [12]. The RBF NN is a two-layer network whose structure is presented in Fig. 3.1, which implies that the input space is mapped into a new space. The hidden layer of RBF performs a fixed nonlinear transformation with no adjustable parameters, and the output layer then combines the outputs linearly.

Generally, the RBF NN is described as

$$Q_{nn}(\boldsymbol{Z}) = \boldsymbol{W}^{\mathrm{T}}\boldsymbol{\phi}(\boldsymbol{Z}) \tag{3.3}$$

where, $\boldsymbol{Z} \in \boldsymbol{\Omega}_Z \subset \mathbf{R}^q$ in the input vector, $\boldsymbol{W} = [w_1, w_2, \ldots, w_l]^{\mathrm{T}} \in \mathbf{R}^l$ is the weight vector, the number of neurons is $l > 1$, the basis function vector is expressed as $\boldsymbol{\phi}(\boldsymbol{Z}) = [\varphi_1(\boldsymbol{Z}), \ldots, \varphi_l(\boldsymbol{Z})]^{\mathrm{T}}$, $\varphi_i(\boldsymbol{Z})$ denotes the commonly used Gaussian function, i.e., $\varphi_i(\boldsymbol{Z}) = e^{-(\boldsymbol{Z}-\boldsymbol{\mu}_i)^{\mathrm{T}}(\boldsymbol{Z}-\boldsymbol{\mu}_i)/\sigma_i^2}$, $i = 1, \ldots, l$, $\boldsymbol{\mu}_i = \left[\mu_{i1}, \mu_{i2}, \ldots, \mu_{iq}\right]^{\mathrm{T}}$ is the center of the receptive field, σ_i is the width of Gaussian function. It has been proven that the RBF NN can approximate any continuous nonlinear function $Q(\boldsymbol{Z})$ in the

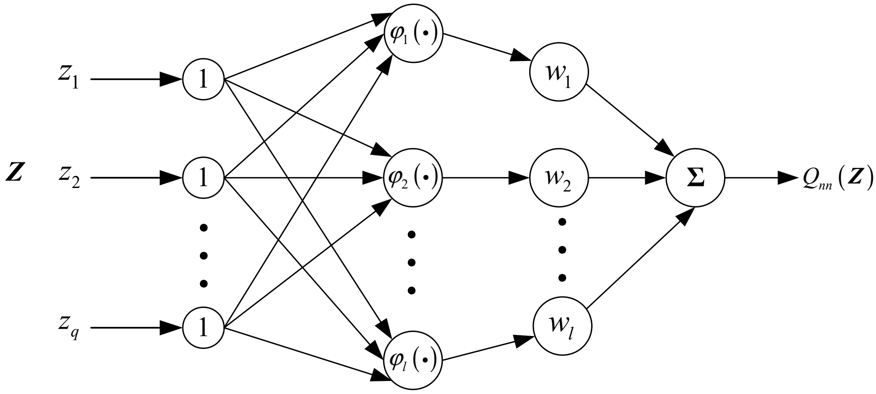

Fig. 3.1 The structure of RBF NN

form of $Q(\boldsymbol{Z}) = \boldsymbol{W}^{*\mathrm{T}}\boldsymbol{\phi}(\boldsymbol{Z}) + \varepsilon(\boldsymbol{Z})$ on a compact set $\boldsymbol{\Omega}_Z \subset \mathbf{R}^q$ with arbitrarily high accuracy provided $l > 1$ is sufficiently large, $\forall \boldsymbol{Z} \in \boldsymbol{\Omega}_Z \subset \mathbf{R}^q$, where $\boldsymbol{W}^*$ is the optimal constant weight vector, $\varepsilon(\boldsymbol{Z})$ is the NN approximation error which is bounded on the compact set, i.e., $|\varepsilon(\boldsymbol{Z})| \le \varepsilon^*$, $\forall \boldsymbol{Z} \in \boldsymbol{\Omega}_Z$, with $\varepsilon^* > 0$ as an unknown constant upper bound. The optimal weight vector $\boldsymbol{W}^*$ represents the ideal value for NN weight and only used for analytical purposes, it is defined as the value $\boldsymbol{W}$ of that can minimize $|\varepsilon(\boldsymbol{Z})|$ for all $\boldsymbol{Z} \in \boldsymbol{\Omega}_Z \subset \mathbf{R}^q$, i.e., $\boldsymbol{W}^* := \arg\min_{\boldsymbol{W}\in R^l}\left\{\sup_{\boldsymbol{Z}\in\boldsymbol{\Omega}_Z}\left|h(\boldsymbol{Z}) - \boldsymbol{W}^{\mathrm{T}}\boldsymbol{\phi}(\boldsymbol{Z})\right|\right\}$.

In control system design, when neural networks are used to approximate unknown functions, updating laws for estimating the weight vector need to be designed. In the early stage, the gradient-based back-propagation algorithms and its variants are the most popular algorithms for training neural networks. Along with the applications in traditional adaptive control framework, differential type learning laws were developed in the control scheme design and stability analysis by using Lyapunov method. Over the past few decades, a large number of adaptive neural control schemes have been presented [12, 14–20], However, difficulties arise when using (3.3) to approximate unknown time-varying function $Q(\boldsymbol{Z}, t)$ in the form of $Q(\boldsymbol{Z}) = \boldsymbol{W}^{*\mathrm{T}}\boldsymbol{\phi}(\boldsymbol{Z}) + \varepsilon(\boldsymbol{Z})$. In order to deal with this problem, a kind of time-varying neural networks is proposed to approximate the unknown time-varying functions in the form of

$$Q(\boldsymbol{Z}, t) = \boldsymbol{W}^{*\mathrm{T}}(t)\boldsymbol{\phi}(\boldsymbol{Z}) + \varepsilon(\boldsymbol{Z}, t) \tag{3.4}$$

where, the ideal weight vector $\boldsymbol{W}^*(t)$ is time-varying as well. In ILC design, we can design adaptive laws along iteration axis to estimate $\boldsymbol{W}^*(t)$.

3.3 RBF NN AILC Design

The definitions of $e_{sk}(t)$ and $s_k(t)$ remain the same as Chap. 2. It follows from the definition of $s_k(t)$ that

$$s_k(t)\text{sat}\left(\frac{e_{sk}(t)}{\eta(t)}\right) = \begin{cases} 0, & if \left|\frac{e_{sk}(t)}{\eta(t)}\right| \le 1 \\ s_k(t)\text{sgn}(e_{sk}(t)), & if \left|\frac{e_{sk}(t)}{\eta(t)}\right| > 1 \end{cases}$$
$$= s_k(t)\text{sgn}(s_k(t)) = |s_k(t)| \tag{3.5}$$

According to Eq. (3.1) and the definition of tracking errors, we can get the dynamical equation of $e_{n,k}(t)$ as follows

$$\begin{aligned}\dot{e}_{n,k}(t) &= f(\boldsymbol{X}_k(t),t) + h\big(\boldsymbol{X}_{\tau,k}(t),t\big) + g(\boldsymbol{X}_k(t),t)u_k + d(t) - y_d^{(n)}(t) \\ &= f(\boldsymbol{X}_k(t),t) + h\big(\boldsymbol{X}_{\tau,k}(t),t\big) + g(\boldsymbol{X}_k(t),t)(m(t)v_k(t) - d_1(v_k(t))) \\ &\quad + d(t) - y_d^{(n)}(t) \\ &= f(\boldsymbol{X}_k(t),t) + h\big(\boldsymbol{X}_{\tau,k}(t),t\big) + g(\boldsymbol{X}_k(t),t)m(t)v_k(t) \\ &\quad + d_2(\boldsymbol{X}_k(t),t) - y_d^{(n)}(t)\end{aligned} \tag{3.6}$$

where, $d_2(\boldsymbol{X}_k(t),t) = -g(\boldsymbol{X}_k(t),t)d_1(v_k(t)) + d(t)$. From Assumption 3.3, Assumption 2.6 and Assumption 2.8, we know that $d_2(\boldsymbol{X}_k,t)$ is bounded, i.e., there exists an un known continuous positive function $\overline{d}(\boldsymbol{X}_k)$ satisfying $|d_2(\boldsymbol{X}_k,t)| \le \overline{d}(\boldsymbol{X}_k)$. For the simplification of expression, denote $g_m(\boldsymbol{X}_k(t),t) \triangleq g(\boldsymbol{X}_k(t),t)m(t)$. It is clear that $\underline{g}_m = m_{\min}g_{\min} \le g_m(x_k,t) \le m_{\max}g_{\max} = \overline{g}_m$.

Choose the Lyapunov function as

$$V_{s_k}(t) = \frac{1}{2}s_k^2(t) \tag{3.7}$$

Taking the derivative of $V_{s_k}(t)$ along (3.6), it results in

$$\begin{aligned}\dot{V}_{s_k}(t) &= s_k(t)\dot{s}_k(t) \\ &= s_k(t)(\dot{e}_{sk}(t) - \dot{\eta}(t)\text{sgn}(s_k(t))) \\ &= s_k(t)\Bigg[\sum_{j=1}^{n-1}\lambda_j e_{j+1,k}(t) - \dot{\eta}(t)\text{sgn}(s_k(t)) + f(\boldsymbol{X}_k(t),t) + h\big(\boldsymbol{X}_{\tau,k}(t),t\big) \\ &\qquad + g_m(\boldsymbol{X}_k(t),t)v_k(t) + d_2(\boldsymbol{X}_k(t),t) - y_d^{(n)}(t)\Bigg] \\ &= s_k(t)\Bigg[\sum_{j=1}^{n-1}\lambda_j e_{j+1,k}(t) + Ke_{sk}(t) - Ke_{sk}(t)\end{aligned}$$

$$
\begin{aligned}
&+ K\eta(t)\mathrm{sgn}(s_k(t)) + f(\boldsymbol{X}_k(t), t) \\
&+h\big(\boldsymbol{X}_{\tau,k}(t), t\big) + g_m(\boldsymbol{X}_k(t), t)v_k(t) + d_2(\boldsymbol{X}_k(t), t) - y_d^{(n)}(t)\Big] \\
&= s_k(t)\big[\big(f(\boldsymbol{X}_k(t), t) + h\big(\boldsymbol{X}_{\tau,k}(t), t\big) + g_m(\boldsymbol{X}_k(t), t)v_k(t) \\
&+\mu_k(t) + d_2(\boldsymbol{X}_k(t), t)\big] - Ks_k^2(t)
\end{aligned}
\tag{3.8}
$$

where, $\mu_k(t) = \sum_{j=1}^{n-1}\lambda_j e_{j+1,k}(t) + Ke_{sk}(t) - y_d^{(n)}(t)$ and using the relationship (2.13).

Using Youngs inequality and noting Assumption 3, we have

$$
\begin{aligned}
s_k(t)h\big(\boldsymbol{X}_{\tau,k}(t), t\big) &\le |s_k(t)|\theta(t)\sum_{j=1}^{n}\rho_j\big(x_{\tau_j,k}(t)\big) \\
&\le \frac{n}{2}s_k^2(t)\theta^2(t) + \frac{1}{2}\sum_{j=1}^{n}\rho_j^2\big(x_{\tau_j,k}(t)\big)
\end{aligned}
\tag{3.9}
$$

$$
s_k(t)d_2(\boldsymbol{X}_k(t), t) \le \frac{s_k^2(t)\overline{d}^2(\boldsymbol{X}_k(t))}{2a_1^2} + \frac{a_1^2}{2}
\tag{3.10}
$$

where, a_1 is a given arbitrary positive constant.

Substituting (3.9) and (3.10) back into (3.8) yields

$$
\begin{aligned}
\dot{V}_{s_k}(t) \le s_k(t)\Big[&(f(\boldsymbol{X}_k(t), t) + g_m(\boldsymbol{X}_k(t), t)v_k(t) + \mu_k(t) + \frac{n}{2}s_k(t)\theta^2(t) \\
&+\frac{s_k(t)\overline{d}^2(\boldsymbol{X}_k(t))}{2a_1^2}\Big] - Ks_k^2(t) + \frac{1}{2}\sum_{j=1}^{n}\rho_j^2\big(x_{\tau_j,k}(t)\big) + \frac{a_1^2}{2}
\end{aligned}
\tag{3.11}
$$

To overcome the design difficulty arising from the unknown time-varying delay term $\rho_j^2\big(x_{\tau_j,k}(t)\big)$, consider the following Lyapunov–Krasovskii functional

$$
V_{U_k}(t) = \frac{1}{2(1-\kappa)}\sum_{j=1}^{n}\int_{t-\tau_j(t)}^{t}\rho_j^2\big(x_{j,k}(\sigma)\big)\mathrm{d}\sigma
\tag{3.12}
$$

Recalling Assumption 3.1, taking the time derivative of $V_{U_k}(t)$ leads to

$$
\begin{aligned}
\dot{V}_{U_k}(t) &= \frac{1}{2(1-\kappa)}\sum_{j=1}^{n}\rho_j^2\big(x_{j,k}\big) - \frac{1}{2}\sum_{j=1}^{n}\frac{1-\dot{\tau}_j(t)}{(1-\kappa)}\rho_j^2\big(x_{\tau_j,k}\big) \\
&\le \frac{1}{2(1-\kappa)}\sum_{j=1}^{n}\rho_j^2\big(x_{j,k}\big) - \frac{1}{2}\sum_{j=1}^{n}\rho_j^2\big(x_{\tau_j,k}\big)
\end{aligned}
\tag{3.13}
$$

Define a Lyapunov functional as $V_k(t) = V_{s_k}(t) + V_{U_k}(t)$, combining (3.11) and (3.13), we can obtain the time derivative of $V_k(t)$ as follows

$$\dot{V}_k(t) \leq s_k(t)\Big[(f(\boldsymbol{X}_k(t),t) + g_m(\boldsymbol{X}_k(t),t)v_k(t) + \mu_k(t) + \frac{n}{2}s_k(t)\theta^2(t) + \frac{s_k(t)\overline{d}^2(\boldsymbol{X}_k(t))}{2a_1^2}\Big] - Ks_k^2(t) + \frac{1}{2(1-\kappa)}\sum_{j=1}^{n}\rho_j^2\big(x_{j,k}\big) + \frac{a_1^2}{2} \tag{3.14}$$

For the convenience of expression, denote $\xi(\boldsymbol{X}_k(t)) \triangleq \frac{a_1^2}{2} + \frac{1}{2(1-\kappa)}\sum_{j=1}^{n}\rho_j^2\big(x_{j,k}(t)\big)$, then Eq. (3.14) can be simplified as

$$\dot{V}_k(t) \leq s_k(t)\Big[(f(\boldsymbol{X}_k(t),t) + g_m(\boldsymbol{X}_k(t),t)v_k(t) + \mu_k(t) + \frac{n}{2}s_k(t)\theta^2(t) + \frac{s_k(t)\overline{d}^2(\boldsymbol{X}_k(t))}{2a_1^2} + \frac{\xi(\boldsymbol{X}_k(t))}{s_k(t)}\Big] - Ks_k^2(t) \tag{3.15}$$

To avoid the possible singularity problem, we still employ the hyperbolic tangent function as Chap. 2, then transform Eq. (3.15) to

$$\begin{aligned}
\dot{V}_k(t) \leq\ & s_k(t)\left[f(\boldsymbol{X}_k(t),t) + g_m(\boldsymbol{X}_k(t),t)v_k(t) + \mu_k(t) + \frac{n}{2}s_k(t)\theta^2(t) + \frac{s_k(t)\overline{d}^2(\boldsymbol{X}_k(t))}{2a_1^2}\right] \\
& - Ks_k^2(t) + \xi(\boldsymbol{X}_k(t)) - b\tanh^2\left(\frac{s_k(t)}{\eta(t)}\right)\xi(\boldsymbol{X}_k(t)) + b\tanh^2\left(\frac{s_k(t)}{\eta(t)}\right)\xi(\boldsymbol{X}_k(t)) \\
=\ & s_k(t)\Big[f(\boldsymbol{X}_k(t),t) + g_m(\boldsymbol{X}_k(t),t)v_k(t) + \mu_k(t) + \frac{n}{2}s_k(t)\theta^2(t) + \frac{s_k(t)\overline{d}^2(\boldsymbol{X}_k(t))}{2a_1^2} \\
& + \frac{b}{s_k(t)}\tanh^2\left(\frac{s_k(t)}{\eta(t)}\right)\xi(\boldsymbol{X}_k(t))\Big] - Ks_k^2(t) + \left(1 - b\tanh^2\left(\frac{s_k(t)}{\eta(t)}\right)\right)\xi(\boldsymbol{X}_k(t))
\end{aligned} \tag{3.16}$$

Upon multiplication of both sides of (3.16) by $1\big/g_m(\boldsymbol{X}_k,t)$, it becomes

$$\begin{aligned}
\frac{\dot{V}_k(t)}{g_m(\boldsymbol{X}_k(t),t)} \leq\ & s_k(t)\Bigg[\frac{1}{g_m(\boldsymbol{X}_k(t),t)}\Bigg(f(\boldsymbol{X}_k(t),t) + \frac{n}{2}s_k(t)\theta^2(t) + \frac{s_k(t)\overline{d}^2(\boldsymbol{X}_k(t))}{2a_1^2} \\
& + \frac{b}{s_k(t)}\tanh^2\left(\frac{s_k(t)}{\eta(t)}\right)\xi(\boldsymbol{X}_k(t))\Bigg) + v_k(t) + \frac{1}{g_m(\boldsymbol{X}_k(t),t)}\mu_k(t)\Bigg] \\
& - \frac{K}{g_m(\boldsymbol{X}_k(t),t)}s_k^2(t) + \frac{1}{g_m(\boldsymbol{X}_k(t),t)}\left(1 - b\tanh^2\left(\frac{s_k(t)}{\eta(t)}\right)\right)\xi(\boldsymbol{X}_k(t)) \\
=\ & s_k(t)\big[\Xi(\boldsymbol{X}_k,t) + \Psi(\boldsymbol{X}_k,t)\mu_k(t) + v_k(t)\big] - \frac{K}{g_m(\boldsymbol{X}_k(t),t)}s_k^2(t) \\
& + \frac{1}{g_m(\boldsymbol{X}_k(t),t)}\left(1 - b\tanh^2\left(\frac{s_k(t)}{\eta(t)}\right)\right)\xi(\boldsymbol{X}_k(t))
\end{aligned} \tag{3.17}$$

where, $\Xi(\boldsymbol{X}_k, t) = \frac{1}{g_m(\boldsymbol{X}_k(t),t)}\Big[f(\boldsymbol{X}_k(t), t) + \frac{n}{2}s_k(t)\theta^2(t) + \frac{b}{s_k(t)}\tanh^2\Big(\frac{s_k(t)}{\eta(t)}\Big)\times \xi(\boldsymbol{X}_k) + \frac{s_k(t)\overline{d}^2(\boldsymbol{X}_k)}{2a_1^2}\Big]$, $\Psi(\boldsymbol{X}_k, t) = \frac{1}{g_m(\boldsymbol{X}_k(t),t)}$. In order to deal with the uncertainties in the controller design, we apply the RBF NNs to approximate the unknown nonlinear functions $\Xi(\boldsymbol{X}_k, t)$ 和 $\Psi(\boldsymbol{X}_k, t)$

$$\Xi(\boldsymbol{X}_k, t) = \boldsymbol{W}_\Xi^{*\mathrm{T}}(t)\boldsymbol{\Phi}_\Xi\big(\boldsymbol{X}_k^\Xi\big) + \varepsilon_\Xi\big(\boldsymbol{X}_k^\Xi, t\big) \tag{3.18}$$

$$\Psi(\boldsymbol{X}_k, t) = \boldsymbol{W}_\Psi^{*\mathrm{T}}(t)\boldsymbol{\Phi}_\Psi\big(\boldsymbol{X}_k^\Psi\big) + \varepsilon_\Psi\big(\boldsymbol{X}_k^\Psi, t\big) \tag{3.19}$$

where, $\boldsymbol{X}_k^\Xi = \big[\boldsymbol{X}_k^T, \boldsymbol{X}_d^T\big]^T \in \boldsymbol{\Omega}_\Xi \subset \mathbf{R}^{2n}$ and $\boldsymbol{X}_k^\Psi = \boldsymbol{X}_k \in \boldsymbol{\Omega}_\Psi \subset \mathbf{R}^n$ are the input vector with $\boldsymbol{\Omega}_\Xi$ and $\boldsymbol{\Omega}_\Psi$ as two compact sets; $\delta_\Xi\big(\boldsymbol{X}_k^\Xi, t\big)$ 和 $\delta_\Psi\big(\boldsymbol{X}_k^\Psi, t\big)$ are inherent NN approximation errors which can be decreased arbitrarily by increasing the NN node number, so we can assume that $\big|\varepsilon_\Xi\big(\boldsymbol{X}_k^\Xi, t\big)\big| \le \varepsilon_\Xi$, $\big|\varepsilon_\Xi\big(\boldsymbol{X}_k^\Xi, t\big)\big| \le \varepsilon_\Psi$, $\forall t \in [0, T]$, with $\varepsilon_\Xi, \varepsilon_\Psi > 0$ being unknown positive constants. Define $\beta(t)$ as $\beta(t) = \max\big\{\big|\delta_\Xi\big(\boldsymbol{X}_k^\Xi, t\big)\big|, \big|\delta_\Xi\big(\boldsymbol{X}_k^\Xi, t\big)\big|\big\}$. $\Phi_\Xi\big(\boldsymbol{X}_k^\Xi\big)$ and $\Phi_\Psi\big(\boldsymbol{X}_k^\Psi\big)$ are Gaussian basis function vectors which is given by

$$\boldsymbol{\Phi}_\Xi\big(\boldsymbol{X}_k^\Xi\big) = \big[\varphi_1\big(\boldsymbol{X}_k^\Xi\big), \varphi_2\big(\boldsymbol{X}_k^\Xi\big), \ldots, \varphi_{l^\Xi}\big(\boldsymbol{X}_k^\Xi\big)\big]^\mathrm{T} : \mathbf{R}^{2n} \mapsto \mathbf{R}^{l_\Xi} \tag{3.20}$$

$$\boldsymbol{\Phi}_\Psi\big(\boldsymbol{X}_k^\Psi\big) = \big[\varphi_1\big(\boldsymbol{X}_k^\Psi\big), \varphi_2\big(\boldsymbol{X}_k^\Psi\big), \ldots, \varphi_{l^\Psi}\big(\boldsymbol{X}_k^\Psi\big)\big]^\mathrm{T} : \mathbf{R}^{n} \mapsto \mathbf{R}^{l_\Psi} \tag{3.21}$$

where, $\varphi_i(\boldsymbol{Z}) = \exp\big(-\|\boldsymbol{Z} - \boldsymbol{c}_i\|^2\big/\sigma_i^2\big)$, $\boldsymbol{c}_i \in \boldsymbol{\Omega}_Z$ and $\sigma_i \in \mathbf{R}$ are the center and width of the i-th neuron respectively, l_Ξ and l_Ψ are the number of neurons of two NNs. $\boldsymbol{W}_\Xi^*(t) \in \mathbf{R}^{l_\Xi}$ and $\boldsymbol{W}_\Psi^*(t) \in \mathbf{R}^{l_\Psi}$ denote the optimal time-varying NN weights which are specifically defined as

$$\boldsymbol{W}_\Xi^*(t) = \arg \min_{\boldsymbol{W}_\Xi(t)\in\mathbf{R}^{l_\Xi}} \left\{ \sup_{\boldsymbol{X}_k^\Psi\in\mathbf{R}^n} \big|\Xi(\boldsymbol{X}_k, t) - \boldsymbol{W}_\Xi^\mathrm{T}(t)\boldsymbol{\Phi}_\Xi\big(\boldsymbol{X}_k^\Xi\big)\big| \right\} \tag{3.22}$$

$$\boldsymbol{W}_\Psi^*(t) = \arg \min_{\boldsymbol{W}_\Psi(t)\in\mathbf{R}^{l_\Psi}} \left\{ \sup_{\boldsymbol{X}_k^\Psi\in R^n} \big|\Psi(\boldsymbol{X}_k, t) - \boldsymbol{W}_\Psi^\mathrm{T}(t)\boldsymbol{\Phi}_\Psi\big(\boldsymbol{X}_k^\Psi\big)\big| \right\} \tag{3.23}$$

For NN ideal weights, the following assumption holds.

Assumption 3.4 The optimal weight vector $\boldsymbol{W}_\Xi^*(t)$ and $\boldsymbol{W}_\Psi^*(t)$ are bounded, i.e.,

$$\max_{t\in[0,T]}\big\|\boldsymbol{W}_\Xi^*(t)\big\| \le \varepsilon_{W_\Xi^*},\ \max_{t\in[0,T]}\big\|\boldsymbol{W}_\Psi^*(t)\big\| \le \varepsilon_{W_\Psi^*} \tag{3.24}$$

where, $\varepsilon_{W_\Xi^*}$ and $\varepsilon_{W_\Psi^*}$ are unknown positive constants.

Based on above analysis, design an adaptive iterative learning controller as

$$v_k(t) = -\hat{\boldsymbol{W}}^{\mathrm{T}}_{\Xi,k}(t)\boldsymbol{\Phi}_{\Xi}\big(\boldsymbol{X}^{\Xi}_k\big) - \hat{\boldsymbol{W}}^{\mathrm{T}}_{\Psi,k}(t)\boldsymbol{\Phi}_{\Psi}\big(\boldsymbol{X}^{\Psi}_k\big)\mu_k(t) \\ - \mathrm{sat}\left(\frac{e_{sk}}{\eta(t)}\right)\hat{\beta}_k(t)(1 + |\mu_k(t)|) \tag{3.25}$$

where, $\hat{\boldsymbol{W}}^{T}_{\Xi,k}(t)$, $\hat{\boldsymbol{W}}^{T}_{\Psi,k}(t)$ and $\hat{\beta}_k(t)$ are the estimates of $\boldsymbol{W}^*_{\Xi}(t)$, $\boldsymbol{W}^*_{\Psi}(t)$ and β, respectively. Design the adaptive learning law for above unknown parameters as follows

$$\begin{cases} \hat{\boldsymbol{W}}_{\Xi,k}(t) = \hat{\boldsymbol{W}}_{\Xi,k-1}(t) + q_1 s_k(t)\boldsymbol{\Phi}_{\Xi}\big(\boldsymbol{X}^{\Xi}_k\big) \\ \hat{\boldsymbol{W}}_{\Xi,0}(t) = 0, t \in [0, T] \end{cases} \tag{3.26}$$

$$\begin{cases} \hat{\boldsymbol{W}}_{\Psi,k}(t) = \hat{\boldsymbol{W}}_{\Psi,k-1}(t) + q_2 s_k(t)\mu_k(t)\boldsymbol{\Phi}_{\Psi}\big(\boldsymbol{X}^{\Psi}_k\big) \\ \hat{\boldsymbol{W}}_{\Psi,0}(t) = 0, t \in [0, T] \end{cases} \tag{3.27}$$

$$\begin{cases} (1-\gamma)\dot{\hat{\beta}}_k(t) = -\gamma\hat{\beta}_k(t) + \gamma\hat{\beta}_{k-1}(t) + q_3|s_k(t)|(1 + |\mu_k(t)|) \\ \hat{\beta}_k(0) = \hat{\beta}_{k-1}(T), \hat{\beta}_0(t) = 0, t \in [0, T] \end{cases} \tag{3.28}$$

where, $q_1, q_2, q_3 > 0$ and $0 < \gamma < 1$ are design parameters.

In order to show how controller (3.25) can guarantee stability and convergence of tracking errors later, we define the estimation error as $\tilde{\boldsymbol{W}}_{\Xi,k}(t) = \hat{\boldsymbol{W}}_{\Xi,k}(t) - \boldsymbol{W}^*_{\Xi}(t)$, $\tilde{\boldsymbol{W}}_{\Psi,k}(t) = \hat{\boldsymbol{W}}_{\Psi,k}(t) - \boldsymbol{W}^*_{\Psi}(t)$, $\tilde{\beta}_k(t) = \hat{\beta}_k(t) - \beta$. Then, substituting controller (3.25) back into (3.17) yields

$$\frac{\dot{V}_k(t)}{g_m(\boldsymbol{X}_k(t), t)} \\ \leq s_k(t)\Big[\boldsymbol{W}^{*\mathrm{T}}_{\Xi}(t)\boldsymbol{\Phi}_{\Xi}\big(\boldsymbol{X}^{\Xi}_k\big) + \delta_{\Xi}\big(\boldsymbol{X}^{\Xi}_k, t\big) + \big(\boldsymbol{W}^{*\mathrm{T}}_{\Psi}(t)\boldsymbol{\Phi}_{\Psi}\big(\boldsymbol{X}^{\Psi}_k\big) + \delta_{\Xi}\big(\boldsymbol{X}^{\Psi}_k, t\big)\big)\mu_k(t) \\ -\hat{\boldsymbol{W}}^{\mathrm{T}}_{\Xi,k}(t)\boldsymbol{\Phi}_{\Xi}\big(\boldsymbol{X}^{\Xi}_k\big) - \hat{\boldsymbol{W}}^{\mathrm{T}}_{\Psi,k}(t)\boldsymbol{\Phi}_{\Psi}\big(\boldsymbol{X}^{\Psi}_k\big)\mu_k(t) - \mathrm{sat}\left(\frac{e_{sk}}{\eta(t)}\right)\hat{\beta}_k(1 + |\mu_k(t)|)\Big] \\ - \frac{K}{g_m(\boldsymbol{X}_k(t), t)}s^2_k(t) + \frac{1}{g_m(\boldsymbol{X}_k(t), t)}\left(1 - b\tanh^2\left(\frac{s_k(t)}{\eta(t)}\right)\right)\xi(\boldsymbol{X}_k(t)) \\ \leq -s_k(t)\tilde{\boldsymbol{W}}^{\mathrm{T}}_{\Xi,k}(t)\boldsymbol{\Phi}_{\Xi}\big(\boldsymbol{X}^{\Xi}_k\big) - s_k(t)\tilde{\boldsymbol{W}}^{\mathrm{T}}_{\Psi,k}(t)\boldsymbol{\Phi}_{\Psi}\big(\boldsymbol{X}^{\Psi}_k\big)\mu_k(t) - |s_k(t)|\tilde{\beta}_k(1 + |\mu_k(t)|) \\ - \frac{K}{g_m(\boldsymbol{X}_k(t), t)}s^2_k(t) + \frac{1}{g_m(\boldsymbol{X}_k(t), t)}\left(1 - b\tanh^2\left(\frac{s_k(t)}{\eta(t)}\right)\right)\xi(\boldsymbol{X}_k(t)) \tag{3.29}$$

Equation (3.29) can be further written as

$$s_k(t)\tilde{\boldsymbol{W}}^{\mathrm{T}}_{\Xi,k}(t)\boldsymbol{\Phi}_{\Xi}\big(\boldsymbol{X}^{\Xi}_k\big) + s_k(t)\tilde{\boldsymbol{W}}^{\mathrm{T}}_{\Psi,k}(t)\boldsymbol{\Phi}_{\Psi}\big(\boldsymbol{X}^{\Psi}_k\big)\mu_k(t) + |s_k(t)|\tilde{\beta}_k(1 + |\mu_k(t)|) \leq \\ - \frac{\dot{V}_k(t)}{g_m(\boldsymbol{X}_k(t), t)} - \frac{K}{g_m(\boldsymbol{X}_k(t), t)}s^2_k(t) \\ + \frac{1}{g_m(\boldsymbol{X}_k(t), t)}\left(1 - b\tanh^2\left(\frac{s_k(t)}{\eta(t)}\right)\right)\xi(\boldsymbol{X}_k(t)) \tag{3.30}$$

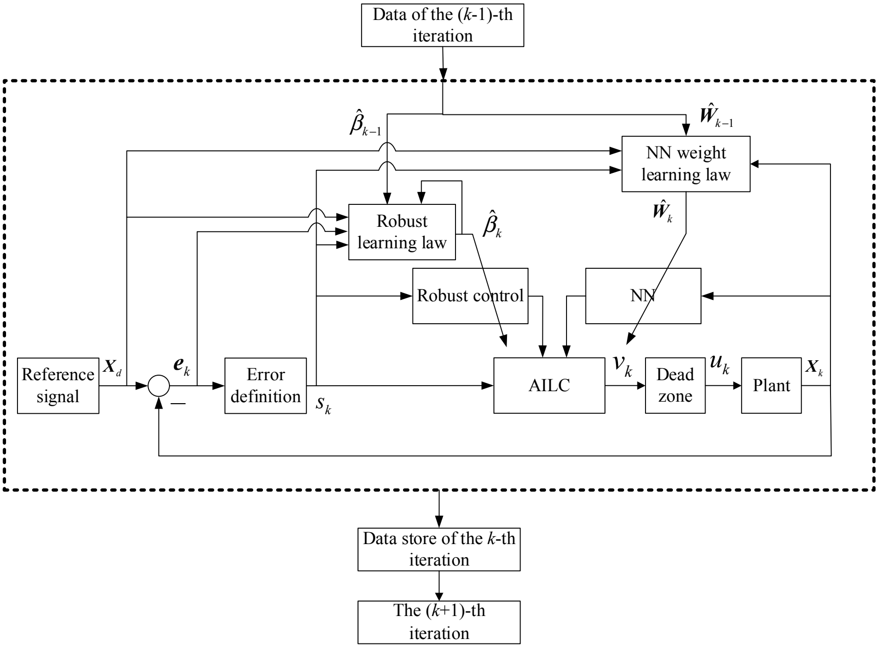

Fig. 3.2 The block diagram of the proposed NN AILC system

The block diagram of proposed NN AILC system is shown in Fig. 3.2.

3.4 Stability Analysis

In this section, we will analyze the stability of the closed loop system and the convergence of tracking errors.

The stability of the proposed NN AILC scheme is summarized as follows.

Theorem 3.1 *Considering the nonlinear time-delay systems described by* (3.1) *and running on the finite interval* $[0, T]$ *repeatedly, if* Assumptions 3.1–3.4 *and* Assumptions 2.4–2.8 *hold, design NN adaptive iterative learning controller* (3.25) *with adaptive learning laws* (3.26)–(3.28), *we can obtain the same conclusions as Theorem* 2.1, *i.e.*, ① *all the signals of the closed-loop system are bounded*; ② $\lim_{k\to\infty} \int_0^T (e_{sk}(\sigma))^2 \mathrm{d}\sigma \le \varepsilon_{esk}, \varepsilon_{esk} = \frac{1}{2K}(1+m)^2\varepsilon^2$; ③ *the system transient performance: the output tracking error satisfies* $\lim_{k\to\infty} \left|e_{1,k}(t)\right| = k_0 \sum_{i=1}^{n-1} \sqrt{\varepsilon_i^2 e^{-\lambda_0 t}} +(1+m)\varepsilon k_0 \frac{1}{\lambda_0 - K}\left(e^{-Kt} - e^{-\lambda_0 t}\right)$.

Proof According to Lemma 2.2, consider the following two cases:

Case 1. $s_k(t) \in \boldsymbol{\Omega}_{s_k}$

According to the analysis in Sect. 2.4, in the case of $s_k(t) \in \boldsymbol{\Omega}_{s_k}$, $|e_{sk}(t)| \leq (1+m)\eta(t)$ holds. Then followed by the boundedness of the desired reference state vector $X_d(t)$, $x_{i,k}(t)$ is bounded. According to adaptive iterative learning laws Eqs. (3.26)–(3.28), we can conclude that $\hat{\boldsymbol{W}}_{\Xi,k}(t)$, $\hat{\boldsymbol{W}}_{\Psi,k}(t)$ and $\hat{\beta}_k(t)$ are bounded provided $s_k(t) \in \boldsymbol{\Omega}_{s_k}$. On the basis of above analysis, it is easy to obtain the boundedness of $v_k(t)$. In summary, all the closed-loop signals are bounded and the tracking error satisfies $|e_{sk}(t)| \leq (1+m)\eta(t)$.

Case 2. $s_k(t) \notin \boldsymbol{\Omega}_{s_k}$

According to Lemma 2.2, for $s_k(t) \notin \boldsymbol{\Omega}_{s_k}$, the last term in the right side of Eq. (3.30) is less than zero and can be removed, then Eq. (3.30) is simplified as

$$
\begin{aligned}
&s_k(t)\tilde{\boldsymbol{W}}^{\mathrm{T}}_{\Xi,k}(t)\boldsymbol{\Phi}_{\Xi}\left(\boldsymbol{X}_k^{\Xi}\right) + s_k(t)\tilde{\boldsymbol{W}}^{\mathrm{T}}_{\Psi,k}(t)\boldsymbol{\Phi}_{\Psi}\left(\boldsymbol{X}_k^{\Psi}\right)\mu_k(t) + |s_k(t)|\tilde{\beta}_k(1+|\mu_k(t)|) \\
&\quad \leq -\frac{\dot{V}_k(t)}{g_m(\boldsymbol{X}_k(t),t)} - \frac{K}{g_m(\boldsymbol{X}_k(t),t)}s_k^2(t)
\end{aligned} \tag{3.31}
$$

Choose the Lyapunov-like CEF as follows

$$
\begin{aligned}
E_k(t) =& \frac{1}{2q_1}\int_0^t \tilde{\boldsymbol{W}}^{\mathrm{T}}_{\Xi,k}(\sigma)\tilde{\boldsymbol{W}}_{\Xi,k}(\sigma)\mathrm{d}\sigma + \frac{1}{2q_2}\int_0^t \tilde{\boldsymbol{W}}^{\mathrm{T}}_{\Psi,k}(\sigma)\tilde{\boldsymbol{W}}_{\Psi,k}(\sigma)\mathrm{d}\sigma \\
&+ \frac{\gamma}{2q_3}\int_0^t \tilde{\beta}_k^2(\sigma)\mathrm{d}\sigma + \frac{(1-\gamma)}{2q_3}\tilde{\beta}_k^2
\end{aligned} \tag{3.32}
$$

Remark 3.4 The CEF should contains the information concerning tracking error and parameter estimation errors. However, from the analysis in Sect. 2.4 we can see that even if the CEF is chosen as of index function of parameter estimation errors, we can also obtain the convergence of tracking error. Therefore, here we choose the CEF as the index function of three parameter estimation errors. Moreover, the last two terms in Eq. (3.32) are chosen in accordance with the adaptive learning law (3.28) for $\hat{\beta}_k(t)$.

The following proof contains four parts. And the main idea is presented is Fig. 3.3.

(1) The difference of $E_k(t)$.

From Eq. (3.32), we can get the difference of $E_k(t)$

$$
\begin{aligned}
\Delta E_k(t) =& \frac{1}{2q_1}\int_0^t \left(\tilde{\boldsymbol{W}}^{\mathrm{T}}_{\Xi,k}(\sigma)\tilde{\boldsymbol{W}}_{\Xi,k}(\sigma) - \tilde{\boldsymbol{W}}^{\mathrm{T}}_{\Xi,k-1}(\sigma)\tilde{\boldsymbol{W}}_{\Xi,k-1}(\sigma)\right)\mathrm{d}\sigma \\
&+ \frac{1}{2q_2}\int_0^t \left(\tilde{\boldsymbol{W}}^{\mathrm{T}}_{\Psi,k}(\sigma)\tilde{\boldsymbol{W}}_{\Psi,k}(\sigma) - \tilde{\boldsymbol{W}}^{\mathrm{T}}_{\Psi,k-1}(\sigma)\tilde{\boldsymbol{W}}_{\Psi,k-1}(\sigma)\right)\mathrm{d}\sigma
\end{aligned}
$$

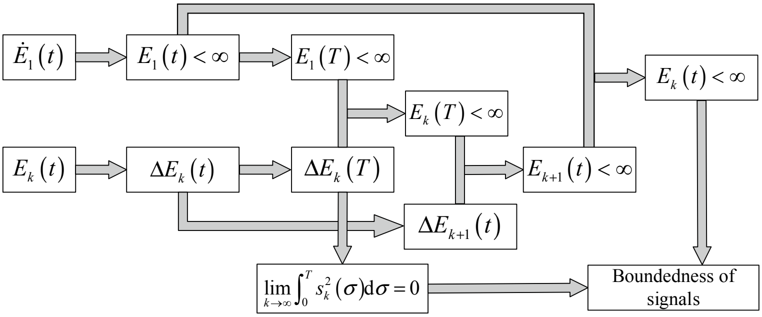

Fig. 3.3 The main idea of CEF-based proof for Theorem 3.1

$$+\frac{\gamma}{2q_3}\int_0^t\left(\tilde{\beta}_k^2(\sigma)-\tilde{\beta}_{k-1}^2(\sigma)\right)\mathrm{d}\sigma+\frac{(1-\gamma)}{2q_3}\left(\tilde{\beta}_k^2(t)-\tilde{\beta}_{k-1}^2(t)\right) \tag{3.33}$$

Considering adaptive iterative learning laws (3.26) and (3.27), we can obtain the following equalities

$$\begin{aligned}&\frac{1}{2q_1}\int_0^t\left(\tilde{\boldsymbol{W}}_{\Xi,k}^{\mathrm{T}}(\sigma)\tilde{\boldsymbol{W}}_{\Xi,k}(\sigma)-\tilde{\boldsymbol{W}}_{\Xi,k-1}^{\mathrm{T}}(\sigma)\tilde{\boldsymbol{W}}_{\Xi,k-1}(\sigma)\right)\mathrm{d}\sigma\\&=\int_0^t s_k(\sigma)\tilde{\boldsymbol{W}}_{\Xi,k}^{\mathrm{T}}(\sigma)\boldsymbol{\Phi}_{\Xi}\left(\boldsymbol{X}_k^{\Xi}\right)\mathrm{d}\sigma-\frac{q_1}{2}\int_0^t s_k^2(\sigma)\left\|\boldsymbol{\Phi}_{\Xi}\left(\boldsymbol{X}_k^{\Xi}\right)\right\|^2\mathrm{d}\sigma\end{aligned} \tag{3.34}$$

$$\begin{aligned}&\frac{1}{2q_2}\int_0^t\left(\tilde{\boldsymbol{W}}_{\Psi,k}^{\mathrm{T}}(\sigma)\tilde{\boldsymbol{W}}_{\Psi,k}(\sigma)-\tilde{\boldsymbol{W}}_{\Psi,k-1}^{\mathrm{T}}(\sigma)\tilde{\boldsymbol{W}}_{\Psi,k-1}(\sigma)\right)\mathrm{d}\sigma\\&=\int_0^t s_k(\sigma)\tilde{\boldsymbol{W}}_{\Psi,k}^{\mathrm{T}}(\sigma)\boldsymbol{\Phi}_{\Psi}\left(\boldsymbol{X}_k^{\Psi}\right)\mu_k(\sigma)\mathrm{d}\sigma-\frac{q_2}{2}\int_0^t s_k^2(\sigma)\mu_k^2(\sigma)\left\|\boldsymbol{\Phi}_{\Psi}\left(\boldsymbol{X}_k^{\Psi}\right)\right\|^2\mathrm{d}\sigma\end{aligned} \tag{3.35}$$

Recalling adaptive learning laws (3.28), the last two terms in Eq. (3.33) can be transformed to

$$\begin{aligned}&\frac{\gamma}{2q_3}\int_0^t\left(\tilde{\beta}_k^2(\sigma)-\tilde{\beta}_{k-1}^2(\sigma)\right)\mathrm{d}\sigma+\frac{(1-\gamma)}{2q_3}\left(\tilde{\beta}_k^2(t)-\tilde{\beta}_{k-1}^2(t)\right)\\&=\frac{\gamma}{2q_3}\int_0^t\left(\tilde{\beta}_k^2(\sigma)-\tilde{\beta}_{k-1}^2(\sigma)\right)\mathrm{d}\sigma+\frac{(1-\gamma)}{q_3}\int_0^t\tilde{\beta}_k(\sigma)\dot{\tilde{\beta}}_k(\sigma)\mathrm{d}\sigma\end{aligned}$$

$$
\begin{aligned}
&+\frac{(1-\gamma)}{2q_3}\Big[\tilde{\beta}_k^2(0)-\tilde{\beta}_{k-1}^2(t)\Big]\\
&=\int_0^t |s_k(\sigma)|\tilde{\beta}_k(\sigma)(1+|\mu_k(\sigma)|)\mathrm{d}\sigma-\frac{\gamma}{q_3}\int_0^t \tilde{\beta}_k(\sigma)\Big(\hat{\beta}_k(\sigma)-\hat{\beta}_{k-1}(\sigma)\Big)\mathrm{d}\sigma\\
&+\frac{\gamma}{2q_3}\int_0^t \Big(\tilde{\beta}_k^2(\sigma)-\tilde{\beta}_{k-1}^2(\sigma)\Big)\mathrm{d}\sigma+\frac{(1-\gamma)}{2q_3}\Big[\tilde{\beta}_k^2(0)-\tilde{\beta}_{k-1}^2(t)\Big]\\
&=\int_0^t |s_k(\sigma)|\tilde{\beta}_k(\sigma)(1+|\mu_k(\sigma)|)\mathrm{d}\sigma-\frac{\gamma}{q_3}\int_0^t \tilde{\beta}_k(\sigma)\Big(\tilde{\beta}_k(\sigma)-\tilde{\beta}_{k-1}(\sigma)\Big)\mathrm{d}\sigma\\
&+\frac{\gamma}{2q_3}\int_0^t \Big(\tilde{\beta}_k^2(\sigma)-\tilde{\beta}_{k-1}^2(\sigma)\Big)d\sigma+\frac{(1-\gamma)}{2q_3}\Big[\tilde{\beta}_k^2(0)-\tilde{\beta}_{k-1}^2(t)\Big]\\
&=\int_0^t |s_k(\sigma)|\tilde{\beta}_k(\sigma)(1+|\mu_k(\sigma)|)\mathrm{d}\sigma+\frac{(1-\gamma)}{2q_3}\Big[\tilde{\beta}_k^2(0)-\tilde{\beta}_{k-1}^2(t)\Big]\\
&-\frac{\gamma}{2q_3}\int_0^t \Big(\tilde{\beta}_k(\sigma)-\tilde{\beta}_{k-1}(\sigma)\Big)^2\mathrm{d}\sigma
\end{aligned}
\tag{3.36}
$$

Substituting (3.34)–(3.36) back into (3.33), it follows that

$$
\begin{aligned}
\Delta E_k(t)&\le-\int_0^t \frac{\dot{V}_k(\sigma)}{g_m(\boldsymbol{X}_k(\sigma),\sigma)}\mathrm{d}\sigma-\int_0^t \frac{K}{g_m(\boldsymbol{X}_k(\sigma),\sigma)}s_k^2(\sigma)\mathrm{d}\sigma\\
&\quad+\frac{(1-\gamma)}{2q_3}\Big[\tilde{\beta}_k^2(0)-\tilde{\beta}_{k-1}^2(t)\Big]\\
&\le-\frac{1}{\underline{g}_m}V_k(t)-\int_0^t \frac{K}{g_m(\boldsymbol{X}_k(\sigma),\sigma)}s_k^2(\sigma)\mathrm{d}\sigma+\frac{(1-\gamma)}{2q_3}\Big[\tilde{\beta}_k^2(0)-\tilde{\beta}_{k-1}^2(t)\Big]
\end{aligned}
\tag{3.37}
$$

Let $t=T$ in Eq. (3.37), from $\hat{\beta}_k(0)=\hat{\beta}_{k-1}(T)$ and $\hat{\beta}_1(0)=0$, it leads to

$$
\Delta E_k(T)<-\frac{1}{\underline{g}_m}V_k(T)-\int_0^T \frac{K}{g_m(\boldsymbol{X}_k(\sigma),\sigma)}s_k^2(\sigma)\mathrm{d}\sigma\le 0 \tag{3.38}
$$

The inequality (3.38) shows that $E_k(T)$ is decreasing along iteration axis. Hence, as long as $E_1(T)$ is bounded, the bounded of $E_k(T)$ can be ensured.

(2) The boundedness of $E_1(T)$.
From the definition of $E_k(t)$ we know

$$E_1(t) = \frac{1}{2q_1}\int_0^t \tilde{\boldsymbol{W}}_{\Xi,1}^{\mathrm{T}}(\sigma)\tilde{\boldsymbol{W}}_{\Xi,1}(\sigma)\mathrm{d}\sigma + \frac{1}{2q_2}\int_0^t \tilde{\boldsymbol{W}}_{\Psi,1}^{\mathrm{T}}(\sigma)\tilde{\boldsymbol{W}}_{\Psi,1}(\sigma)\mathrm{d}\sigma + \frac{\gamma}{2q_3}\int_0^t \tilde{\beta}_1^2(\sigma)\mathrm{d}\sigma + \frac{(1-\gamma)}{2q_3}\tilde{\beta}_1^2 \tag{3.39}$$

Then the time derivative of $E_1(t)$ is

$$\dot{E}_1(t) = \frac{1}{2q_1}\tilde{\boldsymbol{W}}_{\Xi,1}^{\mathrm{T}}(t)\tilde{\boldsymbol{W}}_{\Xi,1}(t) + \frac{1}{2q_2}\tilde{\boldsymbol{W}}_{\Psi,1}^{\mathrm{T}}(t)\tilde{\boldsymbol{W}}_{\Psi,1}(t) + \frac{\gamma}{2q_3}\tilde{\beta}_1^2(t) + \frac{(1-\gamma)}{q_3}\tilde{\beta}_1\dot{\tilde{\beta}}_1 \tag{3.40}$$

Recalling parameter adaptive learning laws (3.26)–(3.28), we have $\hat{\boldsymbol{W}}_{\Xi,1}(t) = q_1 s_1(t)\boldsymbol{\Phi}_\Xi\left(\boldsymbol{X}_1^\Xi\right)$, $\hat{\boldsymbol{W}}_{\Psi,1}(t) = q_2 s_1(t)\mu_1(t)\boldsymbol{\Phi}_\Psi\left(\boldsymbol{X}_1^\Psi\right)$, $(1-\gamma)\dot{\hat{\beta}}_1 = -\gamma\hat{\beta}_1 + q_3|s_1(t)|(1+|\mu_1(t)|)$, then we can obtain

$$\begin{aligned}
&\frac{1}{2q_1}\tilde{\boldsymbol{W}}_{\Xi,1}^{\mathrm{T}}(t)\tilde{\boldsymbol{W}}_{\Xi,1}(t)\\
&\quad= \frac{1}{2q_1}\left(\tilde{\boldsymbol{W}}_{\Xi,1}^{\mathrm{T}}(t)\tilde{\boldsymbol{W}}_{\Xi,1}(t) - 2\tilde{\boldsymbol{W}}_{\Xi,1}^{\mathrm{T}}(t)\hat{W}_{\Xi,1}(t)\right) + \frac{1}{q_1}\tilde{\boldsymbol{W}}_{\Xi,1}^{\mathrm{T}}(t)\hat{W}_{\Xi,1}(t)\\
&\quad= \frac{1}{2q_1}\left(\left(\hat{W}_{\Xi,1}(t) - W_\Xi^*(t)\right)^{\mathrm{T}}\left(\hat{W}_{\Xi,1}(t) - W_\Xi^*(t)\right)\right.\\
&\quad\left.-2\left(\hat{W}_{\Xi,1}(t) - W_\Xi^*(t)\right)^{\mathrm{T}}\hat{W}_{\Xi,1}(t)\right)\\
&\quad+ s_1(t)\tilde{\boldsymbol{W}}_{\Xi,1}^{T}(t)\Phi_\Xi\left(\boldsymbol{X}_1^\Xi\right)\\
&\quad= \frac{1}{2q_1}\left(-\hat{\boldsymbol{W}}_{\Xi,1}^{T}(t)\hat{\boldsymbol{W}}_{\Xi,1}(t) + W_\Xi^{*\mathrm{T}}(t)W_\Xi^*(t)\right) + s_1(t)\tilde{\boldsymbol{W}}_{\Xi,1}^{\mathrm{T}}(t)\Phi_\Xi\left(\boldsymbol{X}_1^\Xi\right)
\end{aligned} \tag{3.41}$$

$$\begin{aligned}
\frac{1}{2q_2}\tilde{\boldsymbol{W}}_{\Psi,1}^{T}(t)\tilde{\boldsymbol{W}}_{\Psi,1}(t) &= \frac{1}{2q_2}\left(-\hat{\boldsymbol{W}}_{\Psi,1}^{T}(t)\hat{\boldsymbol{W}}_{\Psi,1}(t) + \boldsymbol{W}_\Psi^{*T}(t)\boldsymbol{W}_\Psi^*(t)\right)\\
&\quad+ s_1(t)\tilde{\boldsymbol{W}}_{\Psi,1}^{T}(t)\boldsymbol{\Phi}_\Psi\left(\boldsymbol{X}_1^\Psi\right)
\end{aligned} \tag{3.42}$$

$$\begin{aligned}
&\frac{\gamma}{2q_3}\tilde{\beta}_1^2(t) + \frac{(1-\gamma)}{q_3}\tilde{\beta}_1(t)\dot{\tilde{\beta}}_1(t)\\
&\quad= \frac{\gamma}{2q_3}\tilde{\beta}_1^2(t) - \frac{\gamma}{q_3}\tilde{\beta}_1(t)\hat{\beta}_1(t) + |s_1(t)|\tilde{\beta}_1(t)(1+|\mu_1(t)|)\\
&\quad= \frac{\gamma}{2q_3}\left(\hat{\beta}_1^2(t) - 2\tilde{\beta}_1(t)\hat{\beta}_1(t) + \tilde{\beta}_1^2(t)\right) - \frac{\gamma}{2q_3}\hat{\beta}_1^2(t) + |s_1(t)|\tilde{\beta}_1(t)(1+|\mu_1(t)|)
\end{aligned}$$

$$\leq \frac{\gamma}{2q_3}\left(\hat{\beta}_1(t) - \tilde{\beta}_1(t)\right)^2 + |s_1(t)|\tilde{\beta}_1(t)(1 + |\mu_1(t)|)$$
$$= \frac{\gamma}{2q_3}\beta^2 + |s_1(t)|\tilde{\beta}_1(t)(1 + |\mu_1(t)|) \tag{3.43}$$

Substituting (3.41)–(3.43) back into (3.40), the $\dot{E}_1(t)$ changes to

$$\begin{aligned}\dot{E}_1(t) \leq\ & s_1(t)\tilde{\boldsymbol{W}}^{\mathrm{T}}_{\Xi,1}(t)\boldsymbol{\Phi}_{\Xi}\left(\boldsymbol{X}_1^{\Xi}\right) + s_1(t)\tilde{\boldsymbol{W}}^{\mathrm{T}}_{\Psi,1}(t)\boldsymbol{\Phi}_{\Psi}\left(\boldsymbol{X}_1^{\Psi}\right) + |s_1(t)|\tilde{\beta}_1(1 + |\mu_1(t)|)\\ & + \frac{1}{2q_1}\boldsymbol{W}^{*\mathrm{T}}_{\Xi}(t)\boldsymbol{W}^{*}_{\Xi}(t) + \frac{1}{2q_2}\boldsymbol{W}^{*\mathrm{T}}_{\Psi}(t)\boldsymbol{W}^{*}_{\Psi}(t) + \frac{\gamma}{2q_3}\beta^2(t)\\ \leq & -\frac{\dot{V}_k(t)}{g_m(X_k, t)} - \frac{k}{g_m(X_k, t)}s_k^2(t) + \frac{1}{2q_1}\boldsymbol{W}^{*\mathrm{T}}_{\Xi}(t)\boldsymbol{W}^{*}_{\Xi}(t)\\ & + \frac{1}{2q_2}\boldsymbol{W}^{*\mathrm{T}}_{\Psi}(t)\boldsymbol{W}^{*}_{\Psi}(t) + \frac{\gamma}{2q_3}\beta^2(t)\end{aligned} \tag{3.44}$$

For convenience of expression, denote $c_{\max} = \max_{t\in[0,T]}\left\{\frac{1}{2q_1}\boldsymbol{W}^{*\mathrm{T}}_{\Xi}(t)\boldsymbol{W}^{*}_{\Xi}(t) + \frac{1}{2q_2}\boldsymbol{W}^{*\mathrm{T}}_{\Psi}(t)\boldsymbol{W}^{*}_{\Psi}(t) + \frac{\gamma}{2q_3}\beta^2\right\}$. Integrating the inequality (3.44) over $[0, t]$ results in

$$E_1(t) - E_1(0) \leq -\frac{1}{\underline{g}_m}V_1(t) - \int_0^t \frac{K}{g_m(\boldsymbol{X}_1(\sigma), \sigma)}s_1^2(\sigma)\mathrm{d}\sigma + t\cdot c_{\max} \tag{3.45}$$

According to $\hat{\beta}_1(0) = 0$, we have

$$E_1(0) = \frac{(1-\gamma)}{2q_3}\tilde{\beta}_1^2(0) = \frac{(1-\gamma)}{2q_3}\beta^2(0) \tag{3.46}$$

Combining (3.45) and (3.46) yields

$$E_1(t) \leq t\cdot c_{\max} + \frac{(1-\gamma)}{2q_3}\beta^2(0) < \infty \tag{3.47}$$

In result, $E_1(t)$ is bounded on $[0, T]$. When $t = T$, Eq. (3.47) becomes

$$E_1(T) \leq T\cdot c_{\max} + \frac{(1-\gamma)}{2q_3}\beta^2(0) < \infty \tag{3.48}$$

Based on the above analysis, we can arrive at the boundedness of $E_k(T)$.

(3) The boundedness of $E_k(t)$.

Next we will prove the boundedness of $E_k(t)$ by induction method. Firstly, separate $E_k(t)$ into two parts as follows

$$E_k^1(t) = \frac{1}{2q_1}\int_0^t \tilde{\boldsymbol{W}}_{\Xi,k}^T(\sigma)\tilde{\boldsymbol{W}}_{\Xi,k}(\sigma)d\sigma + \frac{1}{2q_2}\int_0^t \tilde{\boldsymbol{W}}_{\Psi,k}^T(\sigma)\tilde{\boldsymbol{W}}_{\Psi,k}(\sigma)d\sigma + \frac{\gamma}{2q_3}\int_0^t \tilde{\beta}_k^2(\sigma)d\sigma \tag{3.49}$$

$$E_k^2(t) = \frac{(1-\gamma)}{2q_3}\tilde{\beta}_k^2(t) \tag{3.50}$$

According to preceding analysis, the boundedness of $E_k^1(T)$ and $E_k^2(T)$ is guaranteed for $\forall k \in \mathbf{N}$. Consequently, $\forall k \in \mathbf{N}$, there exist finite constants M_1 and M_2 satisfying

$$E_k^1(t) \le E_k^1(T) \le M_1 < \infty \tag{3.51}$$

$$E_k^2(T) \le M_2 \tag{3.52}$$

Then we have

$$E_k(t) = E_k^1(t) + E_k^2(t) \le E_k^2(t) + M_1 \tag{3.53}$$

On the other hand, from (3.28) we know $E_{k+1}^2(0) = E_k^2(T)$, then it results in

$$\Delta E_{k+1}(t) < \frac{(1-\gamma)}{2q_3}\left[\tilde{\beta}_{k+1}^2(0) - \tilde{\beta}_k^2(t)\right] \le M_2 - E_k^2(t) \tag{3.54}$$

Adding (3.53) and (3.54) leads to

$$E_{k+1}(t) = E_k(t) + \Delta E_{k+1}(t) \le M_1 + M_2 \tag{3.55}$$

As we have proven that $E_1(t)$ is bounded, therefore, from induction method we can known $E_k(t)$ is bounded as well. Furthermore, From the form of $E_k(t)$ we can obtain the boundedness of $\hat{\boldsymbol{W}}_{\Xi,k}(t)$, $\hat{\boldsymbol{W}}_{\Psi,k}(t)$ and $\hat{\beta}_k(t)$.

(4) The convergence of tracking error

It follows from (3.38) that

$$E_k(T) = E_1(T) + \sum_{l=2}^{k}\Delta E_l(T) < E_1(T) - \frac{1}{\overline{g}_m}\sum_{l=2}^{k}V_l(T) - \sum_{l=2}^{k}\int_0^T \frac{K}{g_m(\boldsymbol{X}_k(\sigma),\sigma)}s_l^2(\sigma)\mathrm{d}\sigma$$

$$\leq E_1(T) - \sum_{l=2}^{k} \int_0^T \frac{K}{g_m(\boldsymbol{X}_k(\sigma), \sigma)} s_l^2(\sigma)\mathrm{d}\sigma \tag{3.56}$$

Rewriting the previous inequality as the following from

$$\frac{K}{\overline{g}_m} \sum_{l=2}^{k} \int_0^T s_l^2(\sigma)\mathrm{d}\sigma \leq \sum_{l=2}^{k} \int_0^T \frac{K}{g_m(\boldsymbol{X}_k(\sigma), \sigma)} s_l^2(\sigma)\mathrm{d}\sigma \leq E_1(T) - E_k(T) \leq E_1(T) \tag{3.57}$$

Taking the limitation of (3.57), it yields

$$\lim_{k\to\infty} \sum_{l=2}^{k} \int_0^T s_l^2(\sigma)\mathrm{d}\sigma \leq \frac{\overline{g}_m}{k}(E_1(T) - E_k(T)) \leq \frac{\overline{g}_m}{k} E_1(T) \tag{3.58}$$

Since $E_1(T)$ is bounded, according to the convergence theorem of the sum of series, it results in $\lim\limits_{k\to\infty} \int_0^T s_k^2(\sigma)\mathrm{d}\sigma = 0$, which implies that $\lim\limits_{k\to\infty} s_k(t) = s_\infty(t) = 0$, $\forall t \in [0, T]$. It follows form the definition of $s_k(t)$ that when $|e_{sk}(t)| \leq \eta(t)$, $s_k(t) = 0$ holds. Then $\lim\limits_{k\to\infty} \int_0^T s_k^2(\sigma)\mathrm{d}\sigma = 0$ is equivalent to $\lim\limits_{k\to\infty} |e_{sk}(t)| \leq \eta(t)$. Furthermore, $\lim\limits_{k\to\infty} \int_0^T (e_{sk}(\sigma))^2\mathrm{d}\sigma \leq \int_0^T (\eta(\sigma))^2\mathrm{d}\sigma$.

In previous part, we have got the boundedness of $\hat{W}_{\Xi,k}(t)$, $\hat{W}_{\Psi,k}(t)$ and $\hat{\beta}_k(t)$ from the boundedness of $E_k(t)$. Here we can obtain the boundedness of $s_k(t)$ from $\int_0^t s_k^2(\sigma)\mathrm{d}\sigma \leq \int_0^T s_k^2(\sigma)\mathrm{d}\sigma$, then we can further get the boundedness of $x_{i,k}(t)$ on the basis of the boundedness of $X_d(t)$. Similar to case 1, the boundedness of $\upsilon_k(t)$ can be established.

Summarizing the conclusions in two cases, we can know that the proposed control algorithm is able to guarantee that all closed-loop signals are bounded and $\lim\limits_{k\to\infty} |e_{sk}(t)| \leq (1+m)\eta(t)$. Therefore, we can further conclude that $\lim\limits_{k\to\infty} \int_0^T (e_{sk}(\sigma))^2\mathrm{d}\sigma \leq \varepsilon_e$, $\varepsilon_e = \int_0^T ((1+m)\eta(\sigma))^2\mathrm{d}\sigma = \frac{1}{2K}(1+m)^2\varepsilon^2\left(1 - e^{-2KT}\right) \leq \frac{1}{2K}(1+m)^2\varepsilon^2 = \varepsilon_{esk}$. Moreover, $e_{s\infty}(t)$ satisfies $\lim\limits_{k\to\infty} |e_{sk}(t)| = e_{s\infty}(t) = (1+m)\varepsilon e^{-Kt}$, $\forall t \in [0, T]$.

The proof of the transient performance for tracking error is same as Sect. 2.4.

This concludes the proof. □

3.5 Simulation Analysis

In this section, a simulation study is presented to verify the effectiveness of the proposed AILC scheme. Consider the following second-order nonlinear system with unknown time-varying delays and unknown dead-zone running on finite time interval repetitively

$$\begin{cases} \dot{x}_{1,k}(t) = x_{2,k}(t) \\ \dot{x}_{2,k}(t) = f(\boldsymbol{X}_k(t), t) + h\big(\boldsymbol{X}_{\tau,k}(t), t\big) + g(\boldsymbol{X}_k(t), t)u_k(t) + d(t) \\ y_k(t) = x_{1,k}(t), u_k(t) = D(v_k(t)) \end{cases} \tag{3.59}$$

where, $f(\boldsymbol{X}_k(t), t) = -x_{1,k}(t)x_{2,k}(t)\sin\big(x_{1,k}(t)x_{2,k}(t)\big)$, $g(X_k(t), t) = 0.9 + 0.1|\cos(2t)|^2 \sin^2\big(x_{1,k}x_{2,k}\big)$, $h\big(\boldsymbol{X}_{\tau,k}(t), t\big) = 0.2\sin(t)\mathrm{e}^{-|\cos(2t)|}\big[x_{1,k}(t-\tau_1)\sin\big(x_{1,k}(t-\tau_1)\big) + x_{2,k}(t-\tau_2(t))\sin\big(x_{2,k}(t-\tau_2(t))\big)\big]$. The unknown time-varying delays are given by $\tau_1(t) = 0.5(1+\sin t)$, $\tau_2(t) = 1 - 0.5\cos(t)$, then $\tau_{1\max} = 1$, $\dot{\tau}_1 \le 0.5$, $\tau_{2\max} = 1.5$, $\dot{\tau}_2 \le 0.5$. The unknown external disturbance is $d(t) = 0.5 * rand * \sin t$, where $rand$ presents Gaussian noise signal that takes value on [0, 1] randomly.

3.5.1 *Verification of the RBF NN AILC Scheme*

To demonstrate the validity of above conclusion, we design three mathematical simulation experiments as follows.

Experiment 1 Choose the desired reference trajectory vector as $\boldsymbol{X}_d(t) = [\sin t, \cos t]^{\mathrm{T}}$ and the design parameters as $\varepsilon_1 = \varepsilon_2 = 1$, $\lambda = 2$, $K = 3$, $\gamma = 0.5$, $q_1 = q_2 = 1$, $q_3 = 0.01$, $\varepsilon = \lambda\varepsilon_1 + \varepsilon_2 = 3$. The parameters for dead-zone is given by $m = 1 + 0.2\sin t$, $b_r = 0.25$, $b_l = -0.25$. The NN parameters are chosen as $l^{\Xi} = 30$, $\mu_{\Xi j} = \frac{1}{l^{\Xi}}\big(2j - l^{\Xi}\big)[2, 3, 1, 1.5]$, $\sigma_{\Xi j} = 2$, $j = 1, 2, \ldots, l^{\Xi}$; $l^{\Psi} = 20$, $\mu_{\Psi j} = \frac{1}{l^{\Xi}}\big(2j - l^{\Xi}\big)[2, 3]$, $\sigma_{\Psi j} = 2$, $j = 1, 2, \ldots, l^{\Psi}$. The initial condition for $x_{1,k}(0)$ and $x_{2,k}(0)$ are generated randomly on intervals $[-0.5, 0.5]$ and $[0.5, 1.5]$, respectively. The system runs on the finite time interval $[0, 4\pi]$ for five times. Part simulation results are presented in Figs. 3.4, 3.5, 3.6, 3.7 and 3.8.

Figures 3.4 and 3.5 show the tracking curves of the 1st iteration ($k = 1$) and the 5th iteration (k = 5), respectively, which shows that the tracking performance has been improved through four times of learning. In Fig. 3.5, we can see that the it has achieved complete tracking except for the initial stage that is influenced by resetting error. This improvement performance is clearly presented by Fig. 3.8. Figures 3.6 and 3.7 show the control curves of the 1st iteration and 5th iteration respectively, which shows the boundedness of control signal and the influence of dead-zone characteristic.

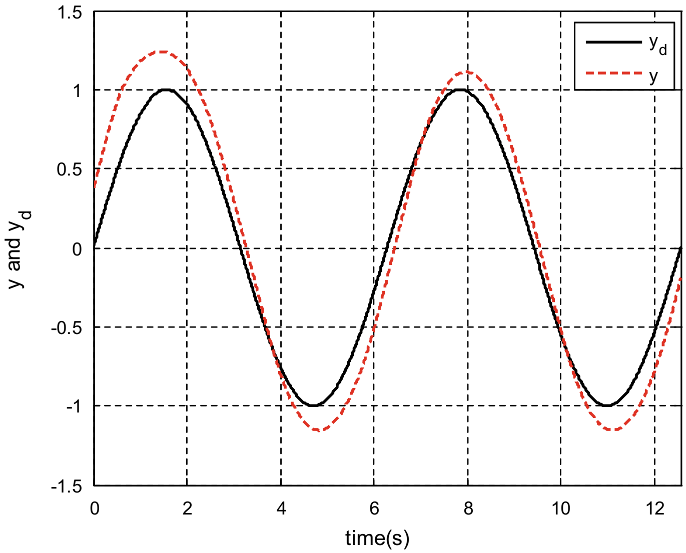

Fig. 3.4 System output y_k versus y_d $(k = 1)$

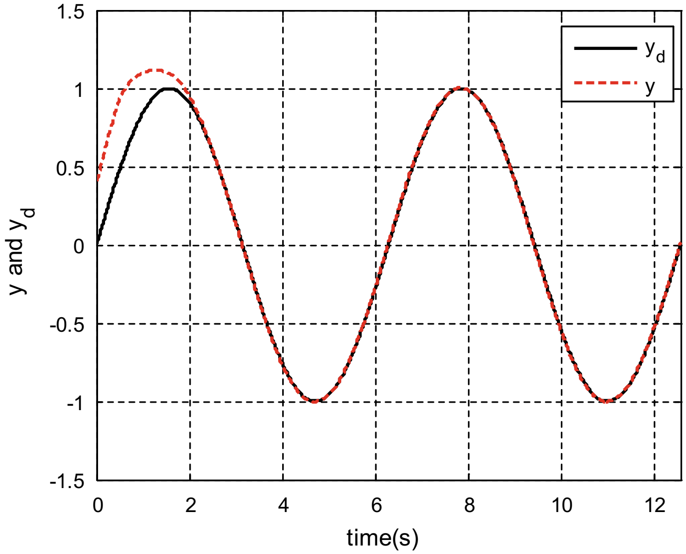

Fig. 3.5 System output y_k versus y_d $(k = 5)$

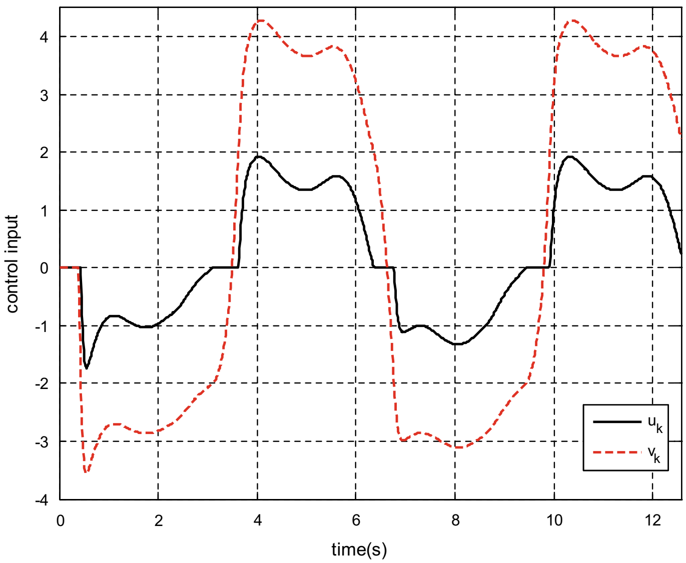

Fig. 3.6 The input v_k and output u_k of dead-zone characteristic ($k = 1$)

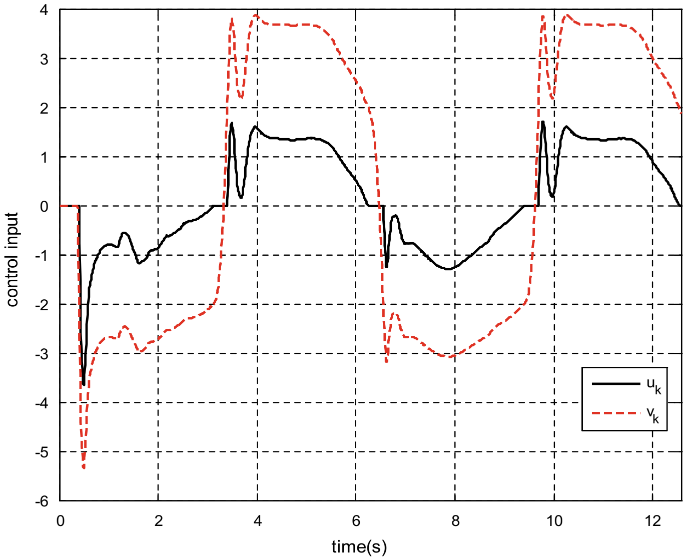

Fig. 3.7 The input v_k and output u_k of dead-zone characteristic ($k = 5$)

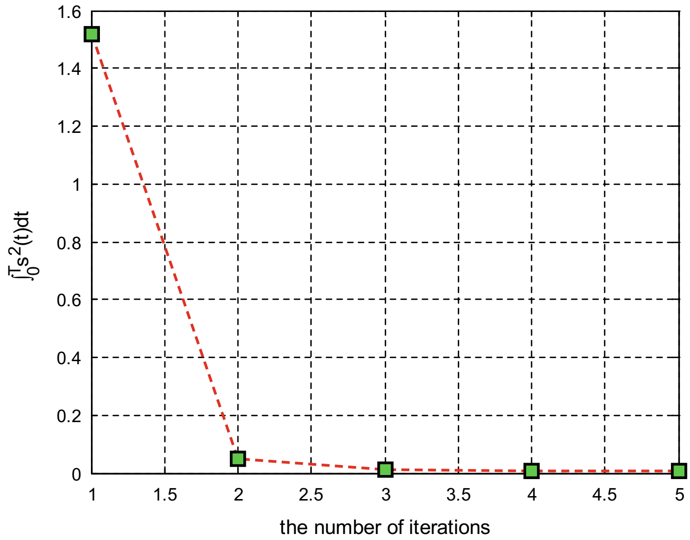

Fig. 3.8 $\int_0^T s_k^2(t)dt$ versus the number of iterations (Experiment 1)

Experiment 2 To show the control performance for more complicated desired reference trajectory, we choose the desired reference signal as $\boldsymbol{X}_d(t) = [\sin t + \sin(2t), \cos t + 2\cos(2t)]^T$. The design parameters keep the same as Experiment 1. The initial conditions for states $x_{1,k}(0)$ and $x_{2,k}(0)$ are generated randomly on the intervals $[-0.5, 0.5]$ and $[2.5, 3.5]$ respectively. The system runs on finite time interval $[0, 4\pi]$ for fifteen iterations. The simulation results are presented in Figs. 3.9, 3.10, 3.11, 3.12 and 3.13.

As shown in simulation Figures, we can see that the proposed controller can also achieve perfect tracking performance for more complicated desired trajectory and accomplish the control objective.

Experiment 3 To study the control performance of different design parameters, the following case is investigated. The desired trajectory is the same as that in Case 2. The parameters are chosen $\lambda = 3$, $K = 4$, $\gamma = 0.5$, $q_1 = q_2 = 2$, $q_3 = 0.02$, $\varepsilon = \lambda\varepsilon_1 + \varepsilon_2 = 4$. Other parameters remain unchanged. Here we only give the results of $\int_0^T s_k^2(t)dt$ versus the number of iterations which is shown in Fig. 3.14.

Comparing Fig. 3.13 with Fig. 3.14, it shows that fast adaption may improve the convergence rate in terms of iteration times. But in practice, the parameters can be chosen too large, as it may generate over-large control signal and eventually results in large overshot and oscillations.

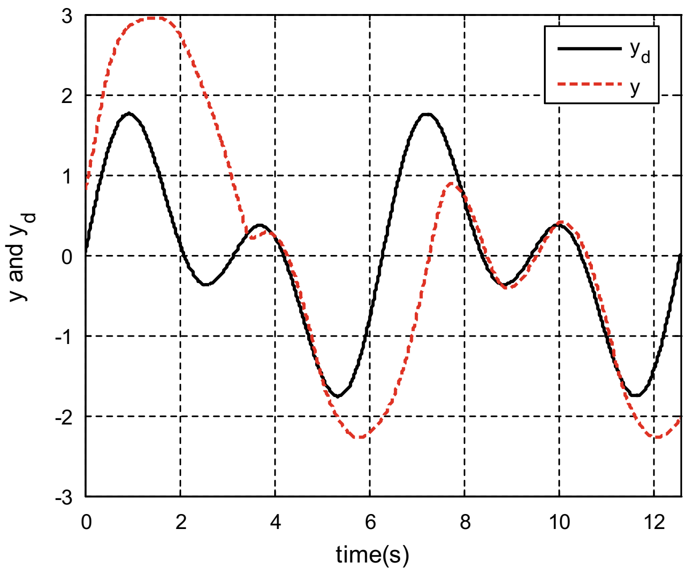

Fig. 3.9 System output y_k versus y_d $(k = 1)$

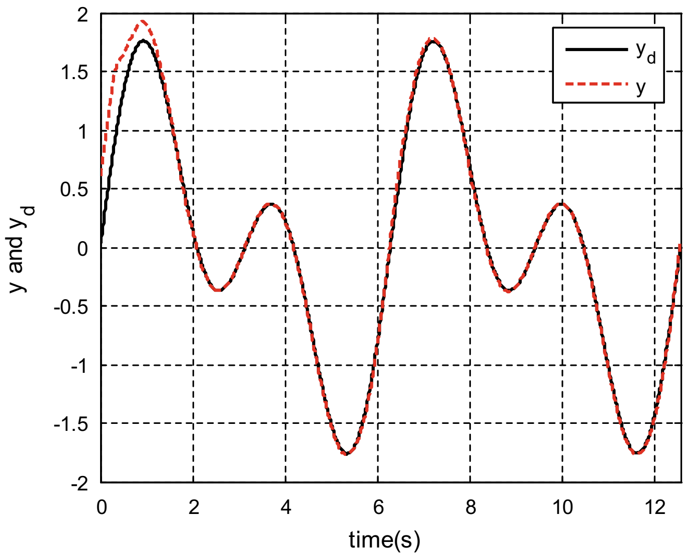

Fig. 3.10 System output y_k versus y_d $(k = 15)$

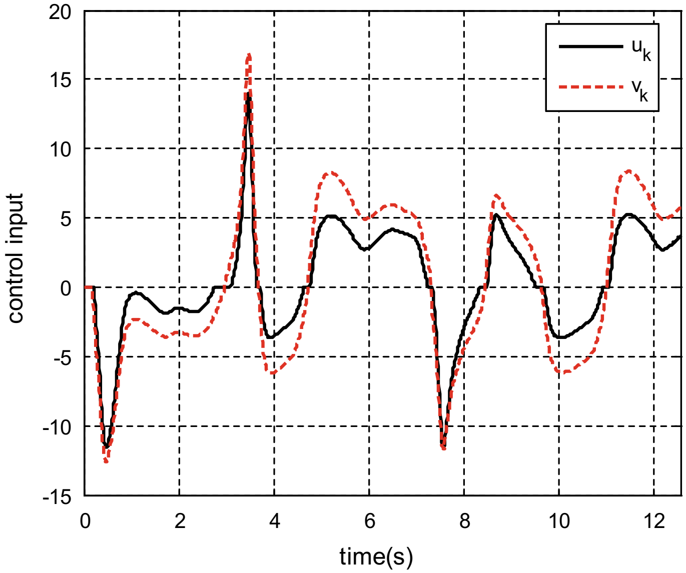

Fig. 3.11 The input v_k and output u_k of dead-zone characteristic ($k = 1$)

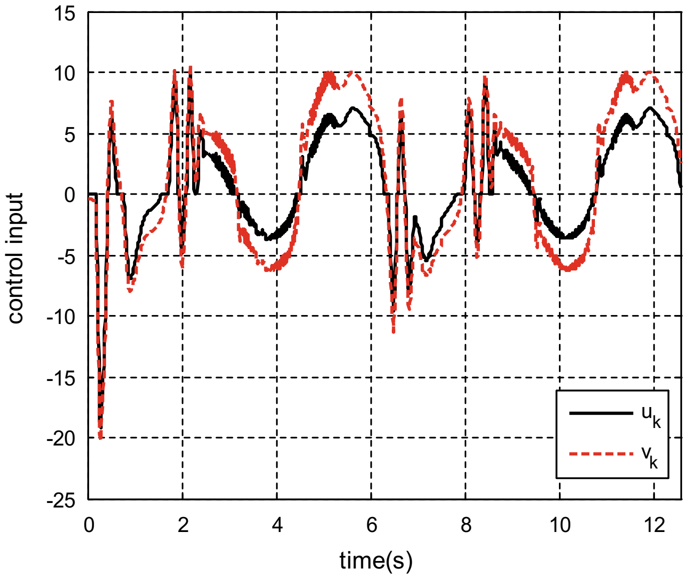

Fig. 3.12 The input v_k and output u_k of dead-zone characteristic ($k = 15$)

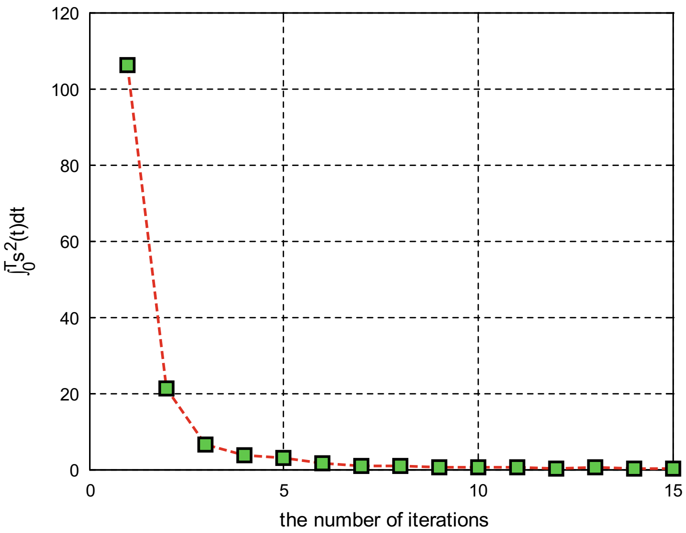

Fig. 3.13 $\int_0^T s_k^2(t)dt$ versus the number of iterations (Experiment 2)

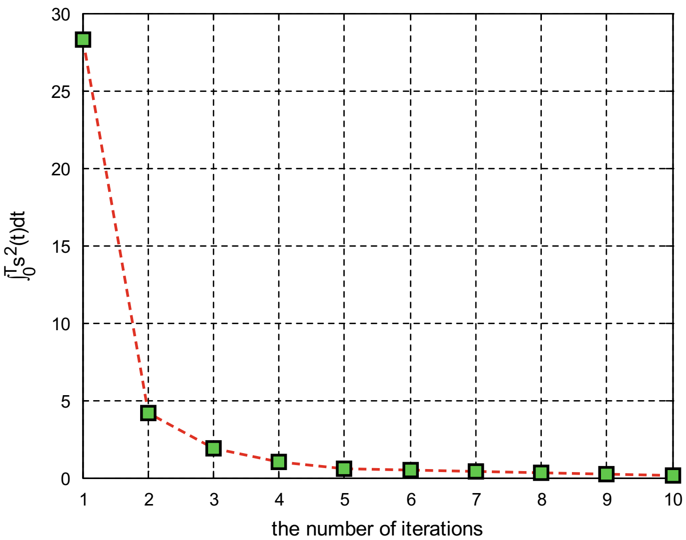

Fig. 3.14 $\int_0^T s_k^2(t)dt$ versus the number of iterations (Experiment 3)

3.5.2 Comparison Simulation: Adaptive NN Control

Experiment 4 Finally, the contribution of the proposed NN AILC is shown by comparing the proposed controller with traditional adaptive NN controller. We employ the adaptive NN controller in [12] to control the systems (3.59). The controller is as same as (3.25). But the adaptive laws for unknown parameters are changed to the following forms according to adaptive NN control method:

$$\dot{\hat{\boldsymbol{W}}}_{\Xi,k} = -\boldsymbol{\Gamma}_{W_\Xi}\left[\boldsymbol{\Phi}_\Xi\left(\boldsymbol{X}_k^\Xi\right)s_k + \sigma_1\hat{\boldsymbol{W}}_{\Xi,k}\right],\ \hat{\boldsymbol{W}}_{\Xi,k}(0) = 0$$

$$\dot{\hat{\boldsymbol{W}}}_{\Psi,k}(t) = -\boldsymbol{\Gamma}_{W_\Psi}\left[s_k\mu_k\boldsymbol{\Phi}_\Psi^T\left(X_k^\Psi\right) + \sigma_2\hat{\boldsymbol{W}}_{\Psi,k}\right],\ \hat{\boldsymbol{W}}_{\Psi,k}(0) = 0$$

$$\dot{\hat{\beta}}_k = -\gamma\hat{\beta}_k + q_3|s_k(t)|(1 + |\mu_k(t)|),\ \hat{\beta}_k(0) = 0$$

The design parameters are chosen as $\boldsymbol{\Gamma}_{W_\Xi} = \text{diag}\{2\}$, $\boldsymbol{\Gamma}_{W_\Psi} = \text{diag}\{2\}$, $\sigma_1 = \sigma_2 = 0.5$, $\gamma = 0.5$, $q_3 = 0.02$. The desired reference trajectory is $\boldsymbol{X}_d(t) = [\sin t + \sin(2t), \cos t + 2\cos(2t)]^{\mathrm{T}}$, and other design parameter keep the same as Experiment 2. Since traditional adaptive NN controller runs in time domain, the subscript "k" in controller and adaptive updating laws does not have any practical meaning. Fig. 3.15 shows the tracking curve for y_d and Fig. 3.16 shows the input and output curves of dead-zone characteristic. From the simulation results shown below, it is obvious that the adaptive NN controller performs much worse than the proposed approach and the tracking error can't be eliminated through differential-type adaptive laws for unknown parameters.

As observed in the simulation results above, the proposed NN AILC can achieve a good tracking performance for non-parameterized nonlinear time-delay systems with dead-zone input and realize the control objective, which is in accord with the

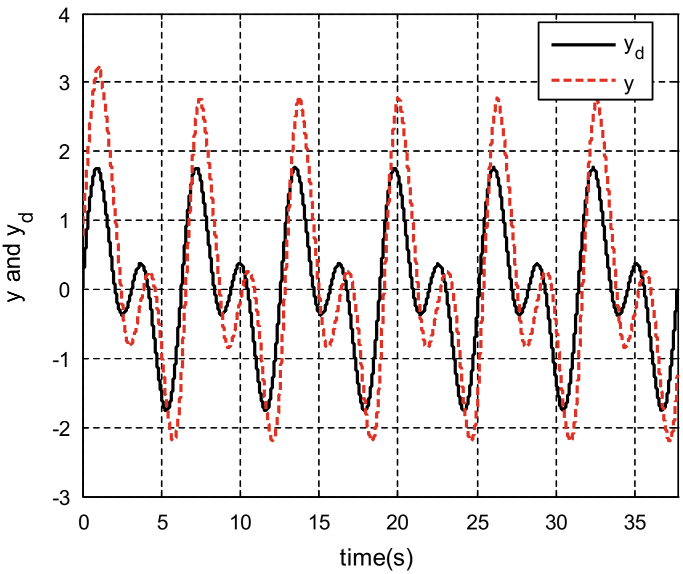

Fig. 3.15 System output y_k versus y_d

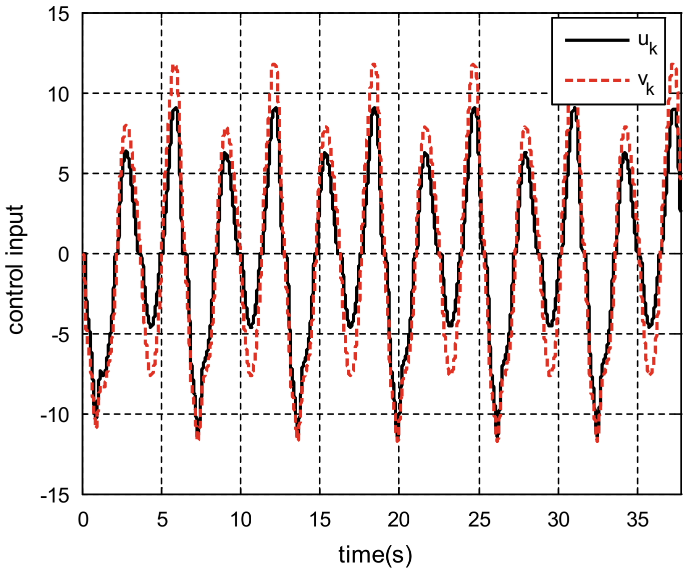

Fig. 3.16 The input v_k and output u_k of dead-zone

conclusions in Theorem 3.1 and adequately demonstrates the validity of the AILC approach in this chapter.

3.6 Summary and Comments

On the basis of Chap. 2, in this chapter we investigated the AILC problem for a class of nonlinear time-varying systems with unknown time-varying delays and unknown input dead-zone nonlinearity and proposed a RBF NN-based AILC scheme by comprehensively using L-K functional method, time-varying NN approximation technique and robust control method. By constructing appropriate Lyapunov–Krasovskii functional in the Lyapunov function candidates, the uncertainties from unknown time varying delays are removed such that control law is delay independent. RBF NNs are then used to compensate for the system's uncertainties and robust learning term is designed to deal with NN approximation remaining term. Theoretical analysis by constructing Lyapunov-like CEF has shown that the tracking errors converge to a small residual domain around the origin as iteration number goes to infinity. At the same time, all the closed-loop signals remain bounded. Simulation results have been provided to show the effectiveness of the proposed control scheme and the superiority comparing with traditional adaptive NN control method. Moreover, the proposed scheme relaxes the limitation of globally or locally Lipschitz condition, thus broadening the range of application of AILC method.

References

1. Sheng Zhu, Ming-xuan Sun. Iterative learning control of a class of nonlinear systems with unknown input dead-zone[J]. Control and Decision, 2009, 24(1): 96–100.
2. Sun M X. Iterative learning neurocomputing[C]. 2009 International Conference on Wireless Networks and Information Systems, Shanghai, China, 2009: 158–161.
3. Sun M X. Time-varying neurocomputing: An iterative learning perspective[C]. Proceedings of Intelligent Computing Theories and Applications- 8th International Conference, Huangshan, China, 2012: 18–26.
4. Hua G, Sun M. Neural networks iterative learning control: a terminal sliding mode approach[C]. Proceedings of the 7th World Congress on Intelligent Control and Automation, Chongqing, China, 2008: 3119–3124.
5. Wei-li Yan, Ming-xuan Sun. Time-varying neural networks based indirect adaptive ILC for discrete-time varying nonlinear systems[C]. Proceedings. of the 29th Chinese Control Conference, Beijing, China, 2010: 2060–2065.
6. Jun-min Li. Adaptive iterative learning control for nonlinearly parameterized systems with time-varying delays[J]. Acta Mathematica Scientia, 2011, 31A(3): 682–290.
7. Jun-min Li, Yuan-liang Wang, Xin-min Li. Adaptive iterative learning control for nonlinear parameterized-systems with unknown time-varying delays[J]. Control Theory & Applications, 2011, 28(6): 861–868.
8. Chen W, Zhang L. Adaptive iterative learning control for nonlinearly parameterized systems with unknown time-varying delays[J]. International Journal of Control, Automation and Systems, 2010, 8(2): 177–186.
9. Zhang C L, Li J M. Adaptive iterative learning control for nonlinear time-delay systems with periodic disturbances using FSE-neural network[J]. International Journal of Automation and Computing, 2011, 8(4): 403–410.
10. Li D, Li J M. Adaptive iterative learning control for nonlinearly parameterized systems with unknown time-varying delay and unknown control direction[J]. International Journal of Automation and Computing, 2012, 9(6): 578–586.
11. Broomhead D S, Lowe D. Multivariable functional interpolation and adaptive networks[J]. 1988, Complex Systems, 2: 321–355.
12. Ge S S, Hang C C, Lee T H, et al. Stable adaptive neural network control[M]. Norwell: Kluwer Academic Publishers, 2001.
13. Gupta M M, Rao D H. Neuro-control systems: theory and applications[M]. New York: IEEE Press, 1994.
14. Hätönen J, Owens D H, Feng K. Basis functions and parameter optimisation in high-order iterative learning control[J]. Automatica, 2006, 42(2): 287–294.
15. Ge S S, Hong F, Lee T H. Adaptive neural control of nonlinear time-delay systems with unknown virtual control coefficients[J]. IEEE Transactions on Systems, Man, and Cybernetics, Part B: Cybernetics, 2004, 34(1): 499–516.
16. Ge S S, Hong F, Lee T H. Robust adaptive control of nonlinear systems with unknown time delays[J]. Automatica, 2005, 41(7): 1181–1190.
17. Zhang T P, Ge S S. Adaptive neural control of MIMO nonlinear state time-varying delay systems with unknown dead-zones and gain signs[J]. Automatica, 2007, 43(6): 1021–1033.
18. Bresch-Pietri D, Chauvin J, Petit N. Adaptive control scheme for uncertain time-delay systems[J]. Automatica, 2012, 48(8): 1536–1552.
19. Zhang X, Liu L, Feng G, et al. Output feedback control of large-scale nonlinear time-delay systems in lower triangular form[J]. Automatica, 2013, 49(11): 3476–3483.
20. Zhou B. Truncated predictor feedback for time-delay systems[M]. Heidelberg: Springer, 2014.

Chapter 4
AILC of Nonlinear Time-Delay Systems with Unknown Control Direction

4.1 Introduction

In Chap. 3, the proposed RBF NN-based AILC scheme solved the AILC problem for nonlinear time-delay systems with dead-zone input. However, an important precondition for this scheme is that the sign of unknown control gain function is known, but this condition may not be satisfied in some practical control systems which are referred to as unknown control direction. In such case, the NN-based AILC method is no longer applicable.

Nowadays, the control problem of nonlinear systems with unknown control directions is a hot topic in the control field. When there is no priori knowledge about the signs of control coefficients, the control of such systems becomes much more difficult. For this problem, there are mainly two solutions: one is to directly estimate the unknown control parameter [1–3], the other is Nussbaum gain technique [4]. There into, the Nussbaum-type gain has been proved to be one of the most effective tools, and it was first proposed by Nussbaum for a class of first-order systems in 1983 [4]. In the decades that followed, this method was widely used in various kinds of control systems with unknown control direction, a large number of correlational studies have been reported in literature to promote the development of Nussbaum-type gain for a variety of control systems [5–7]. Among tremendous research results, only a few are conducted from the perspective of AILC [8–10]. The main obstacles of the problem include the manipulation of unknown control direction and stability analysis with CEF, which are different from adaptive control. Therefore, when using nonlinear control techniques to solve the ILC problem for uncertain systems with unknown direction, we have to face many new challenges. Although a few existing literatures have made some exploratory studies, the studied objects are mostly first-order system and the time-varying uncertainties exist in the parameterized form [9, 11]. Moreover, some studies also required the uncertainties to satisfy Lipschitz condition [8]. All these requirements greatly limited the extension of these methods.

Except for the dead-zone nonlinearity characteristics in the previous two chapters, hysteresis is another important non-smooth nonlinearities in a wide range of

J. Wei et al., *Iterative Learning Control for Nonlinear Time-Delay System*,
https://doi.org/10.1007/978-981-19-6317-9_4

physical systems and devices, for example, electromagnetic fields, mechanical actuators, and electronic relay circuits, which is caused by the backlash between the motion devices of gears. The existence of hysteresis can severely limit system performances and usually lead to undesirable inaccuracies, oscillations and instability. Therefore, the control design for nonlinear systems preceded by hysteresis is a challenging and rewarding research subject. To address such a problem, the principal work is to model the hysteresis nonlinearity for control design. So far, various kinds of mathematical models have been proposed for hysteresis, such as Ishlinskii hysteresis operator [12], Preisach model [13], Krasnoskl'skii-Pokrovskii hysteron [12], Duhem hysteresis [14], backlash-like hysteresis [15]. Among those models, the backlash-like hysteresis model was widely used owing to its better representation of the hysteresis nonlinearity and its facilitation for the controller design. In time domain, many various methods have been put forward for various systems with backlash-like hysteresis [16–18]. However, there are few works conducted from the viewpoint of AILC to deal with nonlinear systems with hysteresis nonlinearity in the literature. All the control strategies mentioned above are not applicable to the AILC problem of uncertain time-varying systems due to the particular design process and stability analysis tool. As far as we know, only Zhu discussed the ILC problem for a class of parameterized systems with hysteresis nonlinearity [19].

Motivated by the above observations, in this chapter, we study the AILC problem specifically for a class of nonlinear systems with unknown time-varying delays and control direction preceded by a backlash-like hysteresis input. To the best of our knowledge, up to now, no works has been reported in the field of AILC which can deal with this kind of systems. The design difficulty mainly comes from the interactions of unknown time varying delays, backlash-like hysteresis nonlinearity, unknown control direction and time-varying uncertainties. In order to overcome above difficulties, we will synthetically utilize neural approximation technique, Nussbaum function method and robust control to design the iterative learning controller.

4.2 Problem Formulation and Preliminaries

4.2.1 Problem Formulation

Consider a class of nonlinear time-delay systems with unknown control direction and uncertain backlash-like hysteresis running on a finite time interval $[0, T]$ repeatedly, which is given by

$$\begin{cases} \dot{x}_{i,k}(t) = x_{i+1,k}(t), i = 1, \ldots, n-1 \\ \dot{x}_{n,k}(t) = f(\boldsymbol{X}_k(t), t) + h\big(\boldsymbol{X}_{\tau,k}(t), t\big) + g(\boldsymbol{X}_k(t), t)u_k(v_k(t)) + d(t) \\ y_k(t) = x_{1,k}(t), t \in [0, T] \\ x_k(t) = \varpi(t), t \in [-\tau_{\max}, 0) \end{cases} \tag{4.1}$$

where, $g(\cdot, \cdot)$ is the unknown time-varying control gain and its sign is unknown; $u_k(v_k(t))$ presents backlash-like hysteresis nonlinearity, where v_k and u_k present the input and output of backlash-like nonlinearity respectively. Other notations are as same as those in Chap. 3.

The control goal remains the same as previous chapters. On the basis of Chap. 3, make the following assumption on control gain function.

Assumption 4.1 The nonlinear gain function $g(\cdot, \cdot)$ and its sign are both unknown, and its sign is either strictly positive or negative. There exist positive constants $0 < g_{\min} \leq g_{\max}$ such that $g_{min} \leq |g(\cdot, \cdot)| \leq g_{max})$.

Remark 4.1 Assumption 4.1 a reasonable assumption since $g(\cdot, \cdot)$ being away from zero is the controllable condition of nonlinear systems (4.1), which is required in most control schemes [20, 21]. Besides, the control gain bounds $g_{\min}$ and $g_{\max}$ are only required for analytical purposes, their true values are not necessarily known as they are not used for controller design.

4.2.2 *Backlash-Like Hysteresis Nonlinearity*

Traditionally, the backlash hysteresis nonlinearity can be given by the following expression.

$$\dot{u}_k(t) = \begin{cases} c\dot{v}_k, \text{ if } \dot{v}_k > 0, \ u_k = c(v_k - B) \\ c\dot{v}_k, \text{ if } \dot{v}_k < 0, \ u_k = c(v_k + B) \\ 0, \ \text{otherwise} \end{cases} \tag{4.2}$$

where $c > 0$ is the slope of the lines and $B > 0$ is the backlash distance. This model is discontinuous and not suitable for controller design. Here, we use the backlash-like hysteresis dynamic model in [15] to model the backlash-like hysteresis nonlinearity, which is given by

$$\frac{\mathrm{d}u_k}{\mathrm{d}t} = \alpha \left| \frac{\mathrm{d}v_k}{\mathrm{d}t} \right| (cv_k - u_k) + B_1 \frac{\mathrm{d}v_k}{\mathrm{d}t} \tag{4.3}$$

where β, c and B_1 are unknown constants, satisfying $c > B_1$. Based on the analysis in [15], Eq. (4.3) can be solved explicitly

$$u_k(t) = cv_k(t) + d_1(v_k) \tag{4.4}$$

where,

$$d_1(v_k) = (u_k(0) - cv_k(0))\mathrm{e}^{-\alpha(v_k - v_k(0))\mathrm{sgn}\dot{v}_k}$$

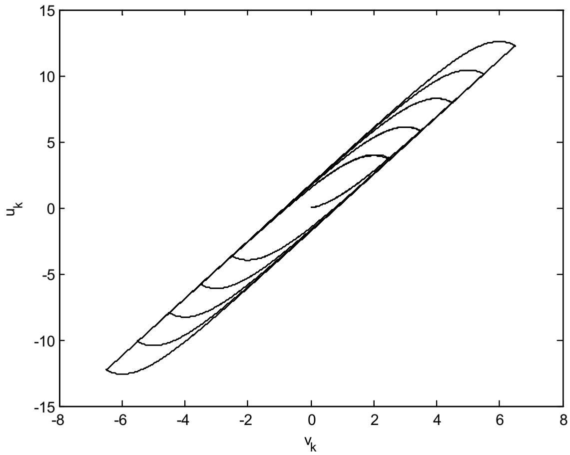

Fig. 4.1 Backlash-like hysteresis curves for model (4.3) with $\beta = 1$, $c = 1.1635$, and $B_1 = 0.345$ for $v_k(t) = m\sin(2.3t)$ with $m = 2.5, 3.5, 4.5, 5.5$ and 6.5

$$+\, \mathrm{e}^{-\alpha v_k \mathrm{sgn}\dot{v}_k} \int_{v_k(0)}^{v_k(t)} (B_1 - c)\mathrm{e}^{\alpha\sigma(\mathrm{sgn}\dot{v}_k)} \mathrm{d}\sigma \tag{4.5}$$

Examining (4.4), it shows that the backlash-like hysteresis nonlinearity is composed of a line with the slope c, together with $d_1(v_k)$ which is bounded. Furthermore, we have

$$\begin{cases} \lim\limits_{v_k \to -\infty} d_1(v_k) = \lim\limits_{v_k \to -\infty} (u_k(v_k; v_k(0), u_k(0)) - cv_k) = \dfrac{c - B_1}{\alpha} \\ \lim\limits_{v_k \to +\infty} d_1(v_k) = \lim\limits_{v_k \to +\infty} (u_k(v_k; v_k(0), u_k(0)) - cv_k) = -\dfrac{c - B_1}{\alpha} \end{cases} \tag{4.6}$$

It indicates that β determines the rate where u_k switches between $-(c - B_1)/\beta$ and $(c - B_1)/\beta$, i.e., the larger the parameter β is, the faster the transition frequency in u_k is going to be [22]. The backlash distance is determined by $(c - B_1)/\beta$. Therefore, a suitable choose of parameter set $\{\beta, c, B_1\}$ enable us to model the required shape of backlash-like hysteresis. A graphical representation of backlash-like hysteresis is shown in Fig. 4.1, where the parameters $\beta = 1$, $c = 1.1635$, and $B_1 = 0.345$, the input signal $v_k(t) = m\sin(2.3t)$ ($m = 2.5$, 3.5, 4.5, 5.5 and 6.5) and the initial condition $u_k(0) = 0$.

4.2.3 Nussbaum Gain Method

In order to deal with unknown control direction, the Nussbaum gain technique is used in this paper. The Nussbaum type function is defined as follows.

Definition 4.1 A continuous function $N(\zeta)$ is called a Nussbaum-type function when it has the following properties:

$$\lim_{s\to+\infty}\sup\frac{1}{s}\int_0^s N(\zeta)\mathrm{d}\zeta = +\infty \tag{4.7}$$

$$\lim_{s\to+\infty}\inf\frac{1}{s}\int_0^s N(\zeta)\mathrm{d}\zeta = -\infty \tag{4.8}$$

Commonly used Nussbaum-type functions include: $\zeta^2\cos\zeta$, $\zeta^2\sin\zeta$ and $\exp(\zeta^2)\cos((\pi/2)\zeta)$. Taking $N(\zeta) = \zeta^2\sin\zeta$ for example, it is sufficient to prove that

$$\lim_{n\to\infty}\frac{1}{2n\pi}\int_0^{2n\pi} N(\zeta)\mathrm{d}\zeta = -\infty \tag{4.9}$$

$$\lim_{n\to\infty}\frac{1}{2n\pi+\pi}\int_0^{2n\pi+\pi} N(\zeta)\mathrm{d}\zeta = +\infty \tag{4.10}$$

The proof for (4.9) is as follows

$$\begin{aligned}
\lim_{n\to\infty}\frac{1}{2n\pi}\int_0^{2n\pi}\zeta^2\sin\zeta\,\mathrm{d}\zeta &= -\lim_{n\to\infty}\frac{1}{2n\pi}\int_0^{2n\pi}\zeta^2\mathrm{d}\cos\zeta \\
&= -\lim_{n\to\infty}\frac{1}{2n\pi}\left(\zeta^2\cos(\zeta)\big|_0^{2n\pi} - 2\int_0^{2n\pi}\zeta\cos\zeta\,\mathrm{d}\zeta\right) \\
&= -\lim_{n\to\infty}2n\pi + \lim_{n\to\infty}\frac{1}{n\pi}\int_0^{2n\pi}\zeta\,\mathrm{d}\sin\zeta \\
&= -\lim_{n\to\infty}2n\pi + \lim_{n\to\infty}\frac{1}{n\pi}\left(\zeta\sin\zeta\,|_0^{2n\pi} - \int_0^{2n\pi}\sin\zeta\,\mathrm{d}\zeta\right) \\
&= -\infty
\end{aligned} \tag{4.11}$$

The proof for (4.10) is similar and we will not present it in detail.

Associated with the Nussbaum-type function, we have the following propositions.

Lemma 4.1 [23]. *Let $V(\cdot)$ and $\zeta(\cdot)$ be smooth functions defined on $\left[0, t_f\right)$ with $V(t) \geq 0, \forall t \in \left[0, t_f\right)$, and $N(\cdot)$ be an even smooth Nussbaum-type function. If the following inequality holds*:

$$V(t) \leq c_0 + \int_0^t (g_0 N(\zeta) + 1)\dot{\zeta}\mathrm{d}\sigma, \ \forall t \in \left[0, t_f\right) \tag{4.12}$$

where, g_0 is a nonzero constant and c_0 represents some suitable constant, then $V(t)$, $\zeta(t)$ and $\int_0^t (g_0 N(\zeta) + 1)\dot{\zeta}\mathrm{d}\sigma$ must be bounded on $\left[0, t_f\right)$.

Lemma 4.2 [24]. *For any given positive constant $t_f > 0$, if the solution of the resulting closed-loop system is bounded, then $t_f = \infty$.*

4.3 Nussbuam Gain-Based AILC Scheme Design

The definitions of e_{sk} and s_k are as same as that in previous two chapters. Substituting (4.4) into (4.1), we can obtain the time derivative of $e_{n,k}$ as follows

$$\begin{aligned} \dot{e}_{n,k} &= f(\boldsymbol{X}_k, t) + h\big(\boldsymbol{X}_{\tau,k}, t\big) + g(\boldsymbol{X}_k, t)(cv_k + d_1(v_k)) + d(t) - y_d^{(n)} \\ &= f(\boldsymbol{X}_k, t) + h\big(\boldsymbol{X}_{\tau,k}, t\big) + cg(\boldsymbol{X}_k, t)v_k + d_2(\boldsymbol{X}_k) - y_d^{(n)} \end{aligned} \tag{4.13}$$

where, $d_2(\boldsymbol{X}_k) = g(\boldsymbol{X}_k, t)d_1(v_k) + d(t)$. Obviously, $d_2(\boldsymbol{X}_k)$ is bounded, i.e., there exists unknown smooth positive function $\overline{d}(\boldsymbol{X}_k)$ such that $|d_2(\boldsymbol{X}_k)| \leq \overline{d}(\boldsymbol{X}_k)$. For clarity of notation, we denote $cg(\boldsymbol{X}_k, t)$ by $g_c(\boldsymbol{X}_k, t) \triangleq cg(\boldsymbol{X}_k, t)$. It is clear that, $\underline{g}_c = cg_{\min} \leq |g_c(\boldsymbol{X}_k, t)| \leq cg_{\max} = \overline{g}_c$. For subsequent design, we define a positive function $\beta(\boldsymbol{X}_k) = 1\big/|g_c(\boldsymbol{X}_k, t)|$. For following design, we rewrite $\beta(\boldsymbol{X}_k)$ as $\beta\big(\overline{\boldsymbol{x}}_{n-1,k}, x_{n,k}\big) = 1\big/|g_c(\boldsymbol{X}_k, t)|$ with $\overline{\boldsymbol{x}}_{n-1,k}(t) = \left[x_{1,k}(t), \ldots, x_{n-1,k}(t)\right]^{\mathrm{T}}$. To avoid control singularity, define the following positive integral functional

$$V_{s_k} = \int_0^{s_k} \sigma\beta(\overline{\boldsymbol{x}}_{n-1,k}, \sigma + \omega_k)\mathrm{d}\sigma \tag{4.14}$$

where, $\omega_k = y_d^{(n-1)} - \left[\boldsymbol{\Lambda}^{\mathrm{T}}\ 0\right]\boldsymbol{e}_k + \eta(t)\mathrm{sat}\big(e_{sk}\big/\eta(t)\big)$.

By changing the variable $\sigma = \vartheta s_k$, we may rewrite V_{s_k} as $V_{s_k} = s_k^2 \int_0^1 \vartheta\beta(\overline{x}_{n-1,k}, \theta s_k + \omega_k)\mathrm{d}\vartheta$. Noting that $1\big/\overline{g}_c \leq \beta(\overline{x}_{n-1,k}, \sigma + \omega_k) \leq 1\Big/\underline{g}_c$, we have

$$\frac{s_k^2}{2\overline{g}_c} \leq V_{s_k} \leq \frac{s_k^2}{2\underline{g}_c} \tag{4.15}$$

It is clear that V_{s_k} is positive definite with respect to s_k. Differentiating V_{s_k} with respect to time t, we obtain

$$\begin{aligned}\dot{V}_{s_k} &= \frac{\partial V_{s_k}}{\partial s_k}\dot{s}_k + \dot{\overline{\boldsymbol{x}}}^{\mathrm{T}}_{n-1,k}\frac{\partial V_{s_k}}{\partial \overline{\boldsymbol{x}}_{n-1,k}} + \frac{\partial V_{s_k}}{\partial \omega_k}\dot{\omega}_k \\ &= \beta(\boldsymbol{X}_k)s_k\dot{s}_k + \dot{\overline{\boldsymbol{x}}}^{\mathrm{T}}_{n-1,k}\int_0^{s_k}\sigma\frac{\partial\beta(\overline{\boldsymbol{x}}_{n-1,k},\sigma+\omega_k)}{\partial\overline{\boldsymbol{x}}_{n-1,k}}\mathrm{d}\sigma \\ &\quad + \dot{\omega}_k\int_0^{s_k}\sigma\frac{\partial\beta(\overline{\boldsymbol{x}}_{n-1,k},\sigma+\omega_k)}{\partial\omega_k}\mathrm{d}\sigma \end{aligned} \tag{4.16}$$

Considering the first term of the right side of (4.16), we have

$$\begin{aligned}\beta(\boldsymbol{X}_k)s_k\dot{s}_k &= \begin{cases}\beta(\boldsymbol{X}_k)s_k(\dot{e}_{sk}-\dot{\eta}(t)), & if\ e_{sk}>\eta(t)\\ 0, & if\ |e_{sk}|\le\eta(t)\\ \beta(\boldsymbol{X}_k)s_k(\dot{e}_{sk}+\dot{\eta}(t)), & if\ e_{sk}<-\eta(t)\end{cases} \\ &= \beta(\boldsymbol{X}_k)s_k(\dot{e}_{sk}-\dot{\eta}(t)\mathrm{sgn}(s_k)) \\ &= \beta(\boldsymbol{X}_k)s_k\left[\sum_{j=1}^{n-1}\lambda_j e_{j+1,k} - \dot{\eta}(t)\mathrm{sgn}(s_k) - y_d^{(n)} + f(\boldsymbol{X}_k,t) + h\big(\boldsymbol{X}_{\tau,k},t\big)\right. \\ &\quad \left. + g_c(\boldsymbol{X}_k,t)v_k + d_2(\boldsymbol{X}_k)\right] \end{aligned} \tag{4.17}$$

By changing the variable we obtain

$$\dot{\overline{\boldsymbol{x}}}^{\mathrm{T}}_{n-1,k}\int_0^{s_k}\sigma\frac{\partial\beta(\overline{\boldsymbol{x}}_{n-1,k},\sigma+\omega_k)}{\partial\overline{\boldsymbol{x}}_{n-1,k}}\mathrm{d}\sigma = s_k^2\sum_{i=1}^{n-1}x_{i+1,k}\int_0^1\vartheta\frac{\partial\beta(\overline{\boldsymbol{x}}_{n-1,k},\vartheta s_k+\omega_k)}{\partial x_{i,k}}d\vartheta \tag{4.18}$$

Because $\partial\beta(\overline{\boldsymbol{x}}_{n-1,k},\sigma+\omega_k)/\partial\omega_k = \partial\beta(\overline{\boldsymbol{x}}_{n-1,k},\sigma+\omega_k)/\partial\sigma$, it is clear that

$$\begin{aligned}&\dot{\omega}_k\int_0^{s_k}\sigma\frac{\partial\beta(\overline{\boldsymbol{x}}_{n-1,k},\sigma+\omega_k)}{\partial\omega_k}\mathrm{d}\sigma \\ &= \dot{\omega}_k\left[\sigma\beta(\overline{\boldsymbol{x}}_{n-1,k},\sigma+\omega_k)\Big|_0^{s_k} - \int_0^{s_k}\beta(\overline{\boldsymbol{x}}_{n-1,k},\sigma+\omega_k)d\sigma\right] \\ &= s_k\dot{\omega}_k\left[\beta(\boldsymbol{X}_k) - \int_0^1\beta(\overline{\boldsymbol{x}}_{n-1,k},\vartheta s_k+\omega_k)d\vartheta\right]\end{aligned}$$

$$
= \begin{cases} s_k\left[y_d^{(n)} - \sum_{j=1}^{n-1}\lambda_j e_{j+1,k} + \dot{\eta}(t)\right]\left[\beta(\boldsymbol{X}_k) - \int_0^1 \beta(\overline{\boldsymbol{x}}_{n-1,k}, \vartheta s_k + \omega_k)d\vartheta\right], if\ e_{sk}(t) > \eta(t) \\ 0,\ if\ |e_{sk}(t)| \le \eta(t) \\ s_k\left[y_d^{(n)} - \sum_{j=1}^{n-1}\lambda_j e_{j+1,k} - \dot{\eta}(t)\right]\left[\beta(\boldsymbol{X}_k) - \int_0^1 \beta(\overline{\boldsymbol{x}}_{n-1,k}, \vartheta s_k + \omega_k)d\vartheta\right],\ if\ e_{sk}(t) < -\eta(t) \end{cases}
$$

$$
= s_k\left[y_d^{(n)} - \sum_{j=1}^{n-1}\lambda_j e_{j+1,k} + \dot{\eta}(t)\mathrm{sgn}(s_k)\right]\left[\beta(\boldsymbol{X}_k) - \int_0^1 \beta(\overline{\boldsymbol{x}}_{n-1,k}, \vartheta s_k + \omega_k)d\vartheta\right]
$$

$$
= s_k\beta(\boldsymbol{X}_k)\left[y_d^{(n)} - \sum_{j=1}^{n-1}\lambda_j e_{j+1,k} + \dot{\eta}(t)\mathrm{sgn}(s_k)\right]
$$

$$
- s_k\left[y_d^{(n)} - \sum_{j=1}^{n-1}\lambda_j e_{j+1,k} + \dot{\eta}(t)\mathrm{sgn}(s_k)\right]\int_0^1 \beta(\overline{\boldsymbol{x}}_{n-1,k}, \vartheta s_k + \omega_k)d\vartheta \tag{4.19}
$$

Substituting (4.17)–(4.19) back into (4.16) leads to

$$
\begin{aligned}
\dot{V}_{s_k} &= \frac{\partial V_{s_k}}{\partial s_k}\dot{s}_k + \dot{\overline{\boldsymbol{x}}}_{n-1,k}^{\mathrm{T}}\frac{\partial V_{s_k}}{\partial \overline{\boldsymbol{x}}_{n-1,k}} + \frac{\partial V_{s_k}}{\partial \omega_k}\dot{\omega}_k \\
&= s_k\beta(\boldsymbol{X}_k)\left[f(\boldsymbol{X}_k, t) + h\left(\boldsymbol{X}_{\tau,k}, t\right) + g_c(\boldsymbol{X}_k, t)v_k + d_2(\boldsymbol{X}_k)\right] \\
&+ s_k^2\sum_{i=1}^{n-1} x_{i+1,k}\int_0^1 \vartheta\frac{\partial\beta(\overline{\boldsymbol{x}}_{n-1,k}, \vartheta s_k + \omega_k)}{\partial x_{i,k}}d\vartheta \\
&- s_k\left[y_d^{(n)} - \sum_{j=1}^{n-1}\lambda_j e_{j+1,k} + \dot{\eta}(t)\mathrm{sgn}(s_k)\right]\int_0^1 \beta(\overline{\boldsymbol{x}}_{n-1,k}, \vartheta s_k + \omega_k)d\vartheta \\
&= s_k\Big\{\beta(x_k)\left[f(\boldsymbol{X}_k, t) + h\left(\boldsymbol{X}_{\tau,k}, t\right) + g_c(\boldsymbol{X}_k, t)v_k + d_2(\boldsymbol{X}_k)\right] \\
&+ s_k\sum_{i=1}^{n-1} x_{i+1,k}\int_0^1 \vartheta\frac{\partial\beta(\overline{\boldsymbol{x}}_{n-1,k}, \vartheta s_k + \omega_k)}{\partial x_{i,k}}d\vartheta \\
&- \left[y_d^{(n)} - \sum_{j=1}^{n-1}\lambda_j e_{j+1,k} + \dot{\eta}(t)\mathrm{sgn}(s_k)\right]\int_0^1 \beta(\overline{\boldsymbol{x}}_{n-1,k}, \vartheta s_k + \omega_k)d\vartheta\Big\}
\end{aligned} \tag{4.20}
$$

Using Young's inequality, we have

$$
\begin{aligned}
s_k\beta(\boldsymbol{X}_k)h\left(\boldsymbol{X}_{\tau,k}, t\right) &\le |s_k|\beta(\boldsymbol{X}_k)\theta(t)\sum_{j=1}^{n}\rho_j\left(x_{\tau_j,k}(t)\right) \\
&\le \frac{n}{2}s_k^2(\beta(\boldsymbol{X}_k))^2(\theta(t))^2 + \frac{1}{2}\sum_{j=1}^{n}\rho_j^2(x_{\tau_j,k})
\end{aligned} \tag{4.21}
$$

$$s_k\beta(\boldsymbol{X}_k)d_2(\boldsymbol{X}_k) \le \frac{s_k^2\beta^2(\boldsymbol{X}_k)\overline{d}^2(\boldsymbol{X}_k)}{4a_1} + a_1 \tag{4.22}$$

with a_1 being a given arbitrary positive constant.

Substituting (4.21) and (4.22) into (4.20) results in

$$\begin{aligned}\dot{V}_{s_k} \le\ & s_k\{\beta(\boldsymbol{X}_k)[f(\boldsymbol{X}_k,t) + g_c(\boldsymbol{X}_k,t)v_k] \\ & + s_k\sum_{i=1}^{n-1} x_{i+1,k}\int_0^1 \vartheta\frac{\partial\beta(\overline{\boldsymbol{x}}_{n-1,k},\vartheta s_k+\omega_k)}{\partial x_{i,k}}\mathrm{d}\vartheta \\ & + \frac{n}{2}s_k\beta^2(\boldsymbol{X}_k)\theta^2(t) + \frac{s_k\beta^2(\boldsymbol{X}_k)\overline{d}^2(\boldsymbol{X}_k)}{4a_1} \\ & - \left[y_d^{(n)} - \sum_{j=1}^{n-1}\lambda_j e_{j+1,k} + \dot{\eta}(t)\mathrm{sgn}(s_k)\right]\int_0^1 \beta(\overline{\boldsymbol{x}}_{n-1,k},\vartheta s_k+\omega_k)d\vartheta\Bigg\} \\ & + \frac{1}{2}\sum_{j=1}^{n}\rho_j^2(x_{\tau_j,k}) + a_1\end{aligned} \tag{4.23}$$

To overcome the design difficulty arising from the unknown time-varying delays term in (4.23), define L-K functional as

$$V_{U_k}(t) = \frac{1}{2(1-\kappa)}\sum_{j=1}^{n}\int_{t-\tau_j(t)}^{t}\rho_j^2\big(x_{j,k}(\sigma)\big)\mathrm{d}\sigma \tag{4.24}$$

Taking the time derivative of $V_{U_k}(t)$ yields

$$\begin{aligned}\dot{V}_{U_k}(t) &= \frac{1}{2(1-\kappa)}\sum_{j=1}^{n}\rho_j^2\big(x_{j,k}\big) - \frac{1}{2}\sum_{j=1}^{n}\frac{1-\dot{\tau}_j(t)}{(1-\kappa)}\rho_j^2\big(x_{\tau_j,k}\big) \\ &\le \frac{1}{2(1-\kappa)}\sum_{j=1}^{n}\rho_j^2\big(x_{j,k}\big) - \frac{1}{2}\sum_{j=1}^{n}\rho_j^2\big(x_{\tau_j,k}\big)\end{aligned} \tag{4.25}$$

Define the Lyapunov candidate as $V_k(t) = V_{s_k}(t) + V_{U_k}(t)$, combining (4.23) and (4.25), we can obtain the time derivative of $V_k(t)$ as follows

$$\begin{aligned}\dot{V}_k \le\ & s_k\{\beta(\boldsymbol{X}_k)[f(\boldsymbol{X}_k(t),t) + g_c(\boldsymbol{X}_k(t),t)v_k(t)] \\ & + s_k\sum_{i=1}^{n-1} x_{i+1,k}\int_0^1 \vartheta\frac{\partial\beta(\overline{\boldsymbol{x}}_{n-1,k},\vartheta s_k+\omega_k)}{\partial x_{i,k}}d\vartheta\end{aligned}$$

$$+\frac{n}{2}s_k\beta^2(\boldsymbol{X}_k)\theta^2(t)+\frac{s_k\beta^2(\boldsymbol{X}_k)\overline{d}^2(\boldsymbol{X}_k)}{4a_1}$$
$$-\left[y_d^{(n)}-\sum_{j=1}^{n-1}\lambda_j e_{j+1,k}+\dot{\eta}(t)\mathrm{sgn}(s_k)\right]\int_0^1\beta(\overline{\boldsymbol{x}}_{n-1,k},\vartheta s_k+\omega_k)d\vartheta\Bigg\}$$
$$+\frac{1}{2(1-\kappa)}\sum_{j=1}^{n}\rho_j^2(x_{j,k})+a_1 \tag{4.26}$$

For the convenience of expression, denote $\xi(\boldsymbol{X}_k)\triangleq\frac{1}{2(1-\kappa)}\sum_{j=1}^{n}\rho_j^2(x_{j,k})+a_1$. Similar to previous chapters, to avoid possible singularity problem, Employing the hyperbolic tangent function, then Eq. (4.26) becomes

$$\begin{aligned}\dot{V}_k\le{}& s_k\beta(\boldsymbol{X}_k)g_c(\boldsymbol{X}_k,t)v_k(t)+s_k\{\beta(\boldsymbol{X}_k)f(\boldsymbol{X}_k,t)\\&+s_k\sum_{i=1}^{n-1}x_{i+1,k}\int_0^1\vartheta\frac{\partial\beta(\overline{\boldsymbol{x}}_{n-1,k},\vartheta s_k+\omega_k)}{\partial x_{i,k}}\mathrm{d}\vartheta\\&+\frac{n}{2}s_k\beta^2(\boldsymbol{X}_k)\vartheta^2(t)+\frac{s_k\beta^2(\boldsymbol{X}_k)\overline{d}^2(x_k)}{4a_1}\\&-\left[y_d^{(n)}-\sum_{j=1}^{n-1}\lambda_j e_{j+1,k}+\dot{\eta}(t)\mathrm{sgn}(s_k)\right]\int_0^1\beta(\overline{\boldsymbol{x}}_{n-1,k},\vartheta s_k+\omega_k)d\vartheta\\&+\frac{b}{s_k}\tanh^2\big(s_k/\eta(t)\big)\xi(\boldsymbol{X}_k)\Big\}+\big[1-b\tanh^2\big(s_k/\eta(t)\big)\big]\xi(\boldsymbol{X}_k)\\={}&g_0s_kv_k(t)+s_kQ(\boldsymbol{Z}_k,t)+\big[1-b\tanh^2\big(s_k/\eta(t)\big)\big]\xi(\boldsymbol{X}_k)\end{aligned} \tag{4.27}$$

where,

$$\begin{aligned}Q(\boldsymbol{Z}_k,t)={}&\beta(\boldsymbol{X}_k)f(\boldsymbol{X}_k,t)+s_k\sum_{i=1}^{n-1}x_{i+1,k}\int_0^1\vartheta\frac{\partial\beta(\overline{\boldsymbol{x}}_{n-1,k},\vartheta s_k+\omega_k)}{\partial x_{i,k}}d\vartheta\\&+\frac{n}{2}s_k\beta^2(x_k)\theta^2(t)+\frac{s_k\beta^2(\boldsymbol{X}_k)\overline{d}^2(\boldsymbol{X}_k)}{4a_1}\\&-\left[y_d^{(n)}-\sum_{j=1}^{n-1}\lambda_j e_{j+1,k}+\dot{\eta}(t)\mathrm{sgn}(s_k)\right]\int_0^1\beta(\overline{\boldsymbol{x}}_{n-1,k},\vartheta s_k+\omega_k)d\vartheta\\&+\frac{b}{s_k}\tanh^2\left(\frac{s_k}{\eta(t)}\right)\xi(x_k)\end{aligned}$$

$\boldsymbol{Z}_k = \left[\boldsymbol{X}_k^T, \boldsymbol{X}_d^T, y_d^{(n)}\right]^{\mathrm{T}} \subset \boldsymbol{\Omega}_{Z_k}$, with $\boldsymbol{\Omega}_{Z_k}$ being a compact set, $g_0 = \beta(\boldsymbol{X}_k) g_c(\boldsymbol{X}_k, t) = g_c(\boldsymbol{X}_k, t) \big/ |g_c(\boldsymbol{X}_k, t)| = 1$ or -1. Apparently, $Q(\boldsymbol{Z}_k, t)$ is continuous and well-defined on the compact set, then it can be approximated by RBF NN to arbitrary accuracy as:

$$Q(\boldsymbol{Z}_k, t) = \boldsymbol{W}^{*T}(t)\boldsymbol{\phi}(\boldsymbol{Z}_k) + \varepsilon(\boldsymbol{Z}_k, t) \tag{4.28}$$

where, $\boldsymbol{W}^*(t) \in \mathbf{R}^l$ is unknown ideal time-varying weight; $\boldsymbol{\phi}(\boldsymbol{Z}_k) = [\varphi_i(\boldsymbol{Z}_k), \varphi_2(\boldsymbol{Z}_k), \ldots, \varphi_l(\boldsymbol{Z}_k)]^{\mathrm{T}} \in \mathbf{R}^l$ is the Gaussian basis function with $\varphi_i(\boldsymbol{X}_k) = \exp\left(-\left\|\boldsymbol{X}_k - \boldsymbol{\mu}_i\right\|^2 \big/ \sigma_i^2\right)$, $\boldsymbol{\mu}_i \in \mathbf{R}^n$ and $\sigma_i \in R$ are the center and width of neural network respectively, l denotes the NN node number; $\varepsilon(\boldsymbol{Z}_k, t)$ is the approximation error. According to NN approximation characteristic, the approximation error can be made arbitrarily small by increasing NN nodes. Therefore, we can assume that $\max_{t\in[0,T]} |\varepsilon(\boldsymbol{Z}_k, t)| \leq \varepsilon^*$, ε^* is an unknown small constant. Besides, the ideal NN weight $\boldsymbol{W}^*(t)$ is bounded, i.e.,

$$\max_{t\in[0,T]} \left\|\boldsymbol{W}^*(t)\right\| \leq \varepsilon_W \tag{4.29}$$

By using Nussbaum function method, design the adaptive iterative learning control system for system (4.1) as follows:

$$\begin{cases} v_k = N(\zeta_k)\alpha_k(t) \\ \dot{\zeta}_k = s_k\alpha_k, \ \zeta_k(0) = \zeta_{k-1}(T) \\ \alpha_k(t) = k_1 s_k + \hat{\boldsymbol{W}}_k^T(t)\boldsymbol{\phi}(\boldsymbol{Z}_k) + \mathrm{sat}\left(e_{sk} \big/ \eta(t)\right)\hat{\varepsilon}_k \end{cases} \tag{4.30}$$

where, α_k presents the virtual control, ζ_k is the Nussbaum gain, $k_1 > 0$ is the design parameter, $\hat{\boldsymbol{W}}_k(t)$ and $\hat{\varepsilon}_k$ are the estimates for $\boldsymbol{W}^*(t)$ and ε^*, respectively. The adaptive learning algorithms for unknown parameters are designed as follows

$$\begin{cases} \hat{\boldsymbol{W}}_k(t) = \hat{\boldsymbol{W}}_{k-1}(t) + q_1 s_k(t)\boldsymbol{\phi}(\boldsymbol{Z}_k) \\ \hat{\boldsymbol{W}}_0(t) = 0, t \in [0, T] \end{cases} \tag{4.31}$$

$$\begin{cases} (1-\gamma)\dot{\hat{\varepsilon}}_k(t) = -\gamma\hat{\varepsilon}_k(t) + \gamma\hat{\varepsilon}_{k-1}(t) + q_2|s_k(t)| \\ \hat{\varepsilon}_k(0) = \hat{\varepsilon}_{k-1}(T), \hat{\varepsilon}_0(t) = 0, t \in [0, T] \end{cases} \tag{4.32}$$

where, $q_1, q_2 > 0$ and $0 < \gamma < 1$ are design parameters.

Remark 4.2 In the controller (4.30), three parts are included, which are error feedback term, neural learning term and robust learning term. Feedback term of error is to guarantee the stability in time domain for each iteration. Neural learning term is used to compensate for the uncertainties in the system. Robust learning term deals with the neural approximation error. As shown in (4.31) and (4.32), difference-type and differential-difference-type learning laws are designed for neural weights and upper bound of approximation error, respectively.

Define the estimation error as $\tilde{W}_k(t) = \hat{W}_k(t) - W^*(t)$, $\tilde{\varepsilon}_k(t) = \hat{\varepsilon}_k(t) - \varepsilon^*$. Then, substituting the controller (4.30) back into (4.27), it results in

$$
\begin{aligned}
\dot{V}_k &\le g_0 s_k v_k(t) + s_k Q(\boldsymbol{Z}_k) + \left[1 - b\tanh^2\left(s_k / \eta(t)\right)\right]\xi(\boldsymbol{X}_k) \\
&= g_0 N(\zeta_k)\dot{\zeta}_k + \dot{\zeta}_k - \dot{\zeta}_k + s_k\left(\boldsymbol{W}^{*\mathrm{T}}(t)\boldsymbol{\phi}(\boldsymbol{Z}_k) + \varepsilon(\boldsymbol{Z}_k, t)\right) \\
&\quad + \left[1 - b\tanh^2\left(s_k / \eta(t)\right)\right]\xi(\boldsymbol{X}_k) \\
&= (g_0 N(\zeta_k) + 1)\dot{\zeta}_k - s_k\left[k_1 s_k + \hat{\boldsymbol{W}}_k^{\mathrm{T}}(t)\boldsymbol{\phi}(\boldsymbol{Z}_k) + \mathrm{sat}\left(e_{sk} / \eta(t)\right)\hat{\varepsilon}_k\right] \\
&\quad + s_k\left(\boldsymbol{W}^{*\mathrm{T}}(t)\boldsymbol{\phi}(\boldsymbol{Z}_k) + \varepsilon(\boldsymbol{Z}_k)\right) + \left[1 - b\tanh^2\left(s_k / \eta(t)\right)\right]\xi(\boldsymbol{X}_k) \\
&\le (g_0 N(\zeta_k) + 1)\dot{\zeta}_k - s_k\tilde{\boldsymbol{W}}_k^{\mathrm{T}}(t)\boldsymbol{\phi}(\boldsymbol{Z}_k) - |s_k|\hat{\varepsilon}_k + |s_k|\varepsilon^* \\
&\quad + \left[1 - b\tanh^2\left(s_k / \eta(t)\right)\right]\xi(\boldsymbol{X}_k) - k_1 s_k^2(t) \\
&= (g_0 N(\zeta_k) + 1)\dot{\zeta}_k - s_k\tilde{\boldsymbol{W}}_k^{\mathrm{T}}(t)\boldsymbol{\phi}(\boldsymbol{Z}_k) - |s_k|\tilde{\varepsilon}_k \\
&\quad + \left[1 - b\tanh^2\left(s_k / \eta(t)\right)\right]\xi(\boldsymbol{X}_k) - k_1 s_k^2(t)
\end{aligned}
\tag{4.33}
$$

For subsequent discussion, we rewrite (4.33) as

$$
\begin{aligned}
s_k\tilde{\boldsymbol{W}}_k^{\mathrm{T}}(t)\boldsymbol{\phi}(\boldsymbol{Z}_k) + |s_k|\tilde{\varepsilon}_k \le -\dot{V}_k + (g_0 N(\zeta_k) + 1)\dot{\zeta}_k - k_1 s_k^2 \\
+ \left[1 - b\tanh^2\left(s_k / \eta(t)\right)\right]\xi(\boldsymbol{X}_k)
\end{aligned}
\tag{4.34}
$$

The block diagram of the proposed Nussbaum-based AILC scheme is presented in Fig. 4.2.

4.4 Stability Analysis

The stability of the proposed AILC scheme in this chapter is summarized as follows.

Theorem 4.1 *Considering the nonlinear time-delay system* (4.1) *with unknown control direction preceded by backlash-like hysteresis nonlinearity running on the finite interval* $[0, T]$ *repetitively, if Assumptions* 2.4–2.7, 3.1, 3.2 *and* 4.1 *hold, design the Nussbaum gain-based AILC* (4.30) *with parameter adaptive iterative learning laws* (4.31) and (4.32), *we can obtain the same conclusion as Theorem* 2.1.

Proof Similar to previous two chapters, we will discuss in two cases according to Lemma 2.2.

Case 1. $s_k(t) \in \boldsymbol{\Omega}_{s_k}$.

According to the analysis in Sect. 2.4, in the case of $s_k(t) \in \boldsymbol{\Omega}_{s_k}$, $|e_{sk}(t)| \le (1 + m)\eta(t)$. Based on adaptive iterative learning laws (4.31) and (4.32), we know

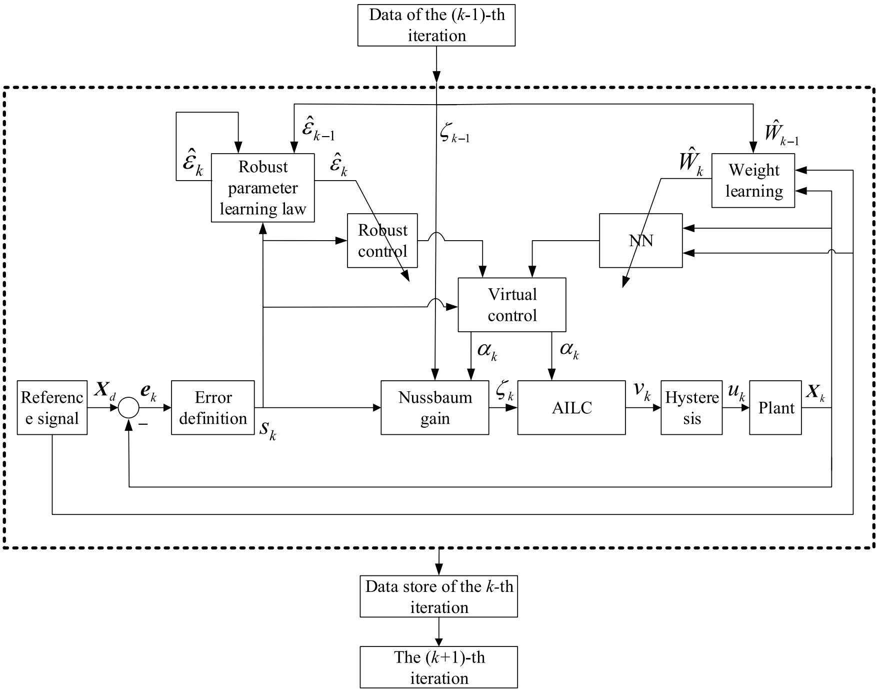

Fig. 4.2 Nussbaum gain based NN AILC scheme

that $\hat{\boldsymbol{W}}_k(t)$ and $\hat{\varepsilon}_k(t)$ are bounded in L_T^∞-norm, which leads to the boundedness of $v_k(t)$. Thus, all the closed-loop signals are bounded.

Case 2. $s_k(t) \notin \boldsymbol{\Omega}_{s_k}$.

According to Lemma 2.2, it follows from (4.34) that

$$s_k \tilde{\boldsymbol{W}}_k^{\mathrm{T}}(t)\boldsymbol{\phi}(\boldsymbol{Z}_k) + |s_k|\tilde{\varepsilon}_k \leq -\dot{V}_k + (g_0 N(\zeta_k) + 1)\dot{\zeta}_k - k_1 s_k^2 \tag{4.35}$$

Define a Lyapunov-like CEF as follows:

$$\begin{aligned} E_k(t) = &\frac{1}{2q_1}\int_0^t \tilde{\boldsymbol{W}}_k^{\mathrm{T}}\tilde{\boldsymbol{W}}_k \mathrm{d}\sigma + \frac{1}{2q_1}\int_t^T \tilde{\boldsymbol{W}}_{k-1}^{\mathrm{T}}\tilde{\boldsymbol{W}}_{k-1}\mathrm{d}\sigma \\ &+ \frac{\gamma}{2q_2}\int_0^t \tilde{\varepsilon}_k^2 \mathrm{d}\sigma + \frac{(1-\gamma)}{2q_2}\tilde{\varepsilon}_k^2 + \frac{\gamma}{2q_2}\int_t^T \tilde{\varepsilon}_{k-1}^2\mathrm{d}\sigma \end{aligned} \tag{4.36}$$

Remark 4.3 From (4.36) we can see that there are two extra terms $\frac{1}{2q_1}\int_t^T \tilde{\boldsymbol{W}}_{k-1}^T\tilde{\boldsymbol{W}}_{k-1}\mathrm{d}\sigma$ and $\frac{\gamma}{2q_2}\int_t^T \tilde{\varepsilon}_{k-1}^2\mathrm{d}\sigma$ in (4.36) compared with the CEF (3.32) in Chap. 3, they are mainly used to meet the needs for Nussbaum gain technique based analysis, which will be given in detail later.

The following proof are separated into three parts.

(1) Difference of $E_k(t)$.

Based on (4.36), computing the difference of $E_k(t)$, we obtain

$$\begin{aligned}\Delta E_k(t) = &\frac{1}{2q_1}\int_0^t \left[\tilde{\boldsymbol{W}}_k^{\mathrm{T}}\tilde{\boldsymbol{W}}_k - \tilde{\boldsymbol{W}}_{k-1}^{\mathrm{T}}\tilde{\boldsymbol{W}}_{k-1}\right]\mathrm{d}\sigma \\ &+ \frac{1}{2q_1}\int_t^T \left[\tilde{\boldsymbol{W}}_{k-1}^{\mathrm{T}}\tilde{\boldsymbol{W}}_{k-1} - \tilde{\boldsymbol{W}}_{k-2}^{\mathrm{T}}\tilde{\boldsymbol{W}}_{k-2}\right]\mathrm{d}\sigma \\ &+ \frac{\gamma}{2q_2}\int_0^t \left[\tilde{\varepsilon}_k^2 - \tilde{\varepsilon}_{k-1}^2\right]\mathrm{d}\sigma + \frac{(1-\gamma)}{2q_2}\left[\tilde{\varepsilon}_k^2 - \tilde{\varepsilon}_{k-1}^2\right] \\ &+ \frac{\gamma}{2q_2}\int_t^T \left[\tilde{\varepsilon}_{k-1}^2 - \tilde{\varepsilon}_{k-2}^2\right]\mathrm{d}\sigma \end{aligned} \tag{4.37}$$

Taking the adaptive learning law (4.31) into consideration, the first term on the right-hand said of (4.37) can be expressed as

$$\begin{aligned}&\frac{1}{2q_1}\int_0^t \left[\tilde{\boldsymbol{W}}_k^{T}\tilde{\boldsymbol{W}}_k - \tilde{\boldsymbol{W}}_{k-1}^{T}\tilde{\boldsymbol{W}}_{k-1}\right]\mathrm{d}\sigma \\ &= \int_0^t s_k\tilde{\boldsymbol{W}}_k^{T}\boldsymbol{\phi}(\boldsymbol{Z}_k)\mathrm{d}\sigma - \frac{q_1}{2}\int_0^t s_k^2\|\boldsymbol{\phi}(\boldsymbol{Z}_k)\|^2\mathrm{d}\sigma \end{aligned} \tag{4.38}$$

Considering adaptive learning law (4.32), we can obtain the following equality

$$\begin{aligned}&\frac{\gamma}{2q_2}\int_0^t \left[\tilde{\varepsilon}_k^2 - \tilde{\varepsilon}_{k-1}^2\right]\mathrm{d}\sigma + \frac{(1-\gamma)}{2q_2}\left[\tilde{\varepsilon}_k^2 - \tilde{\varepsilon}_{k-1}^2\right] \\ &= \frac{\gamma}{2q_2}\int_0^t \left[\tilde{\varepsilon}_k^2 - \tilde{\varepsilon}_{k-1}^2\right]\mathrm{d}\sigma + \frac{(1-\gamma)}{q_2}\int_0^t \tilde{\varepsilon}_k\dot{\tilde{\varepsilon}}_k\mathrm{d}\sigma \\ &\quad + \frac{(1-\gamma)}{2q_2}\left[\tilde{\varepsilon}_k^2(0) - \tilde{\varepsilon}_{k-1}^2(t)\right] \\ &= \int_0^t |s_k|\tilde{\varepsilon}_k\mathrm{d}\sigma - \frac{\gamma}{q_2}\int_0^t \tilde{\varepsilon}_k\left(\hat{\varepsilon}_k - \hat{\varepsilon}_{k-1}\right)\mathrm{d}\sigma \end{aligned}$$

$$+\frac{\gamma}{2q_2}\int_0^t\left(\tilde{\varepsilon}_k^2-\tilde{\varepsilon}_{k-1}^2\right)\mathrm{d}\sigma+\frac{(1-\gamma)}{2q_2}\left[\tilde{\varepsilon}_k^2(0)-\tilde{\varepsilon}_{k-1}^2(t)\right]$$

$$=\int_0^t|s_k|\tilde{\varepsilon}_k\mathrm{d}\sigma-\frac{\gamma}{q_2}\int_0^t\tilde{\varepsilon}_k(\tilde{\varepsilon}_k-\tilde{\varepsilon}_{k-1})\mathrm{d}\sigma$$

$$+\frac{\gamma}{2q_2}\int_0^t\left(\tilde{\varepsilon}_k^2-\tilde{\varepsilon}_{k-1}^2\right)\mathrm{d}\sigma+\frac{(1-\gamma)}{2q_2}\left[\tilde{\varepsilon}_k^2(0)-\tilde{\varepsilon}_{k-1}^2(t)\right]$$

$$=\int_0^t|s_k|\tilde{\varepsilon}_k\mathrm{d}\sigma+\frac{(1-\gamma)}{2q_2}\left[\tilde{\varepsilon}_k^2(0)-\tilde{\varepsilon}_{k-1}^2(t)\right]-\frac{\gamma}{2q_2}\int_0^t\left[\tilde{\varepsilon}_k-\tilde{\varepsilon}_{k-1}\right]^2\mathrm{d}\sigma \tag{4.39}$$

Substituting (4.38) and (4.39) back into (4.37), it follows that

$$\begin{aligned}\Delta E_k(t)=&\int_0^t s_k\tilde{\boldsymbol{W}}_k^{\mathrm{T}}(\sigma)\boldsymbol{\phi}(\boldsymbol{Z}_k)\mathrm{d}\sigma-\frac{q_1}{2}\int_0^t s_k^2\|\boldsymbol{\phi}(\boldsymbol{Z}_k)\|^2\mathrm{d}\sigma\\&+\int_0^t|s_k|\tilde{\varepsilon}_k\mathrm{d}\sigma+\frac{(1-\gamma)}{2q_2}\left[\tilde{\varepsilon}_k^2(0)-\tilde{\varepsilon}_{k-1}^2(t)\right]-\frac{\gamma}{2q_3}\int_0^t\left[\tilde{\varepsilon}_k-\tilde{\varepsilon}_{k-1}\right]^2\mathrm{d}\sigma\\&+\frac{1}{2q_1}\int_t^T\left[\tilde{\boldsymbol{W}}_{k-1}^{\mathrm{T}}\tilde{\boldsymbol{W}}_{k-1}-\tilde{\boldsymbol{W}}_{k-2}^{\mathrm{T}}\tilde{\boldsymbol{W}}_{k-2}\right]\mathrm{d}\sigma+\frac{\gamma}{2q_2}\int_t^T\left[\tilde{\varepsilon}_{k-1}^2-\tilde{\varepsilon}_{k-2}^2\right]\mathrm{d}\sigma\\&\le -V_k(t)+V_k(0)+\int_0^t(g_0N(\zeta_k)+1)\dot{\zeta}_k\mathrm{d}\sigma\\&-k_1\int_0^t s_k^2\mathrm{d}\sigma+\frac{(1-\gamma)}{2q_2}\left[\tilde{\varepsilon}_k^2(0)-\tilde{\varepsilon}_{k-1}^2(t)\right]\\&+\frac{1}{2q_1}\int_t^T\left[\tilde{\boldsymbol{W}}_{k-1}^{\mathrm{T}}\tilde{\boldsymbol{W}}_{k-1}-\tilde{\boldsymbol{W}}_{k-2}^{\mathrm{T}}\tilde{\boldsymbol{W}}_{k-2}\right]\mathrm{d}\sigma+\frac{\gamma}{2q_2}\int_t^T\left[\tilde{\varepsilon}_{k-1}^2-\tilde{\varepsilon}_{k-2}^2\right]\mathrm{d}\sigma\end{aligned} \tag{4.40}$$

From Assumption 2.4 and Assumption 2.7, it is clear that $V_k(0)=0$. Let中 $t=T$ in (4.43), according to $\hat{\varepsilon}_k(0)=\hat{\varepsilon}_{k-1}(T)$, $\hat{\varepsilon}_1(0)=0$, we can have

$$\Delta E_k(T)\le -V_k(T)+\int_0^T(g_0N(\zeta_k)+1)\dot{\zeta}_k\mathrm{d}\sigma-k_1\int_0^T s_k^2\mathrm{d}\sigma$$

$$\leq \int_0^T (g_0 N(\zeta_k) + 1)\dot{\zeta}_k \mathrm{d}\sigma - k_1 \int_0^T s_k^2 \mathrm{d}\sigma \tag{4.41}$$

(2) The finiteness of $E_k(t)$.

Applying (4.41) repeatedly, we have

$$\begin{aligned} E_k(T) &= E_1(T) + \sum_{j=2}^{k} \Delta E_j(T) \\ &\leq E_1(T) + \sum_{j=2}^{k} \int_0^T \left(g_0 N\left(\zeta_j\right) + 1\right)\dot{\zeta}_j \mathrm{d}\sigma - k_1 \sum_{j=2}^{k} \int_0^T s_j^2 \mathrm{d}\sigma \end{aligned} \tag{4.42}$$

Next let us check the finiteness of $E_1(T)$. According to the definition of E_k, we know

$$\dot{E}_1(t) = \frac{1}{2q_1}\tilde{\boldsymbol{W}}_1^{\mathrm{T}}\tilde{\boldsymbol{W}}_1 + \frac{\gamma}{2q_2}\tilde{\varepsilon}_1^2 + \frac{(1-\gamma)}{q_2}\tilde{\varepsilon}_1\dot{\tilde{\varepsilon}}_1 \tag{4.43}$$

Taking the time derivative of $E_1(t)$ yields

$$\dot{E}_1(t) = \frac{1}{2q_1}\tilde{\boldsymbol{W}}_1^{\mathrm{T}}\tilde{\boldsymbol{W}}_1 + \frac{\gamma}{2q_2}\tilde{\varepsilon}_1^2 + \frac{(1-\gamma)}{q_2}\tilde{\varepsilon}_1\dot{\tilde{\varepsilon}}_1 \tag{4.44}$$

Recalling parameter adaptive laws, we have $\hat{\boldsymbol{W}}_1(t) = q_1 s_1 \boldsymbol{\phi}(\boldsymbol{Z}_1)$, $(1-\gamma)\dot{\hat{\varepsilon}}_1 = -\gamma\hat{\varepsilon}_1 + q_2|s_1(t)|$, then we can obtain

$$\begin{aligned} \frac{1}{2q_1}\tilde{\boldsymbol{W}}_1^{\mathrm{T}}\tilde{\boldsymbol{W}}_1 &= \frac{1}{2q_1}\left[\tilde{\boldsymbol{W}}_1^{\mathrm{T}}\tilde{\boldsymbol{W}}_1 - 2\tilde{\boldsymbol{W}}_1^{\mathrm{T}}\hat{\boldsymbol{W}}_1\right] + \frac{1}{q_1}\tilde{\boldsymbol{W}}_1^{\mathrm{T}}\hat{\boldsymbol{W}}_1 \\ &= \frac{1}{2q_1}\left[\left(\hat{\boldsymbol{W}}_1 - \boldsymbol{W}^*\right)^T\left(\hat{\boldsymbol{W}}_1^T - \boldsymbol{W}^*\right) - 2\left(\hat{\boldsymbol{W}}_1 - \boldsymbol{W}^*\right)^T\hat{\boldsymbol{W}}_1\right] \\ &\quad + s_1\tilde{\boldsymbol{W}}_1^T\boldsymbol{\phi}(\boldsymbol{Z}_1) \\ &= \frac{1}{2q_1}\left[-\hat{\boldsymbol{W}}_1^{\mathrm{T}}\hat{\boldsymbol{W}}_1 + \boldsymbol{W}^{*\mathrm{T}}\boldsymbol{W}^*\right] + s_1\tilde{\boldsymbol{W}}_1^{\mathrm{T}}\boldsymbol{\phi}(\boldsymbol{Z}_1) \\ &\leq \frac{1}{2q_1}\boldsymbol{W}^{*\mathrm{T}}\boldsymbol{W}^* + s_1\tilde{\boldsymbol{W}}_1^T\boldsymbol{\phi}(\boldsymbol{Z}_1) \end{aligned} \tag{4.45}$$

$$\begin{aligned} \frac{\gamma}{2q_2}\tilde{\varepsilon}_1^2 + \frac{(1-\gamma)}{q_2}\tilde{\varepsilon}_1\dot{\tilde{\varepsilon}}_1 &= \frac{\gamma}{2q_2}\tilde{\varepsilon}_1^2 - \frac{\gamma}{q_2}\tilde{\varepsilon}_1\hat{\varepsilon}_1(t) + |s_1|\tilde{\varepsilon}_1 \\ &= \frac{\gamma}{2q_2}\left(\hat{\varepsilon}_1^2 - 2\tilde{\varepsilon}_1\hat{\varepsilon}_1 + \tilde{\varepsilon}_1^2\right) - \frac{\gamma}{2q_2}\hat{\varepsilon}_1^2 + |s_1|\tilde{\varepsilon}_1 \\ &\leq \frac{\gamma}{2q_2}\left(\hat{\varepsilon}_1 - \tilde{\varepsilon}_1\right)^2 + |s_1|\tilde{\varepsilon}_1 \end{aligned}$$

$$= \frac{\gamma}{2q_2}\left(\varepsilon^*\right)^2 + |s_1|\tilde{\varepsilon}_1 \tag{4.46}$$

Substituting (4.45) and (4.46) back into (4.44) leads to

$$\begin{aligned} \dot{E}_1(t) &\le \frac{1}{2q_1}\boldsymbol{W}^{*\mathrm{T}}\boldsymbol{W}^* + s_1\tilde{\boldsymbol{W}}_1^{\mathrm{T}}\boldsymbol{\phi}(\boldsymbol{Z}_1) + \frac{\gamma}{2q_3}\left(\varepsilon^*\right)^2 + |s_1|\tilde{\varepsilon}_1 \\ &\le -\dot{V}_1 + (g_0N(\zeta_1)+1)\dot{\zeta}_1 - Ks_1^2 + \frac{1}{2q_1}\boldsymbol{W}^{*\mathrm{T}}\boldsymbol{W}^* + \frac{\gamma}{2q_3}\left(\varepsilon^*\right)^2 \end{aligned} \tag{4.47}$$

Denote $c_{\max} = \max\limits_{t\in[0,T]}\left\{\frac{1}{2q_1}\boldsymbol{W}^{*\mathrm{T}}(t)\boldsymbol{W}^*(t) + \frac{1}{2q_2}(\varepsilon^*)^2\right\}$. Integrating the above inequality over $[0, t]$ results in

$$E_1(t) - E_1(0) \le -V_1(t) + \int_0^t (g_0N(\zeta_1)+1)\dot{\zeta}_1\mathrm{d}\sigma - k_1\int_0^t s_1^2\mathrm{d}\sigma + t\cdot c_{\max} \tag{4.48}$$

Based on $\widehat{\varepsilon}_1(0)0$, we have

$$E_1(0) = \frac{(1-\gamma)}{2q_2}\tilde{\varepsilon}_1^2(0) = \frac{(1-\gamma)}{2q_2}\left(\varepsilon^*\right)^2 \tag{4.49}$$

Then, Eq. (4.48) changes to

$$E_1(t) \le -k_1\int_0^t s_1^2\mathrm{d}\sigma + \int_0^t (g_0N(\zeta_1)+1)\dot{\zeta}_1\mathrm{d}\sigma + t\cdot c_{\max} + \frac{(1-\gamma)}{2q_2}\left(\varepsilon^*\right)^2 \tag{4.50}$$

Letting $t = T$ in (4.50), it becomes

$$E_1(T) \le -k_1\int_0^T s_1^2\mathrm{d}\sigma + \int_0^T (g_0N(\zeta_1)+1)\dot{\zeta}_1\mathrm{d}\sigma + T\cdot c_{\max} + \frac{(1-\gamma)}{2q_2}\left(\varepsilon^*\right)^2 \tag{4.51}$$

Further, substituting (4.51) into (4.42) yields

$$\begin{aligned} E_k(T) &\le -k_1\sum_{j=1}^{k}\int_0^T s_j^2\mathrm{d}\sigma + \sum_{j=1}^{k}\int_0^T \left(g_0N\left(\zeta_j\right)+1\right)\dot{\zeta}_j\mathrm{d}\sigma + T\cdot c_{\max} + \frac{(1-\gamma)}{2q_2}\left(\varepsilon^*\right)^2 \\ &\le \sum_{j=1}^{k}\int_0^T \left(g_0N\left(\zeta_j\right)+1\right)\dot{\zeta}_j\mathrm{d}\sigma + T\cdot c_{\max} + \frac{(1-\gamma)}{2q_2}\left(\varepsilon^*\right)^2 \end{aligned} \tag{4.52}$$

According to the relationship $\zeta_k(0) = \zeta_{k-1}(T)$ for Nussbaum gain, we can know Nussbaum gain is continuous along with iterative running. Then we can denote $\zeta(t + (k-1)T) \triangleq \zeta_k(t)$, $j \in \mathbf{N}$. Consequently, $\zeta(t)$ and $\dot{\zeta}(t)$ are both continuous for $\forall t \in [0, kT]$. Then from $\zeta_k(0) = \zeta_{k-1}(T)$ we have

$$\begin{aligned}\sum_{j=1}^{k}\int_{0}^{T}\big(g_0 N(\zeta_j) + 1\big)\dot{\zeta}_j \mathrm{d}\sigma &= \int_{0}^{T}(g_0 N(\zeta_1) + 1)\dot{\zeta}_1 \mathrm{d}\sigma + \int_{0}^{T}(g_0 N(\zeta_2) + 1)\dot{\zeta}_2 \mathrm{d}\sigma \\ &\quad + \cdots + \int_{0}^{T}(g_0 N(\zeta_k) + 1)\dot{\zeta}_k \mathrm{d}\sigma \\ &= \int_{0}^{T}(g_0 N(\zeta) + 1)\dot{\zeta}\mathrm{d}\sigma + \int_{T}^{2T}(g_0 N(\zeta) + 1)\dot{\zeta}\mathrm{d}\sigma \\ &\quad + \cdots + \int_{(k-1)T}^{kT}(g_0 N(\zeta) + 1)\dot{\zeta}\mathrm{d}\sigma \\ &= \int_{0}^{kT}(g_0 N(\zeta) + 1)\dot{\zeta}\mathrm{d}\sigma \end{aligned} \tag{4.53}$$

Therefor, we can get

$$E_k(T) \le \int_{0}^{kT}(g_0 N(\zeta) + 1)\dot{\zeta}\mathrm{d}\sigma + T \cdot c_{\max} + \frac{(1-\gamma)}{2q_2}\big(\varepsilon^*\big)^2 \tag{4.54}$$

On the other hand, for $k \ge 2$, we have

$$\begin{aligned}\dot{E}_k(t) &= \frac{1}{2q_1}\Big(\tilde{\boldsymbol{W}}_k^{\mathrm{T}}\tilde{\boldsymbol{W}}_k - \tilde{\boldsymbol{W}}_{k-1}^{\mathrm{T}}\tilde{\boldsymbol{W}}_{k-1}\Big) + \frac{\gamma}{2q_2}\tilde{\varepsilon}_k^2 + \frac{(1-\gamma)}{q_2}\tilde{\varepsilon}_k\dot{\tilde{\varepsilon}}_k - \frac{\gamma}{2q_2}\tilde{\varepsilon}_{k-1}^2 \\ &= s_k\tilde{\boldsymbol{W}}_k^{\mathrm{T}}(t)\boldsymbol{\phi}(\boldsymbol{Z}_k) - \frac{q_1}{2}s_k^2\|\boldsymbol{\phi}(\boldsymbol{Z}_k)\|^2 + |s_k|\tilde{\varepsilon}_k - \frac{\gamma}{2q_2}(\tilde{\varepsilon}_k - \tilde{\varepsilon}_{k-1})^2 \\ &\le \dot{V}_k + (g_0 N(\zeta_k) + 1)\dot{\zeta}_k - k_1 s_k^2 \end{aligned} \tag{4.55}$$

It is obvious that $E_k(0) = E_{k-1}(T)$ from the definition of $E_k(t)$. Then integrating (4.55) over $[0, t]$ and letting $k = k-1$ in (4.54), we can obtain

$$E_k(t) \le -V_k + \int_{0}^{t}(g_0 N(\zeta_k) + 1)\dot{\zeta}_k \mathrm{d}\sigma - k_1\int_{0}^{t}s_k^2 \mathrm{d}\sigma + E_k(0)$$

$$\leq \int_0^t (g_0 N(\zeta_k)+1)\dot{\zeta}_k \mathrm{d}\sigma + \int_0^{(k-1)T} (g_0 N(\zeta)+1)\dot{\zeta}\mathrm{d}\sigma$$
$$+ T\cdot c_{\max} + \frac{(1-\gamma)}{2q_2}\left(\varepsilon^*\right)^2$$
$$= c_0 + \int_0^{(k-1)T+t} (g_0 N(\zeta)+1)\dot{\zeta}\mathrm{d}\sigma \tag{4.56}$$

where, $c_0 = T\cdot c_{\max} + \frac{(1-\gamma)}{2q_2}(\varepsilon^*)^2$. From Lemma 2, we know that any $[0,T]\subset [0,t_f)$. According to the Lemma 4.1, we can conclude that: $E_k(t)$, $\zeta(t)$ and $\int_0^{(k-1)T+t}(g_0N(\zeta)+1)\dot{\zeta}\mathrm{d}\sigma$ are all bounded, which further leads to the boundedness of $\zeta_k(t)$, $\hat{\boldsymbol{W}}_k(t)$ and $\hat{\varepsilon}_k(t)$, $\forall k\in\mathbf{N}$.

(3) Learning convergence property.

Letting $t=T$ in (4.56), we can know that $E_k(T)$ is bounded. From (4.52) it leads to

$$k_1\sum_{j=1}^{k}\int_0^T s_j^2\mathrm{d}\sigma \leq -E_k(T) + \sum_{j=1}^{k}\int_0^T \left(g_0 N\left(\zeta_j\right)+1\right)\dot{\zeta}_j\mathrm{d}\sigma + c_0$$
$$\leq \int_0^{kT}(g_0N(\zeta)+1)\dot{\zeta}\mathrm{d}\sigma + c_0 \tag{4.57}$$

Taking the limitation of (4.57), it follows

$$\lim_{k\to\infty}\sum_{j=1}^{k}\int_0^T s_j^2\mathrm{d}\sigma \leq \lim_{k\to\infty}\frac{1}{k_1}\left[\int_0^{kT}(g_0N(\zeta)+1)\dot{\zeta}\mathrm{d}\sigma + T\cdot c_{\max} + \frac{(1-\gamma)}{2q_2}(\varepsilon^*)^2\right] \leq M \tag{4.58}$$

According to the convergence theorem of the sum of series, we have $\lim_{k\to\infty}\int_0^T s_k^2(\sigma)\mathrm{d}\sigma = 0$ which implies that $\lim_{k\to\infty} s_k(t) = s_\infty(t) = 0$, $\forall t\in[0,T]$. Furthermore, from the definition $s_k(t)$ we know that when $|e_{sk}(t)|\leq\eta(t)$, $s_k(t)=0$, then $\lim_{k\to\infty}\int_0^T s_k^2(\sigma)\mathrm{d}\sigma = 0$ is equivalent to $\lim_{k\to\infty}|e_{sk}(t)|\leq\eta(t)$, finally resulting in $\lim_{k\to\infty}\int_0^T(e_{sk}(\sigma))^2\mathrm{d}\sigma \leq \int_0^T(\eta(\sigma))^2\mathrm{d}\sigma$.

Based on the boundedness of $E_k(t)$, we have got the boundedness of $\hat{\boldsymbol{W}}_k(t)$ and $\hat{\varepsilon}_k(t)$. From the inequality $\int_0^t s_k^2(\sigma)\mathrm{d}\sigma \leq \int_0^T s_k^2(\sigma)\mathrm{d}\sigma$ we can obtain the boundedness of $s_k(t)$, then from the boundedness of $\boldsymbol{X}_d(t)$ we can further get the boundedness of $x_{i,k}(t)$. Similar to Case 1, we can get the conclusion that $v_k(t)$ and $u_k(t)$ are bounded.

Based on above discussion in two cases, we can see that the proposed Nussbaum gain based AILC scheme is able to ensure the boundedness of all closed-loop signals, and $\lim_{k\to\infty}|e_{sk}(t)| \le (1+m)\eta(t)$. Therefore, we can further obtain $\lim_{k\to\infty}\int_0^T (e_{sk}(\sigma))^2 \mathrm{d}\sigma \le \varepsilon_e$, $\varepsilon_e = \int_0^T ((1+m)\eta(\sigma))^2 \mathrm{d}\sigma = \frac{1}{2K}(1+m)^2\varepsilon^2\big(1-e^{-2KT}\big) \le \frac{1}{2K}(1+m)^2\varepsilon^2 = \varepsilon_{esk}$. Moreover, $e_{s\infty}(t)$ satisfies $\lim_{k\to\infty}|e_{sk}(t)| = e_{s\infty}(t) = (1+m)\varepsilon e^{-Kt}$, $\forall t \in [0, T]$.

The proof of the transient performance for tracking error is same as Sect. 2.4.

This concludes the proof. □

4.5 Simulation Analysis

In this section, we present a simulation example to verify the effectiveness of the AILC scheme. Consider the following second-order nonlinear time delay system with unknown backlash-like hysteresis and control direction:

$$\begin{cases} \dot{x}_{1,k}(t) = x_{2,k}(t) \\ \dot{x}_{2,k}(t) = f(\boldsymbol{X}_k(t), t) + h\big(\boldsymbol{X}_{\tau,k}(t), t\big) + g(\boldsymbol{X}_k(t), t)u_k(v_k) + d(t) \\ y_k(t) = x_{1,k}(t) \end{cases} \tag{4.59}$$

where, the forms of unknown functions $f(\boldsymbol{X}_k(t), t)$, $h\big(\boldsymbol{X}_{\tau,k}(t), t\big)$ and disturbance $d(t)$ are as same as system (3.67), $g(x_k(t), t) = 0.7 + 0.3|\cos(0.5t)|^2 \sin^2\big(x_{1,k}x_{2,k}\big)$. The unknown time-varying delays are $\tau_1(t) = 0.5(1 + \sin(0.3t))$ and $\tau_2 = 0.8(1 + \sin(0.5t))$.

4.5.1 Verification of Nussbuam Gain-Based AILC Scheme

To demonstrate the conclusions in Theorem 4.1, conduct three simulation experiments.

Experiment 1 The desired trajectory is given by $\boldsymbol{X}_d(t) = [\sin t, \cos t]^{\mathrm{T}}$. The design parameters are $\varepsilon_1 = \varepsilon_2 = 1$, $\lambda = 2$, $K = 2$, $k_1 = 1$, $\gamma = 0.5$, $q_1 = 0.8$, $q_2 = 0.1$, $\varepsilon = \lambda\varepsilon_1 + \varepsilon_2 = 3$. The parameters for backlash-like hysteresis are specified by $\alpha = 1$, $c = 1.1635$, $B_1 = 0.345$. The parameters for RBF NN are given by $l = 30$, $\mu_j = \frac{1}{l}(2j - l)[2, 3, 2, 3, 3]^{\mathrm{T}}$, $\eta_j = 2$, $j = 1, 2, \ldots, l$. The initial condition $x_{1,k}(0)$ and $x_{2,k}(0)$ are randomly taken in the intervals $[-0.5, 0.5]$ and $[0.5, 1.5]$, respectively. The system runs on $[0, 4\pi]$ for five iterations. The simulation results are shown in Figs. 4.3, 4.4, 4.5, 4.6, 4.7 and 4.8.

Figures 4.3 and 4.4 show the curve of system output y_k to track y_d in the 1st iteration ($k = 1$) and the 5th iteration ($k = 5$), respectively, which shows that the tracking performance has been improved through four times of learning. This improvement effect is clearly shown in Fig. 4.8 by the curve of $\int_0^T s_k^2(t)dt$ versus iterations. The

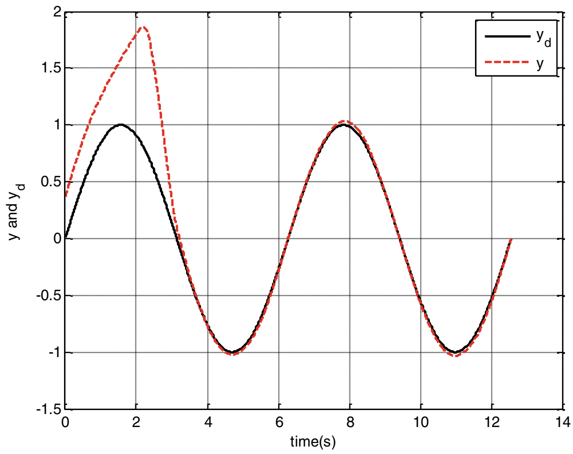

Fig. 4.3 System output y_k versus y_d $(k = 1)$

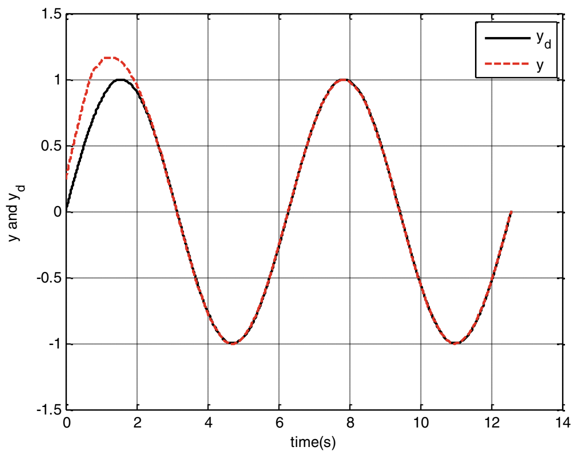

Fig. 4.4 System output y_k versus y_d $(k = 5)$

control curves for the 1st and 5th iteration are presented in Figs. 4.5 and 4.6 respectively, which shows the effect of backlash-like hysteresis nonlinearity on control input. As mentioned above, the Nussbaum gain ζ varies continuously, and Fig. 4.7 presents continuously varying curve for five iterations. It should be pointed out that the horizontal axis of Fig. 4.7 is not real time axis, but a combination of ζ_k for five iterations. From Fig. 4.7 we can see that the Nussbaum gain tends to stability in the 1st iteration.

Experiment 2 To show the control performance for more complicated desired trajectory, we choose the desired trajectory as $\boldsymbol{X}_d(t) = [\sin t + \sin(0.5t), \cos t + 0.5\cos(0.5t)]^{\mathrm{T}}$. The control parameters are chose as $q_1 = 1$, $q_2 = 0.03$, $\gamma = 0.5$, $\lambda = 2$, $K = 2$, $k_1 = 3$, $l = 10$, $\mu_j = \frac{1}{l}(2j - l)[2, 3, 2, 3, 2]^{\mathrm{T}}$, $\eta_j = 2$, $j = 1, 2, \ldots, l$. The initial conditions

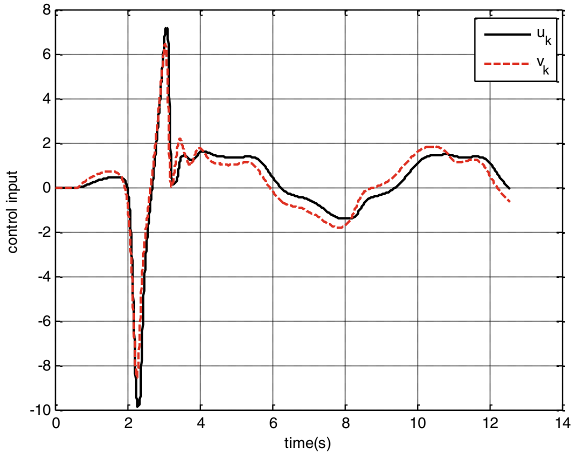

Fig. 4.5 The input v_k and output u_k of backlash-like hysteresis ($k = 1$)

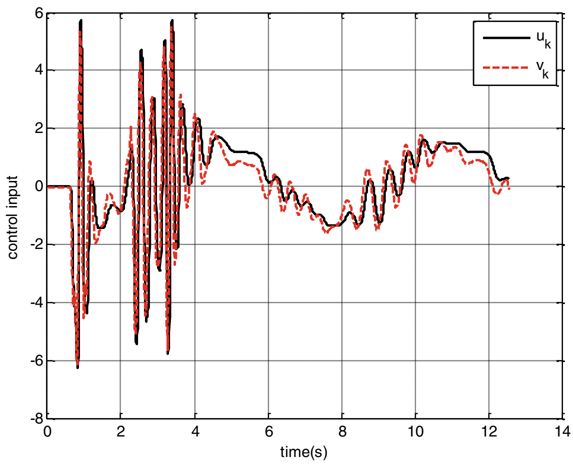

Fig. 4.6 The input v_k and output u_k of backlash-like hysteresis ($k = 5$)

$x_{1,k}(0)$ and $x_{2,k}(0)$ are randomly generated in $[-0.5, 0.5]$ and $[1, 2]$ respectively. The system runs on finite interval $[0, 8\pi]$ for ten times. Simulation results are presented in Figs. 4.9, 4.10, 4.11, 4.12, 4.13 and 4.14.

From above simulation results, it is clear that the proposed AILC scheme can achieve a good tracking performance for the desired reference signal $\boldsymbol{X}_d(t) = [\sin t + \sin(0.5t), \cos t + 0.5\cos(0.5t)]^{\mathrm{T}}$ as well.

Experiment 3 To test the effect of different parameters on tracking performance, we change the parameters in Experiment 2 to $\lambda = 3$, $K = 4$, $\gamma = 0.5$, $q_1 = q_2 = 2$, $q_3 = 0.02$, $\varepsilon = \lambda\varepsilon_1 + \varepsilon_2 = 4$, while remaining other parameters unchanged. Here we only present the curve of $\int_0^T s_k^2(t)\mathrm{d}t$ with respect to iterations.

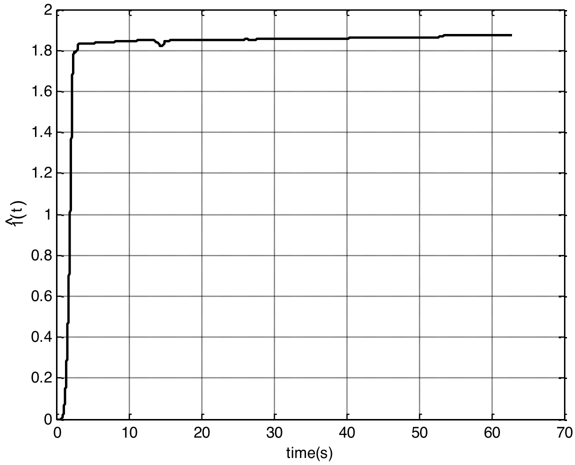

Fig. 4.7 The curve of Nussbaum gain ζ

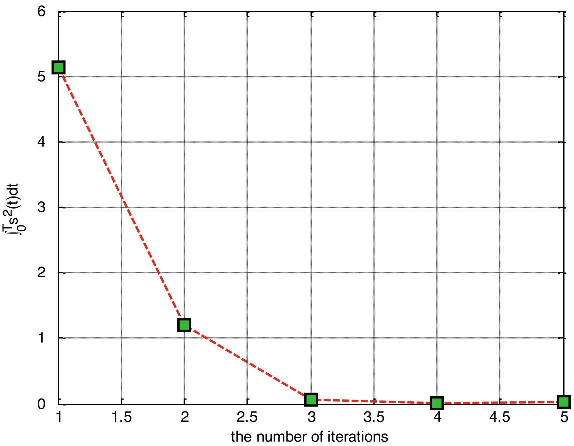

Fig. 4.8 $\int_0^T s_k^2(t)\mathrm{d}t$ versus iterations

By comparing Figs. 4.14 and 4.15, we can see that, for the Nussbaum gain based AILC scheme, larger design parameters can only decrease the index of tracking error $\int_0^T s_k^2(t)\mathrm{d}t$ slightly and don't have remarkable effect on the improvement via learning process. This is mainly because the error feedback term $k_1 s_k$ in controller (4.30) make tracking error converge quickly, which is clearly shown in Fig. 4.9. Moreover, in the controller (3.25) of Chap. 3, since there is no direct effect of error feedback term, the tracking error is not eliminated obviously in the first iteration. To accelerate convergence speed, we can also add the feedback term of tracking error s_k in (3.25). It will not change the stability analysis conclusions in Sect. 3.4.

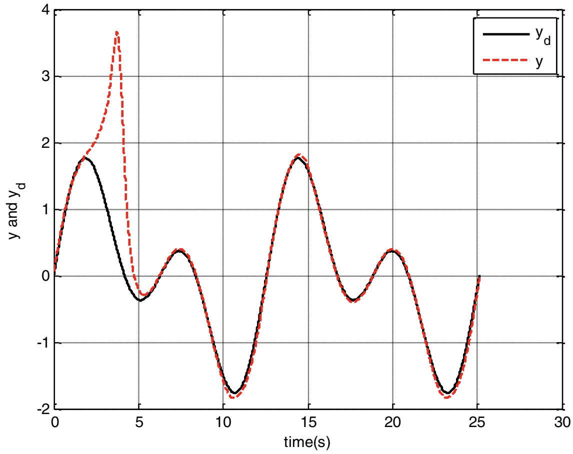

Fig. 4.9 System output y_k versus y_d ($k = 1$)

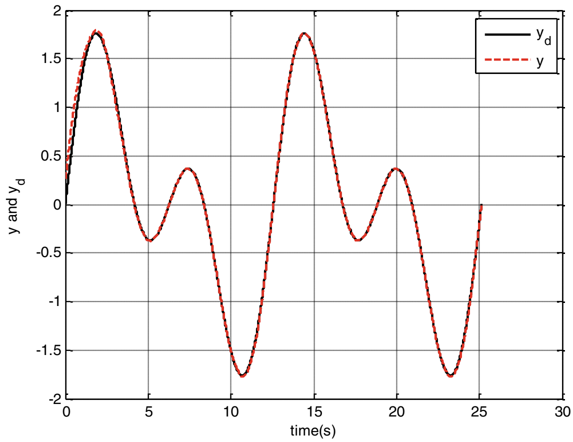

Fig. 4.10 System output y_k versus y_d ($k = 10$)

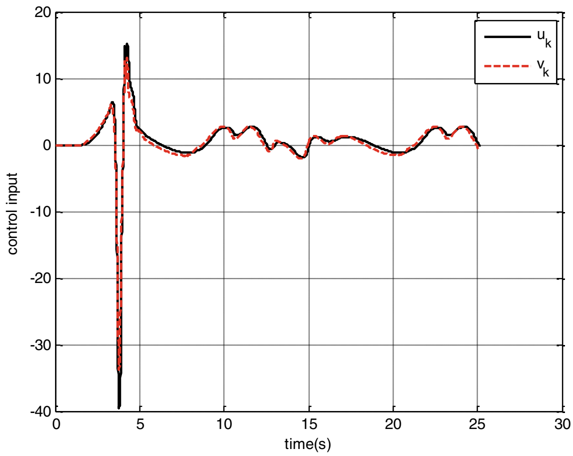

Fig. 4.11 The input v_k and output u_k of backlash-like hysteresis ($k = 1$)

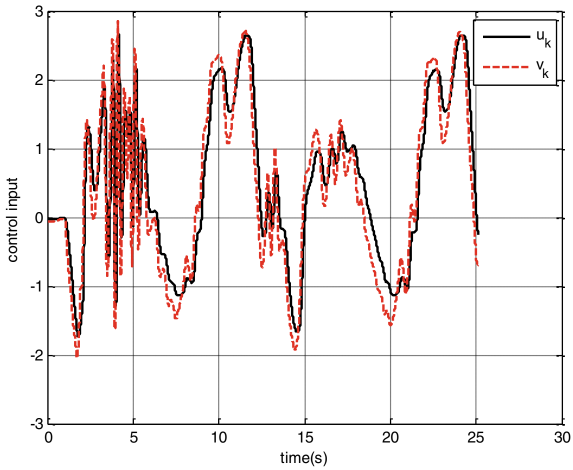

Fig. 4.12 The input v_k and output u_k of backlash-like hysteresis ($k = 10$)

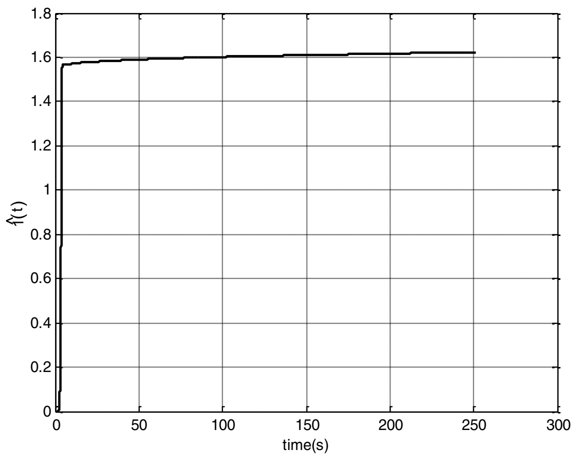

Fig. 4.13 The curve of Nussbaum gain ζ

4.5.2 Comparison Simulation: Nussbuam Gain-Based Adaptive NN Control

Experiment 4 Finally, the contribution of the proposed AILC scheme is shown by comparing the proposed controller with traditional adaptive neural network controller. We utilize the Nussbaum gain based adaptive NN controller in [5] to control the system (4.50) aiming at achieve tracking the desired reference trajectory, in which the controller has the same form as (4.30) and the parameter adaptive law is modified to the following form:

$$\dot{\hat{\boldsymbol{W}}} = -\boldsymbol{\Gamma}\Big[\boldsymbol{\phi}(\boldsymbol{Z}_k)s_k + \sigma_W \hat{\boldsymbol{W}}\Big],$$

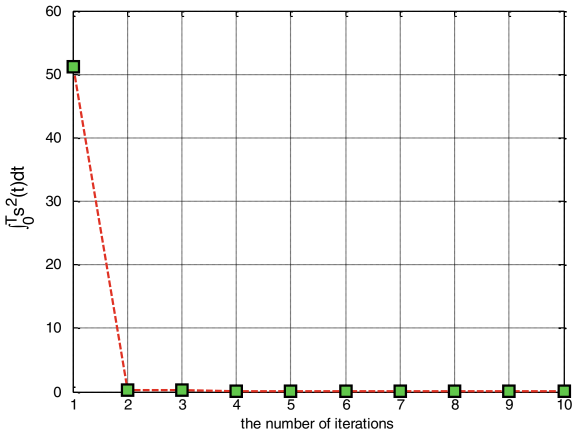

Fig. 4.14 $\int_0^T s_k^2(t)\mathrm{d}t$ versus iterations

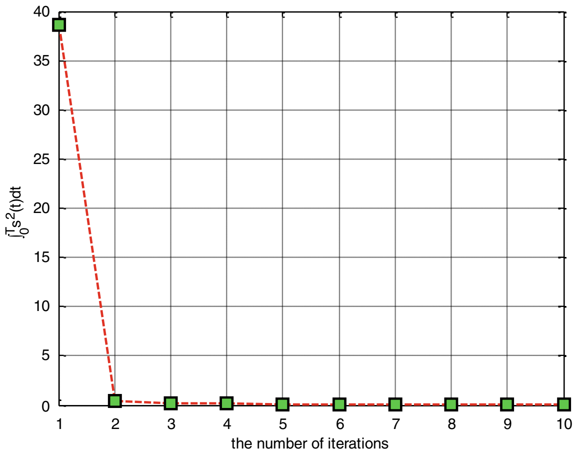

Fig. 4.15 $\int_0^T s_k^2(t)\mathrm{d}t$ versus iterations (Experiment 3)

$$\hat{\boldsymbol{W}}(0) = 0 \quad (1-\gamma)\dot{\hat{\varepsilon}}_k(t) = -\gamma\hat{\varepsilon}_k(t) + q_2|s_k(t)|$$

The design parameters are chosen as $\Gamma = \mathrm{diag}\{2\}$, $\sigma_W = 0.5$, $q_2 = 0.02$. The desired reference trajectory vector is $\boldsymbol{X}_d(t) = [\sin t + \sin(0.5t), \cos t + 0.5\cos(0.5t)]^{\mathrm{T}}$, while other parameters remaining the same as Experiment 2. Similarly, here the subscript "k" in controller and adaptive laws has no practical meaning. Figures 4.16 and 4.17 present the tracking curve and control signal curve respectively. Simulation results show that traditional adaptive control can't achieve perfect tracking performance as iteration continues when there exist time-varying uncertainties in systems, and tracking errors always exist periodically and can't be eliminated by adaptive learning. The simulation results clearly reflect the superiority in dealing with time-varying uncertainties.

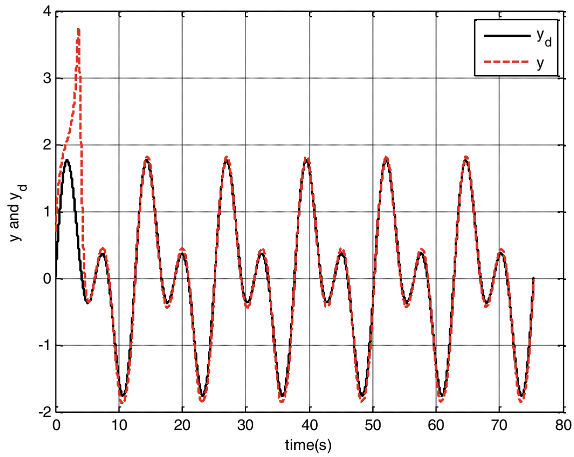

Fig. 4.16 y_k versus y_d

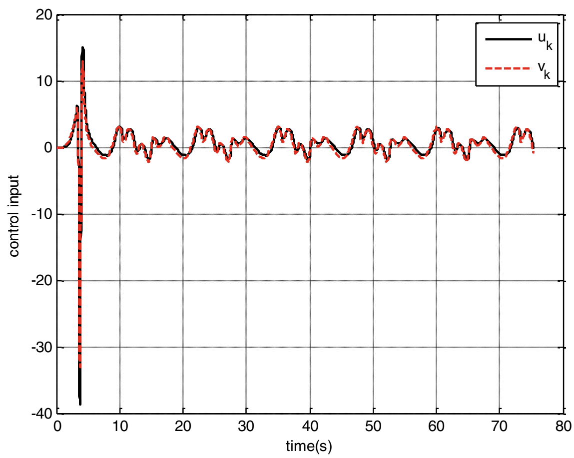

Fig. 4.17 The input v_k and output u_k of backlash-like hysteresis

As observed in above four experiments, the proposed NN AILC can achieve a good tracking performance for nonlinear time-delay systems with unknown control direction and backlash-like hysteresis nonlinearity and realize the control objective, which is in accord with the conclusions in Theorem 4.1. The simulation results adequately demonstrate the validity of the AILC approach in this chapter.

4.6 Summary and Comments

In this chapter, we investigated the control problem for a class of nonlinear time-delay systems with unknown control direction and backlash-like hysteresis nonlinearity. The RBF NN was employed to approximate time-varying uncertainties and robust adaptive learning term was designed to compensate for the NN approximation error, unknown external disturbance and the remaining term of hysteresis. The Nussbaum gain method was used to estimate the unknown control gain and overcome the difficulty of unknown control direction. To solve the problem in stability analysis followed by the introduction of Nussbaum function, we constructed a kind of CEF satisfying alignment condition. In the design, we considered the influence of unknown backlash-like hysteresis nonlinearity input and introduced the integral type Lyapunov function method into AILC design, which avoided the control singularity problem incorporating with the hyperbolic tangent function. This method further extends the application scope of AILC and may provide useful reference for relevant control problems.

References

1. Mudgett D R, Morse A S. Adaptive stabilization of linear systems with unknown high frequency gains[J]. IEEE Transactions on Automatic Control, 1985, 30(6): 549–554.
2. Lozano R, Collado J, Mondie S. Model reference adaptive control without a priori knowledge of the high frequency gain[J]. IEEE Transactions on Automatic Control, 1990, 35(1): 71–78.
3. Kaloust J, Qu Z H. Continuous robust control design for nonlinear uncertain systems without a priori knowledge of control directions[J]. IEEE Transactions on Automatic Control, 1995, 40(2): 275–282.
4. Nussbaum R D. Some remarks on the conjecture in parameter adaptive control[J]. System & Control Letter, 1983, 3(5): 242–246.
5. Ge S S, Hong F, Lee T H. Adaptive neural control of nonlinear time-delay systems with unknown virtual control coefficients[J]. IEEE Transactions on Systems, Man, and Cybernetics, Part B: Cybernetics, 2004, 34(1): 499–516.
6. Zhang T, Ge S S. Adaptive neural network tracking control of MIMO nonlinear systems with unknown dead zones and control directions[J]. IEEE Transactions on Neural Networks, 2009, 20(3): 483–497.
7. Ge S S, Hang C C, Lee T H, et al. Stable adaptive neural network control[M]. Norwell: Kluwer Academic Publishers, 2001.
8. Li D, Li J M. Adaptive iterative learning control for nonlinearly parameterized systems with unknown time-varying delay and unknown control direction[J]. International Journal of Automation and Computing, 2012, 9(6): 578–586.
9. Zhang C L, Li J M. Adaptive iterative learning control of non-uniform trajectory tracking for strict feedback nonlinear time-varying systems with unknown control direction[J]. Applied Mathematical Modelling, 2015, 39(10): 2942–2950.
10. Xu J X, Yan R. Iterative learning control design without a priori knowledge of the control direction[J]. Automatica, 2004, 40(10): 1803–1809.
11. Chen H D, Jiang P. Adaptive iterative learning control for nonlinear systems with unknown control gain[J]. ASME Journal of Dynamic Systems, Measurement and Control, 2004, 126(8): 915–920.

12. Krasnoskl'skii M A, Pokrovskii A V. Systems with hysteresis[M]. Moscow: Nauka, 1983.
13. Chi R, Hou Z, Xu J. Adaptive ILC for a class of discrete-time systems with iteration-varying trajectory and random initial condition[J]. Automatica, 2008, 44(8): 2207–2213.
14. Macki J W, Nistri P, Zecca P. Mathematical models for hysteresis[J]. SIAM review, 1993, 35(1): 94–123.
15. Su C Y, Stepanenko Y, Svoboda J, et al. Robust adaptive control of a class of nonlinear systems with unknown backlash-like hysteresis[J]. IEEE Transactions on Automatic Control, 2000, 45(12): 2427–2432.
16. Wen C Y, Zhou J. Decentralized adaptive stabilization in the presence of unknown backlash-like hysteresis[J]. Automatica, 2007, 43(3): 426–440.
17. Jing Zhou, Changyun Wen. Adaptive backstepping control of uncertain systems[M]. Berlin Heidelberg: Springer-Verlag, 2008.
18. Wang H, Chen B, Liu K, et al. Adaptive neural tracking control for a class of nonstrict-feedback stochastic nonlinear systems with unknown backlash-like hysteresis[J]. IEEE Transactions on Neural Networks and Learning Systems, 2014, 25(5): 947–958.
19. Sheng Zhu, Ming-xuan Sun, Xiong-xiong He. Iterative Learning Control for a Class of Nonlinear Systems with Input Backlash[J]. ACTAAUTOMATICA SINICA, 2011, 37(8): 1014–.1017
20. Krstic M, Kanellakopoulos I, KoKotovic P V. Nonlinear and adaptive control design[M]., New York: Wiley, 1995.
21. Sepulchre R, Jankovic M, Kokotovic P V. Constructive nonlinear control[M]. London: Springer, 1997.
22. CHI R H, SUI S L, HOU Z S. A new discrete-time adaptive ILC for nonlinear systems with time-varying parametric uncertainties[J]. Acta Automatica Sinca, 2008, 34(7): 805–808.
23. Ye X, Jiang J. Adaptive nonlinear design without a priori knowledge of control directions[J]. IEEE Transactions on Automatic Control, 1998, 43(11): 1617–1621.
24. Ryan E P. A universal adaptive stabilizer for a class of nonlinear systems[J]. Systems & Control Letters, 1991, 16(3): 209–218.

Chapter 5
Observer-Based AILC of Nonlinear Time-Delay Systems

5.1 Introduction

In previous three chapters, we designed three kinds of AILC schemes for three different kinds of nonlinear time-delay systems, while considering the influence of dead-zone and backlash-like hysteresis nonlinearity. However, these AILC schemes have a common requirement for the plants: the system states are measurable. In the control community, state feedback control is very powerful for nonlinear systems as the full information of the state vectors is assumed to be accessible for feedback. However, in many practical control systems, only the measured output information, rather than the full state information, is available for feedback. In this situation, the designed approaches are not applicable. In this chapter, we will study the AILC problem for nonlinear systems with un-measurable states.

For systems with only output measurable, the firs task for control systems design is to estimate the states based on priori knowledge. In existing estimation methods, observer technique has been proven to be the most effective scheme, which estimates dynamically the states on the basis of information about output tracking error and other compensation term. Over the past decades, there has been a considerable development in various observer design methodologies using different approaches [1–4]. Although so many results have been developed, only a few results are available from the point of AILC. How to design an AILC for nonlinear systems using only output measurement is an interesting and challenging issue. The main research teams of ILC all studied the problem of observer-based ILC more or less. Tayebi and Xu proposed an observer-based iterative learning control scheme for the tracking problem of a class of time-varying nonlinear systems and gave the sufficient conditions for the boundedness and the convergence to zero of the estimation error by using contraction mapping method [5]. In reference [6], Xu utilized the observer in [7] to design an observer-based AILC scheme for a class of time-varying parameterized nonlinear systems based on CEF analysis method. Chen et al. extended the result in [6] and proposed an observer-based AILC for nonlinear systems with unknown time-varying parametric uncertainties and the delayed output, where the Lyapunov-Krasovskii-like

J. Wei et al., *Iterative Learning Control for Nonlinear Time-Delay System*,
https://doi.org/10.1007/978-981-19-6317-9_5

composite energy function was constructed to prove the boundedness of all closed-loop signals and the convergence of output tracking error [8]. Sun et al. also used the observer in [7] to estimate the system states and designed observer-based ILC scheme for a class of time-varying parameterized systems, realizing global accurate tracking for non-uniform trajectory on the finite time interval [9]. By contrast, Chien's team obtained more results. In [10], Wang and Chien introduced an error observer to design an iterative learning controller for robotic systems, where a robust learning component using a filtered fuzzy neural network was presented to solve the problem of unknown nonlinearities. Subsequently, then extended the results in [10] to SISO nonlinear systems [11], MIMO nonlinear systems [12], and MIMO nonlinear systems with delayed output [13].

Similar to dead-zone and hysteresis, saturation is another nonlinear characteristic that is commonly encountered in practical control systems. Strictly speaking, in practical control systems, as long as there exist actuators, there exist saturation nonlinearities. In some situations, the magnitude of saturation is relatively large, most control signals will lie between the bounds of saturation. In this case, the influences of saturation on the whole control systems are small and can be neglected in control system design. Inversely, when the influences of saturation are large, if neglected, it may severely limit system performances and usually leads to undesirable inaccuracies and even instability. The saturation has always been a hot topic in control community. The control design for nonlinear systems preceded by input saturation is a challenging but worthwhile and necessary issue. In the field of time control methods, many results have been published in the past several decades [14–16], however in ILC filed, only a few results are available at present stage. A few researchers carried on researches and designed ILC schemes for several classes of systems with input saturation under some necessary assumptions [17–22].

In this chapter, we will consider a class of nonlinear systems that is influenced by unknown time-varying delays and input saturation, with only output available. To the best of our knowledge, up till now no works have been reported in the field of AILC to deal with such kinds of systems. And we will make full use of observer, LMI tool, AILC method and filter and propose two control design schemes to solve this control problem.

5.2 Problem Formulation and Preliminaries

5.2.1 Problem Formulation

Consider a class of nonlinear time delay systems with input saturation which runs on a finite time interval $[0, T]$ repeatedly:

$$\begin{cases} \dot{x}_{i,k}(t) = x_{i+1,k}(t), i = 1, \ldots, n-1 \\ \dot{x}_{n,k}(t) = f(\boldsymbol{X}_k(t)) + h\big(\boldsymbol{y}_{\tau,k}(t), t\big) + u_k(v_k(t)) + d(t) \\ y_k(t) = x_{1,k}(t), t \in [0, T] \end{cases} \tag{5.1}$$

where, $f(\bullet)$ and $h(\bullet, \bullet)$ are unknown smooth continuous functions; $y_{\tau_i,k} \triangleq y_k(t - \tau_i(t))$ $(i = 1, \ldots, n)$, $\boldsymbol{y}_{\tau,k}(t) = \big[y_{\tau_1,k}(t), \ldots, y_{\tau_n,k}(t)\big]^{\mathrm{T}}$ is time-delay output vector; $v_k(t)$ is control input, $u_k(v_k(t))$ presents saturation nonlinearity. Here, The states are assumed to be unavailable for measurement and only output $y_k(t)$ is measurable. Moreover, the system is bounded-input-bounded-output (BIBO) stable. Define $\boldsymbol{C} = [1, 0, \ldots, 0]^{\mathrm{T}}$, then it is known that $y_k(t) = \boldsymbol{C}^{\mathrm{T}}\boldsymbol{X}_k(t)$.

The control objective of this chapter is as same as that in previous chapters. On the basis of assumptions on unknown time-varying delay, desired reference trajectories and unknown external disturbance, we make the following assumption on $h(\bullet, \bullet)$:

Assumption 5.1 The unknown continuous function $h(\cdot, \cdot)$ is bounded and satisfies the following inequality

$$\big|h\big(y_{\tau,k}, t\big)\big| \le \sum_{j=1}^{n} \rho_j\big(y_{\tau_j,k}(t)\big) \tag{5.2}$$

where, $\rho_j(\cdot)$ is unknown positive continuous function.

5.2.2 *Input Saturation Nonlinearity*

In this chapter, the output of a control u_k with input v_k subjected to the condition of saturation is given by

$$u_k = \begin{cases} v_k, & |v_k| < u_M \\ u_M \operatorname{sgn}(v_k), & |v_k| \ge u_M \end{cases} \tag{5.3}$$

where, u_M is the upper bound of control signal v_k. For convenience of design, we rewrite the saturation nonlinearity as

$$u_k = \beta(v_k) + d_1(v_k) \tag{5.4}$$

where, $\beta(v_k) = u_M \times \tanh\big(v_k / u_M\big)$. Then, $d_1(v_k) = u_k - \beta(v_k)$. It is clear that

$$|d_1(v_k)| = |\mathrm{sat}(v_k) - \beta(v_k)| \le u_M(1 - \tanh(1)) = D_2 \tag{5.5}$$

A graphic presentation of saturation model is shown in Fig. 5.1.

Fig. 5.1 Saturation model

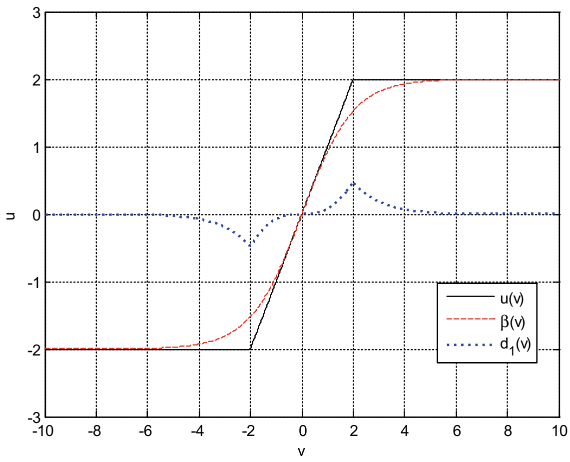

5.2.3 Schur Complementary Lemma

In this paper, the following lemma is used.

Lemma 5.1 [23]. *The Linear Matrix Inequality* (*LMI*)

$$\boldsymbol{S} = \begin{bmatrix} \boldsymbol{S}_{11} & \boldsymbol{S}_{12} \\ \boldsymbol{S}_{21} & \boldsymbol{S}_{22} \end{bmatrix} < 0 \tag{5.6}$$

with $\boldsymbol{S}_{11} = \boldsymbol{S}_{11}^{\mathrm{T}}$ *and* $\boldsymbol{S}_{22} = \boldsymbol{S}_{22}^{\mathrm{T}}$ *is equivalent to*

$$\boldsymbol{S}_{22} < 0,\ \ \boldsymbol{S}_{11} - \boldsymbol{S}_{12}\boldsymbol{S}_{22}^{-1}\boldsymbol{S}_{12}^{\mathrm{T}} < 0 \tag{5.7}$$

5.3 State Observer-Based AILC Design and Stability Analysis

5.3.1 State Observer Design

Rewrite the system (5.1) as

$$\dot{\boldsymbol{X}}_k = \boldsymbol{A}\boldsymbol{X}_k + \boldsymbol{K}_0 y_k + \boldsymbol{B}\big[f(\boldsymbol{X}_k) + h\big(\boldsymbol{y}_{\tau,k}, t\big) + \beta(v_k) + d_1(v_k) + d(t)\big] \tag{5.8}$$

where, $\boldsymbol{K}_0 = [k_1, k_2, \ldots, k_n]^{\mathrm{T}}$, $\boldsymbol{B} = [0, \ldots, 0, 1]^{\mathrm{T}}$, $\boldsymbol{A} = \begin{bmatrix} -k_1 & & & \\ -k_2 & & \boldsymbol{I}_{n-1} & \\ \vdots & & & \\ -k_n & 0 & \cdots & 0 \end{bmatrix}$, $\boldsymbol{I}_{n-1}$ is a unit square matrix of n-1 dimensions. $\boldsymbol{K}_0 \in \mathbf{R}^n$ can be chosen suitably such that $\boldsymbol{A}$ is a strict Hurwitz matrix. Then for a given positive matrix $\boldsymbol{Q} > 0$, there exists a positive matrix $\boldsymbol{P} > 0$ satisfying the following inequality:

$$\boldsymbol{A}^{\mathrm{T}}\boldsymbol{P} + \boldsymbol{P}\boldsymbol{A} + \frac{n+3}{\lambda}\boldsymbol{P}\boldsymbol{P}^{\mathrm{T}} + \frac{\boldsymbol{P}\boldsymbol{P}^{\mathrm{T}}}{\left\|\boldsymbol{C}\boldsymbol{C}^{\mathrm{T}} + \delta\boldsymbol{I}_n\right\|^2} < -\boldsymbol{Q} \tag{5.9}$$

where, λ is a positive constant.

Remark 5.1 To solve inequality (5.9), we decompose the matrix $\boldsymbol{A}$ as $\boldsymbol{A} = \overline{\boldsymbol{A}} + \boldsymbol{K}_0\overline{\boldsymbol{B}}$ with

$$\overline{\boldsymbol{A}} = \begin{bmatrix} 0 & & \\ \vdots & \boldsymbol{I}_{n-1} & \\ 0 & \cdots & 0 \end{bmatrix}, \overline{\boldsymbol{B}} = [-1, 0, \ldots, 0] \tag{5.10}$$

According to Lemma 5.1, the inequality (5.9) is equivalent to the following LMI:

$$\begin{bmatrix} \boldsymbol{P}\overline{\boldsymbol{A}} + \boldsymbol{M}\overline{\boldsymbol{B}} + \overline{\boldsymbol{B}}^{\mathrm{T}}\boldsymbol{M}^{\mathrm{T}} + \overline{\boldsymbol{A}}^{\mathrm{T}}\boldsymbol{P} + \boldsymbol{Q} & \boldsymbol{P} \\ \boldsymbol{P} & -\left(\frac{n+3}{\lambda} + \frac{1}{\left\|\boldsymbol{C}\boldsymbol{C}^{T} + \delta\boldsymbol{I}_n\right\|^2}\right)^{-1}\boldsymbol{I}_n \end{bmatrix} < 0 \tag{5.11}$$

where, $\boldsymbol{I}_n$ is a unit square matrix of n dimensions. Then $\boldsymbol{P}, \boldsymbol{M}$ and λ can be calculated simultaneously via MATLAB LMI toolbox, and the observer gain matrix is further obtained by $\boldsymbol{K}_0 = \boldsymbol{P}^{-1}\boldsymbol{M}$.

For simplicity, define $\overline{d}(t) = d_1(v_k) + d(t)$, obviously, it is bounded, i.e., $\left|\overline{d}(t)\right| \leq D_0$, $D_0 = D_1 + D_2$. To estimate the states of system (5.1), design the observer as

$$\begin{cases} \dot{\hat{\boldsymbol{X}}}_k = \boldsymbol{A}\hat{\boldsymbol{X}}_k + \boldsymbol{K}_o y_k + \boldsymbol{B}[\Psi_k + v_k] \\ \hat{y}_k = \hat{x}_{1,k} \end{cases} \tag{5.12}$$

where, Ψ_k will be given later. For subsequent design, we define $\Delta v_k = \beta(v_k) - v_k$ to describe the effect of input saturation and it can be effectively approximated by using a dynamic neural network.

Define the observer estimation error as $\boldsymbol{z}_k \triangleq \left[z_{1,k}, z_{2,k}, \ldots, z_{n,k}\right] = \boldsymbol{X}_k - \hat{\boldsymbol{X}}_k$, then according to (5.8) and (5.12) we can obtain the dynamical equation of observer error as follows

$$\dot{\boldsymbol{z}}_k = \boldsymbol{A}\boldsymbol{z}_k + \boldsymbol{B}\left[F(\boldsymbol{X}_k) + h\left(\boldsymbol{y}_{\tau,k}, t\right) + \overline{d}(t) - \Psi_k\right] \tag{5.13}$$

where, $F(\boldsymbol{X}_k) = f(\boldsymbol{X}_k) + \Delta v_k$. Choose a positive function of observer error as $V_{z_k} = \boldsymbol{z}_k^{\mathrm{T}} \boldsymbol{P} \boldsymbol{z}_k$, then taking the time derivative of V_{z_k} yields

$$\dot{V}_{z_k} = \boldsymbol{z}_k^{\mathrm{T}}\big(\boldsymbol{A}^{\mathrm{T}}\boldsymbol{P} + \boldsymbol{P}\boldsymbol{A}\big)\boldsymbol{z}_k + 2\boldsymbol{z}_k^{\mathrm{T}}\boldsymbol{P}\boldsymbol{B}\big[F(\boldsymbol{X}_k) + h\big(\boldsymbol{y}_{\tau,k}, t\big) + \overline{d}(t) - \Psi_k\big] \tag{5.14}$$

Considering Assumption 5.1 and utilizing Young's inequality, we can have

$$2\boldsymbol{z}_k^{\mathrm{T}}\boldsymbol{P}\boldsymbol{B}h\big(\boldsymbol{y}_{\tau,k}, t\big) \le 2\big|\boldsymbol{z}_k^{\mathrm{T}}\boldsymbol{P}\boldsymbol{B}\big|\big|h\big(\boldsymbol{y}_{\tau,k}, t\big)\big| \le \frac{n}{\lambda}\boldsymbol{z}_k^{\mathrm{T}}\boldsymbol{P}\boldsymbol{P}^{\mathrm{T}}\boldsymbol{z}_k + \lambda\sum_{j=1}^{n}\rho_j^2\big(y_{\tau_j,k}(t)\big) \tag{5.15}$$

$$2\boldsymbol{z}_k^{\mathrm{T}}\boldsymbol{P}\boldsymbol{B}\overline{d}(t) \le \frac{1}{\lambda}\boldsymbol{z}_k^{\mathrm{T}}\boldsymbol{P}\boldsymbol{P}^{\mathrm{T}}\boldsymbol{z}_k + \lambda D_0^2 \tag{5.16}$$

To compensate for the time delay term, consider the following Lyapunov-Krasovskii functional:

$$V_{U_k}(t) = \frac{\lambda}{(1-\kappa)}\sum_{j=1}^{n}\int_{t-\tau_j(t)}^{t}\rho_j^2(y_k(\sigma))\mathrm{d}\sigma \tag{5.17}$$

On the basis of Assumption 3.1, differentiating $V_{U_k}(t)$ with respect to time leads to

$$\begin{aligned}\dot{V}_{U_k}(t) &= \frac{\lambda}{(1-\kappa)}\sum_{j=1}^{n}\rho_j^2(y_k) - \lambda\sum_{j=1}^{n}\frac{1-\dot{\tau}_j(t)}{(1-\kappa)}\rho_j^2\big(y_{\tau_j,k}\big)\\ &\le \frac{\lambda}{(1-\kappa)}\sum_{j=1}^{n}\rho_j^2(y_k) - \lambda\sum_{j=1}^{n}\rho_j^2\big(y_{\tau_j,k}\big)\end{aligned} \tag{5.18}$$

Combining (5.14)–(5.16) and (5.18), it results in

$$\begin{aligned}\dot{V}_{z_k} + \dot{V}_{U_k} \le{}& \boldsymbol{z}_k^{\mathrm{T}}\left(\boldsymbol{A}^{\mathrm{T}}\boldsymbol{P} + \boldsymbol{P}\boldsymbol{A} + \frac{n+1}{\lambda}\boldsymbol{P}\boldsymbol{P}^{\mathrm{T}}\right)\boldsymbol{z}_k + 2\boldsymbol{z}_k^{\mathrm{T}}\boldsymbol{P}\boldsymbol{B}[F(\boldsymbol{X}_k) - \Psi_k]\\ &+ \frac{\lambda}{(1-\kappa)}\sum_{j=1}^{n}\rho_j^2(y_k) + \lambda D_0^2\end{aligned} \tag{5.19}$$

To overcome the difficulty from unknown time-varying function $F(\boldsymbol{X}_k)$ in (5.19), we utilize time-varying RBF NN to approximate $F(\boldsymbol{X}_k)$ in the following form

$$F(\boldsymbol{X}_k) = \boldsymbol{W}^{*T}\boldsymbol{\phi}(\boldsymbol{X}_k) + \varepsilon(\boldsymbol{X}_k) \tag{5.20}$$

where, $\boldsymbol{W}^* \in \mathbf{R}^l$ denotes the unknown time-varying optimal weight, l is the number of neural nodes, $\boldsymbol{\phi}(\boldsymbol{X}_k) = [\varphi_i(\boldsymbol{X}_k), \varphi_2(\boldsymbol{X}_k), \ldots, \varphi_l(\boldsymbol{X}_k)]^{\mathrm{T}} \in \mathbf{R}^l$, $\varphi_i(x_k) = \exp\left(-\left\|\left(\boldsymbol{X}_k - \boldsymbol{\mu}_i\right)\right\|^2 \Big/ \sigma_i^2\right)$ is the Gaussian radial basis function, $\boldsymbol{\mu}_i \in \mathbf{R}^n$ and $\sigma_i \in \mathbf{R}$ are the center and width of NN respectively, $\varepsilon(\boldsymbol{X}_k)$ presents the approximation error. Denote the bounds of $\boldsymbol{W}^*$ and $\varepsilon(\boldsymbol{X}_k)$ as ε_W and ε_0, respectively, i.e.,

$$\left\|\boldsymbol{W}^*\right\| \leq \varepsilon_W \tag{5.21}$$

$$|\varepsilon(\boldsymbol{X}_k)| \leq \varepsilon_0 \tag{5.22}$$

where, ε_W and ε_0 are unknown constants.

Consequently, we can determine

$$\Psi_k = \hat{\boldsymbol{W}}_k^{\mathrm{T}} \boldsymbol{\phi}\left(\hat{\boldsymbol{X}}_k\right) \tag{5.23}$$

where, $\hat{\boldsymbol{W}}_k(t)$ is the estimated value of $\boldsymbol{W}^*(t)$. Define the error of estimation as $\tilde{\boldsymbol{W}}_k = \hat{\boldsymbol{W}}_k - \boldsymbol{W}^*$, then we can have the following relation

$$\begin{aligned}
&2z_k^{\mathrm{T}} \boldsymbol{P}\boldsymbol{B}[F(\boldsymbol{X}_k) - \Psi_k] \\
&= 2z_k^{\mathrm{T}} \boldsymbol{P}\boldsymbol{B}\left[\boldsymbol{W}^{*T} \boldsymbol{\phi}(\boldsymbol{X}_k) + \varepsilon(\boldsymbol{X}_k) - \hat{\boldsymbol{W}}_k^T \boldsymbol{\phi}\left(\hat{\boldsymbol{X}}_k\right)\right] \\
&= 2z_k^{\mathrm{T}} \boldsymbol{P}\boldsymbol{B}\left[\boldsymbol{W}^{*T} \boldsymbol{\phi}(\boldsymbol{X}_k) - \boldsymbol{W}^{*\mathrm{T}}(t) \boldsymbol{\phi}\left(\hat{\boldsymbol{X}}_k\right) + \varepsilon(\boldsymbol{X}_k) + \boldsymbol{W}^{*T} \boldsymbol{\phi}\left(\hat{\boldsymbol{X}}_k\right) - \hat{\boldsymbol{W}}_k^T \boldsymbol{\phi}\left(\hat{\boldsymbol{X}}_k\right)\right] \\
&= 2z_k^{\mathrm{T}} \boldsymbol{P}\boldsymbol{B}\left[\boldsymbol{W}^{*T} \tilde{\boldsymbol{\phi}}\left(\boldsymbol{X}_k, \hat{\boldsymbol{X}}_k\right) + \varepsilon(\boldsymbol{X}_k) - \tilde{\boldsymbol{W}}_k^{\mathrm{T}} \boldsymbol{\phi}\left(\hat{\boldsymbol{X}}_k\right)\right]
\end{aligned} \tag{5.24}$$

where,

$$\tilde{\boldsymbol{\phi}}\left(\boldsymbol{X}_k, \hat{\boldsymbol{X}}_k\right) = \boldsymbol{\phi}(\boldsymbol{X}_k) - \boldsymbol{\phi}\left(\hat{\boldsymbol{X}}_k\right) \tag{5.25}$$

Based on the form of RBF NN radial basis function, we know that $\tilde{\boldsymbol{\phi}}\left(\boldsymbol{X}_k, \hat{\boldsymbol{X}}_k\right)$ is bounded which satisfies $\tilde{\boldsymbol{\phi}}^{\mathrm{T}}\left(\boldsymbol{X}_k, \hat{\boldsymbol{X}}_k\right)\tilde{\boldsymbol{\phi}}\left(\boldsymbol{X}_k, \hat{\boldsymbol{X}}_k\right) \leq 4l$. Then according to Young's inequality it is clear that

$$2z_k^{\mathrm{T}} \boldsymbol{P}\boldsymbol{B}\left[\boldsymbol{W}^{*T} \tilde{\boldsymbol{\phi}}\left(\boldsymbol{X}_k, \hat{\boldsymbol{X}}_k\right) + \varepsilon(\boldsymbol{X}_k)\right] \leq \frac{2}{\lambda} z_k^{\mathrm{T}} \boldsymbol{P}\boldsymbol{P}^{\mathrm{T}} z_k + 4\lambda l \varepsilon_W^2 + \lambda \varepsilon_0^2 \tag{5.26}$$

$$\begin{aligned}
-2z_k^{\mathrm{T}} \boldsymbol{P}\boldsymbol{B}\tilde{\boldsymbol{W}}_k^{\mathrm{T}} \boldsymbol{\phi}\left(\hat{\boldsymbol{X}}_k\right) &= -2z_k^{\mathrm{T}} \boldsymbol{C}\boldsymbol{C}^{\mathrm{T}}\left(\boldsymbol{C}\boldsymbol{C}^{\mathrm{T}} + \delta \boldsymbol{I}_n\right)^{-1} \boldsymbol{P}\boldsymbol{B}\tilde{\boldsymbol{W}}_k^{\mathrm{T}} \boldsymbol{\phi}\left(\hat{\boldsymbol{X}}_k\right) \\
&\quad - 2z_k^{\mathrm{T}} \delta \boldsymbol{I}_n\left(\boldsymbol{C}\boldsymbol{C}^T + \delta \boldsymbol{I}_n\right)^{-1} \boldsymbol{P}\boldsymbol{B}\tilde{\boldsymbol{W}}_k^{\mathrm{T}} \boldsymbol{\phi}\left(\hat{\boldsymbol{X}}_k\right) \\
&\leq -2z_{1,k} \boldsymbol{C}^{\mathrm{T}}\left(\boldsymbol{C}\boldsymbol{C}^{\mathrm{T}} + \delta \boldsymbol{I}_n\right)^{-1} \boldsymbol{P}\boldsymbol{B}\tilde{\boldsymbol{W}}_k^{\mathrm{T}} \boldsymbol{\phi}\left(\hat{\boldsymbol{X}}_k\right)
\end{aligned}$$

$$+\frac{\boldsymbol{z}_k^{\mathrm{T}}\boldsymbol{P}\boldsymbol{P}^{\mathrm{T}}\boldsymbol{z}_k}{\left\|\boldsymbol{C}\boldsymbol{C}^T+\delta\boldsymbol{I}_n\right\|^2}+\delta^2 l\tilde{\boldsymbol{W}}_k^{\mathrm{T}}\tilde{\boldsymbol{W}}_k \tag{5.27}$$

where, $\delta > 0$ is a small positive constant.

Substituting (5.26) and (5.27) back into (5.19) and using (5.9), it follows that

$$\begin{aligned}
\dot{V}_{z_k}+\dot{V}_{U_k} \le{}& \boldsymbol{z}_k^{\mathrm{T}}\left(\boldsymbol{A}^{\mathrm{T}}\boldsymbol{P}+\boldsymbol{P}\boldsymbol{A}+\frac{n+3}{\lambda}\boldsymbol{P}\boldsymbol{P}^{\mathrm{T}}+\frac{\boldsymbol{P}\boldsymbol{P}^{\mathrm{T}}}{\left\|\boldsymbol{C}\boldsymbol{C}^T+\delta\boldsymbol{I}_n\right\|^2}\right)\boldsymbol{z}_k \\
&-2z_{1,k}\boldsymbol{C}^{\mathrm{T}}\left(\boldsymbol{C}\boldsymbol{C}^{\mathrm{T}}+\delta\boldsymbol{I}_n\right)^{-1}\boldsymbol{P}\boldsymbol{B}\tilde{\boldsymbol{W}}_k^{\mathrm{T}}\boldsymbol{\phi}\left(\hat{\boldsymbol{X}}_k\right) \\
&+\frac{\lambda}{(1-\kappa)}\sum_{j=1}^{n}\rho_j^2(y_k)+\lambda D_0^2+4\lambda l\varepsilon_W^2+\lambda\varepsilon_0^2+\delta^2 l\tilde{\boldsymbol{W}}_k^{\mathrm{T}}\tilde{\boldsymbol{W}}_k \\
\le{}& -\boldsymbol{z}_k^{\mathrm{T}}\boldsymbol{Q}\boldsymbol{z}_k-2z_{1,k}\boldsymbol{C}^{\mathrm{T}}\left(\boldsymbol{C}\boldsymbol{C}^{\mathrm{T}}+\delta\boldsymbol{I}_n\right)^{-1}\boldsymbol{P}\boldsymbol{B}\tilde{\boldsymbol{W}}_k^{\mathrm{T}}\boldsymbol{\phi}\left(\hat{\boldsymbol{X}}_k\right) \\
&+\frac{\lambda}{(1-\kappa)}\sum_{j=1}^{n}\rho_j^2(y_k)+\lambda D_0^2+4\lambda l\varepsilon_W^2+\lambda\varepsilon_0^2+\delta^2 l\tilde{\boldsymbol{W}}_k^{\mathrm{T}}\tilde{\boldsymbol{W}}_k \\
\le{}& -\lambda_{\min}(\boldsymbol{Q})\|\boldsymbol{z}_k\|^2-2z_{1,k}\boldsymbol{C}^{\mathrm{T}}\left(\boldsymbol{C}\boldsymbol{C}^{\mathrm{T}}+\delta\boldsymbol{I}_n\right)^{-1}\boldsymbol{P}\boldsymbol{B}\tilde{\boldsymbol{W}}_k^{\mathrm{T}}\boldsymbol{\phi}\left(\hat{\boldsymbol{X}}_k\right) \\
&+\frac{\lambda}{(1-\kappa)}\sum_{j=1}^{n}\rho_j^2(y_k)+\lambda D_0^2+4\lambda l\varepsilon_W^2+\lambda\varepsilon_0^2+\delta^2 l\tilde{\boldsymbol{W}}_k^{\mathrm{T}}\tilde{\boldsymbol{W}}_k
\end{aligned} \tag{5.28}$$

where, $\lambda_{\min}(\boldsymbol{Q})$ denotes the minimum eigenvalue of matrix $\boldsymbol{Q}$.

5.3.2 NN AILC Scheme Design

Define errors as $e_{1,k}=\hat{x}_{1,k}-y_d, e_{i,k}=\hat{x}_{i,k}-y_d^{(i-1)}, i=2,\ldots,n$, i.e., $\boldsymbol{e}_k=\hat{\boldsymbol{X}}_k-\boldsymbol{X}_d$. Make the following assumptions on initial conditions.

Assumption 5.2 $z_{i,k}(0)=0, i=1,2,\ldots,n$.

Assumption 5.3 Identical initial condition is not necessary for $e_{i,k}(0)$, that is, the initial state errors $e_{i,k}(0)$ at each iteration are not necessarily zero, small or fixed, but assumed to be bounded.

Similar to previous chapters, define errors e_{sk} and s_k. To facilitate following controller design, we give the dynamic equation of $\boldsymbol{e}_k$ as follows

$$\dot{e}_{i,k}=e_{i+1,k}+k_i z_{1,k}, i=1,\ldots,n-1 \tag{5.29}$$

$$\dot{e}_{n,k}=k_n z_{1,k}+v_k+\hat{\boldsymbol{W}}_k^{\mathrm{T}}\boldsymbol{\phi}\left(\hat{\boldsymbol{X}}_k\right)-y_d^{(n)} \tag{5.30}$$

Choose the Lyapunov function for tracking error as $V_{sk} = s_k^2 \big/ 2$, taking the time derivative of V_{sk} yields

$$\begin{aligned}
\dot{V}_{s_k} &= s_k \dot{s}_k \\
&= \begin{cases} s_k(\dot{e}_{sk} - \dot{\eta}(t)), if \;\; e_{sk} > \eta(t) \\ 0 \;, if \;\; |e_{sk}| \le \eta(t) \\ s_k(\dot{e}_{sk} + \dot{\eta}(t)), \; if \; e_{sk} < -\eta(t) \end{cases} \\
&= s_k(\dot{e}_{sk} - \dot{\eta}(t)\mathrm{sgn}(s_k)) \\
&= s_k \Bigg[\sum_{j=1}^{n-1} \left(\lambda_j e_{j+1,k} + \lambda_j k_j z_{1,k} \right) + K\eta(t)\mathrm{sgn}(s_k) \\
&\quad - y_d^{(n)} + k_n z_{1,k} + \hat{\boldsymbol{W}}_k^{\mathrm{T}} \boldsymbol{\phi}\left(\hat{\boldsymbol{X}}_k \right) + v_k \Bigg] \\
&= s_k \Bigg[\sum_{j=1}^{n-1} \lambda_j e_{j+1,k} + \left[\boldsymbol{\Lambda}^T \; 1 \right] K_0 z_{1,k} + K e_{sk} \\
&\quad - y_d^{(n)} + \hat{\boldsymbol{W}}_k^{\mathrm{T}} \boldsymbol{\phi}\left(\hat{\boldsymbol{X}}_k \right) + v_k \Bigg] - K s_k^2
\end{aligned} \tag{5.31}$$

Choose the Lyapunov function of the whole system as $V_k = V_{z_k} + V_{U_k} + V_{s_k}$. Combining (5.28) and (5.31), it follows that

$$\begin{aligned}
\dot{V}_k &\le -\lambda_{\min}(\boldsymbol{Q})\|\boldsymbol{z}_k\|^2 - 2z_{1,k}\boldsymbol{C}^{\mathrm{T}}\left(\boldsymbol{C}\boldsymbol{C}^{\mathrm{T}} + \delta \boldsymbol{I}_n\right)^{-1} \boldsymbol{P}\boldsymbol{B}\tilde{\boldsymbol{W}}_k^{\mathrm{T}} \boldsymbol{\phi}\left(\hat{\boldsymbol{X}}_k \right) \\
&\quad + \frac{\lambda}{(1-\kappa)} \sum_{j=1}^{n} \rho_j^2(y_k) + \lambda D_0^2 + 4\lambda l \varepsilon_W^2 + \lambda \varepsilon_0^2 + \delta^2 l \tilde{\boldsymbol{W}}_k^{\mathrm{T}} \tilde{\boldsymbol{W}}_k \\
&= s_k \left[\sum_{j=1}^{n-1} \lambda_j e_{j+1,k} + \left[\boldsymbol{\Lambda}^T \; 1 \right] K_0 z_{1,k} + K e_{sk} - y_d^{(n)} + \hat{\boldsymbol{W}}_k^{\mathrm{T}} \boldsymbol{\phi}\left(\hat{\boldsymbol{X}}_k \right) + v_k \right] - K s_k^2
\end{aligned} \tag{5.32}$$

For convenience of expression, denote $\Xi(y_k) \triangleq \frac{\lambda}{(1-\kappa)} \sum_{j=1}^{n} \rho_j^2(y_k) + \lambda D_0^2 + 4\lambda l \varepsilon_W^2 + \lambda \varepsilon_0^2$. Employing the hyperbolic tangent function, Eq. (5.32) turns into

$$\begin{aligned}
\dot{V}_k &\le -\lambda_{\min}(\boldsymbol{Q})\|\boldsymbol{z}_k\|^2 - 2z_{1,k}\boldsymbol{C}^{\mathrm{T}}\left(\boldsymbol{C}\boldsymbol{C}^{\mathrm{T}} + \delta \boldsymbol{I}_n\right)^{-1} \boldsymbol{P}\boldsymbol{B}\tilde{\boldsymbol{W}}_k^{\mathrm{T}} \boldsymbol{\phi}\left(\hat{\boldsymbol{X}}_k \right) + \delta^2 l \tilde{\boldsymbol{W}}_k^{\mathrm{T}} \tilde{\boldsymbol{W}}_k \\
&\quad + s_k \Bigg[\sum_{j=1}^{n-1} \lambda_j e_{j+1,k} + \left[\boldsymbol{\Lambda}^T 1 \right] K_0 z_{1,k} + K e_{sk} - y_d^{(n)} + \hat{\boldsymbol{W}}_k^{\mathrm{T}} \boldsymbol{\phi}\left(\hat{\boldsymbol{X}}_k \right) +
\end{aligned}$$

$$v_k + b\frac{\tanh^2\left(s_k/\eta(t)\right)}{s_k}\Xi(y_k)\Bigg] + \left[1 - b\tanh^2\left(s_k/\eta(t)\right)\right]\Xi(y_k) - Ks_k^2 \tag{5.33}$$

Obviously, $\frac{\lambda}{(1-\kappa)}\sum_{j=1}^{n}\rho_j^2(y_k)$ is continuous and well-defined on the compact set $\boldsymbol{\Omega}_y = \{y_k\} \subset \mathbf{R}$. Hence, it can be approximated by a NN with constant weight as follows

$$\frac{\lambda}{(1-\kappa)}\sum_{j=1}^{n}\rho_j^2(y_k) = \boldsymbol{W}_{\Xi}^{*\mathrm{T}}\boldsymbol{\phi}_{\Xi}(y_k) + \varepsilon_{\Xi}(y_k)$$

where, the estimation error satisfies $|\varepsilon_{\Xi}(y_k)| \le \overline{\varepsilon}_{\Xi}$, $\boldsymbol{W}_{\Xi}^{*} \in R^{l_{\Xi}}$ denotes the optimal weight vector, $\boldsymbol{\phi}_{\Xi}(y_k) \in R^{l_{\Xi}}$ is Gaussian basis function vector, l_{Ξ} is the number of neurons. Then $\Xi(y_k)$ can be rewritten as follows

$$\Xi(y_k) = \boldsymbol{W}_{\Xi}^{*\mathrm{T}}\boldsymbol{\phi}_{\Xi}(y_k) + \varepsilon_{\Xi}(y_k) + \lambda D_0^2 + 4\lambda l\varepsilon_W^2 + \lambda\varepsilon_0^2 \tag{5.34}$$

For simplicity of expression, denote $\mu \triangleq \varepsilon_{\Xi}(y_k) + \lambda D_0^2 + 4\lambda l\varepsilon_W^2 + \lambda\varepsilon_0^2$. Then we can further rewrite $\Xi(y_k)$ as $\Xi(y_k) = \boldsymbol{W}_2^{*\mathrm{T}}\boldsymbol{\phi}_2(y_k)$, $\boldsymbol{W}_2^{*} = \left[\boldsymbol{W}_{\Xi}^{*\mathrm{T}}, \mu\right]^{\mathrm{T}}$, $\boldsymbol{\phi}_2(y_k) = \left[\boldsymbol{\phi}_{\Xi}^{\mathrm{T}}(y_k), 1\right]^{\mathrm{T}}$.

Until now, we can design output feedback controller as

$$\begin{aligned} v_k = &-\sum_{j=1}^{n-1}\lambda_j e_{j+1,k} - \left[\boldsymbol{\Lambda}^T \quad 1\right]K_0 z_{1,k} - Ke_{sk} + y_d^{(n)} \\ &- \hat{\boldsymbol{W}}_k^{\mathrm{T}}\phi\left(\hat{\boldsymbol{X}}_k\right) - b\hat{\boldsymbol{W}}_{2,k}^{\mathrm{T}}\boldsymbol{\phi}_2(y_k)\tanh^2\left(s_k/\eta(t)\right)\Big/ s_k \end{aligned} \tag{5.35}$$

where, $\hat{\boldsymbol{W}}_k$ and $\hat{\boldsymbol{W}}_{2,k}$ are the estimated values of $\boldsymbol{W}^*$ and $\boldsymbol{W}_2^*$, respectively.

Design adaptive learning laws for $\hat{\boldsymbol{W}}_k(t)$ and $\hat{\boldsymbol{W}}_{2,k}$ as follows

$$\begin{cases} (1-\gamma_1)\dot{\hat{\boldsymbol{W}}}_k = -\gamma_1\hat{\boldsymbol{W}}_k - \gamma_1\alpha_1\hat{\boldsymbol{W}}_k + \gamma_1\hat{\boldsymbol{W}}_{k-1} + 2q_1 z_{1,k}\boldsymbol{C}^{\mathrm{T}}\left(\boldsymbol{C}\boldsymbol{C}^{\mathrm{T}} + \delta\boldsymbol{I}_n\right)^{-1}\boldsymbol{P}\boldsymbol{B}\boldsymbol{\phi}\left(\hat{\boldsymbol{X}}_k\right) \\ \hat{\boldsymbol{W}}_k(0) = \hat{\boldsymbol{W}}_{k-1}(T),\ \hat{\boldsymbol{W}}_0(t) = 0,\ t \in [0, T] \end{cases} \tag{5.36}$$

$$\begin{cases} (1-\gamma_2)\dot{\hat{\boldsymbol{W}}}_{2,k} = -\gamma_2\hat{\boldsymbol{W}}_{2,k} + \gamma_2\hat{\boldsymbol{W}}_{2,k-1} + q_2 b\tanh^2\left(s_k/\eta(t)\right)\boldsymbol{\phi}_2(y_k) \\ \hat{\boldsymbol{W}}_{2,k}(0) = \hat{\boldsymbol{W}}_{2,k-1}(T),\ \hat{\boldsymbol{W}}_{2,0}(t) = 0,\ t \in [0, T] \end{cases} \tag{5.37}$$

where, $q_1, q_2 > 0$, $0 < \gamma_1, \gamma_2 < 1$ and $\alpha_1 > 0$ are all design parameters.

Define parameter estimation errors as $\tilde{\boldsymbol{W}}_k = \hat{\boldsymbol{W}}_k - \boldsymbol{W}^*$, $\tilde{\boldsymbol{W}}_{2,k} = \hat{\boldsymbol{W}}_{2,k} - \boldsymbol{W}_{2,k}^*$. Substituting controller (5.35) back into (5.33) leads to

$$\dot{V}_k \le -\lambda_{\min}(\boldsymbol{Q})\|\boldsymbol{z}_k\|^2 - 2z_{1,k}\boldsymbol{C}^{\mathrm{T}}\left(\boldsymbol{C}\boldsymbol{C}^{\mathrm{T}} + \delta\boldsymbol{I}_n\right)^{-1}\boldsymbol{P}\boldsymbol{B}\tilde{\boldsymbol{W}}_k^{\mathrm{T}}\boldsymbol{\phi}\left(\hat{\boldsymbol{X}}_k\right) + \delta^2 l\tilde{\boldsymbol{W}}_k^{\mathrm{T}}\tilde{\boldsymbol{W}}_k$$

$$- b\tilde{\boldsymbol{W}}_{2,k}^{\mathrm{T}}\boldsymbol{\phi}_2(y_k)\tanh^2\big(s_k/\eta(t)\big) + \big[1 - b\tanh^2\big(s_k/\eta(t)\big)\big]\Xi(y_k) - Ks_k^2 \tag{5.38}$$

Fro proceeding analysis, we write Eq. (5.38) in the following form

$$2z_{1,k}\boldsymbol{C}^{\mathrm{T}}\big(\boldsymbol{C}\boldsymbol{C}^{\mathrm{T}} + \delta\boldsymbol{I}_n\big)^{-1}\boldsymbol{P}\boldsymbol{B}\tilde{\boldsymbol{W}}_k^{\mathrm{T}}\boldsymbol{\phi}\Big(\hat{\boldsymbol{X}}_k\Big) + b\tilde{\boldsymbol{W}}_{2,k}^{\mathrm{T}}\boldsymbol{\phi}_2(y_k)\tanh^2\big(s_k/\eta(t)\big) \leq$$
$$- \dot{V}_k - \lambda_{\min}(\boldsymbol{Q})\|z_k\|^2 + \big[1 - b\tanh^2\big(s_k/\eta(t)\big)\big]\Xi(y_k) - Ks_k^2 + \delta^2 l\tilde{\boldsymbol{W}}_k^{\mathrm{T}}\tilde{\boldsymbol{W}}_k \tag{5.39}$$

The block diagram of the proposed state observer based adaptive NN ILC scheme is presented in Fig. 5.2.

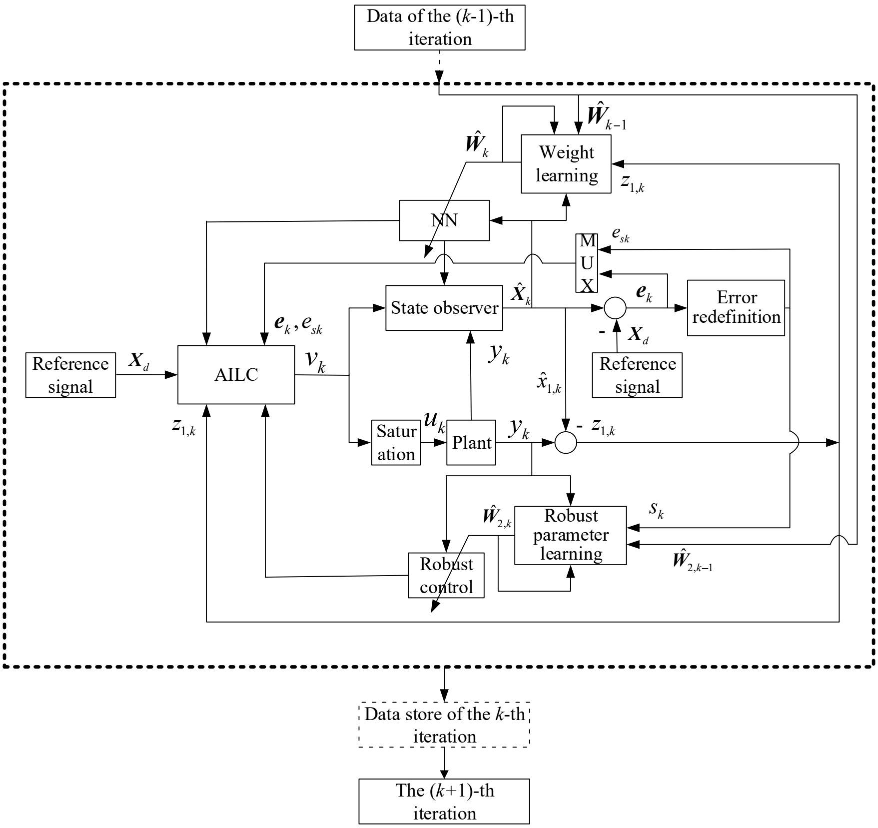

Fig. 5.2 The block diagram of the state observer based adaptive NN ILC system

5.3.3 Stability Analysis

The convergence and boundedness property of the proposed observer-based AILC scheme are summarized in the following theorem.

Theorem 5.1 *Considering the closed-loop system consisting of plant* (5.1) *and input saturation model* (5.3) *under Assumptions* 2.5, 2.6, 3.1, *and Assumptions* 5.1–5.3 *running on the finite time interval* $[0, T]$ *repeatedly, if only the output variable, design state observer* (5.12), *output feedback controller* (5.35) *with parameter adaptive iterative learning laws* (5.36) *and* (5.37), *the following conclusions can be guaranteed*: (1) *for* $k \to \infty$, $e_{sk}(t)$ *will converge to a small neighborhood of the origin under the* L_T^2*-norm, i.e.,* $\lim_{k\to\infty} \int_0^T (e_{sk})^2 \mathrm{d}\sigma \le \varepsilon_{esk} = \frac{1}{2K}(1+m)^2\varepsilon^2$; (2) *the tracking error satisfies* $\lim_{k\to\infty} |y_k(t) - y_d(t)| \le \min\left\{k_0 \sum_{i=1}^{n-1} \sqrt{\varepsilon_i^2}\mathrm{e}^{-\lambda_0 t} + (1+m)\frac{\varepsilon k_0}{\lambda_0 - K}\left(\mathrm{e}^{-Kt} - \mathrm{e}^{-\lambda_0 t}\right), \left[p_1 + \frac{1}{k_1}(Kp_1 + p_2)\right]\varepsilon \mathrm{e}^{-Kt}\right\}$, *where,* λ_0, k_0, p_1 and p_2 *are positive constants and will be given later.*

Proof Similar to previous chapters, we will consider two cases according to Lemma 2.2.

Case 1. $s_k \in \boldsymbol{\Omega}_{s_k}$.

In this case, $|e_{sk}(t)| \le (1+m)\eta(t)$. Since $\boldsymbol{X}_d(t)$ is finite, $\hat{x}_{i,k}(t)$ is bounded. From adaptive iterative learning laws (5.36) and (5.37) it is clear that for $s_k(t) \in \Omega_{s_k}$, $\hat{W}_k(t) \in L_T^\infty$, $\hat{W}_{2,k}(t) \in L_T^\infty$, i.e., they have bounds in L_T^∞-norm. Based on above analysis, we can know that $\boldsymbol{z}_k$ and $\boldsymbol{X}_k$ are bounded which naturally leads to the boundedness of $v_k(t)$. Consequently, all the closed-loop signals are bounded. Additionally, from $|e_{sk}| \le (1+m)\eta(t)$ and the definition of e_k, we can know that $e_{1,k}$ and $e_{2,k}$ lies within small neighborhoods of $p_1\eta(t)$ and $p_2\eta(t)$ respectively with p_1 and p_2 being small constants, i.e., $\left|e_{1,k}\right| \le p_1\eta(t)$, $\left|e_{2,k}\right| \le p_2\eta(t)$. Then it can be derived that $\left|\dot{e}_{1,k}\right| \le p_1 K\eta(t)$ which further leads to according to (5.29)

$$k_1\left|z_{1,k}\right| \le \left|e_{2,k}\right| + \left|\dot{e}_{1,k}\right| = (Kp_1 + p_2)\varepsilon \mathrm{e}^{-Kt} \tag{5.40}$$

It means that

$$|y_k - y_d| = \left|z_{1,k} + e_{1,k}\right| \le \left|z_{1,k}\right| + \left|e_{1,k}\right| \le \left[p_1 + \frac{1}{k_1}(Kp_1 + p_2)\right]\varepsilon \mathrm{e}^{-Kt} \tag{5.41}$$

Case 2. $s_k(t) \notin \Omega_{s_k}$.

According to Lemma 2.2, Eq. (5.38) changes to

$$\begin{aligned}
&2z_{1,k}\boldsymbol{C}^{\mathrm{T}}\left(\boldsymbol{C}\boldsymbol{C}^{\mathrm{T}} + \delta \boldsymbol{I}_n\right)^{-1}\boldsymbol{P}\boldsymbol{B}\tilde{\boldsymbol{W}}_k^{\mathrm{T}}\boldsymbol{\phi}\left(\hat{\boldsymbol{X}}_k\right) + b\tilde{\boldsymbol{W}}_{2,k}^{\mathrm{T}}\boldsymbol{\phi}_2(y_k)\tanh^2\left(s_k/\eta(t)\right)\\
&\le -\dot{V}_k - \lambda_{\min}(\boldsymbol{Q})\|\boldsymbol{z}_k\|^2 - Ks_k^2 + \delta^2 l\tilde{\boldsymbol{W}}_k^{\mathrm{T}}\tilde{\boldsymbol{W}}_k
\end{aligned} \tag{5.42}$$

Next we will check the stability of the system by using CEF-based analysis. Choose the following CEF

$$E_k(t) = \frac{\gamma_1}{2q_1}\int_0^t \tilde{\boldsymbol{W}}_k^{\mathrm{T}}\tilde{\boldsymbol{W}}_k \mathrm{d}\sigma + \frac{(1-\gamma_1)}{2q_1}\tilde{\boldsymbol{W}}_k^{\mathrm{T}}\tilde{\boldsymbol{W}}_k + \frac{\gamma_2}{2q_2}\int_0^t \tilde{\boldsymbol{W}}_{2,k}^{\mathrm{T}}\tilde{\boldsymbol{W}}_{2,k}\mathrm{d}\sigma + \frac{(1-\gamma_2)}{2q_2}\tilde{\boldsymbol{W}}_{2,k}^{\mathrm{T}}\tilde{\boldsymbol{W}}_{2,k} \tag{5.43}$$

Similarly, we separate the following proof into five parts.

(1) The difference of $E_k(t)$.

From (5.43) we can compute the difference of $E_k(t)$ as follows

$$\begin{aligned}\Delta E_k(t) &= E_k(t) - E_{k-1}(t)\\ &= \frac{\gamma_1}{2q_1}\int_0^t \left[\tilde{\boldsymbol{W}}_k^{\mathrm{T}}\tilde{\boldsymbol{W}}_k - \tilde{\boldsymbol{W}}_{k-1}^{\mathrm{T}}\tilde{\boldsymbol{W}}_{k-1}\right]\mathrm{d}\sigma + \frac{(1-\gamma_1)}{2q_1}\left[\tilde{\boldsymbol{W}}_k^{\mathrm{T}}\tilde{\boldsymbol{W}}_k - \tilde{\boldsymbol{W}}_{k-1}^{\mathrm{T}}\tilde{\boldsymbol{W}}_{k-1}\right]\\ &\quad + \frac{\gamma_2}{2q_2}\int_0^t \left[\tilde{\boldsymbol{W}}_{2,k}^{\mathrm{T}}\tilde{\boldsymbol{W}}_{2,k} - \tilde{\boldsymbol{W}}_{2,k-1}^{\mathrm{T}}\tilde{\boldsymbol{W}}_{2,k-1}\right]\mathrm{d}\sigma\\ &\quad + \frac{(1-\gamma_2)}{2q_2}\left[\tilde{\boldsymbol{W}}_{2,k}^{\mathrm{T}}\tilde{\boldsymbol{W}}_{2,k} - \tilde{\boldsymbol{W}}_{2,k-1}^{\mathrm{T}}\tilde{\boldsymbol{W}}_{2,k-1}\right]\end{aligned} \tag{5.44}$$

Recalling adaptive iterative learning law (5.36) and using the relationship $2\tilde{\boldsymbol{W}}_k^{\mathrm{T}}\hat{\boldsymbol{W}}_k \geq \tilde{\boldsymbol{W}}_k^{\mathrm{T}}\tilde{\boldsymbol{W}}_k - \boldsymbol{W}^{*\mathrm{T}}\boldsymbol{W}^*$ we can get

$$\begin{aligned}&\frac{\gamma_1}{2q_1}\int_0^t \left[\tilde{\boldsymbol{W}}_k^{\mathrm{T}}\tilde{\boldsymbol{W}}_k - \tilde{\boldsymbol{W}}_{k-1}^{\mathrm{T}}\tilde{\boldsymbol{W}}_{k-1}\right]\mathrm{d}\sigma + \frac{(1-\gamma_1)}{2q_1}\left[\tilde{\boldsymbol{W}}_k^{\mathrm{T}}\tilde{\boldsymbol{W}}_k - \tilde{\boldsymbol{W}}_{k-1}^{\mathrm{T}}\tilde{\boldsymbol{W}}_{k-1}\right]\\ &= \frac{\gamma_1}{2q_1}\int_0^t \left[\tilde{\boldsymbol{W}}_k^{\mathrm{T}}\tilde{\boldsymbol{W}}_k - \tilde{\boldsymbol{W}}_{k-1}^{\mathrm{T}}\tilde{\boldsymbol{W}}_{k-1}\right]\mathrm{d}\sigma + \frac{(1-\gamma_1)}{q_1}\int_0^t \tilde{\boldsymbol{W}}_k^{\mathrm{T}}\dot{\tilde{\boldsymbol{W}}}_k\mathrm{d}\sigma\\ &+ \frac{(1-\gamma_1)}{2q_1}\left[\tilde{\boldsymbol{W}}_k^{\mathrm{T}}(0)\tilde{\boldsymbol{W}}_k(0) - \tilde{\boldsymbol{W}}_{k-1}^{\mathrm{T}}\tilde{\boldsymbol{W}}_{k-1}\right]\\ &= \int_0^t 2z_{1,k}\boldsymbol{C}^{\mathrm{T}}\left(\boldsymbol{C}\boldsymbol{C}^{\mathrm{T}} + \delta\boldsymbol{I}_n\right)^{-1}\boldsymbol{P}\boldsymbol{B}\tilde{\boldsymbol{W}}_k^{\mathrm{T}}\boldsymbol{\phi}\left(\hat{\boldsymbol{X}}_k\right)\mathrm{d}\sigma\\ &- \frac{\gamma_1}{q_1}\int_0^t \tilde{\boldsymbol{W}}_k^{\mathrm{T}}\left(\alpha_1\hat{\boldsymbol{W}}_k + \hat{\boldsymbol{W}}_k - \hat{\boldsymbol{W}}_{k-1}\right)\mathrm{d}\sigma\end{aligned}$$

$$
\begin{aligned}
&+\frac{\gamma_1}{2q_1}\int_0^t\left[\tilde{\boldsymbol{W}}_k^{\mathrm{T}}\tilde{\boldsymbol{W}}_k-\tilde{\boldsymbol{W}}_{k-1}^{\mathrm{T}}\tilde{\boldsymbol{W}}_{k-1}\right]\mathrm{d}\sigma \\
&+\frac{(1-\gamma_1)}{2q_1}\left[\tilde{\boldsymbol{W}}_k^{\mathrm{T}}(0)\tilde{\boldsymbol{W}}_k(0)-\tilde{\boldsymbol{W}}_{k-1}^{\mathrm{T}}\tilde{\boldsymbol{W}}_{k-1}\right] \\
&=\int_0^t 2z_{1,k}\boldsymbol{C}^{\mathrm{T}}\left(\boldsymbol{C}\boldsymbol{C}^{\mathrm{T}}+\delta\boldsymbol{I}_n\right)^{-1}\boldsymbol{P}\boldsymbol{B}\tilde{\boldsymbol{W}}_k^{\mathrm{T}}\boldsymbol{\phi}\left(\hat{\boldsymbol{X}}_k\right)\mathrm{d}\sigma \\
&-\frac{\alpha_1\gamma_1}{q_1}\int_0^t\tilde{\boldsymbol{W}}_k^{\mathrm{T}}\hat{\boldsymbol{W}}_k\mathrm{d}\sigma-\frac{\gamma_1}{q_1}\int_0^t\tilde{\boldsymbol{W}}_k^{\mathrm{T}}\left(\tilde{\boldsymbol{W}}_k-\tilde{\boldsymbol{W}}_{k-1}\right)\mathrm{d}\sigma \\
&+\frac{\gamma_1}{2q_1}\int_0^t\left[\tilde{\boldsymbol{W}}_k^{\mathrm{T}}\tilde{\boldsymbol{W}}_k-\tilde{\boldsymbol{W}}_{k-1}^{\mathrm{T}}\tilde{\boldsymbol{W}}_{k-1}\right]\mathrm{d}\sigma \\
&+\frac{(1-\gamma_1)}{2q_1}\left[\tilde{\boldsymbol{W}}_k^{\mathrm{T}}(0)\tilde{\boldsymbol{W}}_k(0)-\tilde{\boldsymbol{W}}_{k-1}^{\mathrm{T}}\tilde{\boldsymbol{W}}_{k-1}\right] \\
&=\int_0^t 2z_{1,k}\boldsymbol{C}^{\mathrm{T}}\left(\boldsymbol{C}\boldsymbol{C}^{\mathrm{T}}+\delta\boldsymbol{I}_n\right)^{-1}\boldsymbol{P}\boldsymbol{B}\tilde{\boldsymbol{W}}_k^{\mathrm{T}}\boldsymbol{\phi}\left(\hat{\boldsymbol{X}}_k\right)\mathrm{d}\sigma-\frac{\alpha_1\gamma_1}{q_1}\int_0^t\tilde{\boldsymbol{W}}_k^{\mathrm{T}}\hat{\boldsymbol{W}}_k\mathrm{d}\sigma \\
&-\frac{\gamma_1}{2q_1}\int_0^t\left(\tilde{\boldsymbol{W}}_k-\tilde{\boldsymbol{W}}_{k-1}\right)^{\mathrm{T}}\left(\tilde{\boldsymbol{W}}_k-\tilde{\boldsymbol{W}}_{k-1}\right)\mathrm{d}\sigma \\
&+\frac{(1-\gamma_1)}{2q_1}\left[\tilde{\boldsymbol{W}}_k^{\mathrm{T}}(0)\tilde{\boldsymbol{W}}_k(0)-\tilde{\boldsymbol{W}}_{k-1}^{\mathrm{T}}\tilde{\boldsymbol{W}}_{k-1}\right] \\
&\leq\int_0^t 2z_{1,k}\boldsymbol{C}^{\mathrm{T}}\left(\boldsymbol{C}\boldsymbol{C}^{\mathrm{T}}+\delta\boldsymbol{I}_n\right)^{-1}\boldsymbol{P}\boldsymbol{B}\tilde{\boldsymbol{W}}_k^{\mathrm{T}}\boldsymbol{\phi}\left(\hat{\boldsymbol{X}}_k\right)\mathrm{d}\sigma \\
&-\frac{\alpha_1\gamma_1}{2q_1}\int_0^t\tilde{\boldsymbol{W}}_k^{\mathrm{T}}\tilde{\boldsymbol{W}}_k\mathrm{d}\sigma+\frac{\alpha_1\gamma_1}{2q_1}\int_0^t\left\|\boldsymbol{W}^*\right\|^2\mathrm{d}\sigma \\
&+\frac{(1-\gamma_1)}{2q_1}\left[\tilde{\boldsymbol{W}}_k^{\mathrm{T}}(0)\tilde{\boldsymbol{W}}_k(0)-\tilde{\boldsymbol{W}}_{k-1}^{\mathrm{T}}\tilde{\boldsymbol{W}}_{k-1}\right]
\end{aligned}
\tag{5.45}
$$

Similarly, from adaptive iterative learning law (5.37) we can have

$$
\begin{aligned}
&\frac{\gamma_2}{2q_2}\int_0^t\left[\tilde{\boldsymbol{W}}_{2,k}^{\mathrm{T}}\tilde{\boldsymbol{W}}_{2,k}-\tilde{\boldsymbol{W}}_{2,k-1}^{\mathrm{T}}\tilde{\boldsymbol{W}}_{2,k-1}\right]\mathrm{d}\sigma \\
&\quad+\frac{(1-\gamma_2)}{2q_2}\left[\tilde{\boldsymbol{W}}_{2,k}^{\mathrm{T}}\tilde{\boldsymbol{W}}_{2,k}-\tilde{\boldsymbol{W}}_{2,k-1}^{\mathrm{T}}\tilde{\boldsymbol{W}}_{2,k-1}\right]
\end{aligned}
$$

$$\leq \int_0^t b\tanh^2\left(s_k/\eta\right)\tilde{\boldsymbol{W}}_{2,k}^{\mathrm{T}}\boldsymbol{\phi}_2(y_k)\mathrm{d}\sigma + \frac{(1-\gamma_2)}{2q_2}\left[\tilde{\boldsymbol{W}}_{2,k}^{\mathrm{T}}(0)\tilde{\boldsymbol{W}}_{2,k}(0) - \tilde{\boldsymbol{W}}_{2,k-1}^{\mathrm{T}}\tilde{\boldsymbol{W}}_{2,k-1}\right] \tag{5.46}$$

Substituting (5.45) and (5.46) back into (5.44), it results in

$$\begin{aligned}
\Delta E_k(t) \leq & \int_0^t 2z_{1,k}\boldsymbol{C}^{\mathrm{T}}\left(\boldsymbol{C}\boldsymbol{C}^{\mathrm{T}} + \delta\boldsymbol{I}_n\right)^{-1}\boldsymbol{P}\boldsymbol{B}\tilde{\boldsymbol{W}}_k^{\mathrm{T}}\boldsymbol{\phi}\left(\hat{\boldsymbol{X}}_k\right)\mathrm{d}\sigma \\
& + \int_0^t b\tanh^2\left(s_k/\eta\right)\tilde{\boldsymbol{W}}_{2,k}^{\mathrm{T}}\boldsymbol{\phi}_2(y_k)\mathrm{d}\sigma \\
& - \frac{\alpha_1\gamma_1}{2q_1}\int_0^t \tilde{\boldsymbol{W}}_k^{\mathrm{T}}\tilde{\boldsymbol{W}}_k\mathrm{d}\sigma + \frac{\alpha_1\gamma_1}{2q_1}\int_0^t \left\|\boldsymbol{W}^*\right\|^2\mathrm{d}\sigma \\
& + \frac{(1-\gamma_1)}{2q_1}\left[\tilde{\boldsymbol{W}}_k^{\mathrm{T}}(0)\tilde{\boldsymbol{W}}_k(0) - \tilde{\boldsymbol{W}}_{k-1}^{\mathrm{T}}\tilde{\boldsymbol{W}}_{k-1}\right] \\
& + \frac{(1-\gamma_2)}{2q_2}\left[\tilde{\boldsymbol{W}}_{2,k}^{\mathrm{T}}(0)\tilde{\boldsymbol{W}}_{2,k}(0) - \tilde{\boldsymbol{W}}_{2,k-1}^{\mathrm{T}}\tilde{\boldsymbol{W}}_{2,k-1}\right] \\
\leq & -V_k(t) + V_k(0) - K\int_0^t s_k^2\mathrm{d}\sigma \\
& - \lambda_{\min}(\boldsymbol{Q})\int_0^t \|\boldsymbol{z}_k\|^2\mathrm{d}\sigma - \int_0^t \left(\frac{\alpha_1\gamma_1}{2q_1} - l\delta^2\right)\tilde{\boldsymbol{W}}_k^{\mathrm{T}}\tilde{\boldsymbol{W}}_k\mathrm{d}\sigma \\
& + \frac{\alpha_1\gamma_1}{2q_1}\int_0^t \left\|\boldsymbol{W}^*\right\|^2\mathrm{d}\sigma + \frac{(1-\gamma_1)}{2q_1}\left[\tilde{\boldsymbol{W}}_k^{\mathrm{T}}(0)\tilde{\boldsymbol{W}}_k(0) - \tilde{\boldsymbol{W}}_{k-1}^{\mathrm{T}}\tilde{\boldsymbol{W}}_{k-1}\right] \\
& + \frac{(1-\gamma_2)}{2q_2}\left[\tilde{\boldsymbol{W}}_{2,k}^{\mathrm{T}}(0)\tilde{\boldsymbol{W}}_{2,k}(0) - \tilde{\boldsymbol{W}}_{2,k-1}^{\mathrm{T}}\tilde{\boldsymbol{W}}_{2,k-1}\right]
\end{aligned} \tag{5.47}$$

Choose suitable parameters such that $\alpha_1\gamma_1/2q_1 - l\delta^2 > 0$, then (5.47) further changes to

$$\Delta E_k(t) \leq -V_k(t) + V_k(0) - K\int_0^t s_k^2\mathrm{d}\sigma$$

$$
\begin{aligned}
& - \lambda_{\min}(\boldsymbol{Q}) \int_0^t \|\boldsymbol{z}_k\|^2 \mathrm{d}\sigma + \frac{\alpha_1 \gamma_1}{2q_1} \int_0^t \left\| \boldsymbol{W}^* \right\|^2 \mathrm{d}\sigma \\
& + \frac{(1-\gamma_1)}{2q_1} \left[\tilde{\boldsymbol{W}}_k^{\mathrm{T}}(0) \tilde{\boldsymbol{W}}_k(0) - \tilde{\boldsymbol{W}}_{k-1}^{\mathrm{T}} \tilde{\boldsymbol{W}}_{k-1} \right] \\
& + \frac{(1-\gamma_2)}{2q_2} \left[\tilde{\boldsymbol{W}}_{2,k}^{\mathrm{T}}(0) \tilde{\boldsymbol{W}}_{2,k}(0) - \tilde{\boldsymbol{W}}_{2,k-1}^{\mathrm{T}} \tilde{\boldsymbol{W}}_{2,k-1} \right]
\end{aligned} \tag{5.48}
$$

According to Assumption 5.2 and Assumption 5.3, we know $V_k(0) = 0$. Letting $t = T$ in (5.48), from $\hat{\boldsymbol{W}}_k(0) = \hat{\boldsymbol{W}}_{k-1}(T)$, $\hat{\boldsymbol{W}}_1(0) = 0$, $\hat{\boldsymbol{W}}_{2,k}(0) = \hat{\boldsymbol{W}}_{2,k-1}(T)$, $\hat{\boldsymbol{W}}_{2,1}(0) = 0$, we can obtain

$$
\begin{aligned}
\Delta E_k(T) &\le -V_k(T) - K \int_0^T s_k^2 \mathrm{d}\sigma - \lambda_{\min}(\boldsymbol{Q}) \int_0^T \|\boldsymbol{z}_k\|^2 \mathrm{d}\sigma + \frac{\alpha_1 \gamma_1}{2q_1} \left\| \boldsymbol{W}^* \right\|^2 T \\
&\le -K \int_0^T s_k^2 \mathrm{d}\sigma - \lambda_{\min}(\boldsymbol{Q}) \int_0^T \|\boldsymbol{z}_k\|^2 \mathrm{d}\sigma + \frac{\alpha_1 \gamma_1}{2q_1} \left\| \boldsymbol{W}^* \right\|^2 T
\end{aligned} \tag{5.49}
$$

(2) The boundedness of $E_k(T)$.

From (5.43) it is clear that

$$
\begin{aligned}
E_1(t) = & \frac{\gamma_1}{2q_1} \int_0^t \tilde{\boldsymbol{W}}_1^{\mathrm{T}} \tilde{\boldsymbol{W}}_1 \mathrm{d}\sigma + \frac{(1-\gamma_1)}{2q_1} \tilde{\boldsymbol{W}}_1^{\mathrm{T}} \tilde{\boldsymbol{W}}_1 \\
& + \frac{\gamma_2}{2q_2} \int_0^t \tilde{\boldsymbol{W}}_{2,1}^{\mathrm{T}} \tilde{\boldsymbol{W}}_{2,1} \mathrm{d}\sigma + \frac{(1-\gamma_2)}{2q_2} \tilde{\boldsymbol{W}}_{2,1}^{\mathrm{T}} \tilde{\boldsymbol{W}}_{2,1}
\end{aligned} \tag{5.50}
$$

Taking the time derivative of $E_1(t)$ it yields

$$
\dot{E}_1(t) = \frac{\gamma_1}{2q_1} \tilde{\boldsymbol{W}}_1^{\mathrm{T}} \tilde{\boldsymbol{W}}_1 + \frac{(1-\gamma_1)}{q_1} \tilde{\boldsymbol{W}}_1^{\mathrm{T}} \dot{\tilde{\boldsymbol{W}}}_1 + \frac{\gamma_2}{2q_2} \tilde{\boldsymbol{W}}_{2,1}^{\mathrm{T}} \tilde{\boldsymbol{W}}_{2,1} + \frac{(1-\gamma_2)}{q_2} \tilde{\boldsymbol{W}}_{2,1}^{\mathrm{T}} \dot{\tilde{\boldsymbol{W}}}_{2,1} \tag{5.51}
$$

Considering parameter adaptive iterative learning laws, we have $(1-\gamma_1)\dot{\hat{\boldsymbol{W}}}_1 = -\gamma_1 \hat{\boldsymbol{W}}_1 - \gamma_1 \alpha_1 \hat{\boldsymbol{W}}_1 + 2q_1 z_{1,1} \boldsymbol{C}^{\mathrm{T}} \left(\boldsymbol{C}\boldsymbol{C}^{\mathrm{T}} + \delta \boldsymbol{I}_n \right)^{-1} \boldsymbol{P}\boldsymbol{B}\boldsymbol{\phi}\left(\hat{\boldsymbol{X}}_1 \right)$, $(1-\gamma)\dot{\hat{\boldsymbol{W}}}_{2,1} = -\gamma \hat{\boldsymbol{W}}_{2,1} + q_2 b \tanh^2\left(s_1 / \eta(t) \right) \boldsymbol{\phi}_2(y_1)$. Therefore we have

$$
\frac{\gamma_1}{2q_1} \tilde{\boldsymbol{W}}_1^{\mathrm{T}} \tilde{\boldsymbol{W}}_1 + \frac{(1-\gamma_1)}{q_1} \tilde{\boldsymbol{W}}_1^{\mathrm{T}} \dot{\tilde{\boldsymbol{W}}}_1 = \frac{\gamma_1}{2q_1} \tilde{\boldsymbol{W}}_1^{\mathrm{T}} \tilde{\boldsymbol{W}}_1 - \frac{\gamma_1}{q_1} \tilde{\boldsymbol{W}}_1^{\mathrm{T}} \hat{\boldsymbol{W}}_1 - \frac{\alpha_1 \gamma_1}{q_1} \tilde{\boldsymbol{W}}_1^{\mathrm{T}} \hat{\boldsymbol{W}}_1
$$

$$
\begin{aligned}
&+ 2z_{1,1}\boldsymbol{C}^{\mathrm{T}}\left(\boldsymbol{C}\boldsymbol{C}^{\mathrm{T}} + \delta\boldsymbol{I}_n\right)^{-1}\boldsymbol{P}\boldsymbol{B}\tilde{\boldsymbol{W}}_1^{\mathrm{T}}\boldsymbol{\phi}\left(\hat{\boldsymbol{X}}_1\right) \\
&= \frac{\gamma_1}{2q_1}\left[\tilde{\boldsymbol{W}}_1^{\mathrm{T}}\tilde{\boldsymbol{W}}_1 - 2\tilde{\boldsymbol{W}}_1^{\mathrm{T}}\hat{\boldsymbol{W}}_1 + \hat{\boldsymbol{W}}_1^{\mathrm{T}}\hat{\boldsymbol{W}}_1\right] - \frac{\gamma_1}{2q_1}\hat{\boldsymbol{W}}_1^{\mathrm{T}}\hat{\boldsymbol{W}}_1 - \frac{\alpha_1\gamma_1}{q_1}\tilde{\boldsymbol{W}}_1^{\mathrm{T}}\hat{\boldsymbol{W}}_1 \\
&+ 2z_{1,1}\boldsymbol{C}^{\mathrm{T}}\left(\boldsymbol{C}\boldsymbol{C}^{\mathrm{T}} + \delta\boldsymbol{I}_n\right)^{-1}\boldsymbol{P}\boldsymbol{B}\tilde{\boldsymbol{W}}_1^{\mathrm{T}}\boldsymbol{\phi}\left(\hat{\boldsymbol{X}}_1\right) \\
&\leq \frac{\gamma_1}{2q_1}\left[\hat{\boldsymbol{W}}_1 - \tilde{\boldsymbol{W}}_1\right]^{\mathrm{T}}\left[\hat{\boldsymbol{W}}_1 - \tilde{\boldsymbol{W}}_1\right] - \frac{\alpha_1\gamma_1}{2q_1}\tilde{\boldsymbol{W}}_1^{\mathrm{T}}\tilde{\boldsymbol{W}}_1 + \frac{\alpha_1\gamma_1}{2q_1}\boldsymbol{W}^{*\mathrm{T}}\boldsymbol{W}^* \\
&+ 2z_{1,1}\boldsymbol{C}^{\mathrm{T}}\left(\boldsymbol{C}\boldsymbol{C}^{\mathrm{T}} + \delta\boldsymbol{I}_n\right)^{-1}\boldsymbol{P}\boldsymbol{B}\tilde{\boldsymbol{W}}_1^{\mathrm{T}}\boldsymbol{\phi}\left(\hat{\boldsymbol{X}}_1\right) \\
&\leq (1+\alpha_1)\frac{\gamma_1}{2q_1}\boldsymbol{W}^{*\mathrm{T}}\boldsymbol{W}^* \\
&+ 2z_{1,1}\boldsymbol{C}^{\mathrm{T}}\left(\boldsymbol{C}\boldsymbol{C}^{\mathrm{T}} + \delta\boldsymbol{I}_n\right)^{-1}\boldsymbol{P}\boldsymbol{B}\tilde{\boldsymbol{W}}_1^{\mathrm{T}}\boldsymbol{\phi}\left(\hat{\boldsymbol{X}}_1\right) - \frac{\alpha_1\gamma_1}{2q_1}\tilde{\boldsymbol{W}}_1^{T}\tilde{\boldsymbol{W}}_1
\end{aligned}
\tag{5.52}
$$

$$
\begin{aligned}
&\frac{\gamma}{2q_2}\tilde{\boldsymbol{W}}_{2,1}^{\mathrm{T}}\tilde{\boldsymbol{W}}_{2,1} + \frac{(1-\gamma)}{q_2}\tilde{\boldsymbol{W}}_{2,1}^{\mathrm{T}}\dot{\tilde{\boldsymbol{W}}}_{2,1} = \frac{\gamma}{2q_2}\tilde{\boldsymbol{W}}_{2,1}^{\mathrm{T}}\tilde{\boldsymbol{W}}_{2,1} - \frac{\gamma}{q_2}\tilde{\boldsymbol{W}}_{2,1}^{\mathrm{T}}\hat{\boldsymbol{W}}_{2,1} \\
&\quad + b\tanh^2\left(s_1/\eta(t)\right)\tilde{\boldsymbol{W}}_{2,1}^{\mathrm{T}}\boldsymbol{\phi}_2(y_1) \\
&\quad = \frac{\gamma}{2q_2}\left[\tilde{\boldsymbol{W}}_{2,1}^{\mathrm{T}}\tilde{\boldsymbol{W}}_{2,1} - 2\tilde{\boldsymbol{W}}_{2,1}^{\mathrm{T}}\hat{\boldsymbol{W}}_{2,1} + \hat{\boldsymbol{W}}_{2,1}^{\mathrm{T}}\hat{\boldsymbol{W}}_{2,1}\right] \\
&\quad - \frac{\gamma}{2q_2}\hat{\boldsymbol{W}}_{2,1}^{\mathrm{T}}\hat{\boldsymbol{W}}_{2,1} + b\tanh^2\left(s_1/\eta(t)\right)\tilde{\boldsymbol{W}}_{2,1}^{\mathrm{T}}\boldsymbol{\phi}_2(y_1) \\
&\quad \leq \frac{\gamma}{2q_2}\left[\hat{\boldsymbol{W}}_{2,1} - \tilde{\boldsymbol{W}}_{2,1}\right]^{\mathrm{T}}\left[\hat{\boldsymbol{W}}_{2,1} - \tilde{\boldsymbol{W}}_{2,1}\right] \\
&\quad + b\tanh^2\left(s_1/\eta(t)\right)\tilde{\boldsymbol{W}}_{2,1}^{\mathrm{T}}\boldsymbol{\phi}_2(y_1) \\
&\quad = \frac{\gamma}{2q_2}\boldsymbol{W}_2^{*\mathrm{T}}\boldsymbol{W}_2^* + b\tanh^2\left(s_1/\eta(t)\right)\tilde{\boldsymbol{W}}_{2,1}^{\mathrm{T}}\boldsymbol{\phi}_2(y_1)
\end{aligned}
\tag{5.53}
$$

Considering above two inequalities, $\dot{E}_1(t)$ becomes

$$
\begin{aligned}
\dot{E}_1(t) &\leq (1+\alpha_1)\frac{\gamma_1}{2q_1}\boldsymbol{W}^{*\mathrm{T}}\boldsymbol{W}^* + \frac{\gamma}{2q_2}\boldsymbol{W}_2^{*\mathrm{T}}\boldsymbol{W}_2^* \\
&\quad + 2z_{1,1}\boldsymbol{C}^{\mathrm{T}}\left(\boldsymbol{C}\boldsymbol{C}^{\mathrm{T}} + \delta\boldsymbol{I}_n\right)^{-1}\boldsymbol{P}\boldsymbol{B}\tilde{\boldsymbol{W}}_1^{\mathrm{T}}\boldsymbol{\phi}\left(\hat{\boldsymbol{X}}_1\right) \\
&\quad + b\tanh^2\left(s_1/\eta(t)\right)\tilde{\boldsymbol{W}}_{2,1}^{\mathrm{T}}\boldsymbol{\phi}_2(y_1) - \frac{\alpha_1\gamma_1}{2q_1}\tilde{\boldsymbol{W}}_1^{T}\tilde{\boldsymbol{W}}_1 \\
&\leq -\dot{V}_1 - \lambda_{\min}(\boldsymbol{Q})\|\boldsymbol{z}_1\|^2 - Ks_1^2 + (1+\alpha_1)\frac{\gamma_1}{2q_1}\boldsymbol{W}^{*\mathrm{T}}\boldsymbol{W}^* \\
&\quad + \frac{\gamma}{2q_2}\boldsymbol{W}_2^{*\mathrm{T}}\boldsymbol{W}_2^* - \left(\frac{\alpha_1\gamma_1}{2q_1} - l\delta^2\right)\tilde{\boldsymbol{W}}_1^{T}\tilde{\boldsymbol{W}}_1 \\
&\leq -\dot{V}_1 - \lambda_{\min}(\boldsymbol{Q})\|\boldsymbol{z}_1\|^2 - Ks_1^2 + (1+\alpha_1)\frac{\gamma_1}{2q_1}\boldsymbol{W}^{*\mathrm{T}}\boldsymbol{W}^* + \frac{\gamma}{2q_2}\boldsymbol{W}_2^{*\mathrm{T}}\boldsymbol{W}_2^*
\end{aligned}
\tag{5.54}
$$

For convenience of expression, denote $c = (1+\alpha_1)\frac{\gamma_1}{2q_1}\boldsymbol{W}^{*\mathrm{T}}\boldsymbol{W}^* + \frac{\gamma}{2q_2}\boldsymbol{W}_2^{*\mathrm{T}}\boldsymbol{W}_2^*$. Integrating (5.54) over $[0, t]$ leads to

$$E_1(t) - E_1(0) \le -V_1(t) + V_1(0) - \lambda_{\min}(\boldsymbol{Q})\int_0^t \|z_1\|^2 \mathrm{d}\sigma - \int_0^t K s_1^2(\sigma)\mathrm{d}\sigma + ct \tag{5.55}$$

From $\hat{\boldsymbol{W}}_1(0) = \hat{\boldsymbol{W}}_{2,1}(0) = 0$ it is clear that

$$\begin{aligned} E_1(0) &= \frac{(1-\gamma_1)}{2q_1}\tilde{\boldsymbol{W}}_1^{\mathrm{T}}(0)\tilde{\boldsymbol{W}}_1(0) + \frac{(1-\gamma_2)}{2q_2}\tilde{\boldsymbol{W}}_{2,1}^{\mathrm{T}}(0)\tilde{\boldsymbol{W}}_{2,1}(0) \\ &= \frac{(1-\gamma_1)}{2q_1}\left\|\boldsymbol{W}^*\right\|^2 + \frac{(1-\gamma_2)}{2q_2}\left\|\boldsymbol{W}_2^*\right\|^2 \end{aligned} \tag{5.56}$$

So we have

$$E_1(t) \le ct + \frac{(1-\gamma_1)}{2q_1}\left\|\boldsymbol{W}^*\right\|^2 + \frac{(1-\gamma_2)}{2q_2}\left\|\boldsymbol{W}_2^*\right\|^2, t \in [0, T] \tag{5.57}$$

Therefore, $E_1(t)$ is bounded on $[0, T]$. Letting $t = T$ in above inequality, we can obtain the boundedness of $E_1(T)$:

$$E_1(T) \le cT + \frac{(1-\gamma_1)}{2q_1}\left\|\boldsymbol{W}^*\right\|^2 + \frac{(1-\gamma_2)}{2q_2}\left\|\boldsymbol{W}_2^*\right\|^2 < \infty \tag{5.58}$$

Choose $\alpha_1 = \Delta_k$ with $\{\Delta_k\}$ as a convergent sequence. Here we determine $\Delta_k = \frac{q}{k^p}$, where p and q are design parameters satisfying $q(\in R) > 0$, $p(\in Z_+) \ge 2$. Δ_k has the following property.

Property 5.1 $\lim_{k\to\infty} \sum\limits_{j=1}^{k} \Delta_j \le 2q$.

Proof When $j-1 \le x \le j$, $\frac{1}{j^p} \le \frac{1}{x^p}$. So we have

$$\frac{1}{j^p} = \int_{j-1}^{j} \frac{1}{j^p}\mathrm{d}x \le \int_{j-1}^{j} \frac{1}{x^p}\mathrm{d}x, \quad (j = 2, 3, \ldots)$$

Then the partial sum of the series $\left(1 + \frac{1}{2^p} + \cdots + \frac{1}{k^p} + \cdots\right)$ is bounded by

$$S_k = 1 + \sum_{j=2}^{k} \frac{1}{j^p} \le 1 + \sum_{j=2}^{k} \int_{j-1}^{j} \frac{1}{x^p}\mathrm{d}x$$

$$= 1 + \int_1^k \frac{1}{x^p} \mathrm{d}x = 1 + \frac{1}{p-1}\left(1 - \frac{1}{k^{p-1}}\right) < 1 + \frac{1}{p-1}$$
$$(k = 2, 3, \ldots)$$

Obviously, the sequence $\{S_k\}$ is bounded. Since $p(\in Z_+) \geq 2$, then it is clear that $\lim_{k\to\infty} \sum_{j=1}^{k} \Delta_j \leq 2q$.

Adding Eq. (5.49) repeatedly yields

$$\begin{aligned} E_k(T) &= E_1(T) + \sum_{j=2}^{k} \Delta E_j(T) \\ &\leq E_1(T) - K \sum_{j=2}^{k} \int_0^T s_j^2 \mathrm{d}\sigma - \lambda_{\min}(Q) \sum_{j=2}^{k} \int_0^T \left\| z_j \right\|^2 \mathrm{d}\sigma \\ &+ \frac{\gamma_1}{2q_1} T \left\| W^* \right\|^2 \sum_{j=2}^{k} \Delta_k \end{aligned} \tag{5.59}$$

According to Property 5.1 we can know $\sum_{j=1}^{k} \Delta_k \leq \lim_{k\to\infty} \sum_{j=1}^{k} \Delta_k \leq 2q$, consequently, $E_k(T)$ is bounded.

(3) The boundedness of $E_k(t)$.

Next we will prove the boundedness of by induction method. Firstly, we separate $E_k(t)$ into two parts

$$E_k^1(t) = \frac{\gamma_1}{2q_1} \int_0^t \tilde{W}_k^{\mathrm{T}} \tilde{W}_k \mathrm{d}\sigma + \frac{\gamma_2}{2q_2} \int_0^t \tilde{W}_{2,k}^{\mathrm{T}} \tilde{W}_{2,k} \mathrm{d}\sigma \tag{5.60}$$

$$E_k^2(t) = \frac{(1-\gamma_1)}{2q_1} \tilde{W}_k^{\mathrm{T}} \tilde{W}_k + \frac{(1-\gamma_2)}{2q_2} \tilde{W}_{2,k}^{\mathrm{T}} \tilde{W}_{2,k} \tag{5.61}$$

The boundedness of $E_k(T)$ is guaranteed for all iterations. Consequently, for all $\forall k \in N$, there exist two constants M_1 and M_2 satisfying

$$E_k^1(t) \leq E_k^1(T) \leq M_1 < \infty \tag{5.62}$$

$$E_k^2(T) \leq M_2 \tag{5.63}$$

Then, we have

$$E_k(t) = E_k^1(t) + E_k^2(t) \leq M_1 + E_k^2(t) \tag{5.64}$$

On the other hand, from (5.48) it follows

$$\begin{aligned}\Delta E_{k+1}(t) &< \frac{\Delta_k \gamma_1}{2q_1} \int_0^t \left\| \boldsymbol{W}^* \right\|^2 \mathrm{d}\sigma + \frac{(1-\gamma_1)}{2q_1}\left[\tilde{\boldsymbol{W}}_k^{\mathrm{T}}(0)\tilde{\boldsymbol{W}}_k(0) - \tilde{\boldsymbol{W}}_{k-1}^{\mathrm{T}}\tilde{\boldsymbol{W}}_{k-1}\right] \\ &+ \frac{(1-\gamma_2)}{2q_2}\left[\tilde{\boldsymbol{W}}_{2,k}^{\mathrm{T}}(0)\tilde{\boldsymbol{W}}_{2,k}(0) - \tilde{\boldsymbol{W}}_{2,k-1}^{\mathrm{T}}\tilde{\boldsymbol{W}}_{2,k-1}\right] \\ &\leq \frac{\Delta_k \gamma_1}{2q_1} \int_0^t \left\| \boldsymbol{W}^* \right\|^2 \mathrm{d}\sigma + M_2 - E_k^2(t) \end{aligned} \tag{5.65}$$

Combining (5.64) and (5.65) results in

$$E_{k+1}(t) = E_k(t) + \Delta E_{k+1}(t) \leq M_1 + M_2 + \frac{\Delta_k \gamma_1}{2q_1} \int_0^t \left\| \boldsymbol{W}^* \right\|^2 \mathrm{d}\sigma \tag{5.66}$$

As we have got the boundedness of $E_1(t)$, therefore $E_k(t)$ is finite according to induction principle. Furthermore, we can obtain the boundedness of $\hat{\boldsymbol{W}}_k$ and $\hat{\boldsymbol{W}}_{2,k}$.

(4) Learning convergence property

From (5.59) it is followed by

$$\begin{aligned}\sum_{j=2}^{k} \int_0^T s_j^2 \mathrm{d}\sigma &\leq \frac{1}{K}\left(E_1(T) - E_k(T) + \frac{\gamma_1 T}{2q_1}\left\| \boldsymbol{W}^* \right\|^2 \sum_{j=2}^{k} \Delta_k\right) \\ &\leq \frac{1}{K}\left(E_1(T) + \frac{\gamma_1 T}{2q_1}\varepsilon_W^2 \sum_{j=2}^{k} \Delta_k\right) \end{aligned} \tag{5.67}$$

$$\lim_{k\to\infty} \sum_{j=2}^{k} \int_0^T \left\| \boldsymbol{z}_j \right\|^2 \mathrm{d}\sigma \leq \frac{1}{\lambda_{\min}(\boldsymbol{Q})}\left(E_1(T) + \frac{\gamma_1 T}{2q_1}\varepsilon_W^2 \sum_{j=2}^{k} \Delta_k\right) \tag{5.68}$$

Taking the limitation of the above two inequalities leads to

$$\begin{aligned}\lim_{k\to\infty} \sum_{j=2}^{k} \int_0^T s_j^2(\sigma) \mathrm{d}\sigma &\leq \lim_{k\to\infty} \frac{1}{K}\left(E_1(T) + \frac{\gamma_1 T}{2q_1}\varepsilon_W^2 \sum_{j=2}^{k} \Delta_k\right) \\ &= \frac{1}{K}\left(E_1(T) + \frac{\gamma_1 T q}{q_1}\varepsilon_W^2\right) \end{aligned} \tag{5.69}$$

$$\lim_{k\to\infty}\sum_{j=2}^{k}\int_0^T \left\|z_j\right\|^2 \mathrm{d}\sigma \le \frac{1}{\lambda_{\min}(\boldsymbol{Q})}\left(E_1(T)+\frac{\gamma_1 T q}{q_1}\varepsilon_W^2\right) \tag{5.70}$$

Since $E_1(T)$ is bounded, according to the convergence theorem of the sum of series we have $\lim\limits_{k\to\infty}\int_0^T s_k^2(\sigma)\mathrm{d}\sigma = 0$, $\lim\limits_{k\to\infty}\int_0^T \|z_k\|^2\mathrm{d}\sigma = 0$. Obviously, $\lim\limits_{k\to\infty}\int_0^T \left(y_k-\hat{y}_k\right)^2\mathrm{d}\sigma \le \lim\limits_{k\to\infty}\int_0^T \|z_k\|^2\mathrm{d}\sigma = 0$, $\forall t \in [0,T]$. Additionally, $\lim\limits_{k\to\infty}\int_0^T s_k^2(\sigma)\mathrm{d}\sigma = 0$ means $\lim\limits_{k\to\infty}\int_0^T |s_k(\sigma)|\mathrm{d}\sigma = 0$ which implies that $\lim\limits_{k\to\infty}\int_0^T |e_{sk}(\sigma)|\mathrm{d}\sigma \le \int_0^T \eta(\sigma)\mathrm{d}\sigma$, $\lim\limits_{k\to\infty}\int_0^T (e_{sk}(\sigma))^2\mathrm{d}\sigma \le \int_0^T \eta^2(\sigma)\mathrm{d}\sigma$. From $\int_0^t s_k^2(\sigma)\mathrm{d}\sigma \le \int_0^T s_k^2(\sigma)\mathrm{d}\sigma$ and $\int_0^t \|z_k(\sigma)\|^2\mathrm{d}\sigma \le \int_0^T \|z_k(\sigma)\|^2\mathrm{d}\sigma$, it is known that $s_k(t)$ and $\|z_k\|$ are bounded in L_T^2-norm, which shows that $x_k(t)$ and $\hat{x}_k(t)$ are bounded as well. Based on above reasoning, we arrive at the fact that $v_k(t)$ is bounded.

Synthesizing the discussions in two cases, we can draw the conclusion that, for two cases, the proposed control algorithm is able to guarantee that all closed-loop signals are bounded, $\lim\limits_{k\to\infty}\int_0^T \|z_k\|^2\mathrm{d}\sigma = 0$, $\lim\limits_{k\to\infty}\int_0^T (e_{sk})^2\mathrm{d}\sigma \le \varepsilon_e$, $\varepsilon_e = \int_0^T ((1+m)\eta_1(\sigma))^2\mathrm{d}\sigma = \frac{1}{2K}(1+m)^2\varepsilon^2\left(1-e^{-2KT}\right) \le \frac{1}{2K}(1+m)^2\varepsilon^2 = \varepsilon_{esk}$. Furthermore, the bound of $e_{s\infty}(t)$ will satisfy $\lim\limits_{k\to\infty}|e_{sk}(t)| = e_{s\infty}(t) = (1+m)\varepsilon e^{-Kt}$, $\forall t \in [0,T]$.

(5) Transient Performance

Define the vector $\boldsymbol{\zeta}_k(t) = \left[e_{1,k}(t), e_{2,k}(t), \ldots, e_{n-1,k}(t)\right]^{\mathrm{T}}$, then the dynamical equation of $\boldsymbol{\zeta}_k(t)$ can be express as

$$\dot{\boldsymbol{\zeta}}_k(t) = \boldsymbol{A}_s\boldsymbol{\zeta}_k(t) + \boldsymbol{b}_s e_{sk}(t) + \boldsymbol{K}_s z_{1,k} \tag{5.71}$$

where,

$$\boldsymbol{A}_s = \begin{bmatrix} 0 & 1 & \cdots & 0 \\ \vdots & \vdots & \ddots & \vdots \\ 0 & 0 & \cdots & 1 \\ -\lambda_1 & -\lambda_2 & \cdots & -\lambda_{n-1} \end{bmatrix} \in \mathbf{R}^{(n-1)\times(n-1)},\ \boldsymbol{b}_s = \begin{bmatrix} 0 \\ \vdots \\ 0 \\ 1 \end{bmatrix} \in \mathbf{R}^{n-1},\ \boldsymbol{K}_s = \begin{bmatrix} k_1 \\ \vdots \\ k_{n-1} \end{bmatrix}$$

with $\boldsymbol{A}_s$ being a stable matrix. In addition, there are two constants $k_0 > 0$ and $\lambda_0 > 0$ such that $\left\|\mathrm{e}^{\boldsymbol{A}_s t}\right\| \le k_0\mathrm{e}^{-\lambda_0 t}$. The solution of $\dot{\boldsymbol{\zeta}}_k(t)$ is

$$\boldsymbol{\zeta}_k(t) = e^{\boldsymbol{A}_s t}\boldsymbol{\zeta}_k(0) + \int_0^t \mathrm{e}^{\boldsymbol{A}_s(t-\sigma)}\boldsymbol{b}_s e_{sk}(\sigma)\mathrm{d}\sigma + \int_0^t \mathrm{e}^{\boldsymbol{A}_s(t-\sigma)}\boldsymbol{K}_s z_{1,k}(\sigma)\mathrm{d}\sigma \tag{5.72}$$

Consequently, we have

$$\begin{aligned}\left\|\boldsymbol{\zeta}_k(t)\right\| \le k_0\left\|\boldsymbol{\zeta}_k(0)\right\|\mathrm{e}^{-\lambda_0 t} + k_0\int_0^t \mathrm{e}^{-\lambda_0(t-\sigma)}|e_{sk}(\sigma)|\mathrm{d}\sigma \\ + k_0\|\boldsymbol{K}_s\|\int_0^t \mathrm{e}^{-\lambda_0(t-\sigma)}\left|z_{1,k}(\sigma)\right|\mathrm{d}\sigma\end{aligned} \tag{5.73}$$

If we choose suitable parameters such that $\lambda_0 > K$, then from $\lim_{k\to\infty}|e_{sk}(t)| \le (1+m)\eta(t)$, we can know

$$\begin{aligned}\left\|\boldsymbol{\zeta}_\infty(t)\right\| &= k_0\left\|\boldsymbol{\zeta}_\infty(0)\right\|e^{-\lambda_0 t} + k_0\int_0^t \mathrm{e}^{-\lambda_0(t-\sigma)}|e_{s\infty}(\sigma)|\mathrm{d}\sigma \\ &\quad + k_0\|\boldsymbol{K}_s\|\int_0^t \mathrm{e}^{-\lambda_0(t-\sigma)}\left|z_{1,\infty}(\sigma)\right|\mathrm{d}\sigma \\ &\le k_0\left\|\boldsymbol{\zeta}_\infty(0)\right\| + (1+m)\varepsilon k_0\int_0^t \mathrm{e}^{-\lambda_0(t-\sigma)}e^{-K\sigma}\mathrm{d}\sigma + 0 \\ &= k_0\left\|\boldsymbol{\zeta}_\infty(0)\right\| + (1+m)\varepsilon k_0\frac{1}{\lambda_0 - K}\left(\mathrm{e}^{-Kt} - \mathrm{e}^{-\lambda_0 t}\right) \\ &\le k_0\left\|\boldsymbol{\zeta}_\infty(0)\right\| + \frac{1}{\lambda_0 - K}(1+m)\varepsilon k_0\end{aligned} \tag{5.74}$$

Noting $e_{sk}(t) = \left[\boldsymbol{\Lambda}^{\mathrm{T}} \quad 1\right]\boldsymbol{e}_k(t)$ and $\boldsymbol{e}_k(t) = \left[\boldsymbol{\zeta}_k^{\mathrm{T}}(t)\ e_{n,k}(t)\right]^{\mathrm{T}}$, we may further obtain

$$\begin{aligned}\|\boldsymbol{e}_k(t)\| &\le \left\|\boldsymbol{\zeta}_k(t)\right\| + \left|e_{n,k}(t)\right| \\ &= \left\|\boldsymbol{\zeta}_k(t)\right\| + \left|e_{sk}(t) - \boldsymbol{\Lambda}^T\boldsymbol{\zeta}_k(t)\right| \\ &\le (1+\|\boldsymbol{\Lambda}\|)\left\|\boldsymbol{\zeta}_k(t)\right\| + |e_{sk}(t)|\end{aligned} \tag{5.75}$$

Considering above two inequalities, we can obtain

$$\begin{aligned}\|\boldsymbol{e}_\infty(t)\| &\le (1+\|\boldsymbol{\Lambda}\|)\left\|\boldsymbol{\zeta}_\infty(t)\right\| + |e_{s\infty}(t)| \\ &\le (1+\|\Lambda\|)\left(k_0\left\|\boldsymbol{\zeta}_\infty(0)\right\| + \frac{1}{\lambda_0 - K}(1+m)\varepsilon k_0\right) + (1+m)\eta(t) \\ &\le (1+\|\boldsymbol{\Lambda}\|)\left(k_0\sum_{i=1}^{n-1}\sqrt{\varepsilon_i^2} + \frac{1}{\lambda_0 - K}(1+m)\varepsilon k_0\right) + (1+m)\eta(t)\end{aligned} \tag{5.76}$$

Since $\boldsymbol{\zeta}_k(t) = \left[e_{1,k}(t), e_{2,k}(t), \ldots, e_{n-1,k}(t)\right]^{\mathrm{T}}$, then it is clear that

$$\left|e_{1,k}(t)\right| \leq \left\|\boldsymbol{\zeta}_k(t)\right\| \leq k_0\left\|\boldsymbol{\zeta}_k(0)\right\|\mathrm{e}^{-\lambda_0 t} + k_0\int\limits_0^t \mathrm{e}^{-\lambda_0(t-\sigma)}|e_{sk}(\sigma)|\mathrm{d}\sigma \tag{5.77}$$

When $k \to \infty$, it can be shown that

$$\begin{aligned}
\left|e_{1,\infty}(t)\right| &\leq \left\|\boldsymbol{\zeta}_\infty(t)\right\| \\
&\leq k_0\left\|\boldsymbol{\zeta}_\infty(0)\right\|\mathrm{e}^{-\lambda_0 t} + k_0\int\limits_0^t e^{-\lambda_0(t-\sigma)}|e_{s\infty}(\sigma)|\mathrm{d}\sigma \\
&\leq k_0\left\|\boldsymbol{\zeta}_\infty(0)\right\|\mathrm{e}^{-\lambda_0 t} + (1+m)\varepsilon k_0\int\limits_0^t e^{-\lambda_0(t-\sigma)}\mathrm{e}^{-K\sigma}\mathrm{d}\sigma \\
&= k_0\left\|\boldsymbol{\zeta}_\infty(0)\right\|\mathrm{e}^{-\lambda_0 t} + (1+m)\varepsilon k_0\frac{1}{\lambda_0 - K}\left(\mathrm{e}^{-Kt} - \mathrm{e}^{-\lambda_0 t}\right) \\
&\leq k_0\sum_{i=1}^{n-1}\sqrt{\varepsilon_i^2}e^{-\lambda_0 t} + (1+m)\varepsilon k_0\frac{1}{\lambda_0 - K}\left(e^{-Kt} - e^{-\lambda_0 t}\right)
\end{aligned} \tag{5.78}$$

Define $\boldsymbol{\chi}_k = \left[\chi_{1,k}, \ldots, \chi_{n,k}\right]^{\mathrm{T}} = \boldsymbol{X}_k - \boldsymbol{X}_d$, then it is clear that $\boldsymbol{\chi}_k = z_k + \boldsymbol{e}_k$. From $\lim\limits_{k\to\infty}\int_0^T \|z_k\|^2\mathrm{d}\sigma = 0$ we have $\lim\limits_{k\to\infty}\|z_k(t)\| = 0$, that is, $\|z_\infty(t)\| = 0$, $t \in [0, T]$. Consequently, it is obvious that

$$\begin{aligned}
\left\|\boldsymbol{\chi}_\infty\right\| &\leq \|z_\infty\| + \|\boldsymbol{e}_\infty\| \\
&\leq (1 + \|\boldsymbol{\Lambda}\|)\left(k_0\sum_{i=1}^{n-1}\sqrt{\varepsilon_i^2} + \frac{1}{\lambda_0 - K}(1+m)\varepsilon k_0\right) + (1+m)\eta(t)
\end{aligned} \tag{5.79}$$

$$\begin{aligned}
\left|\chi_{1,\infty}\right| &= |y_\infty - y_d| \\
&\leq \left|z_{1,\infty}\right| + \left|e_{1,\infty}\right| \\
&\leq k_0\sum_{i=1}^{n-1}\sqrt{\varepsilon_i^2}\mathrm{e}^{-\lambda_0 t} + (1+m)\varepsilon k_0\frac{1}{\lambda_0 - K}\left(\mathrm{e}^{-Kt} - \mathrm{e}^{-\lambda_0 t}\right)
\end{aligned} \tag{5.80}$$

This concludes the proof. □

5.3.4 Simulation Analysis

In this section, we present a simulation example to verify the effectiveness of proposed control scheme. Consider the following second-order nonlinear time delay system with input saturation:

$$\begin{cases} \dot{x}_{1,k}(t) = x_{2,k}(t) \\ \dot{x}_{2,k}(t) = f(\boldsymbol{X}_k(t)) + h\big(\boldsymbol{y}_{\tau,k}(t), t\big) + u_k(v_k) + d(t) \\ y_k(t) = x_{1,k}(t) \end{cases} \tag{5.81}$$

where,

$$f(\boldsymbol{X}_k(t)) = -x_{1,k}(t)x_{2,k}(t)\sin\big(x_{1,k}(t)x_{2,k}(t)\big)$$

$$h\big(\boldsymbol{y}_{\tau,k}, t\big) = 0.5\sin(t)\mathrm{e}^{-|\cos(0.5t)|}\big(y_{\tau_{1,k}}\sin\big(y_{\tau_{1,k}}\big) + y_{\tau_{2,k}}\sin\big(y_{\tau_{2,k}}\big)\big)$$

The unknown time-varying delays and external disturbance are as same as those in Chap. 4. We choose $Q = \begin{bmatrix} 0.001 & 0 \\ 0 & 0.002 \end{bmatrix}$. By using Matlab LMI toolbox, we can obtain $K_0 = [3.2894, 2.9764]^{\mathrm{T}}$ and $P = \begin{bmatrix} 0.4741 & -0.2848 \\ -0.2848 & 0.4741 \end{bmatrix}$.

5.3.4.1 The Verification of State Observer Based AILC Scheme

To demonstrate the conclusions in Theorem 5.1, we carry on the following two simulation experiments.

Experiment 1 The desired reference trajectory vector is chosen as $\boldsymbol{X}_d(t) = [\sin t, \cos t]^{\mathrm{T}}$. The design parameters are chosen as $\varepsilon_1 = \varepsilon_2 = 1$, $\lambda = 2$, $K = 2$, $\gamma_1 = \gamma_2 = 0.5$, $\alpha_1 = 0.03 \times 1/k^2$, $q_1 = 0.5$, $q_1 = 0.5$, $q_2 = 1$, $\varepsilon = \lambda\varepsilon_1 + \varepsilon_2 = 3$. The upper bound of saturation input is $u_M = 1.3$. The parameters of two NNs are given by $l = 30$, $\mu_j = \frac{1}{l}(2j - l)[2, 3, 2, 3, 3]^{\mathrm{T}}$, $\sigma_j = 1.5$, $j = 1, 2, \ldots, l$; $l_\Xi = 15$, s, $\sigma_{\Xi j} = 1$, $j = 1, 2, \ldots, l_\Xi$. The initial conditions for $x_{1,k}(0)$ and $x_{2,k}(0)$ are generated on the intervals $[-0.5, 0.5]$ and $[0.5, 1.5]$, respectively. The systems run on $[0, 4\pi]$ for five times. Part simulation results are presented in Figs. 5.3, 5.4, 5.5, 5.6, 5.7, 5.8, 5.9 and 5.10.

Figures 5.3 and 5.6 show the trajectories of the observer output and the desired reference signal of the first iteration and the tenth iteration, respectively; Figs. 5.4 and 5.7 present the trajectories of $x_{1,k}$ and $\hat{x}_{1,k}$. It can be seen that the proposed scheme is able to estimate the system states accurately and steer the system output to track the desired trajectory, which implies achieving the control objective. By comparing the simulation results of the first iteration and the tenth iteration, we can conclude that the tracking performance is improved via iterative learning, which is shown clearly by the curves of $\int_0^T z_{1,k}^2(t)\mathrm{d}t$ and $\int_0^T s_k^2(t)\mathrm{d}t$ in Figs. 5.9 and 5.10. Figures 5.5 and 5.8 show the control curves of the first iteration and the tenth iteration, respectively, which show the boundedness of control signals and the influence of saturation.

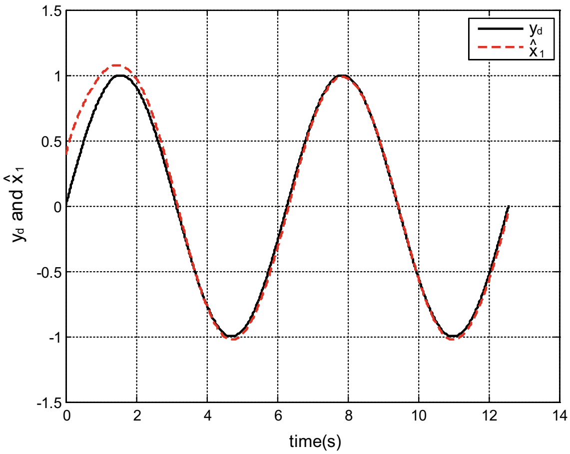

Fig. 5.3 $\hat{x}_{1,k}$ versus y_d ($k = 1$)

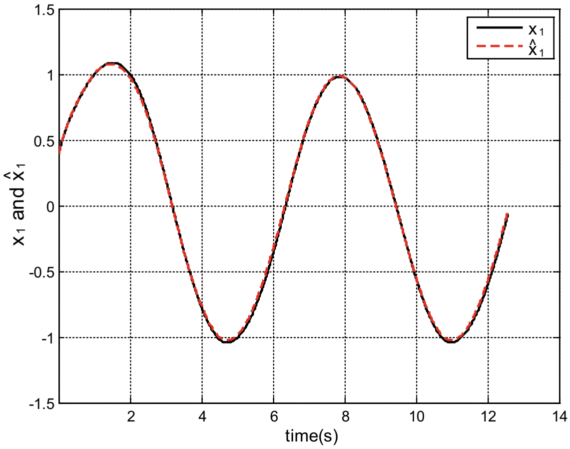

Fig. 5.4 $x_{1,k}$ versus $\hat{x}_{1,k}$ ($k = 1$)

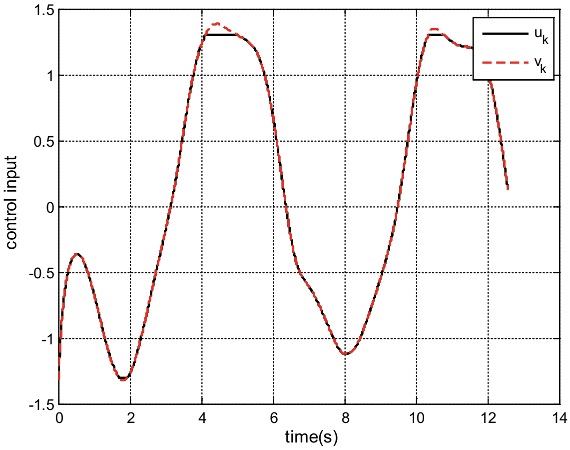

Fig. 5.5 The input v_k and output u_k of saturation ($k = 1$)

Fig. 5.6 $\hat{x}_{1,k}$ versus y_d ($k = 10$)

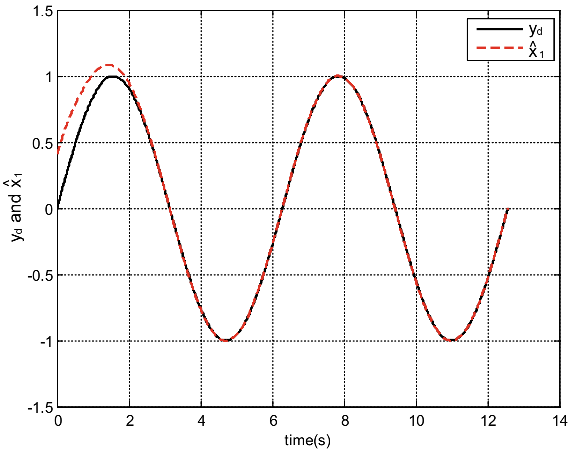

Fig. 5.7 $x_{1,k}$ versus $\hat{x}_{1,k}$ ($k = 10$)

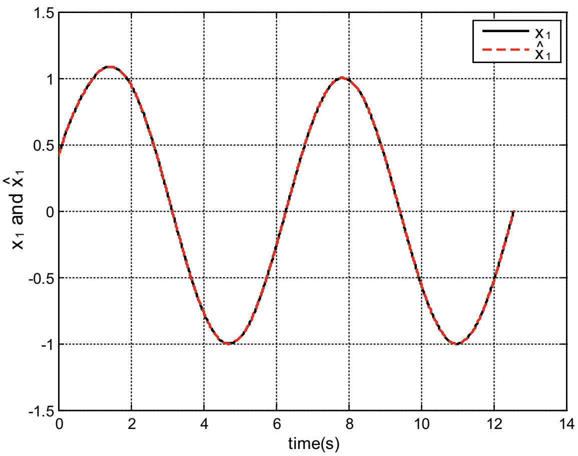

Experiment 2 To show the control performance for more complicated desired trajectory, we choose the desired trajectory as $\boldsymbol{X}_d(t) = [\sin t + \sin(0.5t), \cos t + 0.5\cos(0.5t)]^{\mathrm{T}}$. The control parameters remain the same as those in Experiment 1. The control input is bounded by $u_M = 4$. The system runs on the finite time interval $[0, 8\pi]$ for ten iterations. The simulation results are presented in Figs. 5.11, 5.12, 5.13, 5.14, 5.15, 5.16, 5.17 and 5.18.

From the simulation curves of the first iteration in Figs. 5.11 and 5.12, it is clear that we can't obtain satisfactory tracking performance and state observer estimation effect. Through nine times of learning, the control performance has been improved greatly in the tenth iteration in Figs. 5.14 and 5.15. In other words, it has achieved the control objective.

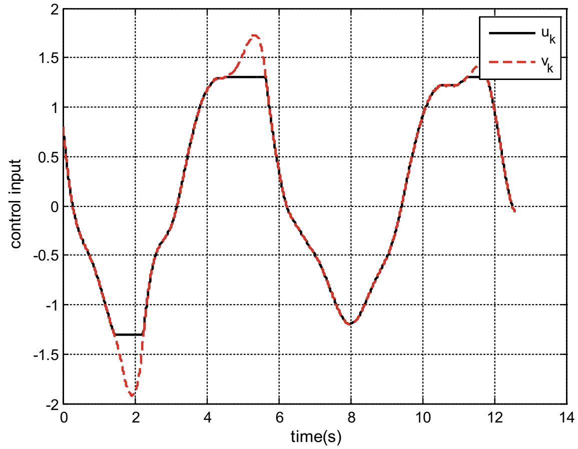

Fig. 5.8 The input v_k and output u_k of saturation ($k = 10$)

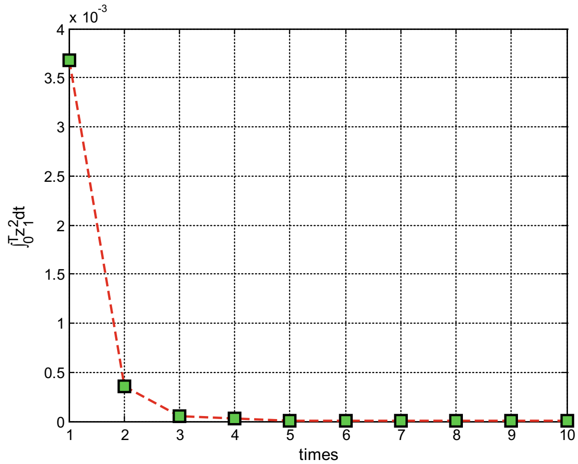

Fig. 5.9 $\int_0^T z_{1,k}^2(t)\mathrm{d}t$ versus the number of iterations

5.3.4.2 Comparison Analysis: State Observer Based Adaptive NN Control

Experiment 3 Finally, the contribution of the proposed observer based AILC scheme is shown by comparing the proposed controller with traditional adaptive neural network controller. The form of controller is as same as the proposed scheme, but the adaptive laws using σ-modification for NN weights are given by

$$\dot{\hat{\boldsymbol{W}}} = \boldsymbol{\Gamma}_W\left(2q_1 z_{1,k}\boldsymbol{C}^{\mathrm{T}}\left(\boldsymbol{C}\boldsymbol{C}^{\mathrm{T}} + \delta\boldsymbol{I}_n\right)^{-1}\boldsymbol{P}\boldsymbol{B}\boldsymbol{\phi}\left(\hat{\boldsymbol{X}}_k\right) - \delta_W\hat{\boldsymbol{W}}\right)$$

$$\dot{\hat{\boldsymbol{W}}}_2 = q_2 s_k \boldsymbol{\phi}_2(y_k) - \gamma\hat{\boldsymbol{W}}_2$$

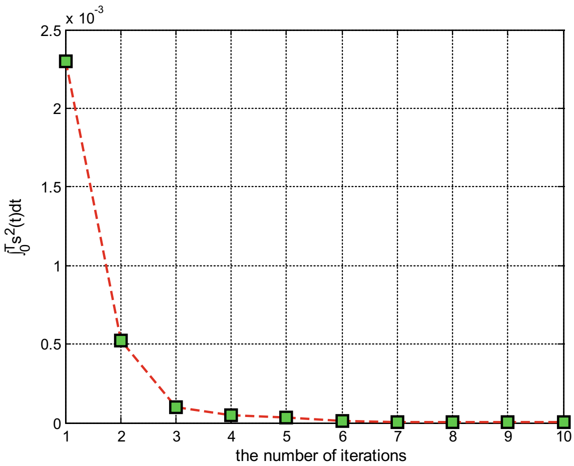

Fig. 5.10 $\int_0^T s_k^2(t)\mathrm{d}t$ versus the number of iterations

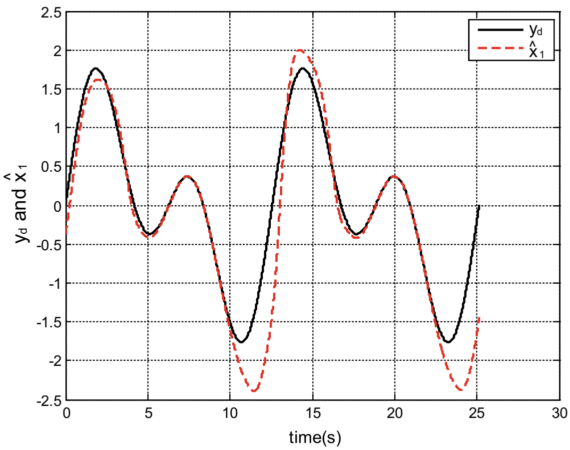

Fig. 5.11 $\hat{x}_{1,k}$ versus y_d (k = 1)

The design parameters are chosen as $\Gamma_W = \mathrm{diag}\{0.2\}$, $\delta_W = 0.5$, $q_2 = 1$, $\gamma = 0.5$, $u_M = 3.5$. The desired reference trajectory vector is $\boldsymbol{X}_d(t) = [\sin t + \sin(0.5t), \cos t + 0.5\cos(0.5t)]^{\mathrm{T}}$, other design parameters keep the same as Experiment 1. Figures 5.19, 5.20 and 5.21 present part simulation results.

From the simulation curves in Figs. 5.19 and 5.20, it shows that traditional adaptive controller can't get good tracking performance for the system (5.81) and tracking error always exists periodically. This is mainly because time-varying uncertainties can't be compensated through differential-type adaptive control effect.

According to the simulation results, it is confirmed that the proposed AILC can guarantee fairly good control performance for uncertain nonlinear systems with unknown time varying delays and control input saturation in the presence of external

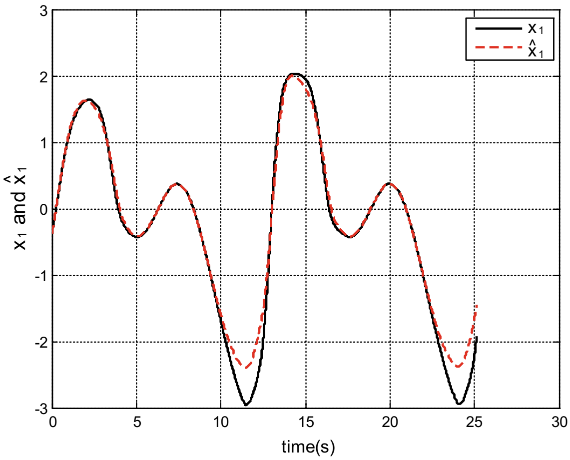

Fig. 5.12 $x_{1,k}$ versus $\hat{x}_{1,k}$ ($k = 1$)

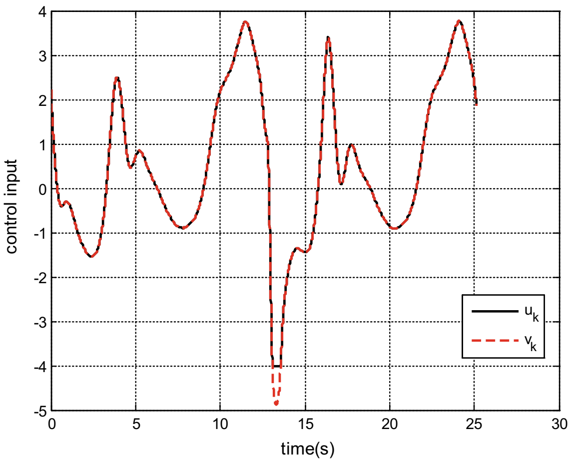

Fig. 5.13 The input v_k and output u_k of saturation ($k = 1$)

disturbance. Moreover, it is verified that our control scheme is more suitable than robust adaptive neural network control methods for finite time repeated problem.

5.4 Error Observer-Based AILC Design and Stability Analysis

In this section, we continue studying the system (5.1) and design a novel error observer-based AILC scheme.

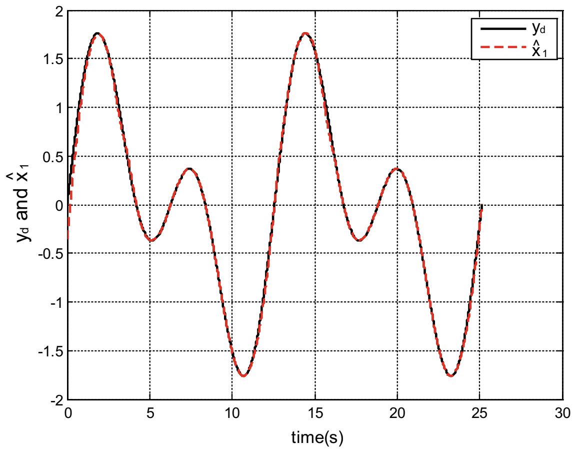

Fig. 5.14 $\hat{x}_{1,k}$ versus y_d ($k = 10$)

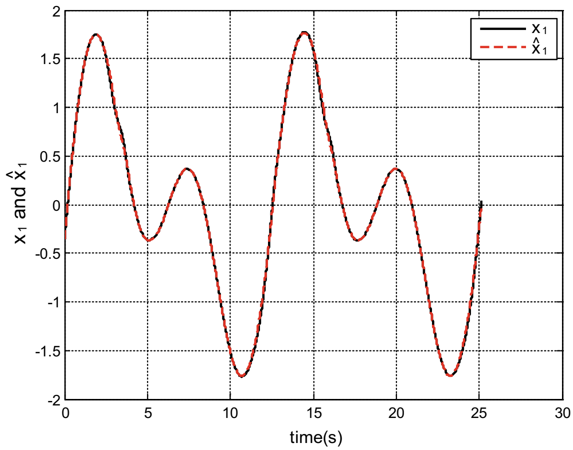

Fig. 5.15 $x_{1,k}$ versus $\hat{x}_{1,k}$ ($k = 10$)

5.4.1 Error Observer-Based AILC Scheme Design

Consider the system (5.1), and the definitions of symbols in (5.1) remain unchanged. In the following part, we will redefine some symbols to meet the needs of controller design, where some symbols may remain the same as mentioned above, but have different meaning.

In this section, we consider the case that time delays is known. For simplicity, we will not consider the influence of saturation input. Rewrite the system (5.1) in the following form

$$\begin{cases} \dot{\boldsymbol{X}}_k = A\boldsymbol{X}_k + B\big[f(\boldsymbol{X}_k) + h\big(\boldsymbol{y}_{\tau,k}, t\big) + u_k(t) + d(t)\big] \\ y_k = \boldsymbol{C}^{\mathrm{T}}\boldsymbol{X}_k \end{cases} \tag{5.82}$$

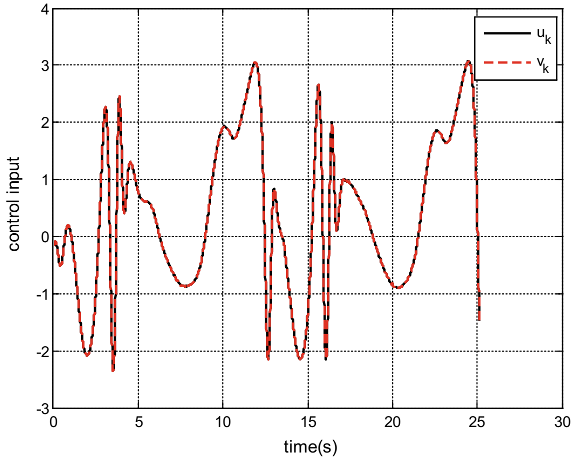

Fig. 5.16 The input v_k and output u_k of saturation ($k = 10$)

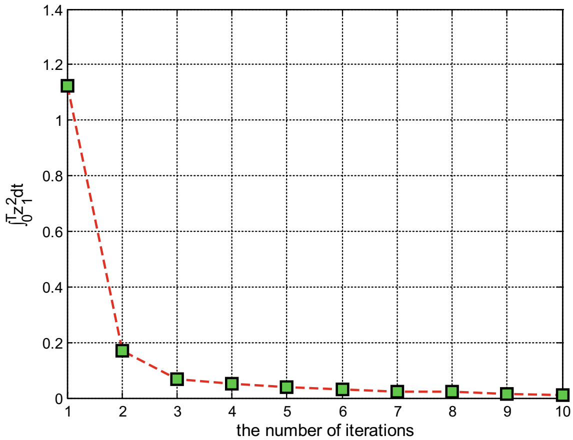

Fig. 5.17 $\int_0^T z_{1,k}^2(t)\mathrm{d}t$ versus the number of iterations

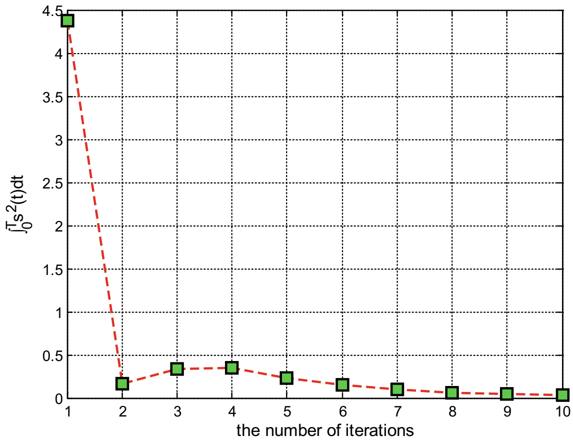

Fig. 5.18 $\int_0^T s_k^2(t)\mathrm{d}t$ versus the number of iterations

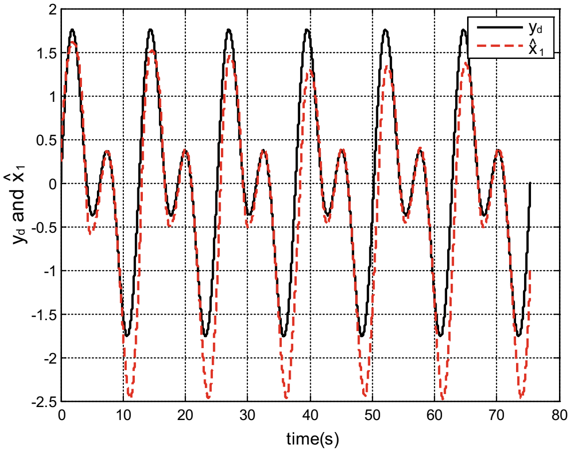

Fig. 5.19 $\hat{x}_{1,k}$ versus y_d

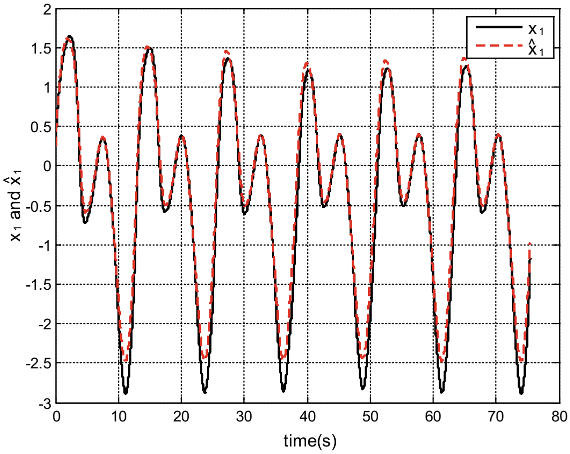

Fig. 5.20 $x_{1,k}$ versus $\hat{x}_{1,k}$

with

$$\boldsymbol{A} = \begin{bmatrix} 0 & & \\ \vdots & \boldsymbol{I}_{n-1} & \\ 0 & \cdots & 0 \end{bmatrix}, \boldsymbol{B} = [0, \ldots, 0, 1]^{\mathrm{T}}, \boldsymbol{C} = [1, 0, \ldots, 0]^{\mathrm{T}}.$$

Define tracking error as $\boldsymbol{z}_k = \left[z_{1,k}, \ldots, z_{n,k}\right]^{\mathrm{T}} = \boldsymbol{X}_k - \boldsymbol{X}_d$, then the dynamical equation of tracking error can be given by

$$\begin{cases} \dot{\boldsymbol{z}}_k = \boldsymbol{A}\boldsymbol{z}_k + \boldsymbol{B}\left[f(\boldsymbol{X}_k) + h\left(\boldsymbol{y}_{\tau,k}, t\right) + u_k(t) + d(t) - y_d^{(n)}\right] \\ z_{1,k} = \boldsymbol{C}^{\mathrm{T}}\boldsymbol{z}_k \end{cases} \tag{5.83}$$

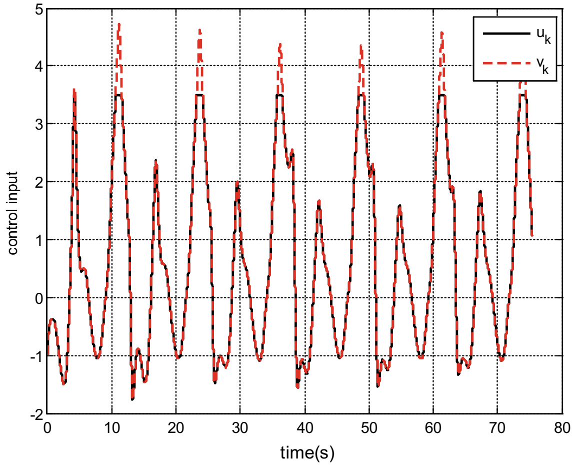

Fig. 5.21 The input v_k and output u_k of saturation

In order to deal with the system uncertainties, we employ two radial basis function (RBF) neural network to approximate unknown functions $f(\boldsymbol{X}_k)$ and $h\left(\boldsymbol{y}_{\tau,k}, t\right)$ as follows

$$f(\boldsymbol{X}_k) = \boldsymbol{W}_f^{*\mathrm{T}}(t)\boldsymbol{\phi}_f(\boldsymbol{X}_k) + \varepsilon_f(\boldsymbol{X}_k) \tag{5.84}$$

$$h\left(\boldsymbol{y}_{\tau,k}, t\right) = \boldsymbol{W}_h^{*\mathrm{T}}(t)\boldsymbol{\phi}_h\left(\boldsymbol{y}_{\tau,k}\right) + \varepsilon_h\left(y_{\tau,k}, t\right) \tag{5.85}$$

where, $\boldsymbol{W}_f^* \in \mathbf{R}^{l_f}$ and $\boldsymbol{W}_h^* \in \mathbf{R}^{l_h}$ are NN optimal weight vectors, $l_f, l_h > 1$ denotes the number of NN nodes; $\boldsymbol{\phi}_f(\boldsymbol{X}_k) \in \mathbf{R}^{l_f}$ and $\boldsymbol{\phi}_h\left(\boldsymbol{y}_{\tau,k}\right) \in \mathbf{R}^{l_h}$ are Gaussian radial basis functions, $\varepsilon_f(\boldsymbol{X}_k)$ and $\varepsilon_h\left(\boldsymbol{y}_{\tau,k}, t\right)$ present NN approximation errors which has their bounds. Then we can rewrite Eq. (5.83) as

$$\begin{cases} \dot{\boldsymbol{z}}_k = \boldsymbol{A}\boldsymbol{z}_k + B\left[\boldsymbol{W}_f^{*\mathrm{T}}\boldsymbol{\phi}_f\left(\hat{\boldsymbol{X}}_k\right) + \boldsymbol{W}_h^{*\mathrm{T}}(t)\boldsymbol{\phi}_h\left(\boldsymbol{y}_{\tau,k}\right) + u_k(t) + \delta_k(t) - y_d^{(n)}\right] \\ z_{1,k} = \boldsymbol{C}^{\mathrm{T}}\boldsymbol{z}_k \end{cases} \tag{5.86}$$

where, $\delta_k(t) = \boldsymbol{W}^{*\mathrm{T}}(t)\left(\boldsymbol{\phi}(\boldsymbol{X}_k) - \boldsymbol{\phi}\left(\hat{\boldsymbol{X}}_k\right)\right) + \varepsilon(\boldsymbol{X}_k) + \varepsilon\left(y_{\tau,k}, t\right) + d(t)$, obviously, $\delta_k(t)$ is bounded. $\hat{\boldsymbol{X}}_k$ can be obtained through the relation $\hat{\boldsymbol{X}}_k = \hat{\boldsymbol{z}}_k + \boldsymbol{X}_d$, where $\hat{\boldsymbol{z}}_k$ denotes the estimated tracking error that is obtained by the following observer:

$$\begin{cases} \dot{\hat{\boldsymbol{z}}}_k = \boldsymbol{A}_c\hat{\boldsymbol{z}}_k + \boldsymbol{K}_o\left(z_{1,k} - \hat{z}_{1,k}\right) \\ \hat{z}_{1,k} = \boldsymbol{C}^{\mathrm{T}}\hat{\boldsymbol{z}}_k \end{cases} \tag{5.87}$$

where, $\boldsymbol{A}_c = \boldsymbol{A} - \boldsymbol{B}\boldsymbol{K}_c^{\mathrm{T}}$, $\boldsymbol{K}_c = [k_{c1}, \ldots, k_{cn}]^{\mathrm{T}} \in \mathbf{R}^n$ should be chosen suitably such that the characteristic polynomial of $\boldsymbol{A}_c$ is Hurwitz; $\boldsymbol{K}_o = [k_{o1}, \ldots, k_{on}]^{\mathrm{T}} \in \mathbf{R}^n$ is the observer gain which makes the characteristic polynomial of $\boldsymbol{A}_o = \boldsymbol{A} - \boldsymbol{K}_o\boldsymbol{C}^{\mathrm{T}}$ be Hurwitz.

Define the estimation error vector as $\boldsymbol{e}_k = \left[e_{1,k}, \ldots, e_{n,k}\right]^{\mathrm{T}} = \boldsymbol{z}_k - \hat{\boldsymbol{z}}_k$, then we can obtain the dynamic equation of estimation error as follows

$$\begin{cases} \dot{\boldsymbol{e}}_k = \boldsymbol{A}_o\boldsymbol{e}_k + \boldsymbol{B}\left[\boldsymbol{W}_f^{*\mathrm{T}}(t)\boldsymbol{\phi}_f\left(\hat{\boldsymbol{X}}_k\right) + \boldsymbol{W}_h^{*\mathrm{T}}(t)\boldsymbol{\phi}_h\left(\boldsymbol{y}_{\tau,k}\right) + u_k(t) + \delta_k(t) - y_d^{(n)} + \boldsymbol{K}_c^{\mathrm{T}}\hat{\boldsymbol{z}}_k\right] \\ e_{1,k} = \boldsymbol{C}^{\mathrm{T}}\boldsymbol{e}_k \end{cases} \tag{5.88}$$

Remark 5.2 Unlike state-based observer design in the previous section, we design an observer to estimate tracking errors, which is to solve the problem of identical initial condition in ILC design. Because the states are unavailable, it is difficult to make the initial values of the state-based observer as same as the system states. However, it is essential in the convergence analysis of ILC method. In this section, we use observer (5.87) estimate the errors in Eq. (5.86). By defining the estimation error, we obtain the dynamic equation of estimation error in Eq. (5.88). In the following design, if we can realize the convergence to zero of estimation error $\boldsymbol{e}_k$ by designing the control system, the estimated error $\hat{\boldsymbol{z}}_k$ will be driven to zero, because $\boldsymbol{A}_c$ is Hurwitz. Then from the definition $\boldsymbol{e}_k = \boldsymbol{z}_k - \hat{\boldsymbol{z}}_k$, it is followed that tracking error $\boldsymbol{z}_k$ will converge to zero simultaneously.

In order to see how to design the control law, we adopt the mixed use of a time signal and a Laplace transfer function to obtain the explicit expression of $e_{1,k}$ in Eq. (5.88) as follows:

$$e_{1,k} = H(s)\left(\boldsymbol{W}_f^{*\mathrm{T}}\boldsymbol{\phi}_f\left(\hat{\boldsymbol{X}}_k\right) + \boldsymbol{W}_h^{*\mathrm{T}}(t)\boldsymbol{\phi}_h\left(\boldsymbol{y}_{\tau,k}\right) + u_k(t) + \delta_k(t) - y_d^{(n)} + \boldsymbol{K}_c^{\mathrm{T}}\hat{\boldsymbol{z}}_k\right) \tag{5.89}$$

where, "s" denotes the complex variable in Laplace transform, $H(s) = C^T(sI - A_o)^{-1}B$ is the transfer function of (5.88). If we choose $\boldsymbol{K}_o = \left[C_n^n\lambda^n, \ldots, C_n^2\lambda^2, C_n^1\lambda\right]^{\mathrm{T}}$ with $C_n^i = n!\big/((n-i)!i!)$, it can easily be shown that $H(s) = 1\big/(s+\lambda)^n$ with λ as a positive design parameter.

In order to design the control term, we construct a new variable $e_{a,k}$ as follows

$$\dot{e}_{a,k} + K_a e_{a,k} = \alpha_0\left(\dot{e}_{1,k} + \lambda e_{1,k}\right), \; e_{a,k}(0) = 0 \tag{5.90}$$

where, K_a and α_0 are positive design parameters. It follows from (5.90) that

$$e_{a,k} = \left[\frac{\alpha_0(s+\lambda)}{s+K_a}\right]e_{1,k} \tag{5.91}$$

Noting Eqs. (5.89), (5.91) becomes

$$e_{a,k} = \frac{L(s)}{s + K_a}\left[\boldsymbol{W}_f^{*\mathrm{T}}\boldsymbol{\phi}_f\left(\hat{\boldsymbol{X}}_k\right) + \boldsymbol{W}_h^{*\mathrm{T}}(t)\boldsymbol{\phi}_h\left(\boldsymbol{y}_{\tau,k}\right) + u_k(t) + \delta_k(t) - y_d^{(n)} + \boldsymbol{K}_c^{\mathrm{T}}\hat{\boldsymbol{z}}_k\right] \tag{5.92}$$

where, $L(s)$ denotes a stable filter which is $L(s) = \alpha_0(s+\lambda)H(s) = \alpha_0 \big/ (s+\lambda)^{n-1}$.

The differential equation, which allows to obtain $e_{a,k}$, can be written as

$$\dot{e}_{a,k} + K_a e_{a,k} = L(s)\left[\boldsymbol{W}_f^{*\mathrm{T}}\boldsymbol{\phi}_f\left(\hat{\boldsymbol{X}}_k\right) + \boldsymbol{W}_h^{*\mathrm{T}}(t)\boldsymbol{\phi}_h\left(\boldsymbol{y}_{\tau,k}\right) + u_k(t) + \delta_k(t) - y_d^{(n)} + \boldsymbol{K}_c^{\mathrm{T}}\hat{\boldsymbol{z}}_k\right] \tag{5.93}$$

For design purpose, we separate the structure of control variable into two parts

$$u_k(t) = u_{c,k}(t) + u_{r,k}(t) \tag{5.94}$$

Here, $u_{c,k}(t)$ is defined as the feedback component of $u_k(t)$ and specified by

$$u_{c,k}(t) = -\hat{\boldsymbol{W}}_{f,k}^{\mathrm{T}}\boldsymbol{\phi}_f\left(\hat{\boldsymbol{X}}_k\right) - \hat{\boldsymbol{W}}_{h,k}^{\mathrm{T}}(t)\boldsymbol{\phi}_h\left(\boldsymbol{y}_{\tau,k}\right) + y_d^{(n)} - \boldsymbol{K}_c^{\mathrm{T}}\hat{\boldsymbol{z}}_k \tag{5.95}$$

where, $\hat{\boldsymbol{W}}_{f,k}$ and $\hat{\boldsymbol{W}}_{h,k}$ denote the estimates of $\boldsymbol{W}_f^*$ and $\boldsymbol{W}_h^*$, respectively. Substituting Eq. (5.95) into Eq. (5.93) yields

$$\begin{aligned}\dot{e}_{a,k} + K_a e_{a,k} &= L(s)\left(-\tilde{\boldsymbol{W}}_{f,k}^{\mathrm{T}}(t)\boldsymbol{\phi}_f\left(\hat{\boldsymbol{X}}_k\right) - \tilde{\boldsymbol{W}}_{h,k}^{\mathrm{T}}(t)\boldsymbol{\phi}_h\left(\boldsymbol{y}_{\tau,k}\right) + u_{r,k}(t) + \delta_k(t)\right)\\ &= -\tilde{\boldsymbol{W}}_{f,k}^{\mathrm{T}}(t)\boldsymbol{\xi}_f\left(\hat{\boldsymbol{X}}_k\right) - \tilde{\boldsymbol{W}}_{h,k}^{T}(t)\boldsymbol{\xi}_h\left(\boldsymbol{y}_{\tau,k}\right) + L(s)\left[u_{r,k}(t)\right] + \delta_{L,k}(t)\end{aligned} \tag{5.96}$$

where, $\boldsymbol{\xi}\left(\hat{\boldsymbol{X}}_k\right) = L(s)\boldsymbol{\phi}\left(\hat{\boldsymbol{X}}_k\right)$, $\boldsymbol{\xi}_h\left(\boldsymbol{y}_{\tau,k}\right) = L(s)\boldsymbol{\phi}_h\left(\boldsymbol{y}_{\tau,k}\right)$, $\delta_{L,k}(t) = L(s)\delta_k(t)$. obvious that $\delta_{L,k}(t)$ is bounded by an unknown constant, i.e., $\left|\delta_{L,k}(t)\right| \le \beta$ with β as an unknown constant. Then we can design the robust control part as follows

$$u_{r,k}(t) = -\frac{1}{L(s)}e_{a,k}\hat{\beta}_k \tanh\left(e_{a,k}\hat{\beta}_k \big/ \Delta_k\right) \tag{5.97}$$

where, $\hat{\beta}_k$ is the estimated value of β, Δ_k denotes a convergent sequence which is specified in the previous section. For preceding analysis, we need the following lemma.

Lemma 5.2 [24]. *For any $\Delta_k > 0$ and $x \in R$, the inequality $|x| - x\tanh\left(x \big/ \Delta_k\right) \le \theta\Delta_k$ holds, where θ is a positive constant and $\theta = e^{-(\theta+1)}$* or $\theta = 0.2785$.

Design adaptive learning laws for unknown parameters as

$$\begin{cases}(1-\gamma_1)\dot{\hat{\boldsymbol{W}}}_{f,k} = -\gamma_1\hat{\boldsymbol{W}}_{f,k} + \gamma_1\hat{\boldsymbol{W}}_{f,k-1} + q_1 e_{a,k}\boldsymbol{\xi}_f\left(\hat{\boldsymbol{X}}_k\right)\\ \hat{\boldsymbol{W}}_{f,k}(0) = \hat{\boldsymbol{W}}_{f,k-1}(T),\ \hat{\boldsymbol{W}}_{f,0}(t) = 0,\ t \in [0, T]\end{cases} \tag{5.98}$$

$$\begin{cases} \hat{\boldsymbol{W}}_{h,k} = \hat{\boldsymbol{W}}_{h,k-1} + q_2 e_{a,k} \boldsymbol{\xi}_h\big(\boldsymbol{y}_{\tau,k}\big) \\ \hat{\boldsymbol{W}}_{h,0}(t) = 0, t \in [0, T] \end{cases} \tag{5.99}$$

$$\begin{cases} (1-\gamma_2)\dot{\hat{\beta}}_k = -\gamma_2\hat{\beta}_k + \gamma_2\hat{\beta}_{k-1} + q_3\left|e_{a,k}\right| \\ \hat{\beta}_k(0) = \hat{\beta}_{k-1}(T), \hat{\beta}_0(t) = 0, t \in [0, T] \end{cases} \tag{5.100}$$

where, $\gamma_1, \gamma_2 \in (0, 1)$ are adjustable parameters, $q_1, q_2, q_3 > 0$ are adaptive learning gains.

Define a Lyapunov function as $V_k = e_{a,k}^2 \big/ 2$. Taking the derivative of V_k with respective to time and utilizing Lemma 5.2 results in

$$\begin{aligned} \dot{V}_k &= e_{a,k}\dot{e}_{a,k} \\ &= -K_a e_{a,k}^2 + e_{a,k}\Big(-\tilde{\boldsymbol{W}}_{f,k}^{\mathrm{T}}(t)\boldsymbol{\xi}_f\Big(\hat{\boldsymbol{X}}_k\Big) - \tilde{\boldsymbol{W}}_{h,k}^{\mathrm{T}}(t)\boldsymbol{\xi}_h\big(\boldsymbol{y}_{\tau,k}\big) + \delta_{L,k}(t)\Big) \\ &- e_{a,k}\hat{\beta}_k \tanh\Big(e_{a,k}\hat{\beta}_k \Big/ \Delta_k\Big) \\ &\le -K_a e_{a,k}^2 - e_{a,k}\tilde{\boldsymbol{W}}_{f,k}^{\mathrm{T}}(t)\boldsymbol{\xi}_f\Big(\hat{\boldsymbol{X}}_k\Big) \\ &\quad - e_{a,k}\tilde{\boldsymbol{W}}_{h,k}^{\mathrm{T}}(t)\boldsymbol{\xi}_h\big(\boldsymbol{y}_{\tau,k}\big) + \left|e_{a,k}\right|\beta - \left|e_{a,k}\right|\hat{\beta}_k + \left|e_{a,k}\right|\hat{\beta}_k \\ &- e_{a,k}\hat{\beta}_k \tanh\Big(e_{a,k}\hat{\beta}_k \Big/ \Delta_k\Big) \\ &\le -K_a e_{a,k}^2 - e_{a,k}\tilde{\boldsymbol{W}}_{f,k}^{\mathrm{T}}(t)\boldsymbol{\xi}_f\Big(\hat{\boldsymbol{X}}_k\Big) - e_{a,k}\tilde{\boldsymbol{W}}_{h,k}^{T}(t)\boldsymbol{\xi}_h\big(\boldsymbol{y}_{\tau,k}\big) - \left|e_{a,k}\right|\tilde{\beta}_k + \theta\Delta_k \end{aligned} \tag{5.101}$$

The block diagram of the proposed error observer based adaptive NN ILC scheme is presented in Fig. 5.22.

5.4.2 Stability Analysis

The stability of the proposed AILC scheme is summarized as follows.

Theorem 5.2 *Considering the nonlinear time-delay system* (5.1), *de designing the tracking error observer* (5.87) *and adaptive iterative learning controller* (5.94) *with parameter adaptive learning algorithms in* Eqs. (5.98)–(5.100), *the following properties can be guaranteed*: ① *all the signals of the closed-loop system are bounded*; ② *the output error $z_{1,k}(t)$ approaches zero as $k \to \infty$, i.e.,* $\lim\limits_{k\to\infty}\int_0^T \big(z_{1,k}(\sigma)\big)^2 \mathrm{d}\sigma = 0$.

Proof Define the parameter estimation error as $\tilde{\beta}_k = \hat{\beta}_k - \beta$. Then we can define a Lyapunov-like CEF as

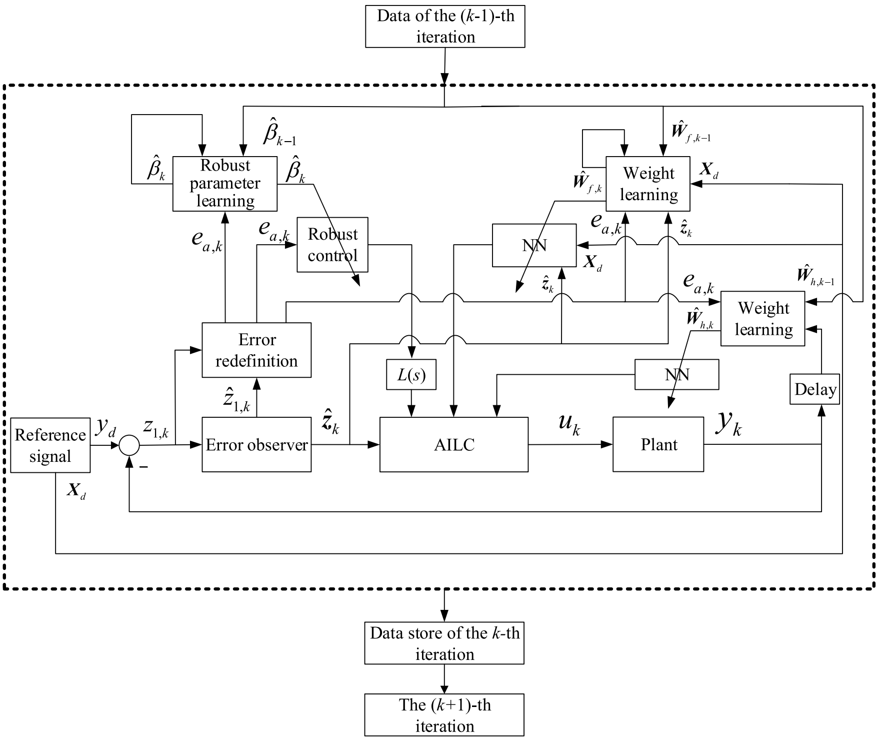

Fig. 5.22 The block diagram of the proposed error observer based adaptive NN ILC scheme

$$
\begin{aligned}
E_k(t) &= V_k + \frac{\gamma_1}{2q_1}\int_0^t \tilde{\boldsymbol{W}}_{f,k}^{\mathrm{T}}\tilde{\boldsymbol{W}}_{f,k}\mathrm{d}\sigma + \frac{1-\gamma_1}{2q_1}\tilde{\boldsymbol{W}}_{f,k}^{\mathrm{T}}\tilde{\boldsymbol{W}}_{f,k} \\
&\quad + \frac{1}{2q_2}\int_0^t \tilde{\boldsymbol{W}}_{h,k}^{\mathrm{T}}\tilde{\boldsymbol{W}}_{h,k}\mathrm{d}\sigma + \frac{\gamma_2}{2q_3}\int_0^t \tilde{\beta}_k^2\mathrm{d}\sigma + \frac{1-\gamma_2}{2q_3}\tilde{\beta}_k^2
\end{aligned}
\tag{5.102}
$$

Similar to previous chapters, the proof includes four parts.

(1) The difference of $E_k(t)$

Computing the difference of $E_k(t)$, which is

$$
\begin{aligned}
\Delta E_k(t) &= E_k(t) - E_{k-1}(t) \\
&= V_k - V_{k-1} + \frac{\gamma_1}{2q_1}\int_0^t \left(\tilde{\boldsymbol{W}}_{f,k}^{\mathrm{T}}\tilde{\boldsymbol{W}}_{f,k} - \tilde{\boldsymbol{W}}_{f,k-1}^{\mathrm{T}}\tilde{\boldsymbol{W}}_{f,k-1}\right)\mathrm{d}\sigma \\
&\quad + \frac{1-\gamma_1}{2q_1}\left(\tilde{\boldsymbol{W}}_{f,k}^{\mathrm{T}}\tilde{\boldsymbol{W}}_{f,k} - \tilde{\boldsymbol{W}}_{f,k-1}^{\mathrm{T}}\tilde{\boldsymbol{W}}_{f,k-1}\right)
\end{aligned}
$$

$$+\frac{1}{2q_2}\int_0^t\left(\tilde{\boldsymbol{W}}_{h,k}^{\mathrm{T}}\tilde{\boldsymbol{W}}_{h,k}-\tilde{\boldsymbol{W}}_{h,k-1}^{\mathrm{T}}\tilde{\boldsymbol{W}}_{h,k-1}\right)\mathrm{d}\sigma$$

$$+\frac{\gamma_2}{2q_3}\int_0^t\left(\tilde{\beta}_k^2-\tilde{\beta}_{k-1}^2\right)\mathrm{d}\sigma+\frac{1-\gamma_2}{2q_3}\left(\tilde{\beta}_k^2-\tilde{\beta}_{k-1}^2\right) \tag{5.103}$$

Considering Eq. (5.101), it is known that

$$\begin{aligned}V_k&=\int_0^t\dot{V}_k\mathrm{d}\sigma-V_k(0)\\&\le -K_a\int_0^t e_{a,k}^2\mathrm{d}\sigma-\int_0^t e_{a,k}\tilde{\boldsymbol{W}}_{f,k}^{\mathrm{T}}\boldsymbol{\xi}\left(\hat{\boldsymbol{X}}_k\right)\mathrm{d}\sigma\\&-\int_0^t e_{a,k}\tilde{\boldsymbol{W}}_{h,k}^{\mathrm{T}}(t)\boldsymbol{\xi}_h\left(\boldsymbol{y}_{\tau,k}\right)\mathrm{d}\sigma-\int_0^t\left|e_{a,k}\right|\tilde{\beta}_k\mathrm{d}\sigma+\int_0^t\theta\Delta_k\mathrm{d}\sigma\end{aligned} \tag{5.104}$$

Recalling the adaptive learning law, we can have

$$\begin{aligned}&\frac{\gamma_1}{2q_1}\int_0^t\left(\tilde{\boldsymbol{W}}_{f,k}^{\mathrm{T}}\tilde{\boldsymbol{W}}_{f,k}-\tilde{\boldsymbol{W}}_{f,k-1}^{\mathrm{T}}\tilde{\boldsymbol{W}}_{f,k-1}\right)\mathrm{d}\sigma+\frac{1-\gamma_1}{2q_1}\left(\tilde{\boldsymbol{W}}_{f,k}^{\mathrm{T}}\tilde{\boldsymbol{W}}_{f,k}-\tilde{\boldsymbol{W}}_{f,k-1}^{\mathrm{T}}\tilde{\boldsymbol{W}}_{f,k-1}\right)\\&=\frac{\gamma_1}{2q_1}\int_0^t\left(\tilde{\boldsymbol{W}}_{f,k}^{\mathrm{T}}\tilde{\boldsymbol{W}}_{f,k}-\tilde{\boldsymbol{W}}_{f,k-1}^{\mathrm{T}}\tilde{\boldsymbol{W}}_{f,k-1}\right)\mathrm{d}\sigma+\frac{(1-\gamma_1)}{q_1}\int_0^t\tilde{\boldsymbol{W}}_{f,k}^{\mathrm{T}}\dot{\tilde{\boldsymbol{W}}}_{f,k}\mathrm{d}\sigma\\&+\frac{(1-\gamma_1)}{2q_1}\left[\tilde{\boldsymbol{W}}_{f,k}^{\mathrm{T}}(0)\tilde{\boldsymbol{W}}_k(0)-\tilde{\boldsymbol{W}}_{f,k-1}^{\mathrm{T}}\tilde{\boldsymbol{W}}_{f,k-1}\right]\\&=\int_0^t e_{a,k}\tilde{\boldsymbol{W}}_{f,k}^{\mathrm{T}}\boldsymbol{\xi}_f\left(\hat{\boldsymbol{X}}_k\right)\mathrm{d}\sigma-\frac{\gamma_1}{q_1}\int_0^t\tilde{\boldsymbol{W}}_{f,k}^{\mathrm{T}}\left(\hat{\boldsymbol{W}}_{f,k}(\sigma)-\hat{\boldsymbol{W}}_{f,k-1}(\sigma)\right)\mathrm{d}\sigma\\&+\frac{\gamma_1}{2q_1}\int_0^t\left(\tilde{\boldsymbol{W}}_{f,k}^{\mathrm{T}}\tilde{\boldsymbol{W}}_k-\tilde{\boldsymbol{W}}_{f,k-1}^{\mathrm{T}}\tilde{\boldsymbol{W}}_{f,k-1}\right)\mathrm{d}\sigma+\frac{(1-\gamma_1)}{2q_1}\left[\tilde{\boldsymbol{W}}_{f,k}^{\mathrm{T}}(0)\tilde{\boldsymbol{W}}_k(0)-\tilde{\boldsymbol{W}}_{f,k-1}^{\mathrm{T}}\boldsymbol{W}_{f,k-1}\right]\\&=\int_0^t e_{a,k}\tilde{\boldsymbol{W}}_{f,k}^{\mathrm{T}}\boldsymbol{\xi}_f\left(\hat{\boldsymbol{X}}_k\right)\mathrm{d}\sigma-\frac{\gamma_1}{q_1}\int_0^t\tilde{\boldsymbol{W}}_{f,k}^{\mathrm{T}}\left(\tilde{\boldsymbol{W}}_{f,k}(\sigma)-\tilde{\boldsymbol{W}}_{f,k-1}(\sigma)\right)\mathrm{d}\sigma\\&+\frac{\gamma_1}{2q_1}\int_0^t\left(\tilde{\boldsymbol{W}}_{f,k}^{\mathrm{T}}\tilde{\boldsymbol{W}}_{f,k}-\tilde{\boldsymbol{W}}_{f,k-1}^{\mathrm{T}}\tilde{\boldsymbol{W}}_{f,k-1}\right)\mathrm{d}\sigma+\frac{(1-\gamma_1)}{2q_1}\left[\tilde{\boldsymbol{W}}_{f,k}^{\mathrm{T}}(0)\tilde{\boldsymbol{W}}_k(0)-\tilde{\boldsymbol{W}}_{f,k-1}^{\mathrm{T}}\tilde{\boldsymbol{W}}_{f,k-1}\right]\\&=\int_0^t e_{a,k}\tilde{\boldsymbol{W}}_{f,k}^{\mathrm{T}}\boldsymbol{\xi}_f\left(\hat{\boldsymbol{X}}_k\right)\mathrm{d}\sigma+\frac{(1-\gamma_1)}{2q_1}\left[\tilde{\boldsymbol{W}}_{f,k}^{\mathrm{T}}(0)\tilde{\boldsymbol{W}}_k(0)-\tilde{\boldsymbol{W}}_{f,k-1}^{\mathrm{T}}\tilde{\boldsymbol{W}}_{f,k-1}\right]\\&-\frac{\gamma_1}{2q_1}\int_0^t\left[\tilde{\boldsymbol{W}}_{f,k}(\sigma)-\tilde{\boldsymbol{W}}_{f,k-1}(\sigma)\right]^{\mathrm{T}}\left[\tilde{\boldsymbol{W}}_{f,k}(\sigma)-\tilde{\boldsymbol{W}}_{f,k-1}(\sigma)\right]\mathrm{d}\sigma\end{aligned} \tag{5.105}$$

$$\frac{1}{2q_2}\int_0^t\left(\tilde{\boldsymbol{W}}_{h,k}^{\mathrm{T}}\tilde{\boldsymbol{W}}_{h,k}-\tilde{\boldsymbol{W}}_{h,k-1}^{\mathrm{T}}\tilde{\boldsymbol{W}}_{h,k-1}\right)\mathrm{d}\sigma=\int_0^t e_{a,k}\tilde{\boldsymbol{W}}_{h,k}^{\mathrm{T}}(t)\boldsymbol{\xi}_h\left(\boldsymbol{y}_{\tau,k}\right)\mathrm{d}\sigma - \frac{q_2}{2}\int_0^t e_{a,k}^2\left\|\boldsymbol{\xi}_h\left(\boldsymbol{y}_{\tau,k}\right)\right\|^2\mathrm{d}\sigma \quad (5.106)$$

$$\begin{aligned}&\frac{\gamma_2}{2q_3}\int_0^t\left(\tilde{\beta}_k^2-\tilde{\beta}_{k-1}^2\right)\mathrm{d}\sigma+\frac{1-\gamma_2}{2q_3}\left(\tilde{\beta}_k^2-\tilde{\beta}_{k-1}^2\right)\\&=\int_0^t\left|e_{a,k}\right|\tilde{\beta}_k\mathrm{d}\sigma+\frac{1-\gamma_2}{2q_3}\left[\tilde{\beta}_k^2(0)-\tilde{\beta}_{k-1}^2(t)\right]-\frac{\gamma_2}{2q_3}\int_0^t\left(\tilde{\beta}_k-\tilde{\beta}_{k-1}\right)^2\mathrm{d}\sigma\end{aligned} \quad (5.107)$$

Combining Eqs. (5.104)–(5.107) results in

$$\begin{aligned}\Delta E_k(t)\le&-K_a\int_0^t e_{a,k}^2\mathrm{d}\sigma+\int_0^t\theta\Delta_k\mathrm{d}\sigma+\frac{(1-\gamma_1)}{2q_1}\left[\tilde{\boldsymbol{W}}_{f,k}^{\mathrm{T}}(0)\tilde{\boldsymbol{W}}_{f,k}(0)-\tilde{\boldsymbol{W}}_{f,k-1}^{\mathrm{T}}\tilde{\boldsymbol{W}}_{f,k-1}\right]\\&+\frac{1-\gamma_2}{2q_3}\left[\tilde{\beta}_k^2(0)-\tilde{\beta}_{k-1}^2(t)\right]-V_{k-1}\end{aligned} \quad (5.108)$$

Letting $t=T$ in Eq. (5.108), and noting $\hat{\boldsymbol{W}}_{f,k}(0)=\hat{\boldsymbol{W}}_{f,k-1}(T)$, $\hat{\beta}_k(0)=\hat{\beta}_{k-1}(T)$, then we can have

$$\Delta E_k(T)\le -K_a\int_0^T e_{a,k}^2\mathrm{d}\sigma+\theta\Delta_k T-V_{k-1} \quad (5.109)$$

(2) The boundedness of $E_k(T)$

Letting $k=1$ in Eq. (5.102), we have

$$\begin{aligned}E_1(t)=&V_1+\frac{\gamma_1}{2q_1}\int_0^t\tilde{\boldsymbol{W}}_{f,1}^{\mathrm{T}}\tilde{\boldsymbol{W}}_{f,1}\mathrm{d}\sigma+\frac{1-\gamma_1}{2q_1}\tilde{\boldsymbol{W}}_{f,1}^{\mathrm{T}}\tilde{\boldsymbol{W}}_{f,1}\\&+\frac{1}{2q_2}\int_0^t\tilde{\boldsymbol{W}}_{h,1}^{\mathrm{T}}\tilde{\boldsymbol{W}}_{h,1}\mathrm{d}\sigma+\frac{\gamma_2}{2q_3}\int_0^t\tilde{\beta}_1^2\mathrm{d}\sigma+\frac{1-\gamma_2}{2q_3}\tilde{\beta}_1^2\end{aligned} \quad (5.110)$$

Taking the time derivative of $E_1(t)$ yields

$$\dot{E}_1(t)=\dot{V}_1+\frac{\gamma_1}{2q_1}\tilde{\boldsymbol{W}}_{f,1}^{\mathrm{T}}\tilde{\boldsymbol{W}}_{f,1}+\frac{1-\gamma_1}{q_1}\tilde{\boldsymbol{W}}_{f,1}^{\mathrm{T}}\dot{\tilde{\boldsymbol{W}}}_{f,1}$$

$$+\frac{1}{2q_2}\tilde{\boldsymbol{W}}_{h,1}^{\mathrm{T}}\tilde{\boldsymbol{W}}_{h,1}+\frac{\gamma_2}{2q_3}\tilde{\beta}_1^2+\frac{1-\gamma_2}{q_3}\tilde{\beta}_1\dot{\tilde{\beta}}_1 \tag{5.111}$$

From parameter adaptive learning laws we know $(1-\gamma_1)\dot{\hat{\boldsymbol{W}}}_{f,1}=-\gamma_1\hat{\boldsymbol{W}}_{f,1}+q_1e_{a,1}\boldsymbol{\xi}_f\left(\hat{\boldsymbol{X}}_1\right)$, $\hat{\boldsymbol{W}}_{h,1}=q_2e_{a,1}\boldsymbol{\xi}_h\left(\boldsymbol{y}_{\tau,1}\right)$, $(1-\gamma_2)\dot{\hat{\beta}}_1=-\gamma_2\hat{\beta}_1+q_3\left|e_{a,1}\right|$, then we can obtain

$$\begin{aligned}
&\frac{\gamma_1}{2q_1}\tilde{\boldsymbol{W}}_{f,1}^{\mathrm{T}}\tilde{\boldsymbol{W}}_{f,1}+\frac{1-\gamma_1}{q_1}\tilde{\boldsymbol{W}}_{f,1}^{\mathrm{T}}\dot{\tilde{\boldsymbol{W}}}_{f,1}\\
&\quad=\frac{\gamma_1}{2q_1}\tilde{\boldsymbol{W}}_{f,1}^{\mathrm{T}}\tilde{\boldsymbol{W}}_{f,1}-\frac{\gamma_1}{q_1}\tilde{\boldsymbol{W}}_{f,1}^{\mathrm{T}}\hat{\boldsymbol{W}}_{f,1}+e_{a,1}\tilde{\boldsymbol{W}}_{f,1}^{\mathrm{T}}\boldsymbol{\xi}_f\left(\hat{\boldsymbol{X}}_1\right)\\
&\quad=\frac{\gamma_1}{2q_1}\left[\tilde{\boldsymbol{W}}_{f,1}^{\mathrm{T}}\tilde{\boldsymbol{W}}_{f,1}-2\tilde{\boldsymbol{W}}_{f,1}^{\mathrm{T}}\hat{\boldsymbol{W}}_{f,1}+\hat{\boldsymbol{W}}_{f,1}^{\mathrm{T}}\hat{\boldsymbol{W}}_{f,1}\right]\\
&\quad-\frac{\gamma_1}{2q_1}\hat{\boldsymbol{W}}_{f,1}^{\mathrm{T}}\hat{\boldsymbol{W}}_{f,1}+e_{a,1}\tilde{\boldsymbol{W}}_{f,1}^{\mathrm{T}}\boldsymbol{\xi}_f\left(\hat{\boldsymbol{X}}_1\right)\\
&\quad\le\frac{\gamma_1}{2q_1}\left[\hat{\boldsymbol{W}}_{f,1}-\tilde{\boldsymbol{W}}_{f,1}\right]^{\mathrm{T}}\left[\hat{\boldsymbol{W}}_{f,1}-\tilde{\boldsymbol{W}}_{f,1}\right]+e_{a,1}\tilde{\boldsymbol{W}}_{f,1}^{\mathrm{T}}\boldsymbol{\xi}_f\left(\hat{\boldsymbol{X}}_1\right)\\
&\quad=\frac{\gamma_1}{2q_1}\boldsymbol{W}_f^{*\mathrm{T}}\boldsymbol{W}_f^*+e_{a,1}\tilde{\boldsymbol{W}}_{f,1}^{\mathrm{T}}\boldsymbol{\xi}_f\left(\hat{\boldsymbol{X}}_1\right)
\end{aligned} \tag{5.112}$$

$$\frac{1}{2q_2}\tilde{\boldsymbol{W}}_{h,1}^{\mathrm{T}}\tilde{\boldsymbol{W}}_{h,1}=\frac{1}{2q_2}\left(-\hat{\boldsymbol{W}}_{h,1}^{\mathrm{T}}\hat{\boldsymbol{W}}_{h,1}+\boldsymbol{W}_h^{*\mathrm{T}}\boldsymbol{W}_h^*\right)+e_{a,1}\tilde{\boldsymbol{W}}_{h,1}^{\mathrm{T}}\boldsymbol{\xi}_h\left(\boldsymbol{y}_{\tau,1}\right) \tag{5.113}$$

$$\frac{\gamma_2}{2q_3}\tilde{\beta}_1^2+\frac{1-\gamma_2}{q_3}\tilde{\beta}_1\dot{\tilde{\beta}}_1\le\frac{\gamma_2}{2q_3}\beta^2+\left|e_{a,k}\right|\tilde{\beta}_1 \tag{5.114}$$

Considering Eq. (5.101) and substituting Eqs. (5.112)–(5.114) back into Eq. (5.111), we can further get

$$\dot{E}_1(t)\le-K_ae_{a,1}^2+\theta\Delta_1+\frac{\gamma_1}{2q_1}\boldsymbol{W}_f^{*\mathrm{T}}\boldsymbol{W}_f^*+\frac{1}{2q_2}\boldsymbol{W}_h^{*\mathrm{T}}\boldsymbol{W}_h^*+\frac{\gamma_2}{2q_3}\beta^2 \tag{5.115}$$

Denote $c_{\max}=\max\limits_{t\in[0,T]}\left\{\frac{\gamma_1}{2q_1}\boldsymbol{W}_f^{*\mathrm{T}}\boldsymbol{W}_f^*+\frac{1}{2q_2}\boldsymbol{W}_h^{*\mathrm{T}}(t)\boldsymbol{W}_h^*(t)+\frac{\gamma_2}{2q_3}\beta^2\right\}$. Integrating Eq. (5.115) over $[0,t]$ leads to

$$E_1(t)-E_1(0)\le-K_a\int_0^t e_{a,1}^2\mathrm{d}\sigma+t\cdot c_{\max}+\theta\Delta_1t \tag{5.116}$$

From the adaptive learning laws we have $\hat{\boldsymbol{W}}_{f,1}(0)=0$, $\hat{\beta}_1(0)=0$. Further, we arrive at

$$E_1(0) = \frac{1-\gamma_1}{2q_1}\tilde{\boldsymbol{W}}_{f,1}^{\mathrm{T}}(0)\tilde{\boldsymbol{W}}_{f,1}(0) + \frac{1-\gamma_2}{2q_3}\tilde{\beta}_1^2 = \frac{1-\gamma_1}{2q_1}\left\|\boldsymbol{W}_f^*\right\|^2 + \frac{1-\gamma_2}{2q_3}\beta^2 \tag{5.117}$$

Substituting Eq. (5.117) back into Eq. (5.116) results in

$$E_1(t) \le t\cdot c_{\max} + \theta\Delta_1 t + \frac{1-\gamma_1}{2q_1}\left\|\boldsymbol{W}_f^*\right\|^2 + \frac{1-\gamma_2}{2q_2}\beta^2,\ \ t\in[0,T] \tag{5.118}$$

which implies that $E_1(t)$ is bounded on $[0, T]$. Letting $t = T$ in Eq. (5.118), we can obtain the upper bound of $E_1(T)$

$$E_1(T) \le T\cdot(c_{\max} + \theta\Delta_1 t) + \frac{1-\gamma_1}{2q_1}\left\|\boldsymbol{W}_f^*\right\|^2 + \frac{1-\gamma_2}{2q_2}\beta^2 < \infty \tag{5.119}$$

Applying Eq. (5.109) repeatedly, we obtain

$$\begin{aligned} E_k(T) &= E_1(T) + \sum_{j=2}^{k}\Delta E_j(T) \\ &\le -K_a\sum_{j=2}^{k}\int_0^T e_{a,j}^2\mathrm{d}\sigma + T\cdot c_{\max} + \theta T\sum_{j=1}^{k}\Delta_k + \frac{1-\gamma_1}{2q_1}\left\|\boldsymbol{W}_f^*\right\|^2 + \frac{1-\gamma_2}{2q_2}\beta^2 \\ &\le T\cdot c_{\max} + \theta T\sum_{j=1}^{k}\Delta_k + \frac{1-\gamma_1}{2q_1}\left\|\boldsymbol{W}_f^*\right\|^2 + \frac{1-\gamma_2}{2q_2}\beta^2 \end{aligned} \tag{5.120}$$

According to Property 5.1 we know $\theta T\sum_{j=1}^{k}\Delta_k \le \lim_{k\to\infty}\theta T\sum_{j=1}^{k}\Delta_k \le 2\theta T q$, therefore, it means that $E_k(T)$ is bounded.

(3) The boundedness of $E_k(t)$

Similarly, separate $E_k(t)$ into two parts

$$E_k^1(t) = \frac{\gamma_1}{2q_1}\int_0^t \tilde{\boldsymbol{W}}_{f,k}^{\mathrm{T}}\tilde{\boldsymbol{W}}_{f,k}\mathrm{d}\sigma + \frac{\gamma_2}{2q_2}\int_0^t \tilde{\beta}_k^2\mathrm{d}\sigma + \frac{1}{2q_2}\int_0^t \tilde{\boldsymbol{W}}_{h,k}^{\mathrm{T}}\tilde{\boldsymbol{W}}_{h,k}\mathrm{d}\sigma \tag{5.121}$$

$$E_k^2(t) = V_k + \frac{1-\gamma_1}{2q_1}\tilde{\boldsymbol{W}}_k^{\mathrm{T}}\tilde{\boldsymbol{W}}_k + \frac{1-\gamma_2}{2q_2}\tilde{\beta}_k^2 \tag{5.122}$$

According to foregoing derivation, the boundedness of $E_k^1(T)$ and $E_k^2(T)$ is guaranteed for all iterations. Consequently, $\forall k\in N$, there are two constants M_1 and M_2 such that

$$E_k^1(t) \le E_k^1(T) \le M_1 < \infty \tag{5.123}$$

$$E_k^2(T) \le M_2 \tag{5.124}$$

Then we know

$$E_k(t) = E_k^1(t) + E_k^2(t) \le M_1 + E_k^2(t) \tag{5.125}$$

On the other hand, from Eq. (5.108), we obtain

$$\begin{aligned}\Delta E_{k+1}(t) &< \int_0^t (\theta\Delta_{k+1})\mathrm{d}\sigma + \frac{(1-\gamma_1)}{2q_1}\Big[\tilde{\boldsymbol{W}}_{k+1}^{\mathrm{T}}(0)\tilde{\boldsymbol{W}}_{k+1}(0) - \tilde{\boldsymbol{W}}_k^{\mathrm{T}}\tilde{\boldsymbol{W}}_k\Big] \\ &+ \frac{1-\gamma_2}{2q_2}\Big[\tilde{\beta}_{k+1}^2(0) - \tilde{\beta}_k^2(t)\Big] - V_k(t) \\ &\le \theta\Delta_{k+1}t + M_2 - E_k^2(t)\end{aligned} \tag{5.126}$$

Adding Eq. (5.125) and Eq. (5.126) together yields

$$E_{k+1}(t) = E_k(t) + \Delta E_{k+1}(t) \le M_1 + M_2 + \theta\Delta_k t \tag{5.127}$$

Since we have proven that $E_1(t)$ is bounded, so we can conclude that $E_k(t)$ is bounded as well according to induction method. Furthermore, we can say that $\hat{\boldsymbol{W}}_{f,k}$, $\hat{\boldsymbol{W}}_{h,k}$ and $\hat{\beta}_k$ are all bounded.

(4) The convergence of tracking errors

Rewrite Eq. (5.119) as

$$\sum_{j=2}^{k}\int_0^T e_{a,j}^2\mathrm{d}\sigma \le \frac{1}{K_a}\left[T\cdot c_{\max} + \theta T\sum_{j=1}^{k}\Delta_k + \frac{1-\gamma_1}{2q_1}\|W^*\|^2 + \frac{1-\gamma_2}{2q_2}\beta^2 - E_k(T)\right] \tag{5.128}$$

Taking the limitation of Eq. (5.128), it follows that

$$\lim_{k\to\infty}\sum_{j=2}^{k}\int_0^T e_{a,j}^2\mathrm{d}\sigma \le \frac{1}{K_a}\left[T\cdot c_{\max} + 2q\theta T + \frac{1-\gamma_1}{2q_1}\|W^*\|^2 + \frac{1-\gamma_2}{2q_2}\beta^2\right] \tag{5.129}$$

According to the convergence theorem of the sum of series, $\lim\limits_{k\to\infty}\int_0^T e_{a,k}^2\mathrm{d}\sigma = 0$, from $e_{a,k} = \left[\frac{\alpha_0(s+\lambda)}{s+K_a}\right]e_{1,k}$, it is followed by $\lim\limits_{k\to\infty}\int_0^T e_{1,k}^2\mathrm{d}\sigma = 0$. Because $\boldsymbol{A}_c$ and $\boldsymbol{A}_o$ are Hurwitz, then from Eq. (5.87) we get $\lim\limits_{k\to\infty}\int_0^T \hat{z}_{1,k}^2\mathrm{d}\sigma = 0$, which further implies

$\lim_{k\to\infty}\int_0^T z_{1,k}^2 \mathrm{d}\sigma = \lim_{k\to\infty}\int_0^T (y_k - y_d)^2 \mathrm{d}\sigma = 0$. This means that we have achieved the tracking control for system output to the desired reference signals. Based on the above reasoning, we can finally obtain the boundedness of $u_k(t)$.

This concludes the proof. □

5.4.3 Simulation Analysis

Consider the second-order system (5.81), here time delays are known. To verify the validity of the proposed AILC scheme, we conduct the following two simulation experiments.

Experiment 1 The desired reference signals are chosen as $\boldsymbol{X}_d(t) = [\sin t, \cos t]^{\mathrm{T}}$. Choose the design parameters as $\boldsymbol{K}_c = [1, 2]^{\mathrm{T}}$, $\boldsymbol{K}_o = [6, 9]^{\mathrm{T}}$, $\lambda = 3$, $K_a = 2$, $\alpha_0 = 2$, $q_1 = 1$, $q_2 = 1$, $\gamma_1 = \gamma_2 = 0.5$. The parameters for RBF NN are chosen as $l_f = 30$, $\mu_{f,j} = \frac{1}{l_f}\big(2j - l_f\big)[2, 3]^{\mathrm{T}}$, $\sigma_{f,j} = 2$, $j = 1, 2, \ldots, l_f$; $l_h = 20$, $\mu_{h,j} = \frac{1}{l_h}(2j - l_h)[2, 2]^{\mathrm{T}}$, $\sigma_{h,j} = 2$, $j = 1, 2, \ldots, l_h$. The system runs on $[0, 4\pi]$ for five iterations. Some simulation results are presented in Figs. 5.23, 5.24, 5.25, 5.26, 5.27, 5.28 and 5.29.

From simulation results we can see that for the desired reference trajectory $\boldsymbol{X}_d(t) = [\sin t, \cos t]^{\mathrm{T}}$ the proposed error observer based AILC scheme can also obtain perfect control effect and achieve the control objective.

Experiment 2 Further we choose the desired trajectory as $\boldsymbol{X}_d(t) = [\sin t + \cos(0.5t), \cos t - 0.5\sin(0.5t)]^{\mathrm{T}}$, the control parameters remain the same as Experiment 1. The system runs on $[0, 8\pi]$ repeatedly. Simulation results are shown in Figs. 5.30, 5.31, 5.32, 5.33, 5.34, 5.35 and 5.36.

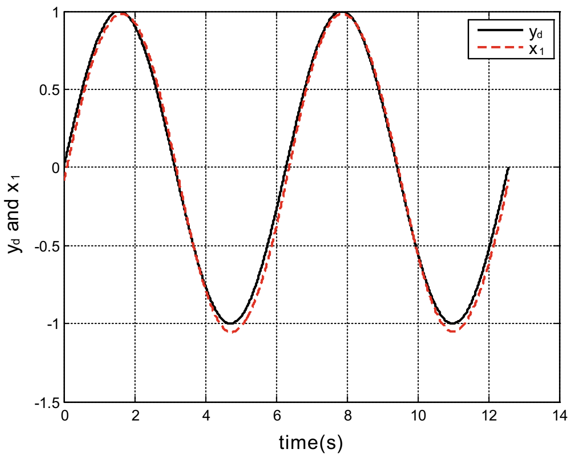

Fig. 5.23 $x_{1,k}$ versus y_d ($k = 1$)

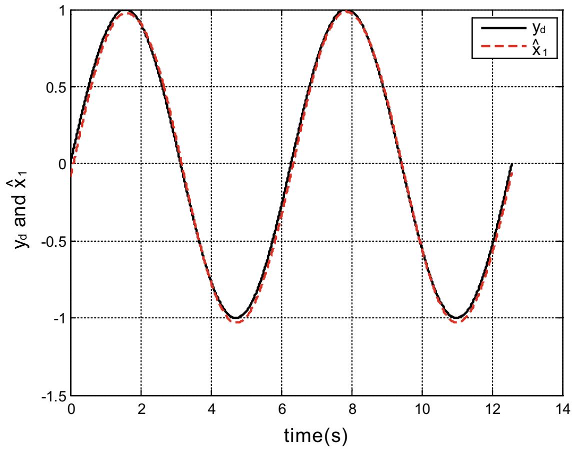

Fig. 5.24 $\hat{x}_{1,k}$ versus y_d ($k = 1$)

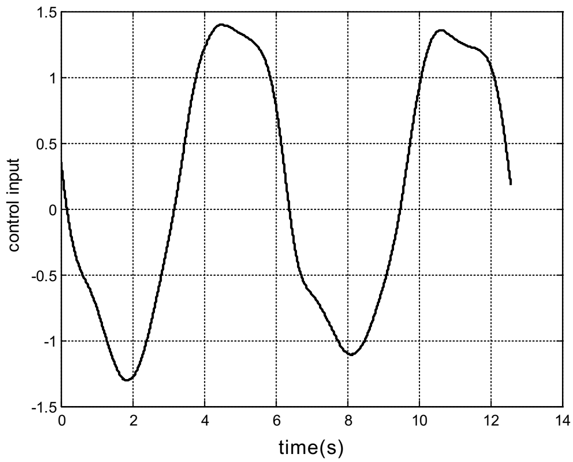

Fig. 5.25 Control input u_k ($k = 1$)

From the simulation results in Experiment 2, it can be seen that the proposed error observer based AILC scheme obtains good control effect for more complex desired reference trajectory.

5.5 Summary and Comments

In this chapter, a deep investigation is carried out for the AILC problem of nonlinear systems with states un-measurable and two kinds of observer-based AILC schemes are proposed, which overcomes the design difficulty from time delays, input saturation and the absence of measurement of states. In the state observer-based AILC

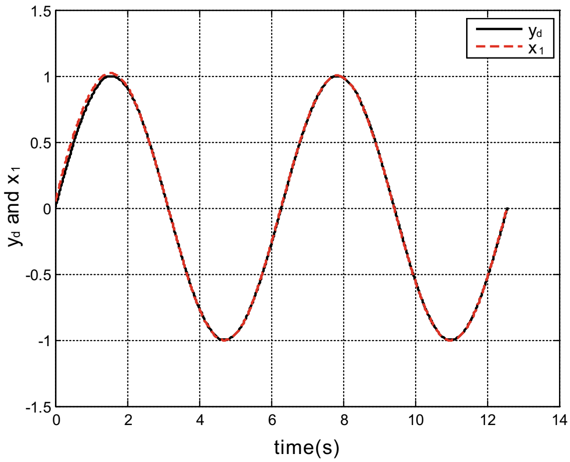

Fig. 5.26 $x_{1,k}$ versus y_d ($k = 5$)

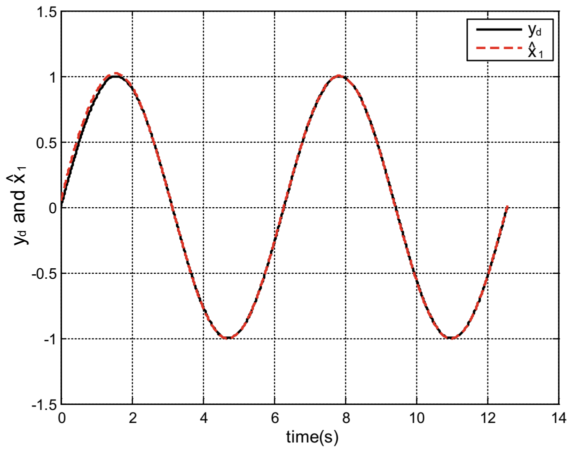

Fig. 5.27 $\hat{x}_{1,k}$ versus y_d ($k = 5$)

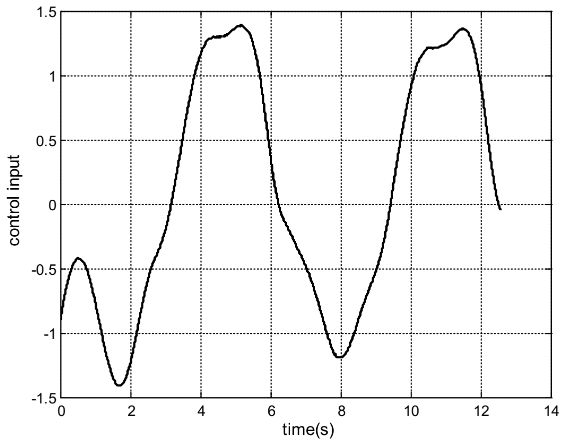

Fig. 5.28 Control input u_k ($k = 5$)

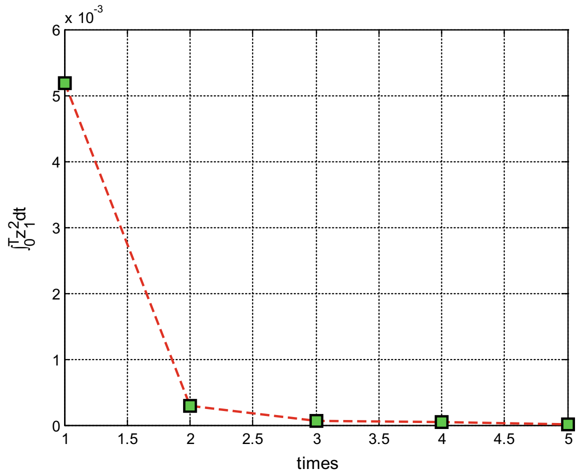

Fig. 5.29 $\int_0^T z_{1,k}^2 \mathrm{d}t$ versus the number of iterations

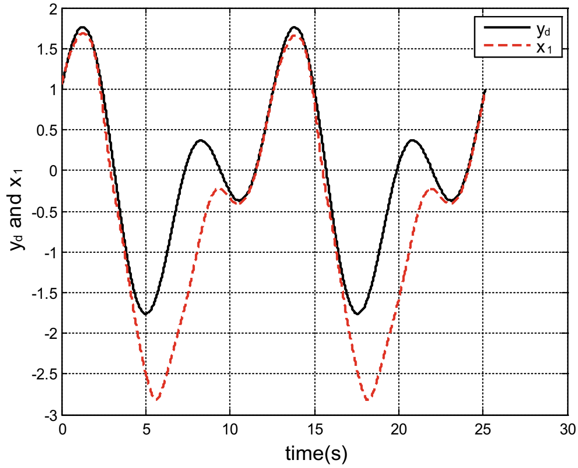

Fig. 5.30 $x_{1,k}$ versus y_d ($k = 1$)

scheme, state observer is designed on the basis of neural network compensation. The observer gain is determined by using LMI method, which avoids the SPR condition. In the error observer-based AILC scheme, a new error variable is defined by introducing filter, which removes the identical initial condition and SPR condition. A new robust learning term is chosen by using hyperbolic tangent function and series convergent sequence to guarantee the learning convergence. Comparing with relative existing results, the proposed AILC is applicable to a broader range and requires for less restrictions on the plant, thus being of lower conservative property.

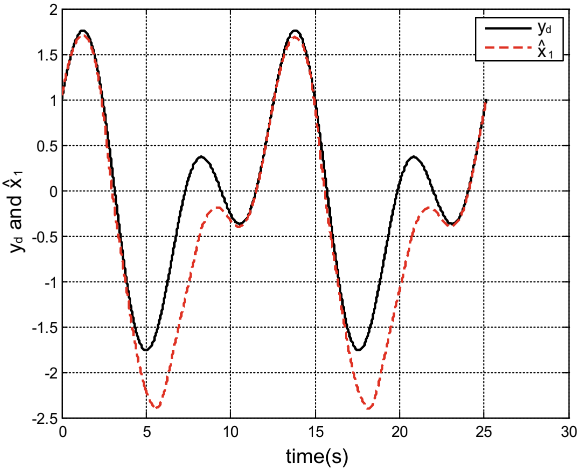

Fig. 5.31 $\hat{x}_{1,k}$ versus y_d ($k = 1$)

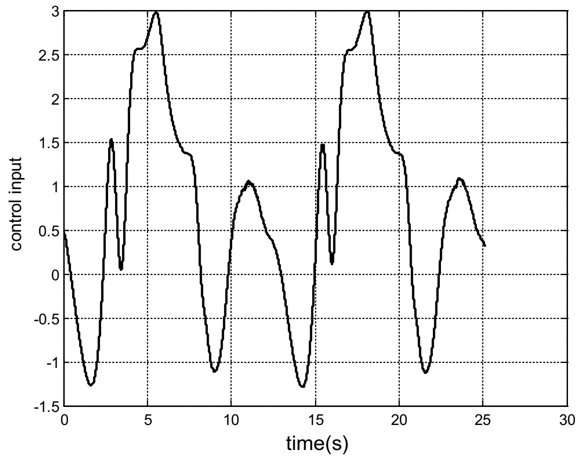

Fig. 5.32 Control input u_k ($k = 1$)

Fig. 5.33 $x_{1,k}$ versus y_d ($k = 10$)

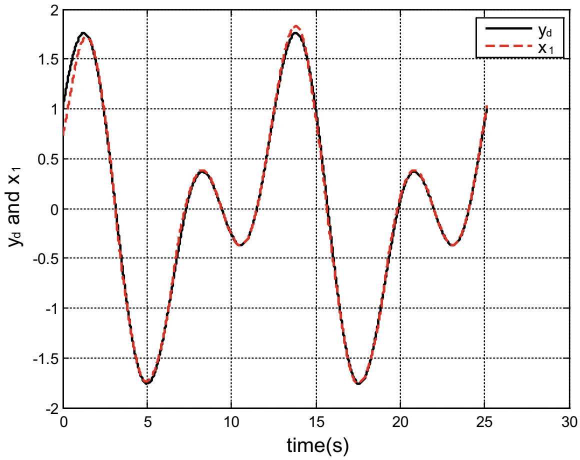

Fig. 5.34 $\hat{x}_{1,k}$ versus y_d ($k = 10$)

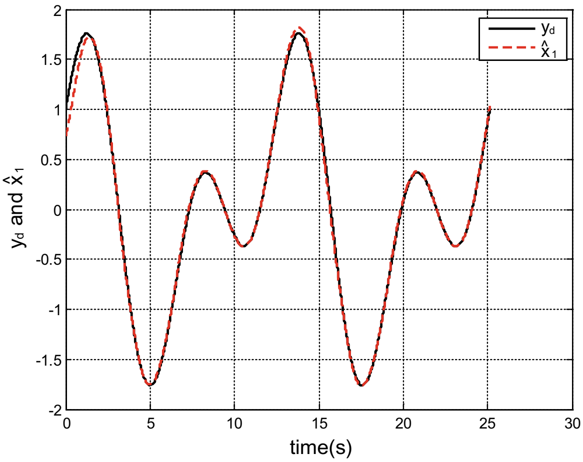

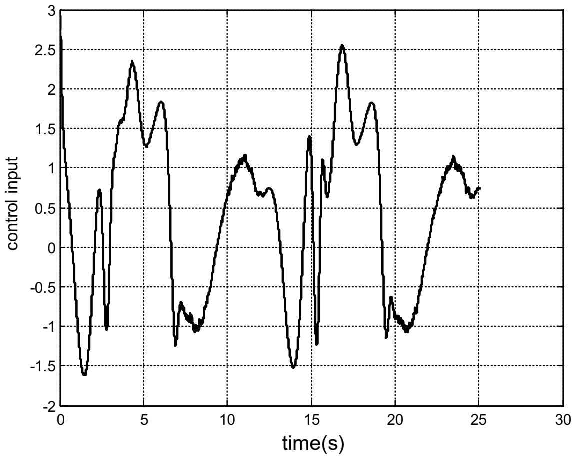

Fig. 5.35 Control input u_k ($k = 10$)

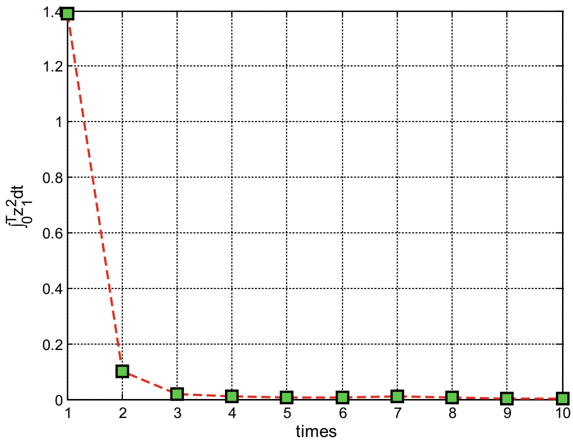

Fig. 5.36 $\int_0^T z_{1,k}^2 \mathrm{d}t$ versus the number of iterations

References

1. Kim Y H, Lewis F L. High-level feedback control with neural networks[M]. NJ: River Edge, 1998.
2. Leu Y G, Wang W Y, Lee T T. Observer-based direct adaptive fuzzy-neural control for nonaffine nonlinear systems[J]. IEEE Transactions on Neural Networks, 2005, 16(4): 853–861.
3. Tong S, Li Y, Li Y, et al. Observer-based adaptive fuzzy backstepping control for a class of stochastic nonlinear strict-feedback systems[J]. IEEE Transactions on Systems, Man, and Cybernetics, Part B: Cybernetics, 2011, 41(6): 1693–1704.
4. Chen B, Lin C, Liu X, et al. Observer-based adaptive fuzzy control for a class of nonlinear delayed systems[J]. IEEE Transactions on Systems Man and Cybernetics: Systems, 2015, 46(1): 27–36.
5. Tayebi A, Xu J X. Observer-based iterative learning control for a class of time-varying nonlinear systems[J]. IEEE Transactions on Circuits and Systems I: Fundamental Theory and Applications, 2003, 50(3): 452–455.

6. Darouach M Z M, Xu S J. Full-order observer for linear systems with unknown inputs[J]. IEEE Trans on Automatic Control, 1994, 39(1): 606–609.
7. Xu J X, Xu J. Observer based learning control for a class of nonlinear systems with time-varying parametric uncertainties[J]. IEEE Transactions on Automatic Control, 2004, 49(2): 275–281.
8. Chen W S, Li R H, Li J. Observer-based adaptive iterative learning control for nonlinear systems with time-varying delays[J]. International Journal of Automation and Computing, 2010, 7(4): 438–446.
9. Dong-mei Zhang, Ming-xuan Sun, Li Yu. Observer-based iterative learning control for non-identical trajectory tracking[J]. Control Theory & Applications, 2006, 23(5): 795–799.
10. Wang Y C, Chien C J. An observer based adaptive iterative learning control for robotic systems[C]. IEEE International Conference on Fuzzy Systems, 2011, Taipei, Taiwan, 2011: 2876–2881.
11. Wang Y C, Chien C J. An observer-based fuzzy neural network adaptive ILC for nonlinear systems[C]. 13th International Conference on Control, Automation and Systems, Gwangju, Korea, 2013: 226–232.
12. Wang Y C, Chien C J, Er M J. An observer-based model reference adaptive iterative learning controller for MIMO nonlinear systems[C]. 11th IEEE International Conference on Control & Automation, Taiwan, 2014: 1168–1173.
13. Wang Y C, Chien C J, Er M J. An observer-based adaptive iterative learning controller for MIMO nonlinear systems with delayed output[C]. 13th International Conference on Control, Automation, Robotics & Vision, Singapore, 2014: 157–162.
14. Zhou B, Gao H J, Lin Z L, et al. Stabilization of linear systems with distributed input delay and input saturation[J]. Automatica, 2012, 48(5): 712–724.
15. Wen C, Zhou J, Liu Z, et al. Robust adaptive control of uncertain nonlinear systems in the presence of input saturation and external disturbance[J]. Automatic Control, IEEE Transactions on, 2011, 56(7): 1672–1678.
16. Esfandiari K, Abdollahi F, Talebi H A. Adaptive control of uncertain nonaffine nonlinear systems with input saturation using neural networks[J]. IEEE Transactions on Neural Networks and Learning Systems, 2014, 26(10): 2311–2322.
17. Xu J X, Tan Y, Tong-Heng Lee. Iterative learning control design based on composite energy function with input saturation[C]. Proceedings of the American Control Conference, Denver, Colorado, 2003: 5129–5134.
18. Xu J X, Tan Y, Lee T H. Iterative learning control design based on composite energy function with input saturation[J]. Automatica, 2004, 40(8): 1371–1377.
19. Zhang R, Hou Z, Ji H, et al. Adaptive iterative learning control for a class of non-linearly parameterised systems with input saturations[J]. International Journal of Systems Science, 2016, 47(5): 1084–1094.
20. Zhang R, Hou Z, Chi R H, et al. Adaptive iterative learning control for nonlinearly parameterised systems with unknown time-varying delays and input saturations[J]. International Journal of Control, 2015, 88(6): 1133–1141.
21. Ji H, Hou Z, Zhang R. Adaptive iterative learning control for high-speed trains with unknown speed delays and input saturations[J]. IEEE Transactions on Automation Science and Engineering, 2015, 13(1): 260–273.
22. Fan L. Iterative learning and adaptive fault-tolerant control with application to high-speed trains under unknown speed delays and control input saturations[J]. IET Control Theory & Applications, 2014, 8(9): 675–687.
23. Boyd S P, El Ghaoui L, Feron E, et al. Linear matrix inequalities in system and control theory[M]. Philadelphia: Society for industrial and applied mathematics, 1994.
24. Pollycarpou M M. Stable adaptive neural control scheme for nonlinear systems[J]. IEEE Transations on Automatic Control, 1996, 41(3): 447–451.

Chapter 6
Observer-Based AILC Design for Robotic Manipulator

6.1 Introduction

In last chapter, we investigate AILC problem for uncertain nonlinear systems with un-measurable states which is described by (5.1). From the form of (5.1), we can find that the proposed observer based AILC schemes are only effective for systems whose control gain is 1. As for systems whose control gain is not 1, the proposed schemes in last chapter are not applicable any more. To solve this problem, in this chapter we will take the manipulator systems with time-delays and only output measurable as example and design a new observer based AILC scheme.

6.2 Problem Formulation and Preliminaries

6.2.1 Problem Formulation

Consider the following n degrees-of-freedom rigid robotic manipulator system

$$\boldsymbol{M}(\boldsymbol{q}_k(t))\ddot{\boldsymbol{q}}_k(t) + \boldsymbol{C}(\boldsymbol{q}_k(t), \dot{\boldsymbol{q}}_k(t))\dot{\boldsymbol{q}}_k(t) + \boldsymbol{G}(\boldsymbol{q}_k(t)) + \boldsymbol{H}\left(\boldsymbol{q}_{k,\tau}\right) = \boldsymbol{u}_k(t) + \boldsymbol{d}_k(t) \tag{6.1}$$

where, $\boldsymbol{q}_k(t) = \left[q_{1,k}(t), \ldots, q_{n,k}(t)\right]^{\mathrm{T}} \in \mathbf{R}^n$, $\boldsymbol{q}_k(t), \dot{\boldsymbol{q}}_k(t)$ and $\ddot{\boldsymbol{q}}_k(t)$ are the joint position, velocity and acceleration vectors, respectively; $\boldsymbol{M}\left(\boldsymbol{q}_k(t)\right) \in \mathbf{R}^{n\times n}$ is the inertia matrix; $\boldsymbol{C}\left(\boldsymbol{q}_k(t), \dot{\boldsymbol{q}}_k(t)\right) \in R^n$ from Coriolis and centrifugal forces; $\boldsymbol{G}\left(\boldsymbol{q}_k(t)\right) \in \mathbf{R}^n$ is the vector resulting from the gravitational forces; $\boldsymbol{u}_k(t) \in \mathbf{R}^n$ is the control input vector. $\boldsymbol{d}_k(t) \in \mathbf{R}^n$ is the vector containing the unknown external disturbances. The time delay term is $\boldsymbol{q}_{k,\tau} \triangleq \left[q_{1,k}(t-\tau_1(t)), \ldots, q_{n,k}(t-\tau_n(t))\right]^{\mathrm{T}}$, where $\tau_i(t)$ is unknown time-varying delay with the upper bound $\tau_{\max}$, $i = 1, 2, \ldots, n$. $\boldsymbol{H}\left(\boldsymbol{q}_{k,\tau}\right)$ is a bounded unknown smooth functions of time-delay position. It is well known

J. Wei et al., *Iterative Learning Control for Nonlinear Time-Delay System*,
https://doi.org/10.1007/978-981-19-6317-9_6

that the inertia matrix $\boldsymbol{M}\big(\boldsymbol{q}_k(t)\big)$ is positive definite and bounded, i.e., for $\forall \boldsymbol{q}_k(t)$, it satisfies

$$0 < m_1 \boldsymbol{I}_n \leq \boldsymbol{M}\big(\boldsymbol{q}_k(t)\big) \leq m_2 \boldsymbol{I}_n \tag{6.2}$$

where, $m_1, m_2 > 0$ are constants, $\boldsymbol{I}_n$ is the n-order unit matrix. Since the inverse of inertia matrix always exists, then the dynamic formulation (6.1) can be rewritten as

$$\begin{aligned}\ddot{\boldsymbol{q}}_k(t) = & -\boldsymbol{M}^{-1}(\boldsymbol{q}_k)\big(\boldsymbol{C}(\boldsymbol{q}_k, \dot{\boldsymbol{q}}_k)\dot{\boldsymbol{q}}_k(t) + \boldsymbol{G}(\boldsymbol{q}_k)\big) - \boldsymbol{M}^{-1}(\boldsymbol{q}_k)\boldsymbol{H}\big(\boldsymbol{q}_{k,\tau}\big) \\ & + \boldsymbol{M}^{-1}(\boldsymbol{q}_k)\boldsymbol{u}_k(t) + \boldsymbol{M}^{-1}(\boldsymbol{q}_k)\boldsymbol{d}_k(t)\end{aligned} \tag{6.3}$$

Define the state variable at the k-th iteration as $\boldsymbol{x}_{1,k}(t) = \boldsymbol{q}_k(t)$, $\boldsymbol{x}_{2,k}(t) = \dot{\boldsymbol{q}}_k(t)$, $\boldsymbol{x}_k(t) = \big[\boldsymbol{x}_{1,k}^{\mathrm{T}}(t), \boldsymbol{x}_{2,k}^{\mathrm{T}}(t)\big]^{\mathrm{T}}$, choose the output variable as $\boldsymbol{y}_k(t) = \boldsymbol{q}_k(t)$, denote $f\big(\boldsymbol{q}_k, \dot{\boldsymbol{q}}_k\big) = -\boldsymbol{M}^{-1}(\boldsymbol{q}_k)\big(\boldsymbol{C}(\boldsymbol{q}_k, \dot{\boldsymbol{q}}_k)\dot{\boldsymbol{q}}_k(t) + \boldsymbol{G}(\boldsymbol{q}_k)\big)$, $\boldsymbol{g}\big(\boldsymbol{x}_{1,k}\big) \triangleq \boldsymbol{M}^{-1}\big(\boldsymbol{x}_{1,k}\big)$. Then we can rewrite Eq. (6.3) as

$$\begin{cases}\dot{\boldsymbol{x}}_{1,k}(t) = \boldsymbol{x}_{2,k}(t) \\ \dot{\boldsymbol{x}}_{2,k}(t) = \boldsymbol{f}(\boldsymbol{x}_k) - \boldsymbol{g}\big(\boldsymbol{x}_{1,k}\big)\boldsymbol{H}\big(\boldsymbol{y}_{k,\tau}\big) + \boldsymbol{g}\big(\boldsymbol{x}_{1,k}\big)\boldsymbol{u}_k(t) + \boldsymbol{g}\big(\boldsymbol{x}_{1,k}\big)\boldsymbol{d}_k(t) \\ \boldsymbol{y}_k(t) = \boldsymbol{C}\boldsymbol{x}_k(t), t \in [0, T] \\ \boldsymbol{y}_k(t) = 0, t \in [-\tau_{\max}, 0)\end{cases} \tag{6.4}$$

where, $\boldsymbol{y}_{k,\tau} \triangleq \big[y_{k,\tau_1}, \ldots, y_{k,\tau_n}\big]^{\mathrm{T}} = \big[y_{1,k}(t - \tau_1(t)), \ldots, y_{n,k}(t - \tau_n(t))\big]^{\mathrm{T}} \in \mathbf{R}^n$, $\boldsymbol{C} = [\boldsymbol{I}_n, \boldsymbol{O}]^{\mathrm{T}} \in \mathbf{R}^{2n \times n}$, $\boldsymbol{O}$ is the $n \times n$ zero matrix. The velocity variables are assumed to be unmeasurable and only the joint position is available for measurement. In constrast with system (5.1), the control gain of system (6.4) is unknown.

The design objective is to design an observer-based AILC scheme for robotic manipulator (1) to steer the output $\boldsymbol{y}_k$ tracking a reference signal $\boldsymbol{y}_d$ over $[0, T]$ as $k \to \infty$, while guaranteeing that all the system signals remain bounded. Define the desired reference trajectory $\boldsymbol{x}_d = \big[\boldsymbol{y}_d^{\mathrm{T}}, \dot{\boldsymbol{y}}_d^{\mathrm{T}}\big]^{\mathrm{T}}$. To facilitate control design, we make following reasonable assumptions.

Assumption 6.1 The unknown time delays $\tau_i(t)$ satisfy: $0 \leq \tau_i(t) \leq \tau_{\max}$, $\dot{\tau}_i(t) \leq \kappa < 1$, $i = 1, 2, \ldots, n$, where $\tau_{\max}$ is the known upper bound of time delays, κ is an unknown constant.

Assumption 6.2 The unknown smooth continuous function $H(\cdot)$ satisfies the following inequality

$$\Big\|\boldsymbol{H}(\cdot)\Big\| \leq \sum_{j=1}^{n} \rho_j(\cdot) \tag{6.5}$$

where, $\rho_j(\cdot)$ is unknown positive smooth function.

Assumption 6.3 The desired signal $\boldsymbol{y}_d(t)$ and its derivatives $\dot{\boldsymbol{y}}_d(t)$ and $\ddot{\boldsymbol{y}}_d(t)$ are continuous and derivable.

Assumption 6.4 The unknown external disturbance $\boldsymbol{d}_k(t)$ is bounded, i.e., $\|\boldsymbol{d}_k(t)\| \leq D_0$, with D_0 as an unknown upper bound.

Assumption 6.5 The control input $\boldsymbol{u}_k(t)$ is bounded.

Remark 6.1 In Assumption 6.5, we made boundedness assumption on control input. This is reasonable. Actually, in all control systems, control input is bounded when the system achieves the control objective.

6.2.2 'GL' Matrix and Operators

To facilitate the analysis of RBF NN, the GL matrix and its product operator [] are briefly introduced here for completeness [1]. Denote the GL vectors and matrices by $\{\cdot\}$ and the GL product operator by "$\cdot$". To avoid any possible confusion, $[\cdot]$ is used to denote the conventional vector and matrix.

Generally, the GL matrix is a rectangular array of vectors and the elements of GL matrix are $\boldsymbol{W}_{ij}, \boldsymbol{\phi}_{ij} \in \mathbf{R}^{n_{ij}}, n_{ij} \in N, i = 1, 2, \ldots, n, j = 1, 2, \ldots, m$. The GL row vector $\{\boldsymbol{W}_i\}$ and its transpose $\{\boldsymbol{W}_i\}^{\mathrm{T}}$ are defined as

$$\{\boldsymbol{W}_i\} = \left\{ \boldsymbol{W}_{i1} \ \boldsymbol{W}_{i2} \cdots \boldsymbol{W}_{im} \right\}$$

$$\{\boldsymbol{W}_i\}^{\mathrm{T}} = \left\{ \boldsymbol{W}_{i1}^{\mathrm{T}} \ \boldsymbol{W}_{i2}^{\mathrm{T}} \cdots \boldsymbol{W}_{im}^{\mathrm{T}} \right\}$$

The GL matrix $\{\boldsymbol{W}\}$ and its transpose $\{\boldsymbol{W}\}^{\mathrm{T}}$ are accordingly defined as

$$\{\boldsymbol{W}\} = \begin{Bmatrix} \boldsymbol{W}_{11} & \boldsymbol{W}_{12} & \cdots & \boldsymbol{W}_{1m} \\ \boldsymbol{W}_{21} & \boldsymbol{W}_{22} & \cdots & \boldsymbol{W}_{2m} \\ \vdots & \vdots & \ddots & \vdots \\ \boldsymbol{W}_{n1} & \boldsymbol{W}_{n2} & \cdots & \boldsymbol{W}_{nm} \end{Bmatrix} = \begin{Bmatrix} \{\boldsymbol{W}_1\} \\ \{\boldsymbol{W}_2\} \\ \vdots \\ \{\boldsymbol{W}_n\} \end{Bmatrix}$$

$$\{\boldsymbol{W}\}^{\mathrm{T}} = \begin{Bmatrix} \boldsymbol{W}_{11}^{\mathrm{T}} & \boldsymbol{W}_{12}^{\mathrm{T}} & \cdots & \boldsymbol{W}_{1m}^{\mathrm{T}} \\ \boldsymbol{W}_{21}^{\mathrm{T}} & \boldsymbol{W}_{22}^{\mathrm{T}} & \cdots & \boldsymbol{W}_{2m}^{\mathrm{T}} \\ \vdots & \vdots & \ddots & \vdots \\ \boldsymbol{W}_{n1}^{\mathrm{T}} & \boldsymbol{W}_{n2}^{\mathrm{T}} & \cdots & \boldsymbol{W}_{nm}^{\mathrm{T}} \end{Bmatrix} = \begin{Bmatrix} \{\boldsymbol{W}_1\}^{\mathrm{T}} \\ \{\boldsymbol{W}_2\}^{\mathrm{T}} \\ \vdots \\ \{\boldsymbol{W}_n\}^{\mathrm{T}} \end{Bmatrix}$$

It should be noted that the dimension of each vector in a GL matrix may be different from each other. However, as long as n_{ij} is known, the structure of the GL matrix is well-determined.

For a given GL matrix

$$\{\boldsymbol{\Phi}\} = \begin{Bmatrix} \boldsymbol{\phi}_{11} & \boldsymbol{\phi}_{12} & \cdots & \boldsymbol{\phi}_{1n} \\ \boldsymbol{\phi}_{21} & \boldsymbol{\phi}_{22} & \cdots & \boldsymbol{\phi}_{2n} \\ \vdots & \vdots & \ddots & \vdots \\ \boldsymbol{\phi}_{n1} & \boldsymbol{\phi}_{n2} & \cdots & \boldsymbol{\phi}_{nn} \end{Bmatrix} = \begin{Bmatrix} \{\boldsymbol{\phi}_1\} \\ \{\boldsymbol{\phi}_2\} \\ \vdots \\ \{\boldsymbol{\phi}_n\} \end{Bmatrix}$$

where, $\boldsymbol{\phi}_{ij}$ has the same dimensions as $\boldsymbol{W}_{ij}$. The GL product of $\{\boldsymbol{W}\}^{\mathrm{T}}$ and $\{\boldsymbol{\Phi}\}$ is a $n \times m$ matrix of elementwise products which is specified by

$$\left[\{\boldsymbol{W}\}^{\mathrm{T}} \cdot \{\boldsymbol{\Phi}\}\right] = \begin{bmatrix} \boldsymbol{W}_{11}^{\mathrm{T}}\boldsymbol{\phi}_{11} & \boldsymbol{W}_{12}^{\mathrm{T}}\boldsymbol{\phi}_{12} & \cdots & \boldsymbol{W}_{1m}^{\mathrm{T}}\boldsymbol{\phi}_{1m} \\ \boldsymbol{W}_{21}^{\mathrm{T}}\boldsymbol{\phi}_{21} & \boldsymbol{W}_{22}^{\mathrm{T}}\boldsymbol{\phi}_{22} & \cdots & \boldsymbol{W}_{2m}^{\mathrm{T}}\boldsymbol{\phi}_{2m} \\ \vdots & \vdots & \ddots & \vdots \\ \boldsymbol{W}_{n1}^{\mathrm{T}}\boldsymbol{\phi}_{n1} & \boldsymbol{W}_{n2}^{\mathrm{T}}\boldsymbol{\phi}_{n2} & \cdots & \boldsymbol{W}_{nm}^{\mathrm{T}}\boldsymbol{\phi}_{nm} \end{bmatrix}$$

Clearly, the GL product can be regarded as a generalization of the Hadamard matrix product[2]. The GL product of a square matrix and a GL row vector is defined as follows. Let $\boldsymbol{\Gamma}_i = \boldsymbol{\Gamma}_i^{\mathrm{T}} = \left[\boldsymbol{\gamma}_{i1}\ \boldsymbol{\gamma}_{i2} \cdots \boldsymbol{\gamma}_{in}\right]$, $\boldsymbol{\gamma}_{ij} \in \mathbf{R}^{m \times n_{ij}}$, $m = \sum_{j=1}^{n} n_{ij}$, then we have

$$\boldsymbol{\Gamma}_i \cdot \left\{\boldsymbol{\phi}_i\right\} = \Gamma_i \cdot \{\phi_i\} := \left[\boldsymbol{\gamma}_{i1}\boldsymbol{\phi}_{i1}\ \boldsymbol{\gamma}_{i2}\boldsymbol{\phi}_{i2} \cdots \boldsymbol{\gamma}_{in}\boldsymbol{\phi}_{in}\right] \in \mathbf{R}^{m \times n}$$

Note that the GL product should be computed first in a mixed matrix product. For instance, in $\{\boldsymbol{A}\} \cdot \{\boldsymbol{B}\}\boldsymbol{C}$, the matrix $[\{\boldsymbol{A}\} \cdot \{\boldsymbol{B}\}]$ should be computed firstly, and then followed by the multiplication of $[\{\boldsymbol{A}\} \cdot \{\boldsymbol{B}\}]$ with matrix $\boldsymbol{C}$.

6.3 States Observer Design

Rewrite Eq. (6.4) into the following form

$$\dot{\boldsymbol{x}}_k = \boldsymbol{A}\boldsymbol{x}_k + \boldsymbol{K}_0\boldsymbol{y}_k + \boldsymbol{B}\left[\boldsymbol{f}(\boldsymbol{x}_k) - \boldsymbol{g}(\boldsymbol{x}_{1,k})\boldsymbol{H}(\boldsymbol{y}_{k,\tau}) + \boldsymbol{g}\left(\boldsymbol{x}_{1,k}\right)\boldsymbol{u}_k + \boldsymbol{g}\left(\boldsymbol{x}_{1,k}\right)\boldsymbol{d}_k(t)\right] \tag{6.6}$$

where, $\boldsymbol{A} = \begin{bmatrix} -\boldsymbol{K}_1 & \boldsymbol{I}_n \\ -\boldsymbol{K}_2 & \boldsymbol{O} \end{bmatrix}_{2n \times 2n}$, $\boldsymbol{K}_1 = \begin{bmatrix} k_{11} & & \\ & \ddots & \\ & & k_{1n} \end{bmatrix}_{n \times n}$ and $\boldsymbol{K}_2 = \begin{bmatrix} k_{21} & & \\ & \ddots & \\ & & k_{2n} \end{bmatrix}_{n \times n}$ are diagonal matrices, $\boldsymbol{K}_o = \begin{bmatrix} \boldsymbol{K}_1 \\ \boldsymbol{K}_2 \end{bmatrix}_{2n \times n}$, $\boldsymbol{B} = \begin{bmatrix} \boldsymbol{O} \\ \boldsymbol{I}_n \end{bmatrix}_{2n \times n}$, $\boldsymbol{O}$ is

$n \times n$ zero matrix. $\boldsymbol{K}_1$ and $\boldsymbol{K}_2$ should be chosen suitably so that $\boldsymbol{A}$ is strict Hurwitz. Then, for a given positive matrix $\boldsymbol{Q} > 0$, there exist a matrix $\boldsymbol{P} > 0$ satisfying the following inequality

$$\boldsymbol{A}^{\mathrm{T}}\boldsymbol{P} + \boldsymbol{P}\boldsymbol{A} + \left(\frac{n/m_1 + 1}{\lambda} + \frac{D_2^2 + 1}{\left\|\boldsymbol{C}\boldsymbol{C}^{\mathrm{T}} + \delta\boldsymbol{I}_{2n}\right\|^2}\right)\boldsymbol{P}\boldsymbol{P}^T < -\boldsymbol{Q} \tag{6.7}$$

where, λ is a positive constant.

In order to estimate the states of system (6.6), design a state observer as follows

$$\begin{cases} \dot{\hat{\boldsymbol{x}}}_k = \boldsymbol{A}\hat{\boldsymbol{x}}_k + \boldsymbol{K}_o\boldsymbol{y}_k + \boldsymbol{B}(\boldsymbol{\Psi}_k - \boldsymbol{u}_{rk}) \\ \hat{\boldsymbol{y}}_k = \hat{\boldsymbol{x}}_{1,k} \end{cases} \tag{6.8}$$

where, $\boldsymbol{\Psi}_k \in \mathbf{R}^n$, $\boldsymbol{u}_{rk}$ is defined as the robust term which will be designed later.

Remark 6.2 To solve inequality (6.7), we separate the matrix $\boldsymbol{A}$ into two parts in the form of $\boldsymbol{A} = \overline{\boldsymbol{A}} + \boldsymbol{K}_0\overline{\boldsymbol{B}}$, where

$$\overline{\boldsymbol{A}} = \begin{bmatrix} \boldsymbol{O} & \boldsymbol{I}_n \\ \boldsymbol{O} & \boldsymbol{O} \end{bmatrix}, \overline{\boldsymbol{B}} = \begin{bmatrix} -\boldsymbol{I}_n & \boldsymbol{O} \end{bmatrix} \tag{6.9}$$

By using Lemma 5.1, inequality (6.7) is equivalent to the following LMI

$$\begin{bmatrix} \boldsymbol{P}\overline{\boldsymbol{A}} + \boldsymbol{M}\overline{\boldsymbol{B}} + \overline{\boldsymbol{B}}^{\mathrm{T}}\boldsymbol{M}^{\mathrm{T}} + \overline{\boldsymbol{A}}^{\mathrm{T}}\boldsymbol{P} + \boldsymbol{Q} & \boldsymbol{P} \\ \boldsymbol{P} & -\boldsymbol{I}_{2n} \Big/ \left(\frac{n/m_1+1}{\lambda} + \frac{D_2^2+1}{\left\|\boldsymbol{C}\boldsymbol{C}^{\mathrm{T}}+\delta\boldsymbol{I}_{2n}\right\|^2}\right) \end{bmatrix} < 0 \tag{6.10}$$

where, $\boldsymbol{I}_{2n}$ denote $2n \times 2n$ unit matrix. $\boldsymbol{P}, \boldsymbol{M}$ and λ can be solved by using Matlab LMI toolbox, then we can get the observer gain matrix via $\boldsymbol{K}_0 = \boldsymbol{P}^{-1}\boldsymbol{M}$.

In order to deal with uncertainties in system, we employ two RBF NNs to approximate $\boldsymbol{f}(\boldsymbol{x}_k)$ and $\boldsymbol{g}(\boldsymbol{x}_{1,k})$ on the compact set $\boldsymbol{\Omega}_f = \{\boldsymbol{x}_k\} \subset \mathbf{R}^{2n}$ and $\boldsymbol{\Omega}_g = \{\boldsymbol{x}_{1,k}\} \subset \mathbf{R}^n$, respectively

$$\begin{aligned} \boldsymbol{f}(\boldsymbol{x}_k) &= \begin{bmatrix} \boldsymbol{W}_{f1}^{*\mathrm{T}}(t)\boldsymbol{\phi}_{f1}(\boldsymbol{x}_k) \\ \vdots \\ \boldsymbol{W}_{fn}^{*\mathrm{T}}(t)\boldsymbol{\phi}_{fn}(\boldsymbol{x}_k) \end{bmatrix} + \begin{bmatrix} \varepsilon_{f1}(\boldsymbol{x}_k) \\ \vdots \\ \varepsilon_{fn}(\boldsymbol{x}_k) \end{bmatrix} \\ &= \left[\left\{\boldsymbol{W}_f^*(t)\right\}^{\mathrm{T}} \cdot \left\{\boldsymbol{\phi}_f(\boldsymbol{x}_k)\right\}\right] + \boldsymbol{\varepsilon}_f(\boldsymbol{x}_k) \end{aligned} \tag{6.11}$$

$$g(x_{1,k}) = \begin{bmatrix} W_{g11}^{*\mathrm{T}}(t)\boldsymbol{\phi}_{g11}(\boldsymbol{x}_{1,k}) + \varepsilon_{g11}(\boldsymbol{x}_{1,k}) & \cdots & W_{g1n}^{*\mathrm{T}}(t)\boldsymbol{\phi}_{\sin}(\boldsymbol{x}_{1,k}) + \varepsilon_{g\,\ln}(\boldsymbol{x}_{1,k}) \\ \vdots & \vdots & \vdots \\ W_{gn1}^{*\mathrm{T}}(t)\boldsymbol{\phi}_{gn1}(\boldsymbol{x}_{1k}) + \varepsilon_{gn1}(\boldsymbol{x}_{1,k}) & \cdots & W_{gm}^{*\mathrm{T}}(t)\boldsymbol{\phi}_{gnn}(\boldsymbol{x}_{1,k}) + \varepsilon_{gm}(\boldsymbol{x}_{1,k}) \end{bmatrix}$$
$$= \begin{bmatrix} \overline{\boldsymbol{W}}_{g11}^{*\mathrm{T}}(t)\overline{\boldsymbol{\phi}}_{g11}(\boldsymbol{x}_{1,k}) & \dots & \overline{\boldsymbol{W}}_{g1n}^{*\mathrm{T}}(t)\overline{\boldsymbol{\phi}}_{g1n}(\boldsymbol{x}_{1,k}) \\ \vdots & \vdots & \vdots \\ \overline{\boldsymbol{W}}_{gn1}^{*\mathrm{T}}(t)\overline{\boldsymbol{\phi}}_{gn1}(\boldsymbol{x}_{1,k}) & \cdots & \overline{\boldsymbol{W}}_{gmn}^{*\mathrm{T}}(t)\overline{\boldsymbol{\phi}}_{gm}(\boldsymbol{x}_{1,k}) \end{bmatrix}$$
$$= \left[\left\{\overline{W}_g^{*}(t)\right\}^{\mathrm{T}} \cdot \left\{\overline{\boldsymbol{\phi}}_g(\boldsymbol{x}_{1,k})\right\}\right] \tag{6.12}$$

where, $W_{fi}^{*}(t), \boldsymbol{\phi}_{it}(\cdot) \in \mathbf{R}^{l_{fi}}$, $i = 1,\ldots,n$; $\boldsymbol{W}_{gij}^{*}, \boldsymbol{\phi}_{gij}(\cdot) \in \mathbf{R}^{l_{gj}}$, $\overline{\boldsymbol{W}}_{gij}^{*} = \left[\boldsymbol{W}_{gij}^{*T}(t), \varepsilon_{gij}(x_{1,k})\right]^{\mathrm{T}}$, $\overline{\boldsymbol{\phi}}_{gij}(\boldsymbol{x}_{1,k}) = \left[\boldsymbol{\phi}_{gij}^{\mathrm{T}}(\boldsymbol{x}_{1,k}), 1\right]^{\mathrm{T}}$, $i = 1,\ldots,n, j = 1,\ldots,n$.

Design Ψ_k as

$$\Psi_k = \left\{\widehat{\boldsymbol{W}}_{f,k}(t)\right\}^{\mathrm{T}} \cdot \left\{\boldsymbol{\phi}_f(\widehat{\boldsymbol{x}}_k)\right\} + \left[\left\{\widehat{\boldsymbol{W}}_{g,k}(t)\right\}^{\mathrm{T}} \cdot \left\{\overline{\boldsymbol{g}}_g(\boldsymbol{x}_{1,k})\right\}\right]\boldsymbol{u}_k \tag{6.13}$$

According to the property of RBF NN, we have

$$\begin{aligned} \boldsymbol{f}(\boldsymbol{x}_k) - \widehat{\boldsymbol{f}}(\widehat{\boldsymbol{x}}_k) &= \left\{\boldsymbol{W}_f^{*}(t)\right\}^{\mathrm{T}} \cdot \left\{\boldsymbol{\phi}_f(\boldsymbol{x}_k)\right\} + \boldsymbol{\varepsilon}_f(\boldsymbol{x}_k) - \left\{\widehat{\boldsymbol{W}}_{f,k}\right\}^{\mathrm{T}} \cdot \left\{\boldsymbol{\phi}_f(\widehat{\boldsymbol{x}}_k)\right\} \\ &= \left\{\boldsymbol{W}_f^{*}(t)\right\}^{\mathrm{T}} \cdot \left\{\boldsymbol{\phi}_f(\boldsymbol{x}_k)\right\} - \left\{\boldsymbol{W}_f^{*}(t)\right\}^{\mathrm{T}} \cdot \left\{\boldsymbol{\phi}_f(\widehat{\boldsymbol{x}}_k)\right\} + \boldsymbol{\varepsilon}_f(t) \\ &\quad + \left\{\boldsymbol{W}_f^{*}\right\}^{\mathrm{T}} \cdot \left\{\boldsymbol{\phi}_f(\widehat{\boldsymbol{x}}_k)\right\} - \left\{\hat{W}_{f,k}\right\}^{\mathrm{T}} \cdot \left\{\boldsymbol{\phi}_f(\widehat{\boldsymbol{x}}_k)\right\} \\ &= \left\{\boldsymbol{W}_f^{*}(t)\right\}^{\mathrm{T}} \cdot \left\{\widetilde{\boldsymbol{\phi}}_f(\boldsymbol{x}_k, \widehat{\boldsymbol{x}}_k)\right\} + \boldsymbol{\varepsilon}_f(\boldsymbol{x}_k) - \left\{\widetilde{\boldsymbol{W}}_{f,k}\right\}^{\mathrm{T}} \cdot \left\{\boldsymbol{\phi}_f(\widehat{\boldsymbol{x}}_k)\right\} \\ &= \boldsymbol{\delta}_{fk} - \left\{\widetilde{\boldsymbol{W}}_{f,k}\right\}^{\mathrm{T}} \cdot \left\{\boldsymbol{\phi}_f(\widehat{\boldsymbol{x}}_k)\right\} \end{aligned} \tag{6.14}$$

where, $\tilde{\boldsymbol{W}}_{fk} = \hat{\boldsymbol{W}}_{fk} - \boldsymbol{W}_f^{*}$ is the estimation error, $\boldsymbol{\delta}_{fk} = \left\{\boldsymbol{W}_f^{*}(t)\right\}^{\mathrm{T}} \cdot \left\{\tilde{\boldsymbol{\phi}}_f(\boldsymbol{x}_k, \hat{\boldsymbol{x}}_k)\right\} + \boldsymbol{\varepsilon}_f(\boldsymbol{x}_k)$, whose upper bound is assumed to be $\|\boldsymbol{\delta}_{fk}\| \le \delta^{*}$.

Define observer estimation error as $\boldsymbol{z}_k \triangleq \left[z_{1,k}, z_{2,k}, \ldots, z_{2n,k}\right]^{\mathrm{T}} = \boldsymbol{x}_k - \hat{\boldsymbol{x}}_k$, and denote $\tilde{\boldsymbol{y}}_k = \boldsymbol{y}_k - \hat{\boldsymbol{y}}_k$.

Then from Eqs. (6.6), (6.8) and (6.13) we can obtain

$$\begin{aligned} \dot{z}_k = \boldsymbol{A}\boldsymbol{z}_k + \boldsymbol{B}\Big[-\left\{\widetilde{\boldsymbol{W}}_{f,k}\right\}^{\mathrm{T}} \cdot \left\{\boldsymbol{\phi}_f(\widehat{\boldsymbol{x}}_k)\right\} - \left[\left\{\widetilde{\overline{\boldsymbol{W}}}_{g,k}(t)\right\}^{\mathrm{T}} \cdot \left\{\overline{\boldsymbol{\phi}}_g(\boldsymbol{x}_{1,k})\right\}\right]\boldsymbol{u}_k\Big] \\ - B\boldsymbol{g}(\boldsymbol{x}_{1,k})\boldsymbol{H}(\boldsymbol{y}_{k,r}) + \boldsymbol{B}\left(\delta_{fk} + \boldsymbol{g}(\boldsymbol{x}_{1,k})\boldsymbol{d}_k(t) + \boldsymbol{u}_{rk}\right) \end{aligned} \tag{6.15}$$

Denote $\boldsymbol{\Phi}_k = \boldsymbol{B}\left(\boldsymbol{\delta}_{fk} + \boldsymbol{g}(\boldsymbol{x}_{1,k})\boldsymbol{d}_k(t) + \boldsymbol{u}_{rk}\right)$, on the basis of above analysis it is clear that $\boldsymbol{\Phi}_k$ is bounded, we assume $\|\boldsymbol{\Phi}_k\| \le D_0$.

Defining $V_{z_k} = \boldsymbol{z}_k^{\mathrm{T}}\boldsymbol{P}\boldsymbol{z}_k$ and taking its time derivative we can have

$$\dot{V}_{z_k} = z_k^{\mathrm{T}}\big(\boldsymbol{A}^{\mathrm{T}}\boldsymbol{P} + \boldsymbol{P}\boldsymbol{A}\big)z_k + 2z_k^{\mathrm{T}}\boldsymbol{P}\boldsymbol{\Phi}_k - 2z_k^{\mathrm{T}}\boldsymbol{P}\boldsymbol{B}\boldsymbol{g}\big(\boldsymbol{x}_{1,k}\big)\boldsymbol{H}\big(y_{k,\tau}\big) + 2z_k^{\mathrm{T}}\boldsymbol{P}\boldsymbol{B}\Big[-\big\{\widetilde{\boldsymbol{W}}_{f,k}\big\}^{\mathrm{T}}\cdot\big\{\boldsymbol{\phi}_f\big(\hat{\boldsymbol{x}}_k\big)\big\} - \Big[\Big\{\widetilde{\overline{\boldsymbol{W}}}_{g,k}(t)\Big\}^{\mathrm{T}}\cdot\big\{\overline{\boldsymbol{\phi}}_g\big(\boldsymbol{x}_{1,k}\big)\big\}\Big]\boldsymbol{u}_k\Big] \tag{6.16}$$

Considering Assumption 6.2 and using Young's inequality, we have

$$\begin{aligned} -2z_k^{\mathrm{T}}\boldsymbol{P}\boldsymbol{B}\boldsymbol{g}(\boldsymbol{x}_{1,k})\boldsymbol{H}(\boldsymbol{y}_{k,\tau}) &\le 2\big\|z_k^T\boldsymbol{P}\boldsymbol{B}\big\|\,\big\|\boldsymbol{g}(\boldsymbol{x}_{1,k})\boldsymbol{H}(\boldsymbol{y}_{k,\tau})\big\| \\ &\le \frac{n}{m_1\lambda}z_k^{\mathrm{T}}\boldsymbol{P}\boldsymbol{P}^{\mathrm{T}}\boldsymbol{z}_k + \frac{\lambda}{m_1}\sum_{j=1}^{n}\rho_j^2\big(y_{k,\tau_j}\big) \end{aligned} \tag{6.17}$$

$$2z_k^{\mathrm{T}}\boldsymbol{P}\boldsymbol{\Phi}_k(t) \le \frac{1}{\lambda}z_k^{\mathrm{T}}\boldsymbol{P}\boldsymbol{P}^{\mathrm{T}}z_k + \lambda D_0^2 \tag{6.18}$$

$$\begin{aligned} &-2z_k^{\mathrm{T}}\boldsymbol{P}\boldsymbol{B}\Big[\big\{\widetilde{\boldsymbol{W}}_{f,k}\big\}^{\mathrm{T}}\cdot\big\{\boldsymbol{\phi}_f\big(\hat{\boldsymbol{x}}_k\big)\big\}\Big] \\ &= -2\boldsymbol{z}_k^{\mathrm{T}}\boldsymbol{C}\boldsymbol{C}^{\mathrm{T}}\big(\boldsymbol{C}\boldsymbol{C}^{\mathrm{T}} + \delta\boldsymbol{I}_{2n}\big)^{-1}\boldsymbol{P}\boldsymbol{B}\Big[\big\{\widetilde{\boldsymbol{W}}_{f,k}\big\}^{\mathrm{T}}\cdot\big\{\boldsymbol{\phi}_j\big(\hat{\boldsymbol{x}}_k\big)\big\}\Big] \\ &\quad - 2z_k^{\mathrm{T}}\delta\boldsymbol{I}_{2n}\big(\boldsymbol{C}\boldsymbol{C}^T + \delta\boldsymbol{I}_{2n}\big)^{-1}\boldsymbol{P}\boldsymbol{B}\Big[\big\{\widetilde{\boldsymbol{W}}_{f,k}\big\}^{\mathrm{T}}\cdot\big\{\boldsymbol{\phi}_f\big(\hat{\boldsymbol{x}}_k\big)\big\}\Big] \\ &\le -2\tilde{\boldsymbol{y}}_k^{\mathrm{T}}\boldsymbol{C}^{\mathrm{T}}\big(\boldsymbol{C}\boldsymbol{C}^T + \delta\boldsymbol{I}_{2n}\big)^{-1}\boldsymbol{P}\boldsymbol{B}\Big[\big\{\widetilde{\boldsymbol{W}}_{f,k}\big\}^{\mathrm{T}}\cdot\big\{\boldsymbol{\phi}_f\big(\hat{\boldsymbol{x}}_k\big)\big\}\Big] \\ &\quad + \frac{\boldsymbol{z}_k^{\mathrm{T}}\boldsymbol{P}\boldsymbol{P}^{\mathrm{T}}\boldsymbol{z}_k}{\big\|\boldsymbol{C}\boldsymbol{C}^{\mathrm{T}} + \delta\boldsymbol{I}_{2n}\big\|^2} + \delta^2\sum_{i=1}^{n}l_{fi}\big\|\widetilde{\boldsymbol{W}}_{fi,k}\big\|^2 \end{aligned} \tag{6.19}$$

$$\begin{aligned} &-2z_k^{\mathrm{T}}\boldsymbol{P}\boldsymbol{B}\Big[\Big\{\widetilde{\overline{W}}_{g,k}(t)\Big\}^{\mathrm{T}}\cdot\big\{\overline{\boldsymbol{\phi}}_g\big(\boldsymbol{x}_{1,k}\big)\big\}\Big]\boldsymbol{u}_k \\ &= -2\boldsymbol{z}_k^{\mathrm{T}}\boldsymbol{C}\boldsymbol{C}^{\mathrm{T}}\big(\boldsymbol{C}\boldsymbol{C}^{\mathrm{T}} + \delta\boldsymbol{I}_{2n}\big)^{-1}\boldsymbol{P}\boldsymbol{B}\Big[\big\{\widetilde{\boldsymbol{W}}_{g,k}(t)\big\}^{\mathrm{T}}\cdot\big\{\overline{\boldsymbol{\phi}}_g\big(x_{1,k}\big)\big\}\Big]\boldsymbol{u}_k \\ &\quad - 2z_k^{\mathrm{T}}\delta\boldsymbol{I}_{2n}\big(\boldsymbol{C}\boldsymbol{C}^{\mathrm{T}} + \delta\boldsymbol{I}_{2n}\big)^{-1}\boldsymbol{P}\boldsymbol{B}\Big[\Big\{\widetilde{\overline{\boldsymbol{W}}}_{g,k}(t)\Big\}^{\mathrm{T}}\cdot\big\{\overline{\boldsymbol{\phi}}_g\big(x_{1,k}\big)\big\}\Big]\boldsymbol{u}_k \\ &= -2\tilde{\boldsymbol{y}}_k^{\mathrm{T}}\boldsymbol{C}^{\mathrm{T}}\big(\boldsymbol{C}\boldsymbol{C}^{\mathrm{T}} + \delta\boldsymbol{I}_{2n}\big)^{-1}\boldsymbol{P}\boldsymbol{B}\Big[\Big\{\widetilde{\overline{\boldsymbol{W}}}_{g,k}(t)\Big\}^{\mathrm{T}}\cdot\big\{\overline{\boldsymbol{\phi}}_{\boldsymbol{g}}\big(x_{1,k}\big)\big\}\Big]\boldsymbol{u}_k \\ &\quad + \frac{D_2^2\boldsymbol{z}_k^{\mathrm{T}}\boldsymbol{P}\boldsymbol{P}^{\mathrm{T}}\boldsymbol{z}_k}{\big\|\boldsymbol{C}\boldsymbol{C}^{\mathrm{T}} + \delta\boldsymbol{I}_{2n}\big\|^2} + \delta^2\sum_{i=1}^{n}\sum_{j=1}^{n}l_{gij}^2\Big\|\widetilde{\overline{W}}_{gjj,k}\Big\|^2 \end{aligned} \tag{6.20}$$

where, D_2 is the upper bound of control signal.

To deal with time-delay term, define the following Lyapunov–Krasovskii functional

$$V_{U_k}(t) = \frac{\lambda}{m_1(1-\kappa)}\sum_{j=1}^{n}\int_{t-\tau_j(t)}^{t}\rho_j^2\big(y_{j,k}(\sigma)\big)\mathrm{d}\sigma \tag{6.21}$$

Considering Assumption 6.1 and taking the time derivative of (6.21), it leads to

$$\begin{aligned} \dot{V}_{U_k}(t) &= \frac{\lambda}{m_1(1-\kappa)}\sum_{j=1}^{n}\rho_j^2\big(y_{j,k}\big) - \frac{\lambda}{m_1}\sum_{j=1}^{n}\frac{1-\dot{\tau}_j(t)}{(1-\kappa)}\rho_j^2\big(y_{k,\tau_j}\big) \\ &\le \frac{\lambda}{m_1(1-\kappa)}\sum_{j=1}^{n}\rho_j^2\big(y_{j,k}\big) - \frac{\lambda}{m_1}\sum_{j=1}^{n}\rho_j^2\big(y_{k,\tau_j}\big) \end{aligned} \tag{6.22}$$

Combining Eqs. (6.16)–(6.18) and Eq. (6.20) and considering inequality (6.7), it results in

$$\begin{aligned} &\dot{V}_{z_k} + \dot{V}_{U_k} \\ &\le z_k^{\mathrm{T}}\left(\boldsymbol{A}^{\mathrm{T}}\boldsymbol{P} + \boldsymbol{P}\boldsymbol{A} + \frac{n/m_1+1}{\lambda}\boldsymbol{P}^{\mathrm{T}}\boldsymbol{P} + \frac{D_2^2+1}{\|\boldsymbol{C}\boldsymbol{C}^{\mathrm{T}}+\delta\boldsymbol{I}_{2n}\|^2}\boldsymbol{P}^{\mathrm{T}}\boldsymbol{P}\right)\boldsymbol{z}_k \\ &+ 2\tilde{\boldsymbol{y}}_k^{\mathrm{T}}\boldsymbol{C}^{\mathrm{T}}\big(\boldsymbol{C}\boldsymbol{C}^{\mathrm{T}}+\delta\boldsymbol{I}_{2n}\big)^{-1}\boldsymbol{P}\boldsymbol{B}\Big[-\big\{\widetilde{\boldsymbol{W}}_{f,k}\big\}^{\mathrm{T}}\cdot\{\boldsymbol{\phi}_j(\hat{\boldsymbol{x}}_k)\} - \Big[\big\{\widetilde{\boldsymbol{W}}_{g,k}(t)\big\}^{\mathrm{T}}\cdot\{\overline{\boldsymbol{\phi}}_g(\boldsymbol{x}_{1,k})\}\Big]\boldsymbol{u}_k\Big] \\ &+ \delta^2\sum_{i=1}^{n} l_{fi}\big\|\widetilde{\boldsymbol{W}}_{fi,k}\big\|^2 + \delta^2\sum_{i=1}^{n}\sum_{j=1}^{n} l_{gij}^2\Big\|\tilde{\overline{W}}_{gij,k}\Big\|^2 + \frac{\lambda}{m_1(1-\kappa)}\sum_{j=1}^{n}\rho_j^2\big(y_{j,k}\big) + \lambda D_0^2 \\ &\le -z_k^{\mathrm{T}}\boldsymbol{Q}\boldsymbol{z}_k + \frac{\lambda}{m_1(1-\kappa)}\sum_{j=1}^{n}\rho_j^2\big(y_{j,k}\big) + \lambda D_0^2 \\ &- 2\tilde{\boldsymbol{y}}_k^{\mathrm{T}}\boldsymbol{C}^{\mathrm{T}}\big(\boldsymbol{C}\boldsymbol{C}^{\mathrm{T}}+\delta\boldsymbol{I}_{2n}\big)^{-1}\boldsymbol{P}\boldsymbol{B}\Big[\big\{\widetilde{\boldsymbol{W}}_{f,k}\big\}^{\mathrm{T}}\cdot\{\boldsymbol{\phi}_j(\hat{x}_k)\} + \Big[\Big\{\tilde{\overline{\boldsymbol{W}}}_{g,k}(t)\Big\}^{\mathrm{T}}\cdot\{\overline{\boldsymbol{\phi}}_g(x_{1,k})\}\Big]\boldsymbol{u}_k\Big] \\ &+ \delta^2\sum_{i=1}^{n} l_{fi}\big\|\widetilde{\boldsymbol{W}}_{fi,k}\big\|^2 + \delta^2\sum_{i=1}^{n}\sum_{j=1}^{n} l_{gj}^2\Big\|\tilde{\overline{W}}_{gij,k}\Big\|^2 \end{aligned} \tag{6.23}$$

6.4 AILC Design

Define errors as $\boldsymbol{e}_{1,k} = \big[e_{1,k}^1, \ldots, e_{1,k}^n\big]^{\mathrm{T}} = \hat{\boldsymbol{x}}_{1,k} - \boldsymbol{y}_d$, $\boldsymbol{e}_{2,k} = \big[e_{2,k}^1, \ldots, e_{2,k}^n\big]^{\mathrm{T}} = \hat{\boldsymbol{x}}_{2,k} - \dot{\boldsymbol{y}}_d$, $\boldsymbol{e}_k = \big[\boldsymbol{e}_{1,k}^{\mathrm{T}}, \boldsymbol{e}_{2,k}^{\mathrm{T}}\big]^{\mathrm{T}}$, and make following assumptions.

Assumption 6.7 $z_{i,k}(0) = 0, i = 1, 2, \ldots, n.$

Assumption 6.8 Identical initial condition is not necessary for $\boldsymbol{e}_{i,k}$, i.e., the initial state errors $\boldsymbol{e}_{i,k}(0)$ at each iteration are not necessarily zero small and fixed, but assumed to be bounded.

Define a filtered tracking error as $\boldsymbol{e}_{sk} = \big[e_{sk,1}, \ldots, e_{sk,n}\big]^{\mathrm{T}} = [\boldsymbol{\Lambda}\ I_n]\boldsymbol{e}_k$, where $\boldsymbol{\Lambda}$ is a diagonal matrix:

$$\boldsymbol{\Lambda} = \begin{bmatrix} \lambda_1 & & \\ & \ddots & \\ & & \lambda_n \end{bmatrix}$$

$\lambda_1, \ldots, \lambda_n$ are chosen such that the polynomial $H_i(s) = s + \lambda_i$ is Hurwitz. It is obvious that if $\boldsymbol{e}_{sk}$ approaches zero as $k \to \infty$, then $\|\boldsymbol{e}_k\|$ will converges to the origin asymptotically.

According to Assumption 6.8, there exist known constants ε_1^i and ε_2^i, such that $\left|e_{1,k}^i(0)\right| \le \varepsilon_1^i$, $\left|e_{2,k}^i(0)\right| \le \varepsilon_2^i$, $i = 1, 2, \ldots, n$, $\forall k \in N$. Employing boundary layer function, define auxiliary error as $\boldsymbol{s}_k = \left[s_{1,k}, \ldots, s_{n,k}\right]^{\mathrm{T}}$, where,

$$s_{i,k} = e_{sk,i} - \eta_i(t)\mathrm{sat}\left(\frac{e_{sk,i}}{\eta_i(t)}\right) \tag{6.24}$$

$$\eta_i(t) = \varepsilon_i e^{-Kt}, i = 1, \ldots, n \tag{6.25}$$

with $\varepsilon_i = \lambda_i \varepsilon_1^i + \varepsilon_2^i$, $K > 0$, The saturation function sat($\cdot$) is specified by

$$\mathrm{sat}\left(\frac{e_{sk,i}}{\eta_i(t)}\right) = \mathrm{sgn}\left(e_{sk,i}\right)\min\left\{\left|e_{sk,i}\big/\eta_i(t)\right|, 1\right\} \tag{6.26}$$

According to initial condition, we can easily obtain

$$\begin{aligned}\left|e_{sk,i}(0)\right| &= \left|\lambda_i e_{1,k}^i(0) + e_{2,k}^i(0)\right| \\ &\le \lambda_i\left|e_{1,k}^i(0)\right| + \left|e_{2,k}^i(0)\right| \\ &\le \lambda_i \varepsilon_1^i + \varepsilon_2^i = \eta_i(0)\end{aligned} \tag{6.27}$$

which implies that $s_{i,k}(0) = e_{sk,i}(0) - \eta_i(0)e_{sk,i}(0)\big/\eta_i(0) = 0$ for any $k \in \mathbf{N}$. For further use, we give the following equality

$$\begin{aligned}s_{i,k}\mathrm{sat}\left(\frac{e_{sk,i}}{\eta_i(t)}\right) &= \begin{cases}0, & if\ \left|e_{sk,i}\big/\eta_i(t)\right| \le 1 \\ s_{i,k}\mathrm{sgn}\left(e_{sk,i}\right), & if\ \left|e_{sk,i}\big/\eta_i(t)\right| > 1\end{cases} \\ &= s_{i,k}\mathrm{sgn}\left(s_{i,k}\right) = \left|s_{i,k}\right|\end{aligned} \tag{6.28}$$

To continue the design procedure, we rewrite the observer as

$$\begin{cases}\dot{\hat{x}}_{1,k} = \boldsymbol{K}_1 z_{1,k} + \hat{\boldsymbol{x}}_{2,k} \\ \dot{\hat{x}}_{2,k} = \boldsymbol{K}_2 z_{1,k} + \left\{\widehat{\boldsymbol{W}}_{f,k}(t)\right\}^{\mathrm{T}} \cdot \left\{\boldsymbol{\phi}_f\left(\hat{\boldsymbol{x}}_k\right)\right\} + \left[\left\{\widehat{\overline{\boldsymbol{W}}}_{g,k}(t)\right\}^{\mathrm{T}} \cdot \left\{\overline{\boldsymbol{\phi}}_g\left(\boldsymbol{x}_{1,k}\right)\right\}\right]\boldsymbol{u}_k - \boldsymbol{u}_{rk}\end{cases} \tag{6.29}$$

Define a Lyapunov function as

$$V_{s_k} = \frac{1}{2}\boldsymbol{s}_k^{\mathrm{T}}\boldsymbol{s}_k \tag{6.30}$$

Taking the derivative of V_{s_k} with respective to time, it yields

$$
\begin{aligned}
\dot{V}_{s_k} &= \boldsymbol{s}_k^{\mathrm{T}} \dot{\boldsymbol{s}}_k \\
&= \sum_{i=1}^{n} S_{i,k} \dot{S}_{i,k} \\
&= \sum_{i=1}^{n} \begin{cases} s_{i,k}\big(\dot{e}_{sk,i} - \dot{\eta}_i(t)\big), & \text{if } e_{sk,i} > \eta_i(t) \\ 0, & \text{if } \left|e_{sk,i}\right| \le \eta_i(t) \\ s_{i,k}\big(\dot{e}_{sk,i} + \dot{\eta}_i(t)\big), & \text{if } e_{sk,i} < -\eta_i(t) \end{cases} \\
&= \sum_{i=1}^{n} s_{i,k}\big(\dot{e}_{sk,i} - \dot{\eta}_i(t)\mathrm{sgn}(s_{i,k})\big) \\
&= \boldsymbol{s}_k^{\mathrm{T}}\Big(\dot{\boldsymbol{e}}_{sk} - \dot{\boldsymbol{\eta}}(t)\mathrm{sgn}(s_k)\Big) \\
&= \boldsymbol{s}_k^{\mathrm{T}}\Big[\boldsymbol{\Lambda}\big(\boldsymbol{K}_1 \boldsymbol{z}_{1,k} + \boldsymbol{e}_{2,k}\big) + \boldsymbol{K}_2 \boldsymbol{z}_{1,k} + \Big\{\hat{\boldsymbol{W}}_{f,k}(t)\Big\}^{\mathrm{T}} \cdot \big\{\boldsymbol{\phi}_f\big(\hat{\boldsymbol{x}}_k\big)\big\} \\
&\quad + \Big[\Big\{\hat{\overline{\boldsymbol{W}}}_{g,k}(t)\Big\}^{\mathrm{T}} \cdot \big\{\overline{\boldsymbol{\phi}}_g\big(\boldsymbol{x}_{1,k}\big)\big\}\Big]\boldsymbol{u}_k - \boldsymbol{u}_{rk} - \ddot{\boldsymbol{y}}_d + K\boldsymbol{\eta}(t)\mathrm{sgn}(\boldsymbol{s}_k)\Big] \\
&= \boldsymbol{s}_k^{\mathrm{T}}\Big[\boldsymbol{\Lambda}\big(\boldsymbol{K}_1 \boldsymbol{z}_{1,k} + \boldsymbol{e}_{2,k}\big) + \boldsymbol{K}_2 \boldsymbol{z}_{1,k} + K\boldsymbol{e}_{sk} + \Big\{\hat{\boldsymbol{W}}_{f,k}(t)\Big\}^{\mathrm{T}} \cdot \big\{\boldsymbol{\phi}_f\big(\hat{\boldsymbol{x}}_k\big)\big\} \\
&\quad + \Big[\Big\{\hat{\overline{\boldsymbol{W}}}_{g,k}(t)\Big\}^{\mathrm{T}} \cdot \big\{\overline{\boldsymbol{\phi}}_g\big(\boldsymbol{x}_{1,k}\big)\big\}\Big]\boldsymbol{u}_k - \boldsymbol{u}_{rk} - \ddot{\boldsymbol{y}}_d\Big] - K\boldsymbol{s}_k^{\mathrm{T}}\boldsymbol{s}_k
\end{aligned} \tag{6.31}
$$

where, $\boldsymbol{\eta}(t) = [\eta_1(t), \ldots, \eta_n(t)]^{\mathrm{T}}$, $\mathrm{sgn}(\boldsymbol{s}_k) = \big[\mathrm{sgn}(s_{1,k}), \ldots, sgn(s_{n,k})\big]^{\mathrm{T}}$, and utilizing the following relation

$$
\begin{aligned}
& s_{i,k}\big(-Ke_{sk,i} + K\eta_i(t)\mathrm{sgn}(s_{i,k})\big) \\
&\quad = s_{i,k}\big(-Ks_{i,k} - K\eta_i(t)\mathrm{sat}\big(e_{sk,i}/\eta_i(t)\big) + K\eta_i(t)\mathrm{sgn}(s_{i,k})\big) \\
&\quad = -Ks_{i,k}^2 - K\eta_i(t)\left|s_{i,k}\right| + K\eta_i(t)\left|s_{i,k}\right| \\
&\quad = -Ks_{i,k}^2
\end{aligned} \tag{6.32}
$$

Choose the Lyapunov candidate for the whole closed-loop system as $V_k = V_{z_k} + V_{U_k} + V_{s_k}$, combining Eqs. (6.23) and (6.31), we can obtain the derivative of V_k as follows

$$
\begin{aligned}
\dot{V}_k \le & -\boldsymbol{z}_k^{\mathrm{T}}\boldsymbol{Q}\boldsymbol{z}_k + \frac{\lambda}{m_1(1-\kappa)}\sum_{j=1}^{n}\rho_j^2\big(y_{j,k}\big) \\
& + \lambda D_0^2 + \delta^2\sum_{i=1}^{n} l_{fi}\left\|\widetilde{\boldsymbol{W}}_{f,k}\right\|^2 + \delta^2\sum_{i=1}^{n}\sum_{j=1}^{n} l_{gjj}^2\left\|\widetilde{\overline{\boldsymbol{W}}}_{gj,k}\right\|^2 \\
& - 2\widetilde{\boldsymbol{y}}_k^{\mathrm{T}}\boldsymbol{C}^{\mathrm{T}}\big(\boldsymbol{C}\boldsymbol{C}^{\mathrm{T}} + \delta\boldsymbol{I}_{2n}\big)^{-1}
\end{aligned}
$$

$$\times \boldsymbol{PB}\Big[\big\{\widetilde{\boldsymbol{W}}_{f,k}\big\}^{\mathrm{T}}\cdot\big\{\boldsymbol{\phi}_f(\widehat{\boldsymbol{x}}_k)\big\}+\Big[\big\{\widetilde{\boldsymbol{W}}_{g,k}(t)\big\}^{\mathrm{T}}\cdot\big\{\overline{\boldsymbol{\phi}}_g(x_{1,k})\big\}\Big]\boldsymbol{u}_k\Big]$$
$$+\boldsymbol{s}_k^{\mathrm{T}}\Big[\boldsymbol{\Lambda}\big(\boldsymbol{K}_1 z_{1,k}+\boldsymbol{e}_{2,k}\big)+\boldsymbol{K}_2 z_{1,k}+\boldsymbol{K}\boldsymbol{e}_{sk}+\Big\{\widehat{\boldsymbol{W}}_{f,k}(t)\Big\}^{\mathrm{T}}\cdot\big\{\boldsymbol{\phi}_f(\widehat{\boldsymbol{x}}_k)\big\}$$
$$+\Big[\Big\{\hat{\overline{\boldsymbol{W}}}_{g,k}(t)\Big\}^{\mathrm{T}}\cdot\big\{\overline{\boldsymbol{\phi}}_g(\boldsymbol{x}_{1,k})\big\}\Big]\boldsymbol{u}_k-\boldsymbol{u}_{rk}-\ddot{\boldsymbol{y}}_d\Big]-K\boldsymbol{s}_k^{\mathrm{T}}\boldsymbol{s}_k \tag{6.33}$$

For the convenience of expression, denote $\Xi(y_k)\triangleq\frac{\lambda}{m_1(1-\kappa)}\sum_{j=1}^{n}\rho_j^2(y_k)+\lambda D_0^2$. To avoid possible singularity possible, employing the hyperbolic tangent function leads to

$$\dot{V}_k\le-\lambda_{\min}(\boldsymbol{Q})\|\boldsymbol{z}_k\|^2+\delta^2\sum_{i=1}^{n}l_{fi}\left\|\tilde{\boldsymbol{W}}_{fi,k}\right\|^2+\delta^2\sum_{i=1}^{n}\sum_{j=1}^{n}l_{gij}^2\left\|\tilde{\overline{\boldsymbol{W}}}_{gij,k}\right\|^2$$
$$-2\tilde{\boldsymbol{y}}_k^{\mathrm{T}}\boldsymbol{C}^{\mathrm{T}}\big(\boldsymbol{C}\boldsymbol{C}^T+\delta\boldsymbol{I}_{2n}\big)^{-1}\boldsymbol{PB}\left[\begin{array}{l}\Big\{\tilde{\boldsymbol{W}}_{f,k}\Big\}^{\mathrm{T}}\cdot\big\{\boldsymbol{\phi}_f(\hat{\boldsymbol{x}}_k)\big\}\\ +\Big[\Big\{\tilde{\overline{\boldsymbol{W}}}_{g,k}(t)\Big\}^{\mathrm{T}}\cdot\big\{\overline{\phi}_g(\boldsymbol{x}_{1,k})\big\}\Big]\boldsymbol{u}_k\end{array}\right]$$
$$+\boldsymbol{s}_k^{\mathrm{T}}\big[\boldsymbol{\Lambda}\big(\boldsymbol{K}_1\boldsymbol{z}_{1,k}+\boldsymbol{e}_{2,k}\big)+\boldsymbol{K}_2\boldsymbol{z}_{1,k}+K\boldsymbol{e}_{sk}$$
$$+\Big\{\hat{\boldsymbol{W}}_{f,k}(t)\Big\}^{\mathrm{T}}\cdot\big\{\boldsymbol{\phi}_f(\hat{\boldsymbol{x}}_k)\big\}+\Big[\Big\{\hat{\overline{\boldsymbol{W}}}_{g,k}(t)\Big\}^{\mathrm{T}}\cdot\big\{\overline{\phi}_g(\boldsymbol{x}_{1,k})\big\}\Big]\boldsymbol{u}_k$$
$$-u_{rk}-\ddot{y}_d+\frac{1}{n}b\,\mathbf{Tanh}\big(s_k/\eta(t)\big)\boldsymbol{s}_k^{-1}\Xi(y_k)\Big]$$
$$+\frac{1}{n}\sum_{i=1}^{n}\big[1-b\tanh^2\big(s_{i,k}/\eta_i(t)\big)\big]\Xi(y_k)-K\boldsymbol{s}_k^T\boldsymbol{s}_k \tag{6.34}$$

where,

$$\mathbf{Tanh}\big(\boldsymbol{s}_k/\eta(t)\big)=\begin{bmatrix}\tanh^2\big(s_{1,k}/\eta_1(t)\big) & & \\ & \ddots & \\ & & \tanh^2\big(s_{n,k}/\eta_n(t)\big)\end{bmatrix}$$

Obviously, $b\mathbf{Tanh}\big(\boldsymbol{s}_k/\eta(t)\big)\boldsymbol{s}_k^{-1}\Xi(y_k)$ is continuous and well-defined on the compact set $\boldsymbol{\Omega}_\Xi=\big\{\hat{\boldsymbol{x}}_k,\boldsymbol{x}_d,\boldsymbol{y}_k\big\}\subset\mathbf{R}^{5n}$, so it can be approximated by the following RBF NN

$$b\mathbf{Tanh}\big(\boldsymbol{s}_k/\eta(t)\big)\boldsymbol{s}_k^{-1}\Xi(y_k)/n=\begin{bmatrix}\boldsymbol{W}_{\Xi1}^{*T}\boldsymbol{\phi}_{\Xi1}(\boldsymbol{Z}_k)+\varepsilon_{\Xi1}(\boldsymbol{Z}_k)\\ \vdots\\ \boldsymbol{W}_{\Xi n}^{*T}\boldsymbol{\phi}_{\Xi n}(\boldsymbol{Z}_k)+\varepsilon_{\Xi n}(\boldsymbol{Z}_k)\end{bmatrix}$$

$$= \begin{bmatrix} \overline{W}^{*T}_{\Xi 1}\overline{\phi}_{\Xi 1}(Z_k) \\ \vdots \\ \overline{W}^{*T}_{\Xi n}\overline{\phi}_{\Xi n}(Z_k) \end{bmatrix} = \left\{\overline{W}^{*}_{\Xi}\right\}^{\mathrm{T}} \cdot \left\{\overline{\phi}_{\Xi}(Z_k)\right\}$$

where, $Z_k = \left[\hat{x}_k^{\mathrm{T}}, x_d^{\mathrm{T}}, y_k^{\mathrm{T}}\right]^{\mathrm{T}}$, $W^*_{\Xi i} \in \mathbf{R}^{l_{\Xi i}}$, $\phi_{\Xi i}(Z_k) \in \mathbf{R}^{l_{\Xi i}}$, $\overline{W}^*_{\Xi i} = \left[W^{*\mathrm{T}}_{\Xi i}, \varepsilon_{\Xi i}(Z_k)\right]^{\mathrm{T}}$, $\overline{\phi}_{\Xi i}(Z_k) = \left[\phi^{\mathrm{T}}_{\Xi i}(Z_k), 1\right]^{\mathrm{T}}$, $i = 1, \ldots, n$, then we can further obtain

$$\begin{aligned}
\dot{V}_k \le & -\lambda_{\min}(Q)\|z_k\|^2 + \delta^2 \sum_{i=1}^{n} l_{fi}\left\|\tilde{W}_{fi,k}\right\|^2 + \delta^2 \sum_{i=1}^{n}\sum_{j=1}^{n} l^2_{gij}\left\|\tilde{\overline{W}}_{gij,k}\right\|^2 \\
& - 2\tilde{y}_k^{\mathrm{T}} C^{\mathrm{T}}\left(CC^{\mathrm{T}} + \delta I_{2n}\right)^{-1} \\
& \times PB\left[\left\{\tilde{W}_{f,k}\right\}^{\mathrm{T}} \cdot \left\{\phi_f(\hat{x}_k)\right\} + \left[\left\{\tilde{\overline{W}}_{g,k}(t)\right\}^{\mathrm{T}} \cdot \left\{\overline{\phi}_g(x_{1,k})\right\}\right]u_k\right] \\
& + s_k^{\mathrm{T}}\left[\Lambda\left(K_1 z_{1,k} + e_{2,k}\right) + K_2 z_{1,k} + K e_{sk} + \left\{\hat{W}_{f,k}(t)\right\}^{\mathrm{T}} \cdot \left\{\phi_f(\hat{x}_k)\right\}\right. \\
& + \left[\left\{\hat{\overline{W}}_{g,k}(t)\right\}^{\mathrm{T}} \cdot \left\{\overline{\phi}_g(x_{1,k})\right\}\right]u_k - u_{rk} \\
& - \ddot{y}_d + \left\{\overline{W}^{*}_{\Xi}\right\}^{\mathrm{T}} \cdot \left\{\overline{\phi}_{\Xi}(Z_k)\right\} - \left\{\hat{\overline{W}}_{\Xi}\right\}^{\mathrm{T}} \cdot \left\{\overline{\phi}_{\Xi}(Z_k)\right\} \\
& \left. + \left\{\hat{\overline{W}}_{\Xi}\right\}^{\mathrm{T}} \cdot \left\{\overline{\phi}_{\Xi}(Z_k)\right\}\right] + \frac{1}{n}\sum_{i=1}^{n}\left[1 - b\tanh^2\left(s_{i,k}/\eta_i(t)\right)\right]\Xi(y_k) - K s_k^{\mathrm{T}} s_k \\
= & -\lambda_{\min}(Q)\|z_k\|^2 + \delta^2 \sum_{i=1}^{n} l_{fi}\left\|\tilde{W}_{fi,k}\right\|^2 + \delta^2 \sum_{i=1}^{n}\sum_{j=1}^{n} l^2_{gij}\left\|\tilde{\overline{W}}_{gij,k}\right\|^2 \\
& - 2\tilde{y}_k^{\mathrm{T}} C^{\mathrm{T}}\left(CC^{\mathrm{T}} + \delta I_{2n}\right)^{-1} \\
& \times PB\left[\left\{\tilde{W}_{f,k}\right\}^{\mathrm{T}} \cdot \left\{\phi_f(\hat{x}_k)\right\} + \left[\left\{\tilde{\overline{W}}_{g,k}(t)\right\}^{\mathrm{T}} \cdot \left\{\overline{\phi}_g(x_{1,k})\right\}\right]u_k\right] \\
& - s_k^{\mathrm{T}}\left[\left\{\tilde{\overline{W}}_{\Xi,k}\right\}^{\mathrm{T}} \cdot \left\{\overline{\phi}_{\Xi}(Z_k)\right\}\right] + s_k^{\mathrm{T}}\left[\Lambda\left(K_1 z_{1,k} + e_{2,k}\right) + K_2 z_{1,k} + K e_{sk}\right. \\
& \times \left\{\hat{W}_{f,k}(t)\right\}^{\mathrm{T}} \cdot \left\{\phi_f(\hat{x}_k)\right\} + \left[\left\{\hat{\overline{W}}_{g,k}(t)\right\}^{\mathrm{T}} \cdot \left\{\overline{\phi}_g(x_{1,k})\right\}\right]u_k - u_{rk} \\
& \left. - \ddot{y}_d + \left\{\hat{\overline{W}}_{\Xi}\right\}^{\mathrm{T}} \cdot \left\{\overline{\phi}_{\Xi}(Z_k)\right\}\right] + \frac{1}{n}\sum_{i=1}^{n}\left[1 - b\tanh^2\left(s_{i,k}/\eta_i(t)\right)\right]\Xi(y_k) - K s_k^{\mathrm{T}} s_k
\end{aligned} \tag{6.35}$$

For convenience of presentation, denote $\Upsilon_k = -\Lambda\left(K_1 z_{1,k} + e_{2,k}\right) - K_2 z_{1,k} - K e_{sk} - \left\{\hat{W}_{f,k}(t)\right\}^{\mathrm{T}} \cdot \left\{\phi_f(\hat{x}_k)\right\} + \ddot{y}_d - \left\{\hat{\overline{W}}_{\Xi}\right\}^{\mathrm{T}} \cdot \left\{\overline{\phi}_{\Xi}(Z_k)\right\}$. Then, we can design the output feedback controller as follows

$$u_k = \left[\left\{\hat{\overline{W}}_{g,k}(t)\right\}^{\mathrm{T}} \bullet \left\{\overline{\phi}_g(x_{1,k})\right\}\right]^{-1} \Upsilon_k \tag{6.36}$$

$$u_{rk} = 0 \tag{6.37}$$

Obviously, singularity problem occurs when using the matrix inversion. To avoid singularity of the control law (6.37) in the case that $\hat{\overline{W}}_{gk}^{T}(t)\overline{\phi}_g(x_{1,k})$ is not invertible, the control law is modified as follows

$$u_k = \left[\left\{\hat{\overline{W}}_{g,k}(t)\right\}^{\mathrm{T}} \cdot \{\overline{\phi}_g(x_{1,k})\}\right]\left[\delta_1 I_n + \left[\left\{\hat{\overline{W}}_{g,k}(t)\right\}^{\mathrm{T}} \cdot \{\overline{\phi}_g(x_{1,k})\}\right]^{\mathrm{T}}\left[\left\{\hat{\overline{W}}_{g,k}(t)\right\}^{\mathrm{T}} \cdot \{\overline{\phi}_g(x_{1,k})\}\right]\right]^{-1}\Upsilon_k \tag{6.38}$$

where, δ_1 is a small positive constant, Then, substituting the controller (6.38) back into (6.35) yields

$$\begin{aligned}
\dot{V}_k \le & -\lambda_{\min}(Q)\|z_k\|^2 + \delta^2\sum_{i=1}^{n} l_{fi}\left\|\tilde{W}_{fi,k}\right\|^2 + \delta^2\sum_{i=1}^{n}\sum_{j=1}^{n} l_{gij}^2\left\|\tilde{\overline{W}}_{gij,k}\right\|^2 \\
& - 2\tilde{y}_k^{\mathrm{T}} C^{\mathrm{T}}\left(CC^{\mathrm{T}} + \delta I_{2n}\right)^{-1} PB\left[\left\{\tilde{W}_{f,k}\right\}^{\mathrm{T}} \cdot \{\phi_f(\hat{x}_k)\} + \left[\left\{\tilde{\overline{W}}_{g,k}(t)\right\}^{\mathrm{T}} \cdot \{\overline{\phi}_g(x_{1,k})\}\right]u_k\right] \\
& - s_k^{\mathrm{T}}\left[\left\{\tilde{\overline{W}}_{\Xi,k}\right\}^{\mathrm{T}} \cdot \{\overline{\phi}_{\Xi}(Z_k)\}\right] \\
& + s_k^{T}\left\{-u_{rk} - \delta I_n\left[\delta I_n + \left[\left\{\hat{\overline{W}}_{g,k}(t)\right\}^{\mathrm{T}} \cdot \{\overline{\phi}_g(x_{1,k})\}\right]^{\mathrm{T}}\left[\left\{\hat{\overline{W}}_{g,k}(t)\right\}^{\mathrm{T}} \cdot \{\overline{\phi}_g(x_{1,k})\}\right]\right]^{-1}\Upsilon_k\right\} \\
& + \frac{1}{n}\sum_{i=1}^{n}\left[1 - b\tanh^2\left(s_{i,k}/\eta_i(t)\right)\right]\Xi(y_k) - K s_k^{\mathrm{T}} s_k \\
\le & -\lambda_{\min}(Q)\|z_k\|^2 + \delta^2\sum_{i=1}^{n} l_{fi}\left\|\tilde{W}_{fi,k}\right\|^2 + \delta^2\sum_{i=1}^{n}\sum_{j=1}^{n} l_{gij}^2\left\|\tilde{\overline{W}}_{gij,k}\right\|^2 - s_k^{\mathrm{T}}\left[\left\{\tilde{\overline{W}}_{\Xi,k}\right\}^{\mathrm{T}} \cdot \{\overline{\phi}_{\Xi}(Z_k)\}\right] \\
& - 2\tilde{y}_k^{\mathrm{T}} C^{\mathrm{T}}\left(CC^{\mathrm{T}} + \delta I_{2n}\right)^{-1} PB\left[\left\{\tilde{W}_{f,k}\right\}^{\mathrm{T}} \cdot \{\phi_f(\hat{x}_k)\} + \left[\left\{\tilde{\overline{W}}_{g,k}(t)\right\}^{\mathrm{T}} \cdot \{\overline{\phi}_g(x_{1,k})\}\right]u_k\right] \\
& + \|s_k\|\|\Upsilon_k\|\delta\left[\delta I_n + \left[\left\{\hat{\overline{W}}_{g,k}(t)\right\}^{\mathrm{T}} \cdot \{\overline{\phi}_g(x_{1,k})\}\right]^{\mathrm{T}}\left[\left\{\hat{\overline{W}}_{g,k}(t)\right\}^{\mathrm{T}} \cdot \{\overline{\phi}_g(x_{1,k})\}\right]\right]^{-1} - s_k^{\mathrm{T}} u_{rk} \\
& + \frac{1}{n}\sum_{i=1}^{n}\left[1 - b\tanh^2\left(s_{i,k}/\eta_i(t)\right)\right]\Xi(y_k) - K s_k^{\mathrm{T}} s_k
\end{aligned} \tag{6.39}$$

where using the matrix relationship $GG^{\mathrm{T}}\left[\delta_1 I_n + GG^{\mathrm{T}}\right]^{-1} = I_n - \delta_1\left[\delta_1 I_n + GG^{\mathrm{T}}\right]^{-1}$.

Design u_{rk} as

$$\begin{aligned}
u_{rk} = & \delta_1\left[\delta_1 I_n + \left[\left\{\hat{\overline{W}}_{g,k}(t)\right\}^{\mathrm{T}} \cdot \{\overline{\phi}_g(x_{1,k})\}\right]^{\mathrm{T}}\left[\left\{\hat{\overline{W}}_{g,k}(t)\right\}^{\mathrm{T}} \cdot \{\overline{\phi}_g(x_{1,k})\}\right]\right]^{-1}\Upsilon_k \\
& \times \tanh\left(\frac{s_k^{\mathrm{T}}\delta_1\left[\delta_1 I_n + \left[\left\{\hat{\overline{W}}_{g,k}(t)\right\}^{\mathrm{T}} \cdot \{\overline{\phi}_g(x_{1,k})\}\right]^{\mathrm{T}}\left[\left\{\hat{\overline{W}}_{g,k}(t)\right\}^{\mathrm{T}} \cdot \{\overline{\phi}_g(x_{1,k})\}\right]\right]^{-1}\Upsilon_k}{\Delta_k}\right)
\end{aligned} \tag{6.40}$$

Where Δ_k is the convergent series sequence define in Sect. 5.3.

According to Lemma 5.2, we can know

$$
\begin{aligned}
\dot{V}_k \le & -\lambda_{\min}(\boldsymbol{Q})\|\boldsymbol{z}_k\|^2 + \delta^2 \sum_{i=1}^{n} l_{fi} \left\| \tilde{\boldsymbol{W}}_{fi,k} \right\|^2 \\
& + \delta^2 \sum_{i=1}^{n} \sum_{j=1}^{n} l_{gij}^2 \left\| \tilde{\overline{\boldsymbol{W}}}_{gij,k} \right\|^2 - s_k^{\mathrm{T}} \left[\left\{ \tilde{\overline{\boldsymbol{W}}}_{\Xi,k} \right\}^{\mathrm{T}} \cdot \left\{ \overline{\boldsymbol{\phi}}_{\Xi}(\boldsymbol{Z}_k) \right\} \right] \\
& - 2\tilde{\boldsymbol{y}}_k^{\mathrm{T}} \boldsymbol{C}^{\mathrm{T}} \left(\boldsymbol{C}\boldsymbol{C}^{\mathrm{T}} + \delta \boldsymbol{I}_{2n} \right)^{-1} \\
& \times \boldsymbol{P}\boldsymbol{B} \left[\left\{ \tilde{\boldsymbol{W}}_{f,k} \right\}^{\mathrm{T}} \cdot \left\{ \boldsymbol{\phi}_f(\hat{\boldsymbol{x}}_k) \right\} + \left[\left\{ \tilde{\overline{\boldsymbol{W}}}_{g,k}(t) \right\}^{\mathrm{T}} \cdot \left\{ \overline{\boldsymbol{\phi}}_g(\boldsymbol{x}_{1,k}) \right\} \right] \boldsymbol{u}_k \right] \\
& + \theta \Delta_k + \frac{1}{n} \sum_{i=1}^{n} \left[1 - b \tanh^2 \left(s_{i,k} / \eta_i(t) \right) \right] \Xi(y_k) - K \boldsymbol{s}_k^{\mathrm{T}} \boldsymbol{s}_k
\end{aligned} \tag{6.41}
$$

The difference type and differential-difference type update algorithms are designed as

$$
\begin{cases}
(1-\gamma_1)\left\{ \dot{\hat{\boldsymbol{W}}}_{f,k}(t) \right\} = -(\gamma_1 + \alpha_1)\left\{ \hat{\boldsymbol{W}}_{f,k}(t) \right\} + \gamma_1 \left\{ \hat{\boldsymbol{W}}_{f,k-1}(t) \right\} \\
\qquad + 2\tilde{\boldsymbol{y}}_k^{\mathrm{T}} \boldsymbol{C}^{T} \left(\boldsymbol{C}\boldsymbol{C}^{T} + \delta \boldsymbol{I}_{2n} \right)^{-1} \boldsymbol{P}\boldsymbol{B} \cdot \left\{ \boldsymbol{\phi}_f(\hat{\boldsymbol{x}}_k) \right\} \\
\left\{ \hat{\boldsymbol{W}}_{f,k}(0) \right\} = \left\{ \hat{\boldsymbol{W}}_{f,k-1}(T) \right\}, \left\{ \hat{\boldsymbol{W}}_{f,0}(t) \right\} = 0, t \in [0, T]
\end{cases} \tag{6.42}
$$

$$
\begin{cases}
(1-\gamma_2)\left\{ \dot{\hat{\overline{\boldsymbol{W}}}}_{g,k}(t) \right\} = -(\gamma_2 + \alpha)\left\{ \hat{\overline{\boldsymbol{W}}}_{g,k}(t) \right\} + \gamma_2 \left\{ \hat{\overline{\boldsymbol{W}}}_{g,k-1}(t) \right\} \\
\qquad + 2\tilde{\boldsymbol{y}}_k^{\mathrm{T}} \boldsymbol{C}^{\mathrm{T}} \left(\boldsymbol{C}\boldsymbol{C}^{T} + \delta \boldsymbol{I}_{2n} \right)^{-1} \boldsymbol{P}\boldsymbol{B}\boldsymbol{u}_k \cdot \left\{ \overline{\boldsymbol{\phi}}_g(\boldsymbol{x}_{1,k}) \right\} \\
\left\{ \hat{\overline{\boldsymbol{W}}}_{g,k}(0) \right\} = \left\{ \hat{\overline{\boldsymbol{W}}}_{g,k-1}(T) \right\}, \left\{ \hat{\boldsymbol{W}}_{g,0}(t) \right\} \neq 0, t \in [0, T]
\end{cases} \tag{6.43}
$$

$$
\begin{cases}
(1-\gamma_3)\left\{ \dot{\hat{\overline{\boldsymbol{W}}}}_{\Xi,k} \right\} = -\gamma_3 \left\{ \hat{\overline{\boldsymbol{W}}}_{\Xi,k} \right\} + \gamma_3 \left\{ \hat{\overline{\boldsymbol{W}}}_{\Xi,k-1} \right\} + q_3 \boldsymbol{s}_k^{\mathrm{T}} \cdot \left\{ \overline{\boldsymbol{\phi}}_{\Xi}(\boldsymbol{Z}_k) \right\} \\
\left\{ \hat{\overline{\boldsymbol{W}}}_{\Xi,k}(0) \right\} = \left\{ \hat{\overline{\boldsymbol{W}}}_{\Xi,k-1}(T) \right\}, \left\{ \hat{\overline{\boldsymbol{W}}}_{\Xi,0}(t) \right\} = 0, t \in [0, T]
\end{cases} \tag{6.44}
$$

where, $q_1, q_2, q_3 > 0, 0 < \gamma_1, \gamma_2, \gamma_3 < 1, \alpha > 0$.

Inequality (6.41) can be rewritten as follows

$$
\begin{aligned}
& 2\tilde{\boldsymbol{y}}_k^{\mathrm{T}} \boldsymbol{C}^{\mathrm{T}} \left(\boldsymbol{C}\boldsymbol{C}^{\mathrm{T}} + \delta \boldsymbol{I}_{2n} \right)^{-1} \\
& \quad \times \boldsymbol{P}\boldsymbol{B} \left[\left\{ \tilde{\boldsymbol{W}}_{f,k} \right\}^{\mathrm{T}} \cdot \left\{ \boldsymbol{\phi}_f(\hat{\boldsymbol{x}}_k) \right\} + \left[\left\{ \tilde{\overline{\boldsymbol{W}}}_{g,k}(t) \right\}^{\mathrm{T}} \cdot \left\{ \overline{\boldsymbol{\phi}}_g(\boldsymbol{x}_{1,k}) \right\} \right] \boldsymbol{u}_k \right] \\
& \quad + s_k^{\mathrm{T}} \left[\left\{ \tilde{\overline{\boldsymbol{W}}}_{\Xi,k} \right\}^{\mathrm{T}} \cdot \left\{ \overline{\boldsymbol{\phi}}_{\Xi}(\boldsymbol{Z}_k) \right\} \right]
\end{aligned}
$$

$$\leq -\dot{V}_k - \lambda_{\min}(\boldsymbol{Q})\|\boldsymbol{z}_k\|^2 + \delta^2\sum_{i=1}^{n} l_{fi}\left\|\tilde{\boldsymbol{W}}_{fi,k}\right\|^2 + \delta^2\sum_{i=1}^{n}\sum_{j=1}^{n} l_{gij}^2\left\|\tilde{\overline{\boldsymbol{W}}}_{gij,k}\right\|^2$$
$$+\theta\Delta_k + \frac{1}{n}\sum_{i=1}^{n}\left[1 - b\tanh^2\left(s_{i,k}/\eta_i(t)\right)\right]\Xi(y_k) - K\boldsymbol{s}_k^{\mathrm{T}}\boldsymbol{s}_k \quad (6.45)$$

The stability of the proposed AILC scheme in this chapter is summarized as follows.

Theorem 6.1 *Considering the manipulator plant* (6.1), *under Assumptions* 6.1–6.8, *design the state observer* (6.8) *and adaptive iterative learning controller* (6.38) *and* (6.40) *with parameter update algorithms* (6.42)–(6.44), *the following properties can be guaranteed*: (1) *all the closed-loop signals are bounded*; (2) *the observer estimation error* $\boldsymbol{z}_k$ *and tracking error* $\boldsymbol{e}_{sk}(t)$ *satisfy* $\lim_{k\to\infty}\int_0^T\|\boldsymbol{z}_k\|^2\mathrm{d}\sigma = 0$ *and* $\lim_{k\to\infty}\|\boldsymbol{e}_{sk}(t)\| = \|\boldsymbol{e}_{s\infty}(t)\| = \left(1+m_\eta\right)\|\boldsymbol{\eta}(t)\|$; (3) $\lim_{k\to\infty}\left\|\boldsymbol{y}_k(t) - \boldsymbol{y}_d(t)\right\| \leq k_0\|\boldsymbol{\varepsilon}\| + k_0\left(1+m_\eta\right)\|\boldsymbol{\varepsilon}\|\left(\mathrm{e}^{-(\lambda_0-1)} - \mathrm{e}^{-\lambda_0 t}\right)$, *where*, λ_0 *is a positive constant*.

The proof of Theorem 6.1 is similar to that of Theorem 5.1 and will not presented in detail.

6.5 Simulation Analysis

Consider a two degree-of-freedom robotic manipulator. The parameters are given by $\boldsymbol{M} = [m_{i,j}]_{2\times 2}, m_{1,1} = m_1 l_{c1}^2 + m_2(l_1^2 + l_{c2}^2 + 2l_1 l_{c2}\cos q_2) + I_1 + I_2, m_{1,2} = m_{2,1} = m_2(l_{c2}^2 + l_1 l_{c2}\cos q_2) + I_2$, $m_{2,2} = m_2 l_{c2}^2 + I_2$, $\boldsymbol{C} = [c_{i,j}]_{2\times 2}$, $c_{1,1} = h\dot{q}_2$, $c_{1,2} = h\dot{q}_1 + h\dot{q}_2$, $c_{2,1} = -h\dot{q}_1$ and $c_{2,2} = 0$, where, $h = -m_2 l_1 l_{c2}\sin q_2$. $G = [G_1, G_2]^T$, $G_1 = (m_1 l_{c1} + m_2 l_1)g\cos q_1 + m_2 l_{c2} g\cos(q_1+q_2)$, $G_2 = m_2 l_{c2} g\cos(q_1+q_2)$. The parameters are given by $m_1 = m_2 = 1$ kg, $l_1 = l_2 = 0.5$ m, $l_{c1} = l_{c2} = 0.25$ m, $I_1 = I_2 = 0.1$ kg m^2, $g = 9.81$ m/s^2, the external disturbance is given by $\boldsymbol{d}_k = [0.1 * rand * \sin t, 0.1 * rand * \sin t]^{\mathrm{T}}$, where $rand$ presents Gaussian noise which takes an random value on [0, 1]. $\boldsymbol{y}_k = \left[q_{1,k}, q_{2,k}\right]^{\mathrm{T}}$, $\boldsymbol{x}_k = \left[q_{1,k}, q_{2,k}, \dot{q}_{1,k}, \dot{q}_{2,k}\right]^{\mathrm{T}}$, $\boldsymbol{u}_k = \left[u_{1,k}, u_{2,k}\right]^{\mathrm{T}}$. The effect of time-delay output is given as

$$\boldsymbol{H}\left(y_{k,\tau}\right) = \begin{bmatrix} 0.5\sin(t)e^{-|\cos(0.5t)|}y_{\tau_1}\sin\left(y_{\tau_1}\right) \\ 0.5\cos(t)e^{-|\cos(0.5t)|}y_{\tau_2}\cos\left(y_{\tau_2}\right) \end{bmatrix}$$

The time delays is $\tau_1 = 0.5(1 + \sin(0.3t))$, $\tau_2 = 0.8(1 - \sin(0.5t))$. The desired trajectories for $q_{1,k}$ and $q_{2,k}$ are chosen as $q_{1,d} = \sin(2\pi t)$ and $q_{2,d} = \cos(2\pi t)$. The system runs on [0, 2] repeatedly. We choose $\boldsymbol{Q} = \mathrm{diag}\{0.001, 0.002, 0.003, 0.004\}$. By using LMI toolbox, we can obtain $\boldsymbol{K}_0 = \begin{bmatrix} 3.2821 & 0 \\ 0 & 3.2824 \\ 2.9695 & 0 \\ 0 & 2.9698 \end{bmatrix}$, $\boldsymbol{P} = \begin{bmatrix} 6.6823 & 0 & -4.01 & 0 \\ 0 & 6.6823 & 0 & -4.0102 \\ -4.01 & 0 & 6.6823 & 0 \\ 0 & -4.0102 & 0 & 6.6823 \end{bmatrix}$. The design parameters are chosen as $\boldsymbol{\Lambda} = \begin{bmatrix} \lambda_1 & 0 \\ 0 & \lambda_2 \end{bmatrix} = \begin{bmatrix} 2 & 0 \\ 0 & 2 \end{bmatrix}$, $\varepsilon_{11} = 1$, $\varepsilon_{12} = 1$, $\varepsilon_{21} = 1$, $\varepsilon_{22} = 1$, $\varepsilon_1 = \lambda_1\varepsilon_{11} + \varepsilon_{21} = 3$, $\varepsilon_2 = \lambda_2\varepsilon_{12} + \varepsilon_{22} = 3$, $K = 2$, $\gamma = 0.5$, $q_1 = 0.5$, $q_2 = 1$, $q_3 = 0.5$, $\Delta_k = 1/k^3$. Parts of the simulation results are shown in Figs. 6.1, 6.2, 6.3 and 6.4.

As observed in simulation results above, the proposed adaptive neural ILC can achieve a good tracking performance and tracking errors decrease along the iteration axis, which demonstrates the validity of the proposed approach.

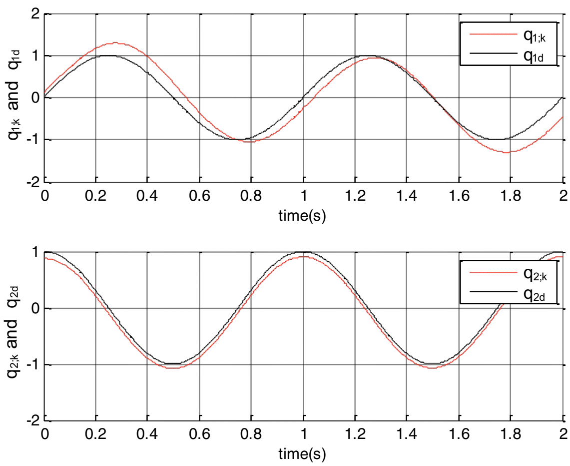

Fig. 6.1 $q_{1,k}$ and $q_{2,k}$ versus q_{1d} and q_{2d} $(k = 1)$

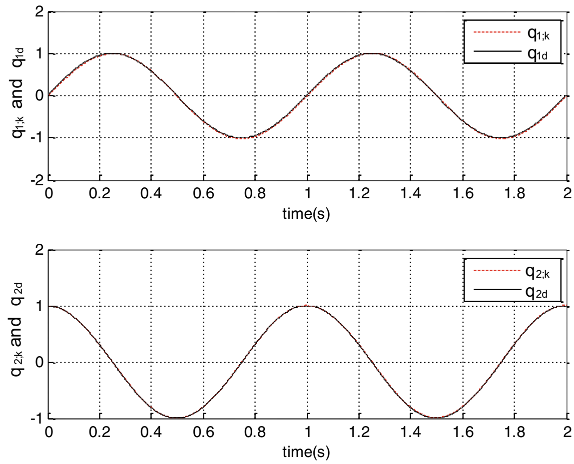

Fig. 6.2 $q_{1,k}$ and $q_{2,k}$ versus q_{1d} and q_{2d} $(k = 10)$

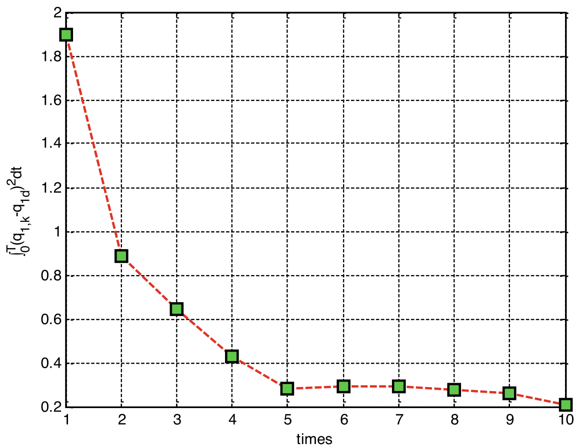

Fig. 6.3 $\int_0^T (q_{1,k} - q_{1d})^2 \mathrm{d}t$ versus the number of iterations

6.6 Summary and Comments

In this chapter, the research for plants with unmeasurable states and unknown control gain is carried out by taking manipulator as investigation object, which successfully overcomes the design difficulty from unknown control gain, absence of measurement of states and output delays. During the design the observer gain is determined by using LMI method and hyperbolic tangent function and convergent sequence are employed to design the robust term for purposed of guaranteeing the learning convergence.

Fig. 6.4 $\int_0^T \left(q_{2,k} - q_{2d}\right)^2 \mathrm{d}t$ versus the number of iterations

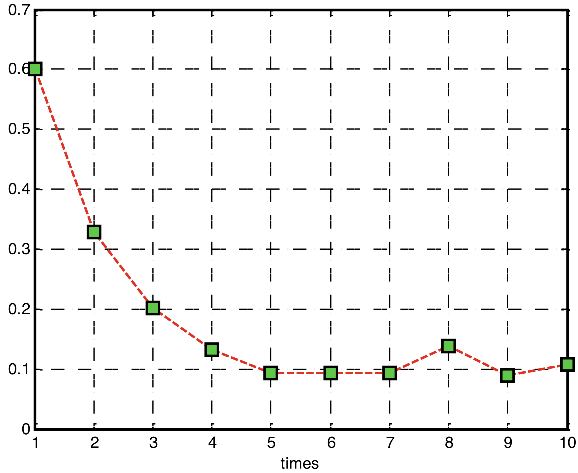

References

1. Ge S S, Lee T H, Harris C J. Adaptive neural network control of robotic manipulators[M]. London: World Scientific, 1998.
2. Agaian S S. Hadamard matrices and their applications[M]. New York: Springer-Verlag, 1985.